THE AUSTRALIAN NATIONAL UNIVERSITY

Functional studies of the Cf-9/Avr9 interaction

Ryan Wilson

19 September 2003

A thesis submitted for the degree of

Doctor of Philosophy at The Australian National University

RESEARCH SCHOOL OF BIOLOGICAL SCIENCES

Cooperative Research Centre Molecular Plant Breeding

Declaration

I hereby declare that this thesis is my own work except where otherwise indicated. The work described here was carried out in requirement of the Doctor of Philosophy degree at The Australian National University.

Ryan J. Wilson

19 September 2003

Table of contents

Acknowledgements

I would firstly like to thank my primary supervisor, Dr David Jones, who is an excellent scientist and supervisor. Thanks for your advice and support, for always being interested in my work and for always having an open door.

I would also like to thank my supervisory panel, Profs Peter Langridge and Adrienne Hardham and Drs Jeff Ellis and Michael Crouch, who have all provided useful and much appreciated input at various stages of my PhD.

I would particularly like to thank the Cooperative Research Centre for Molecular Plant Breeding, for their financial support of my project as well as for the many benefits I have received through being a part of the CRC and through their ongoing commitment to their postgraduate students.

There have been many in the Plant Cell Biology group and the Research School of Biological Sciences with whom I have had useful discussions about aspects of my PhD and who have supplied advice, though I would like to specifically mention the following. Dr Charlie Hocart, for discussions and advice on chemistry and mass spectrometry. Dr Nijat Imin, for similar discussions and advice. Jan Elliott, for numerous useful discussions and advice. Dr David Collings, for suggestions regarding confocal data analysis and for showing me the onion cell bombardment system. Dr Tom Wydrzynski, for useful discussions on assay systems. Also particular thanks to members of the Jones lab past and present for their help, for useful discussions and for being an enjoyable group to have worked with.

I would like to thank my parents for their support, for providing opportunities to me and for always being there. Also thanks to my good friends Penny, Siria (or should I now say Dr Hancock and Dr Natera), Madeleine, Regina and Shane for their friendship and support. I would like to thank Penny in particular, for being my good friend since I moved to Canberra, and for always being keen to go walking, skiing or drinking coffee.

I would like to give a special thanks to Megan, my partner, companion and best friend, not just for putting up with/looking after me while writing my thesis, but also for everything else.

Common abbreviations

alpha	α-cyano-4-hydroxycinnamic acid
amu	Atomic mass units
Avr or *Avr*	Avirulence protein or gene respectively
ER	Endoplasmic Reticulum
ESI-MS	Electrospray Ionisation MS
GFP	Green Fluorescent Protein
GUS	β-glucuronidase
hpi	Hours post infiltration
IEC	Ion-Exchange Chromatography
LRR	Leucine-Rich Repeat
MALDI-TOF	Matrix-Assisted Laser-Desorption Ionisation Time-Of-Flight MS
MS	Mass Spectrometry
m/z	Mass/charge ratio
NBS	Nucleotide Binding Site
PM	Plasma Membrane
PSD	Post-Source Decay
PVX	Potato Virus X
Q-TOF	Quadrupole Time-Of-Flight
R or *R*	Resistance protein or gene, respectively
RTF	Restricted Taxonomic Functionality
6His	Six-histidine

Abstract

Research published on the Cf-9 resistance protein has presented conflicting evidence on its subcellular localisation, suggesting either endoplasmic reticulum (ER) or plasma membrane (PM) residence (Chapter 1). The research described in this thesis aimed to address this issue using functional approaches.

In Chapter 3, this question was addressed using *Agrobacterium*-mediated transient expression (by 'agroinfiltration') of a range of Avr9 variants in *Cf-9* tobacco (see below). To inform this work, preliminary characterisation of the variability of the Cf-9/Avr9 interaction using the agroinfiltration assay was first performed, and is described in Chapter 2. Variation in the assay was observed between plants at slightly different developmental stages and between leaves of different ages on the same plant, whereas little variation was observed within a single leaf. This variation was accounted for in later work by performing within leaf comparisons of test constructs.

The work described in Chapter 3 aimed to ask whether Cf-9 can detect Avr9 from the ER by comparing Avr9 tagged with the C-terminal amino acid sequence KDEL (an ER retrieval motif) with control variants of Avr9. The Cf-9 mediated necrotic response to Avr9-KDEL was delayed by approximately 25 hours compared to Avr9, and this delay was dependent on the biological activity of the retrieval signal. Mutation of the *N*-glycosylation site on Avr9 ruled out differential carbohydrate processing as a cause of this delayed response. Models of Cf-9 function to explain these results are presented, the most likely of which seems to be that Cf-9, or a step in Avr9 perception that is upstream of Cf-9, is present at the PM.

If Cf-9 does function from the ER, one hypothesis is that Avr9 travels to the ER. The work described in Chapter 4 aimed to test this hypothesis by determining whether Avr9 acquires previously identified intracellular modifications when added to plant cells exogenously. This chapter therefore describes the development of methods that would be suitable to detect such modifications to Avr9. A published Avr9 purification procedure was adapted and modified, and semi-purified, bioactive Avr9 was successfully recovered from intercellular fluid washes of transgenic tobacco expressing Avr9. Avr9 was detected in various extracts using a Matrix-Assisted Laser Desorption/Ionisation Time Of Flight mass spectrometry method developed during this work, independently confirming previous analysis of Avr9 expressed in tobacco.

Progress was made towards the application of these methods to the intended experiments, including whole leaf tissue extraction and the preliminary development of an *E. coli* expression system for Avr9. Possible improvements and limitations to this approach as well as alternative approaches to this research are discussed.

The research described in Chapter 5 aimed to determine whether Cf-9 could be engineered to function in wheat. This is of interest to determine whether a resistance gene from a dicotyledonous species could function in a monocotyledonous species. In addition, Cf-9 function in this important crop species could be utilised to engineer a form of non-specific disease resistance, which would be of considerable agricultural value. Microprojectile co-bombardment of Cf-9 and Avr9 into wheat leaves found no evidence for Cf-9 function, suggesting that it does not function in this species.

Chapter 6 describes the production of a six histidine tagged Green Fluorescent Protein (GFP) expression system in *E. coli*, and the subsequent purification of recombinant GFP. Purified GFP was used to generate mouse anti-GFP monoclonal antibodies that were intended for use in the work described in this thesis, but were not utilised. Potential uses of this resource, particularly for future work suggested in this thesis, are outlined.

A general discussion considers broader aspects of Cf-9 function at a cellular level, and approaches for further investigation of this system.

CHAPTER 1

GENERAL INTRODUCTION

Plant disease resistance

IN order to survive, all plants must defend themselves against an assortment of assailants that can affect the plant in a myriad of ways. No one mechanism will suffice for this task – spines may deter herbivores, but more subtle methods are necessary for defence against viral or fungal pathogens. The methods employed by plants for defence against pathogens are usually loosely assembled into two categories: passive (or constitutive) defences and active (or inducible) defences (Lucas 1998). Constitutive defences include structural barriers such as the cuticle and preformed chemicals such as saponins, alkaloids and some antifungal proteins and enzyme inhibitors. Inducible defences include responses such as expression of Pathogenesis Related (PR) proteins, production of active oxygen species and controlled cell death of tissues affected by a specific pathogen.

A well studied form of inducible plant defence is known as gene-for-gene resistance. In this form of resistance, originally described by Flor (1971), plants possessing a dominant resistance ("*R*") gene are resistant to pathogens possessing a dominant gene that confers avirulence ("*Avr*" gene) to the pathogen on the resistant plant. When each of these cognate genes are represented by their dominant allele, *R* and *Avr* in the plant and pathogen respectively, the plant detects the presence of the pathogen and activates defence mechanisms. If either gene is represented by the recessive allele, the plant does not detect the presence of the pathogen and normal disease progression can occur.

The molecular and cellular basis for R protein function

Over the last decade, a number of genes encoding R proteins of diverse structure have been isolated and research attention has shifted towards investigation of R protein function at the cellular and molecular (including biochemical) level (Dangl and Jones 2001). Investigations of the subcellular localisation of R and Avr proteins and the mechanisms or co-factors involved in their function are key aspects of this research.

The subcellular localisation of *R* gene products was initially predicted from primary protein sequence. The largest class of predicted R proteins, the Nucleotide Binding Site-Leucine-Rich Repeat (NBS-LRR) resistance proteins, are generally thought to be cytoplasmic, and in some cases appear to be membrane associated (Dangl and Jones 2001). For example, the RPM1 protein was originally predicted to be cytoplasmic, but with a patch of hydrophobic amino-acids that could be involved in membrane association (Grant *et al.* 1995). This protein was later shown to be a peripheral plasma membrane (PM) localised protein (associated with the membrane, but not anchored in the membrane itself; Boyes *et al.* 1998). An interesting example is the *RPS2* gene which, when isolated, was predicted to encode a protein potentially containing a trans-membrane domain, although no signal peptide sequence was identified (Bent *et al.* 1994). A simultaneously published paper identified an N-terminal hydrophobic sequence that may act as a signal anchor rather than a signal peptide on RPS2 (Mindrinos *et al.* 1994). Interestingly, recent results have suggested that RPS2 is an integral membrane protein (anchored in the hydrophobic part of the membrane), although the role of particular sequence domains was not investigated (Axtell and Staskawicz 2003). Further work is required to determine the subcellular localisation of members of the abundant NBS-LRR class of R proteins, and the mechanisms by which they are localised.

The protein encoded by the *Pto* resistance gene was predicted to be a kinase with no membrane anchor domain, but an N-terminal myristoylation site, suggesting that it may be membrane associated (Martin *et al.* 1993). A later study provided evidence that this motif was not necessary for function of Pto (Loh *et al.* 1998), although this does not necessarily indicate that Pto is not normally membrane anchored.

The transmembrane (as distinct from membrane anchored or associated) class of R proteins is typified by the Cf proteins (Jones and Jones 1997; see below) and Xa21 (Song *et al.* 1995). While Xa21 is predicted to have a large extracellular LRR domain, transmembrane domain and cytoplasmic kinase domain, the Cf proteins are predicted to possess similar large extracytoplasmic and transmembrane domains but only a short cytoplasmic tail, leading to the question of how these proteins transduce signals to activate resistance mechanisms (Jones *et al.* 1994).

R protein function and the guard hypothesis

The simple genetic nature of gene-for-gene disease resistance led to the common speculation that plant *R* genes might encode receptor proteins that detect the pathogen *Avr* gene product (the 'receptor-ligand' model for R protein function). Based on mammalian hormone receptor systems, this model would predict a direct interaction between the R and Avr proteins and subsequent activation of defence signal transduction.

Direct molecular interaction has been shown between Pto/AvrPto (Scofield *et al.* 1996; Tang *et al.* 1996), PiTa/AvrPiTa, (Jia *et al.* 2000) and recently between the broad spectrum resistance protein RRS1-R and the type III effector PopP2 (Deslandes *et al.* 2003). For the resistance protein Cf-9, a range of negative data has been presented suggesting that it may not interact directly with its cognate avirulence gene product Avr9 (Luderer *et al.* 2001). This inability to detect direct interaction between cognate R/Avr proteins is probably more common than the ability to detect direct interactions (Dangl and Jones 2001; Ellis and Jones 2003) but in some cases this could be due to limitations of available techniques (Ellis and Jones 2003).

Although direct R/Avr protein interaction has been demonstrated for the interaction between *Pto* and *AvrPto*, an NBS-LRR protein (Prf) has been identified as necessary for the Pto-dependent response to AvrPto (Salmeron *et al.* 1996). In attempting to explain the role of the Prf protein in the direct Pto/AvrPto interaction, van der Biezen and Jones (1998) suggested that the Prf protein recognises AvrPto interaction with Pto. This idea was later modified and presented as a general hypothesis to explain R gene function, termed the 'guard hypothesis' (Dixon *et al.* 2000; van der Biezen *et al.* 2000). This hypothesis suggests that R proteins 'guard' important host components, which are pathogenicity targets, from pathogenic virulence factors (Figure 1.1). In the case of the Pto/AvrPto system, Pto would be the host component that is targeted by AvrPto, and Prf is the NBS-LRR protein that 'guards' Pto. A variant of this hypothesis is that the pathogen virulence factor modifies the pathogenicity target enzymatically, and this modified host protein is recognised by the R protein guard (Ellis *et al.* 2000).

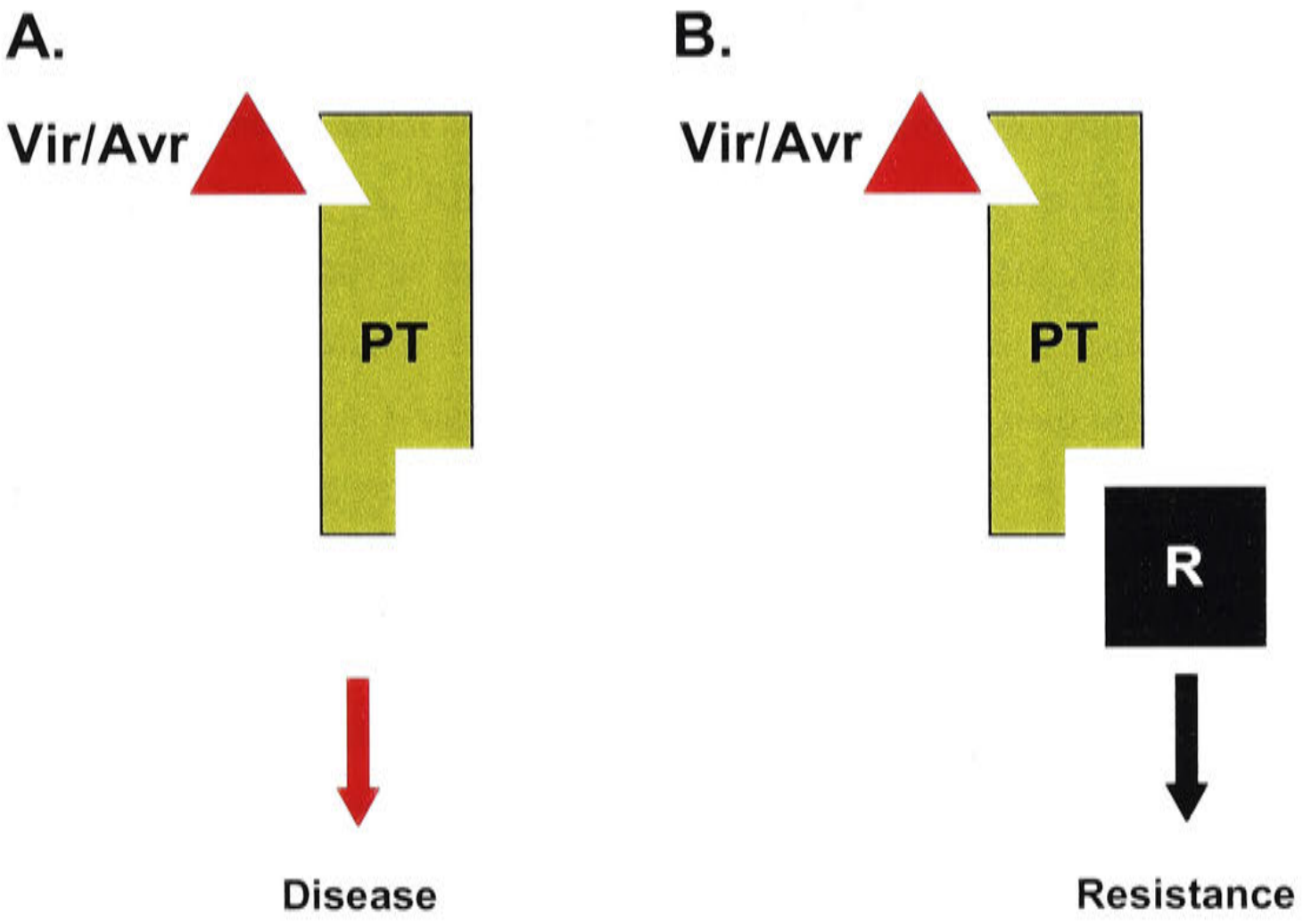

Figure 1.1. The 'guard hypothesis' for R protein function. A pathogen virulence factor (which in the resistant host is an avirulence factor, **Vir/Avr**) interacts with a host plant component (the pathogenicity target, **PT**) for its virulence function. In the susceptible host (**A.**), normal disease occurs due to the absence of the **R** protein, but in the resistant host (**B.**), the R protein initiates a resistance response after detecting the Vir/Avr protein interacting with the pathogenicity target.

The *Arabidopsis/Pseudomonas syringae* (*P.s.*) interaction has provided perhaps the strongest evidence yet to support the guard hypothesis as an explanation for R protein function. The RIN4 protein was first identified as a protein that interacts with the *Arabidopsis* R protein RPM1, and has been suggested to function as a repressor of basal defence responses (Mackey *et al.* 2002). The *P.s.* Avr proteins AvrRpm1 and AvrB proteins were both found to interact with, and promote phosphorylation of, RIN4 *in vivo* thus activating the RPM1 dependent resistance response (Mackey *et al.* 2002). RIN4 was later found to be targeted by yet another *P.s.* Avr protein, AvrRpt2, which mediates the post-transcriptional disappearance of RIN4 and in turn activates RPS2 dependent resistance responses (Axtell and Staskawicz 2003; Mackey *et al.* 2003). Thus, according to the guard hypothesis, RIN4 appears to be a host protein that is an important pathogenicity target, and as such is targeted by multiple bacterial Avr (effector) proteins and guarded by multiple cognate host R proteins (RPM1/AvrRpm1 and AvrB; RPS2/AvrRpt2). This is consistent with a prediction of the guard hypothesis that more than one Avr protein might be found to interact with a host protein that is a key pathogenicity target (Dangl and Jones 2001).

Another example of multiple targeting of a host protein is Pto which, in addition to interacting directly with AvrPto, interacts directly with AvrPtoB and subsequently induces defence responses in a *Prf* dependent manner (Kim *et al.* 2002). According to the guard hypothesis, Pto would be the pathogenicity target that is targeted by multiple Avr/virulence proteins and guarded by the NBS-LRR protein Prf (van der Biezen and Jones 1998).

The tomato Cf proteins

The *Cf-9* gene is the founding member of a family of genes from tomato that confer resistance to specific races of the fungus *Cladosporium fulvum* (Jones *et al.* 1994; Jones and Jones 1997). The Cf-9 protein is predicted to have a large extracellular domain, transmembrane domain and short cytoplasmic tail (Jones *et al.* 1994; Jones and Jones 1997). The extracellular domain consists of 27 LRRs, with the first (N-terminal) 23 LRRs (domain C1) separated from the remaining 4 (domain C3) by a short 'loop out' region, and has a number of predicted N-glycosylation sites (Jones and Jones 1997).

The predicted Cf-9 protein is identical to Cf-4 in the C-terminal portion of the proteins, including the last 5 LRRs of C1 (Thomas *et al.* 1997). Interestingly, the predicted Cf-5

and Cf-2 proteins are highly similar to other Cf proteins in this same C-terminal region (Dixon *et al.* 1996; Dixon *et al.* 1998), leading authors to suggest that this domain may be involved in interactions with other proteins to activate signalling mechanisms (Dixon *et al.* 1996; Jones and Jones 1997; Thomas *et al.* 1997).

Cf-9 and Cf-4, but not Cf-5 and Cf-2, possess a C-terminal KKRY amino acid motif, the dilysine consensus motif (KKXX) for endoplasmic reticulum (ER) localisation of Type I membrane anchored proteins, suggesting that Cf-9 might function in the ER (Jones *et al.* 1994). This localisation would be unusual, as *C. fulvum* does not penetrate the plant cells (Joosten and de Wit 1999) and thus probably produces Avr9 only in the apoplast. The subcellular localisation of Cf-9 was thus of particular interest, and two independent studies have specifically examined this issue (Benghezal *et al.* 2000; Piedras *et al.* 2000).

The subcellular localisation of Cf-9

Piedras *et al.* (2000) used c-myc epitope tagged Cf-9 (one version tagged at the N-terminus, after the signal peptide, and one version tagged in the cytoplasmic domain upstream of the KKXX motif) to perform cell fractionation and immunolocalisation analyses. Two-phase partitioning was used to enrich PM from transgenic tobacco with the tagged Cf-9 (c-myc:Cf-9), and protein gel blots and enzyme assays of resulting fractions suggested an enrichment of c-myc:Cf-9 in the PM fraction (see further comments below). Immunolabelling of transgenic tobacco protoplasts was then performed using c-myc antibodies and silver enhancement, and labelling was observed on non-permeabilised c-myc:Cf-9 protoplasts, suggesting that c-myc:Cf-9 was detected at the PM.

Benghezal *et al.* (2000) focussed on demonstrating that the KKXX motif at the C-terminus of Cf-9 functions as an ER retrieval signal, and this was the first time that it had been shown in plants. Localisation of Cf-9 was examined using full length Cf-9 tagged with the triple hemagglutinin (3-HA) epitope (after the signal peptide) and expressed in tobacco bright yellow 2 (BY-2) cells. Sucrose gradient fractionation of plant cell membranes indicated that 3HA-Cf-9 was absent from the tonoplast and that at least some was present in the ER. When total membranes were separated by two-phase partitioning, no 3HA-Cf-9 could be detected in the PM fraction despite the enrichment

of PM associated with this technique, and the protein could only be detected in the ER containing fraction.

The data from these two studies apparently conflict, suggesting either PM or ER localisation of Cf-9. There are some potential limitations to these studies, which may help explain this apparent conflict. The main criticism levelled at the Benghezal *et al.* (2000) study is that the functionality of 3HA-Cf-9 was not tested (Rivas *et al.* 2002; Van der Hoorn *et al.* 2001b). Aberrant ER retention could therefore be a consequence of the lack of function of the protein. An example of this could be ER retention due to incorrect folding of the fusion protein (Hammond and Helenius 1995), which in this case could be the result of the 3HA tag. However, since Cf-9 was tagged in the same location in this study as it was by Piedras *et al.* (2000) this possibility seems unlikely, although 3HA sequence specific folding disruption is possible. Alternatively, lack of functionality could result in absence of a positive signal for ER export. For example, hormone stimulation (Malide *et al.* 2001) or functional complex formation (Shenkman *et al.* 2000) has been shown to induce ER export of receptor proteins. If Cf-9 relied upon similar mechanisms for ER export (assuming it does not function in the ER), disruption of interaction with signalling or partner proteins involved in export would result in ER retention of a non-functional version of the protein.

Piedras *et al.* (2000) used a CaMV35S promoter to drive expression of their tagged Cf-9 protein, and as KKXX mediated ER retrieval in plants cells can probably be saturated (Benghezal *et al.* 2000) this would allow progress of some protein to the PM. Therefore, in the Piedras *et al.* (2000) study, some progression of Cf-9 to the PM could have occurred even if Cf-9 was normally ER localised (as noted by Van der Hoorn *et al.* 2001b). Benghezal *et al.* (2000) also used the CaMV35S promoter to drive expression of tagged Cf-9, although no protein was observed at the PM in these studies.

Another limitation of the Piedras *et al.* (2000) study is that the immunolocalisation experiment was performed without permeablisation of the whole protoplasts, which would not allow detection of any ER signal, as has been noted (Van der Hoorn *et al.* 2001b). Though this approach was likely intended to reduce intracellular fluorescence, the immunofluorescence data of Piedras *et al.* (2000) does not exclude the possibility that a proportion of Cf-9 was in the ER.

There are some other limitations of the data of Piedras *et al.* (2000) paper that do not appear to have been noted in the literature. One is that this study used an ER marker enzyme that also shows activity on the PM (Askerlund *et al.* 1991; Piedras *et al.* 2000), a consequence of which is that the authors could not conclusively rule out ER contamination of their two-phase partitioning PM preparations. The lack of a western blot control for an ER marker protein also makes it difficult to rule out ER contamination of the PM fraction.

Other functional studies of Cf-9

A later paper examined whether the Cf-9 protein requires the C-terminal KKXX consensus motif for function by using a transient expression assay to compare the activity of Cf-9 with a wildtype C-terminus (KKRY) to Cf-9 with the AARY mutation at the C-terminus (Van der Hoorn *et al.* 2001b). Representative results using this approach suggested that the Cf-9-AARY mutant had lower activity than wildtype Cf-9, although the statistical significance of the result was not indicated. The authors suggest that these results are best explained by a model in which Cf-9 is retained in the ER (by the KKXX signal) until it is assembled into functional complexes, after which it progresses to the PM from where it functions (also suggested by Benghezal *et al.* 2000 and Piedras *et al.* 2000).

In this model, it is suggested that the reduced activity of Cf-9-AARY (at the PM) results from quicker ER exit of this non-retrieved mutant (Van der Hoorn *et al.* 2001b). However, by this same logic (early exit of Cf-9-AARY from the ER), reduced activity of Cf-9-AARY would also be expected if Cf-9 was functional in the ER instead of the PM. It therefore does not seem that reduced activity of Cf-9-AARY compared to wildtype Cf-9 argues clearly in favour of either PM or ER localisation of Cf-9.

A more recent functional study of Cf-9 using gel filtration and blue native PAGE analysis of TAP (Tandem Affinity Purification) tagged Cf-9, found that the protein was present in total membranes in what appeared to be an approximately 420 kDa complex (Rivas *et al.* 2002). Though intended to address distinct issues (i.e. that of the cofactors involved in Cf-9 function), this study does not further clarify the question of localisation of Cf-9 protein, for two reasons. Firstly, this study performed analysis on total membrane extracts, which would include both PM and ER membranes. Secondly, the TAP epitope tag was inserted after the C-terminal KKRY sequence of Cf-9, which

would abolish any ER retention. A recent study found that the apparent large complex containing Cf-9 (and other Cf proteins) was probably an artefact of the gel filtration technique used to perform these experiments rather than a protein complex (Van der Hoorn *et al.* 2003).

Models for Cf-9 function

In summary, the data outlined above from studies on Cf-9 protein function do not conclusively support PM or ER localisation of the protein, and raise the possibility that the localisation of total and functional Cf-9 may be distinct. Consequently, two broad models for the cellular basis of Cf-9 function can be contemplated. One model (Model 1) is that the Cf-9 functions at the PM, and ER retrieval may function as a quality control mechanism, allowing proper assembly of Cf-9 into functional complexes and released to the PM (Benghezal *et al.* 2000; Piedras *et al.* 2000; Van der Hoorn *et al.* 2001b; Figure 1.2). This model could include cleavage of Cf-9 that is not present in properly assembled complexes (Benghezal *et al.* 2000), or possibly release of Cf-9 complexes from the ER to the PM only in the presence of Avr9. Another model (Model 2) is that Cf-9 is an ER resident protein, and that Avr9, or a signal initiated by Avr9 at the PM, travels to the ER whereupon Cf-9 initiates a response (Benghezal *et al.* 2000; Joosten and de Wit 1999; Figure 1.2). Precedents for such models and their relative merits as a model for Cf-9 function are discussed in Chapter 7 (General Discussion).

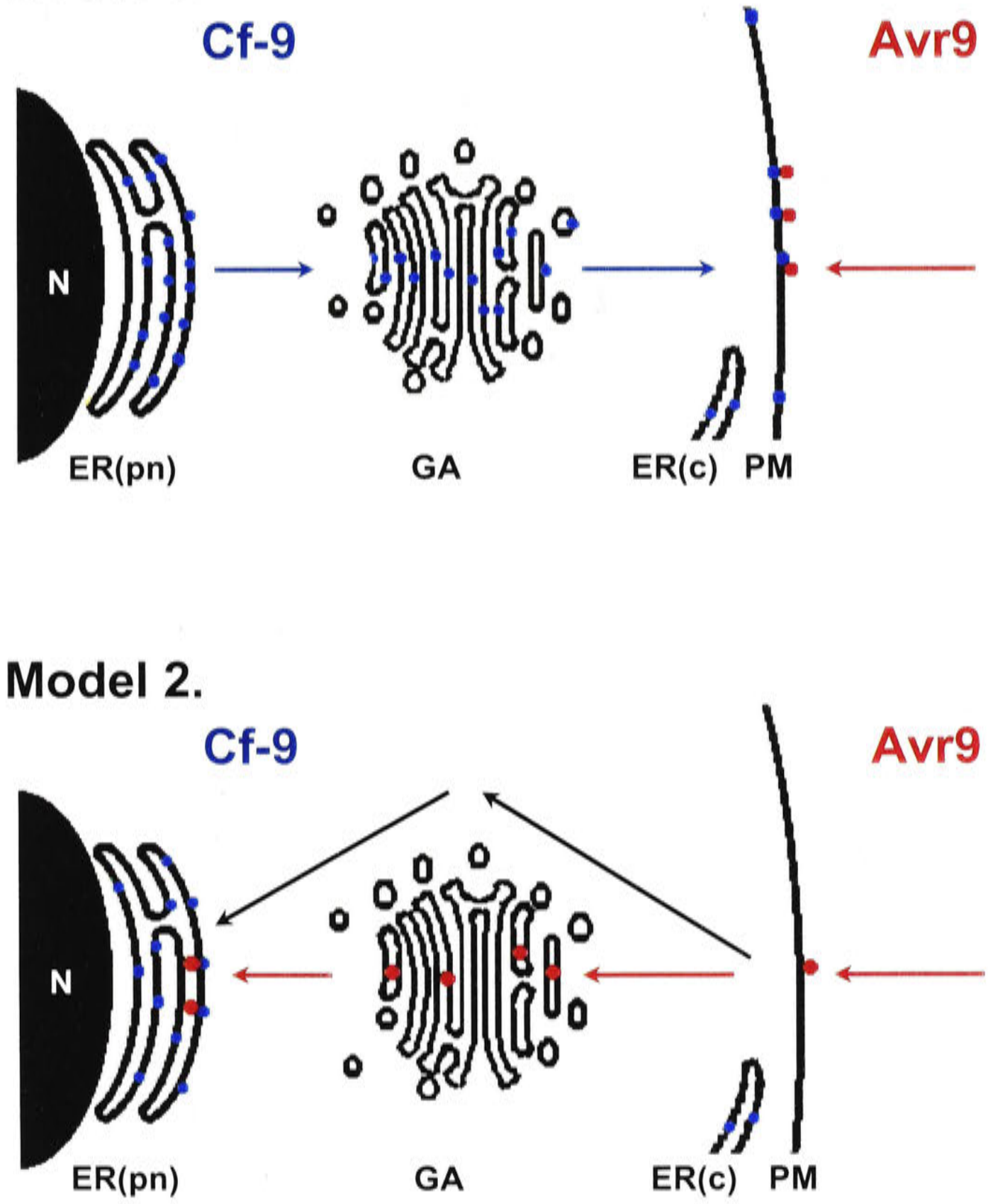

Figure 1.2. Two broad models for the cellular basis of Cf-9 function. **Model 1**. **Cf-9** is present in the **ER** (**pn** indicates perinuclear ER, **c** indicates cortical ER, **N** indicates the nucleus), but functions to detect **Avr9** at the **PM**. ER retention may function as a quality control mechanism, allowing only properly assembled, active complexes to progress to the PM (blue arrows). **Model 2**. Cf-9 is an ER resident protein, and Avr9 is perceived after it travels to the ER (red arrows) or initiates signalling from the PM to the ER (black arrows). Travel to the ER from the PM could be by a pathway that does or does not involve the Golgi apparatus (**GA**). For both models, Cf-9 could be present in cortical and/or perinuclear ER.

Aim of this thesis

The primary aim of this thesis was to examine functional aspects of the Cf-9 disease resistance protein, including to further resolve the key question of the localisation of functional Cf-9. Chapter 3 describes work that aimed to examine this issue by testing whether Cf-9 could respond to Avr9 from the ER. Avr9 with and without ER localisation signals fused to the C-terminus were expressed in *Cf-9* tobacco and changes to the Cf-9-mediated necrotic response compared to controls were analysed. Chapter 2 describes the implementation of a transient expression method to perform these experiments. Some preliminary characterisation of the *Agrobacterium*-mediated transient expression system is also described in this chapter.

In Chapter 4, a complementary approach was planned to address the question of localisation of functional Cf-9, specifically by examining the destination of Avr9 when added exogenously to tobacco suspension cells. If Cf-9 did function from the ER, it would be predicted that Avr9 is probably transported to the ER when added exogenously to cells, whereas if it did not function from the ER, Avr9 would not be expected to travel to the ER. As tools for this approach, Avr9 purification procedures were adapted from the literature and a sensitive mass spectrometry method for Avr9 detection from semi-purified extracts was developed. Although the planned experiments were not performed, development of a system for expression of functional Avr9 in *E. coli* was initiated towards this goal.

The aim of Chapter 5 was to test for function of the Cf-9 protein in the monocotyledonous crop species wheat (*Triticum aestivum*). This project was motivated by current interest in the taxonomic limits of *R* gene function as well as to examine the possibility for engineering novel resistance in wheat with the Cf-9 gene. Modifications were made to the encoded Cf-9 protein to account for predicted limitations to the function of Cf-9 in heterologous species, and a transient microprojectile bombardment approach was used to test for function in wheat cells.

An early plan for analysis of Cf-9 function was to test for direct interaction between GFP tagged Cf-9 and Avr9, as outlined in Chapter 6. An *E. coli* expression construct for six-histidine tagged GFP was produced and the protein expressed and purified. Purified protein was used to generate monoclonal antibodies to facilitate these experiments, however this approach was discontinued.

Chapter 7 is the General Discussion, and considers broader implications and issues related to the research presented in this thesis.

CHAPTER 2

PRELIMINARY CHARACTERISATION OF AGROINFILTRATION VARIABILITY

2.1 SUMMARY

AGROBACTERIUM-mediated transient expression has become an increasingly popular transient expression method over the last decade. As a prelude to studies reported in Chapter 3, a study was conducted in order to characterise some parameters and variables of this method. Considerable variation was demonstrated between leaves and between plants, with some minor variation within leaves. A gradient of assay strength was identified on leaves of different ages on a single plant. This gradient opposed a gradient of sensitivity to Avr9 peptide, also shown in this study, indicating that the agroinfiltration gradient was attributable to properties of this assay rather than Cf-9/Avr9 gene-for-gene interaction. Considerations for application of the assay are discussed and suggestions for further characterisation of this method are then made.

2.2 INTRODUCTION

2.2.1 *Agrobacterium*–mediated transient expression

In recent years, the use of transient expression systems to facilitate the functional analysis of R proteins has proliferated, with *Agrobacterium*-mediated transient expression, or 'agroinfiltration' being particularly popular. This method consists of inserting the gene of interest into an *Agrobacterium* binary vector, as one would for stable plant transformation with this bacterium, then infiltrating a suspension of the *Agrobacterium* culture carrying this plasmid into the intercellular leaf spaces of the plant of interest, typically using a needle-less syringe or vacuum (Kapila *et al.* 1997; Schob *et al.* 1997; Van den Ackerveken *et al.* 1996). The T-DNA and inserted gene construct/s are then transferred to the plant cells by the *Agrobacterium*, and transient

expression of the gene/s of interest in the introduced T-DNA occurs in the plant cells within 1-2 days (Janssen and Gardner 1990; Kapila *et al.* 1997; Van der Hoorn *et al.* 2000). This method is popular because of its speed and ease of use as well as being based upon materials and methods already present in laboratories generating transgenic plants. Additionally, this method can be used on a wide variety of plant species, and is particularly useful for species recalcitrant to stable transformation (Van den Ackerveken *et al.* 1996). Although widely used, and considerably useful, disadvantages or drawbacks to this method have not been widely discussed or analysed in the literature.

The first studies specifically detailing the use of *Agrobacterium* as a general tool for transient gene expression *in planta* were published in 1997 (Kapila *et al.* 1997; Schob *et al.* 1997), although the observation of *Agrobacterium*-mediated transient expression had been made somewhat earlier (Janssen and Gardner 1990; Rossi *et al.* 1993; Tang *et al.* 1996; Van den Ackerveken *et al.* 1996). Agroinfiltration has since been used for a multitude of experimental purposes, including gene-silencing (Johansen and Carrington 2001; Schob *et al.* 1997), promoter analysis (Yang *et al.* 2000), functional analysis of viruses (Palanichelvam and Schoelz 2002), transient expression in ripe fleshy fruit (Spolaore *et al.* 2001), producing recombinant antibodies *in planta* (Vaquero *et al.* 1999), study of the secretory pathway (Batoko *et al.* 2000), isolation of a resistance gene (Bendahmane *et al.* 2000), and functional analysis of resistance and avirulence genes and their interaction (see below).

Analysis of gene-for-gene systems by agroinfiltration

This method of transient gene expression has been variously useful in studying R and Avr protein function. The first examples include *R* gene specific necrosis induced in response to *Agrobacterium*-mediated transient expression of the bacterial avirulence genes *AvrBs3* from *Xanthomonas* (Van den Ackerveken *et al.* 1996) and *AvrPto* from *Pseudomonas* (Scofield *et al.* 1996; Tang *et al.* 1996) in transgenic tobacco expressing *Bs3* or *Pto* respectively.

Agroinfiltration has also been used to study both Cf-9/Avr9 and Cf-4/Avr4 interactions in *Nicotiana tabacum* and *N. benthamiana* (Thomas *et al.* 2000; Van der Hoorn *et al.* 2000). Using wild-type tobacco, gene-for-gene specificity of the interaction was maintained as indicated by the need for Cf-9 and Avr9 or Cf-4 and Avr4 to cause necrosis, whereas other combinations of genes or either gene alone did not result in

necrosis. Furthermore, gene-for-gene specificity was retained when intercellular fluids (IF) containing Avr9 or Avr4 from *C. fulvum*/tomato interactions were infiltrated into tobacco leaves that transiently expressed the corresponding resistance gene (Cf-9 or Cf-4) following agroinfiltration (Van der Hoorn *et al.* 2000). Specific necrosis also resulted when the Avr protein was expressed using a Potato Virus X expression system and the corresponding *R* gene was introduced by agroinfiltration (Van der Hoorn *et al.* 2000).

Comparative analysis by agroinfiltration

A semi-quantitative dose-response approach has previously been used to compare the strength of *Cf-9* and *Cf-4* resistance gene activity (Hammond-Kosack and Jones 1994). This was done by comparing the strength of the response of plants heterozygous or homozygous for these *R* genes to 2-fold serially diluted IF containing the corresponding Avr protein. Visual scoring of the differential necrotic response showed that plants homozygous for the *Cf* gene responded to 2-fold more dilute IF than did heterozygotes.

A similar approach was attempted more recently using agroinfiltration dilution series comparisons and quantification of the necrotic response to compare Cf-9 and Cf-4 function (Van der Hoorn *et al.* 2000). This was feasible because the Cf/Avr genes were on separate plasmids. The experiment was performed by mixing *Cf*-containing *Agrobacterium* with *Avr*-containing *Agrobacterium* in different ratios (presumably diluted against each other), then quantifying the percentage of the infiltrated area that had become necrotic after 7 days, and plotting percentage necrosis against the percentage of culture containing either the Cf or Avr plasmid (Van der Hoorn *et al.* 2000). In interpreting the results from these experiments, it is important to note that 100% necrosis was achieved with less than about 15% of Cf or Avr *Agrobacterium* culture, so that as one component became limiting the cognate component was in considerable excess (e.g. the Cf when the Avr was below 15%, or vice versa).

The percentage of Cf-9 needed for 50% necrosis (NC^{50}) determined from two independent experiments was 1.86% and 3.74% (values are for two experiments, so a standard error was not calculated) while the values for Cf-4 were 1.38% and 4.92%, suggesting that the Cf-9 and Cf-4 constructs had similar activity in this system. One hundred percent necrosis was achieved at approximately 10% for both Cf-9 and Cf-4 containing *Agrobacterium*. The NC^{50} values for Avr9 and Avr4 containing *Agrobacterium* were 2.56 ± 0.88% and 0.27 ± 0.12% (values are for four experiments,

so standard errors were calculated) respectively, suggesting that the Avr4 construct has approximately 10 fold higher activity than the Avr9 construct. One hundred percent necrosis was achieved at approximately 15% and 0.7% for Avr9 and Avr4-containing *Agrobacterium*, respectively (Van der Hoorn *et al.* 2000).

This is consistent with the more rapid response of the Cf-4/Avr4 interaction relative to the Cf-9/Avr9 interaction (Thomas *et al.* 2000; Van der Hoorn *et al.* 2000), and suggests that activity of the *Avr* gene or gene construct may be a causal factor (see below; Van der Hoorn *et al.* 2000). Interestingly, the authors note that at *Avr* concentrations corresponding to NC^{50} values, no difference in timing of response to these genes was observed (although these data were not presented). They argue that this supports the hypothesis that the difference in *activity* of the *Avr* constructs causes the different *timing* of the response. This distinction between activity and timing of necrosis is important, and has relevance to the experiments described in Chapter 3.

It is not clear what results in this different activity, but the authors suggest that the possibilities could include differences in transcription, post-transcriptional modifications, protein stability or perception (Van der Hoorn *et al.* 2000). Consequently, the authors can only ascribe the differential activity to the Avr constructs or genes, and further experiments would be needed to clearly determine what particular stage of transgene expression (e.g. transcript or protein stability) or Avr protein perception caused the different activity. Differences in T-DNA transfer of the Avr plasmids seem unlikely since *Agrobacterium* suspensions were of an equal density and the same leaves were used. Additionally, the CaMV35S promoter was used for all constructs, so the level of transcriptional initiation of the Avr constructs would have been about the same.

Subsequent analyses of Cf-9 mediated responses have also used agroinfiltration. Van der Hoorn *et al.* (2001b) examined the role of the Cf-9 C-terminal dilysine motif (KKXX) in recognition of Avr9. This study suggests that the activity of Cf-9 with a mutated KKXX motif is quantitatively reduced, but the lack of statistical treatment of the data means that statistical certainty of the conclusion is not clear. The same method was also used to compare the activity of a range of variants of Cf-9 and Cf-4 in order to identify specificity determinants for recognition of Avr4 (Van der Hoorn *et al.* 2001a).

In both of these latter studies, results from a single experiment representative of multiple repetitions are presented, rather than statistically treated data from multiple experiments (Van der Hoorn *et al.* 2001a; Van der Hoorn *et al.* 2001b). One consequence of this is that the statistical significance, and therefore level of certainty, of the data cannot be determined from the results presented. While this would not be critical when the difference in necrotic response is very clear and reproducible (as in most cases in the cited papers), minor and/or variable differences in necrosis are unlikely to be reliably detected.

2.2.2 Aim of this chapter

In summary, it is clear there are many potential benefits of using the agroinfiltration approach to investigate the Cf-9/Avr9 gene-for-gene system, most notably abolition of the need for stable transgenic lines and consequent reduction in time needed to perform such analyses. However, this is a relatively new system that has not been widely used in a comparative manner for *R* gene analysis, and therefore requires cautious use. Accordingly, preliminary experiments described in this chapter aimed to characterise the variability of the agroinfiltration method so that experiments reported in Chapter 3 could be performed in a more informed fashion. In particular, variation of Cf-9/Avr9-activated necrosis between plants, between leaves and within leaves was investigated by agroinfiltration of Avr9 into different leaves and leaf panels of different transgenic *Cf-9* tobacco plants.

2.3 MATERIALS AND METHODS

2.3.1 *Agrobacterium* culturing

Agrobacterium tumefaciens strain GV3101 was grown in YEP (liquid) for transient expression experiments in tobacco, or MinA medium (liquid and solid) for selection against *E. coli* after tri-parental mating (see appendix 2 for the composition of the media). Liquid cultures of *Agrobacterium* were grown at 27°C with shaking at approximately 200 rpm. Solid medium contained 1.5% (w/v) agar in addition to other ingredients and was also incubated at 27°C. For selection of GV3101, 50 μg/ml rifampicin and 25 μg/ml gentamycin were added to the medium, and for GV3101

containing a binary vector plasmid, tetracycline (5 μg/ml in liquid or 10 μg/ml in solid) was added to the medium (MinA- or YEP-RGT).

2.3.2 Binary vector plasmid transfer to *Agrobacterium* by tri-parental mating

The construction of the Avr9 binary plasmid used in this chapter (pCBJ243, 'Avr9') is described in Chapter 3. Binary vector plasmids were transferred to GV3101 using the tri-parental mating method, as follows. GV3101 was grown to mid-late exponential phase in MinA or YEP. *E. coli* strains containing the helper plasmid pRK2013 (50 μg/ml kanamycin) and the binary plasmid (10 μg/ml tetracycline) were each grown to stationary phase in LB containing the indicated antibiotics. One millilitre of each culture (i.e. *E. coli* containing pRK2013, *E. coli* with the binary plasmid and GV3101) was pelleted by centrifugation at 1344 x g for 4 minutes, resuspended in LB then pelleted again by centrifugation to remove residual antibiotics. *E. coli* cells were then resuspended in 1ml of LB and GV3101 cells in 0.1ml LB. Twenty microlitres of each suspension were mixed then plated onto solid LB and incubated overnight at 27°C without selection. The helper strain was omitted from one mixture as a negative control. A bacterial loop full of cells from the tri-parental mating plate was then streaked onto solid MinA medium containing 50 μg/ml rifampicin, 25 μg/ml gentamycin and 10 μg/ml tetracycline (MinA-RGT) and incubated at 27°C for 4-5 days. *Agrobacterium* colonies were then re-streaked onto solid MinA-RGT and single colonies isolated for confirmation of binary vector plasmid transfer prior to use.

2.3.3 Tobacco culture

Tobacco seeds were germinated in potting mix with approximately one-quarter volume of sand added, then after 3-4 weeks seedlings were transplanted into large pots containing potting mix and approximately one teaspoon of Osmocote® slow release fertiliser (Scotts, Ohio) per pot. Plants were used for the transient assay (described below) just prior to expansion of the inflorescence (approx. 8 weeks of age, depending upon day length) as described in the text. The glasshouse temperature range was 19-21°C overnight and 29-33°C during the day depending upon the time of year and the weather of a given day.

Assay of Avr9 activity by infiltration of Avr9 into *Cf-9* tobacco leaves ('Avr9 bioassay') was performed using the second to fourth fully expanded leaves essentially as described (Hammond-Kosack *et al.* 1998), unless stated otherwise. Wildtype tobacco was *Nicotiana tabacum* cv. Petit Gerard (cv. Petit Havana homozygous for Tobacco Mosaic Virus resistance gene *N*), *Cf-9* tobacco was a line containing cosmid 34 as described by Hammond-Kosack *et al.* (1998). The Avr9 expressing tobacco line used was line SLJ6201F, which secretes function Avr9 into the apoplast (Hammond-Kosack *et al.* 1994a). SLJ6201F IF containing Avr9 and wildtype IF lacking Avr9 were extracted according to De Wit and Spikman (1982).

2.3.4 *Agrobacterium*–mediated transient expression by agroinfiltration

For agroinfiltration experiments, GV3101 cultures containing binary vectors were each grown to early stationary phase from a glycerol stock (for no longer than 72 hours) in liquid YEP-RGT then subcultured (1:100) and grown overnight (14-16 hours) to late log phase (absorbance at 600nm {A_{600}} of 1.0 to 1.4) in YEP-RGT plus 20mM acetosyringone. Cultures that were to be compared directly were handled identically and used only if they had progressed to equal culture growth stages so as to minimise experimental variability.

The culture A_{600} was measured and the volume of culture required to give an A_{600} of 1.0 in a given resuspended volume (when resuspended in infiltration buffer) was calculated. The required volume of each culture was centrifuged in Oak-Ridge tubes at 5930 x g for 10 minutes at room temperature, the supernatant removed and bacterial pellets resuspended in sterile infiltration buffer (1 x MS salts {pH 5.6}, 3% sucrose, 10mM MES {pH 5.6}, 200μM acetosyringone). The A_{600} was rechecked to ensure that the cultures to be compared had equal density, and adjusted to equalise the A_{600} where necessary.

Approximately 30 minutes prior to infiltration, tobacco plants were watered to ensure stomata were fully open to facilitate infiltration of *Agrobacterium* suspensions into the intercellular leaf spaces. After incubation of the *Agrobacterium* suspensions for 30-60 minutes at room temperature, cultures were gently infiltrated into leaf panels of the 3-4th or 7-8th fully expanded leaf (from the base of the plant) using a needle-less 1 ml

syringe as indicated in the text. Unless otherwise indicated, the full leaf panel was filled with the *Agrobacterium* suspension.

Photographs of tobacco leaves were taken using a Canon PowerShot G1 digital camera (3.3 mega pixels) on the high-resolution setting (2048 x 1536 pixels), using automatic exposure and focus settings and the macro feature. If light was insufficient for a hand held photograph to be taken, the red-eye reduction flash mode was used to minimise reflection from the leaf cuticle. Pictures were taken at the intervals shown in the text. Seven to ten days after infiltration, leaves were removed and photographed using slide film.

2.4 RESULTS

The variability of the agroinfiltration assay was investigated by infiltrating Avr9-containing *Agrobacterium* into *Cf-9* tobacco plant leaves and examining necrosis induction. Between plant, and within plant (between leaf) and with leaf (between leaf panel) variation was investigated.

2.4.1 Within plant variation

Within plant (between leaf) variation was examined by agroinfiltrating four leaves of decreasing age (i.e. the second, third, fourth and seventh fully expanded leaves from the base of the *Cf-9* tobacco plant with an identical pattern of Avr9 and control constructs (Figure 2.1). Leaves were chosen that were oriented in different directions relative to insolation load (i.e. incoming solar radiation), to ensure that any differences in response were not attributable to microhabitat effects such as different insolation load on different parts of the leaf (Figure 2.1B).

It can be seen that the older leaves responded more slowly to Avr9 agroinfiltration than did the next youngest leaves in a gradient from the oldest to the youngest leaves (Figure 2.1A). At the endpoint of the experiment (8 days, 192 hours post infiltration {hpi}), there was only a clear difference between leaf 2 and the other leaves, since the remainder progressed to essentially full necrosis. No necrosis was observed when Avr9 (Figure 2.1C) or empty vector (Figure 2.1D) containing *Agrobacterium* was infiltrated into leaf panels of wild type tobacco. Also, the youngest leaf used (the 7th fully

expanded leaf from the base) developed a dark grey initial necrosis (upon collapse of the tissue) and progressed to full necrosis more rapidly than other leaves in response to Avr9, whereas other leaves developed a light, flat khaki green necrosis (Figure 2.1A, compare leaf panels 2-4 with 7).

It should be noted that this experiment was performed in this specific format on only one occasion. As such, the relative differences between leaves should be considered a preliminary result. However, in six subsequent experiments in which multiple aged leaves on the same plant were infiltrated with Avr9 containing *Agrobacterium* (two leaves compared on four occasions, three on one occasion and four on another) a weaker response to Avr9 in older leaves was always observed (data not shown).

From this experiment, it is not clear whether this difference in sensitivity of leaves of different ages is due to the properties of the expression system (agroinfiltration) or the biological response (Cf-9/Avr9 mediated necrosis). It has previously been reported that Cf-9 is developmentally regulated in tobacco, with no response to infiltrated Avr9 peptide by seedlings of four leaves or less, a weak to moderate response at the five leaf stage and a normal response at the eight leaf stage (Hammond-Kosack *et al.* 1998). However, the sensitivity of different leaves of the same mature plant to Avr9 peptide has not been reported.

To test whether the gradient of responsiveness to agroinfiltrated Avr9 (above) is a result of the properties of the Cf-9/Avr9 activated resistance response or the expression system, the intercellular fluid (IF) of tobacco expressing Avr9 (which contains Avr9 peptide, see Materials and Methods) was injected into a range of leaves on a mature *Cf-9* tobacco plant (Figure 2.2) equivalent to those shown in Figure 2.1 (see figure legend). Images shown are of leaves illuminated by short wave ultraviolet radiation, which causes fluorescence of phenolic compounds produced during the defence reaction, as a convenient method to image leaves after a necrotic resistance response (Tang *et al.* 1996). The sensitivity of *Cf-9* tobacco leaves to Avr9 peptide shows the opposite pattern to agroinfiltration of Avr9: older leaves were much more sensitive to infiltrated Avr9 peptide than younger leaves (Figure 2.2). The oldest leaf (leaf 2) responded with full necrosis of the infiltrated leaf panel, whereas leaf 4 responded with some necrosis outside the infiltration site and leaf 7 only had necrosis at the infiltration sites and some mild fluorescence corresponding to chlorosis. Infiltration of wildtype (control) IF

caused no response in *Cf-9* or wildtype tobacco leaves (other than some damage at the site of infiltration resulting from the syringe used for infiltration) and similarly no reaction was observed in wildtype tobacco to Avr9 IF (leaf 4). Note that the exposure is increased (increasing from leaf 2-7) to aid the visualisation of necrosis (see Eppendorf tube autofluorescence).

The same trend was observed when multiple leaves of different ages on one plant (but not the same leaves as the above experiment) were infiltrated in the same way (data not shown), however this experiment was only performed on this one additional occasion, so these results should be considered preliminary. If these results (Figure 2.1 and 2.2) are real, this suggests that the increasing sensitivity of younger *Cf-9* tobacco leaves to agroinfiltrated Avr9 is due to properties of the agroinfiltration assay system rather than the Cf-9/Avr9 interaction itself.

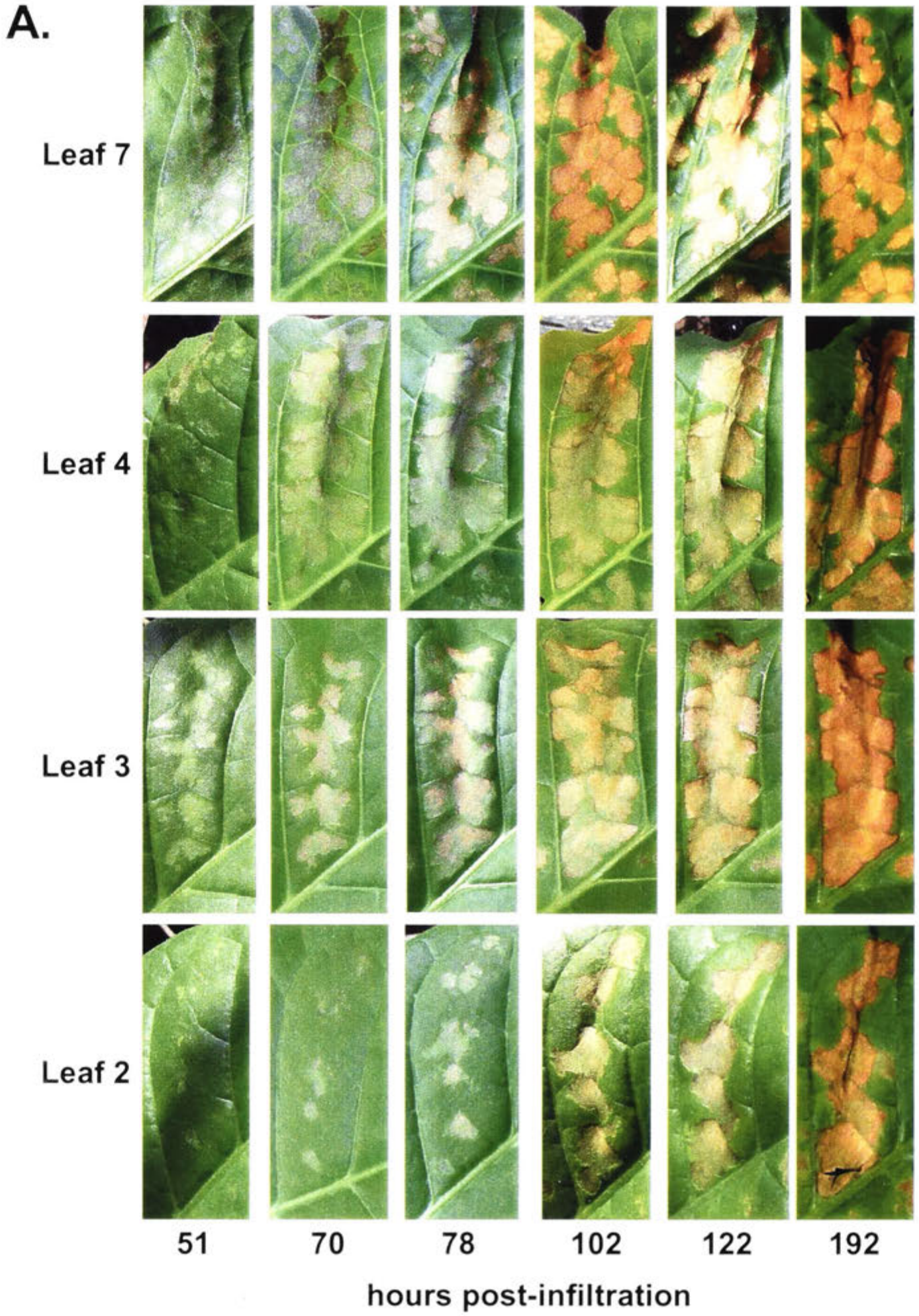

Figure 2.1. Between leaf variation of Cf-9/Avr9 dependent necrosis using *Agrobacterium*-mediated transient expression of Avr9 in *Cf-9 N. tabacum* leaves. **A.** The same *Agrobacterium* suspension containing Avr9 was infiltrated into equivalent leaf panels of four Cf-9 tobacco leaves of different ages (from oldest to youngest leaves: the second, third, fourth and seventh fully expanded leaf from the base of the plant, respectively). Individual leaf panels are shown at intervals after infiltration (hours post-infiltration, hpi). **B.** The plant corresponding to A., with leaf numbers indicated. A diagram indicating the direction each leaf was facing (N = north and S = south) is shown on the right. **C.** and **D.** Wild type *N. tabacum* leaf panels infiltrated with Avr9 (C.) and empty vector (D.) containing *Agrobacterium*. Intervals after infiltration are shown (hpi and days post-infiltration {dpi}). For C., no necrosis was observed after 8 days (not shown).

B.

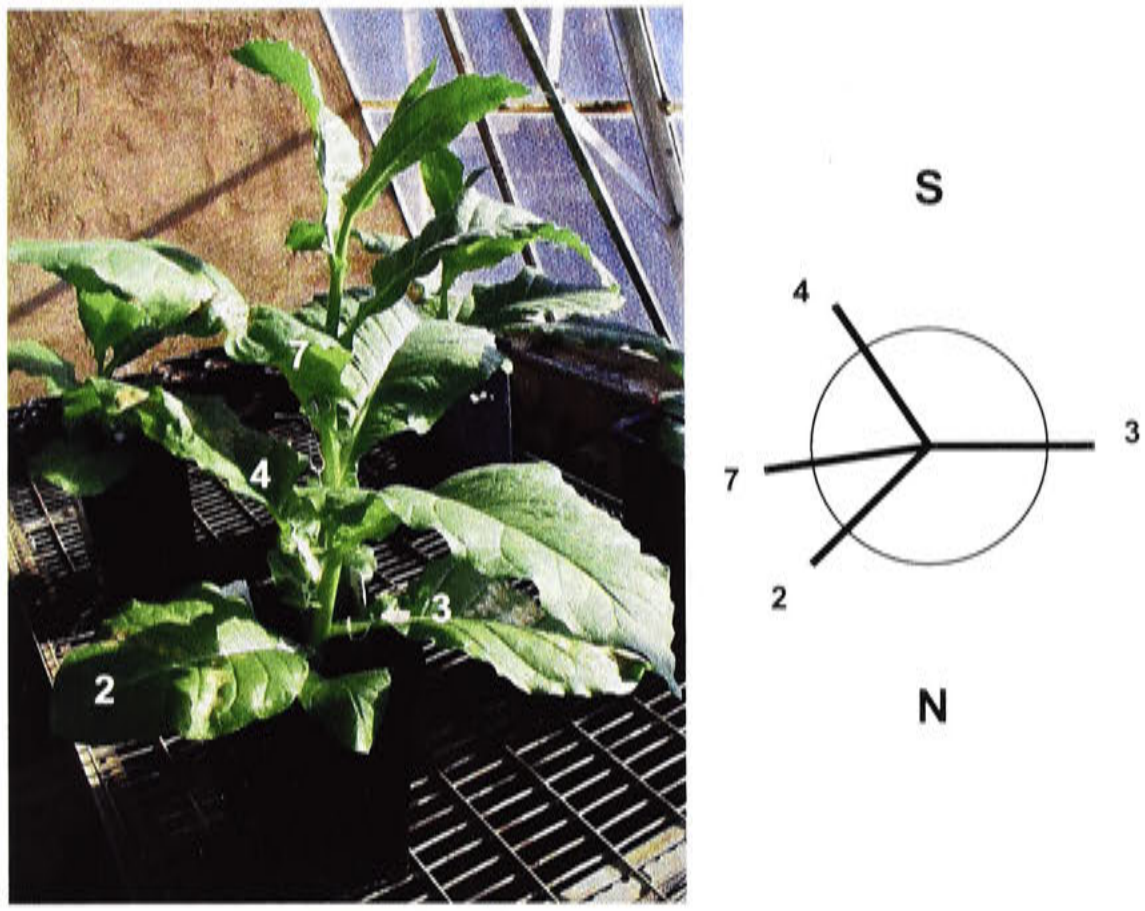

C.

51 70 78

hours post-infiltration

D.

9 dpi

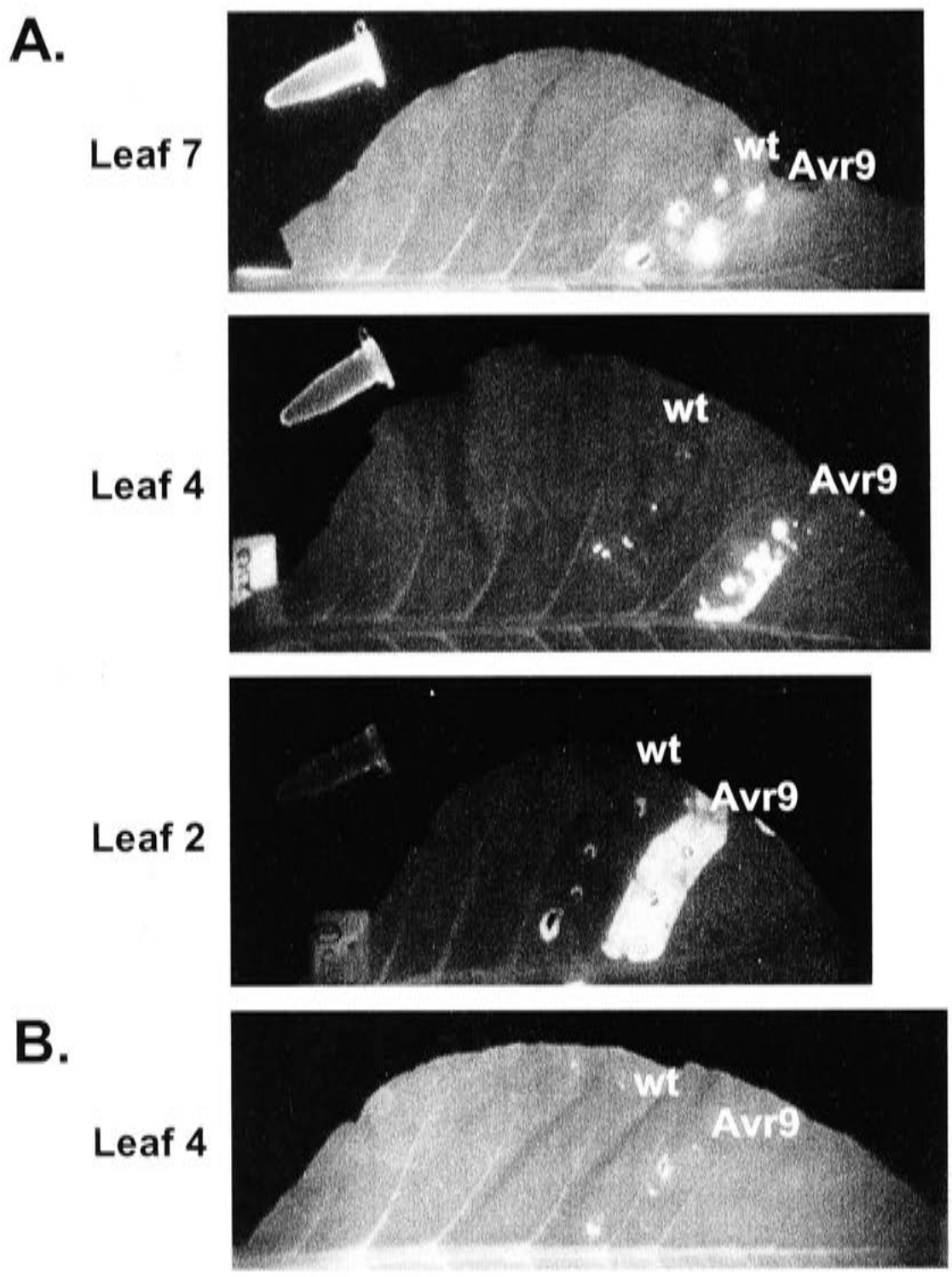

Figure 2.2. Between leaf variation of Cf-9/Avr9 dependent necrosis. Intercellular fluids (IF) from **Avr9** or wild type control (**wt**) tobacco plants were infiltrated into *Cf-9* tobacco leaves (**A.** the second, fourth and seventh fully expanded leaves from the base respectively) or wildtype leaves (**B.** the fourth fully expanded leaf) of different ages. Leaves are shown at 7 days post-infiltration, under ultra-violet illumination. An Eppendorf tube is included as a fluorescence control in A. Images are under the same magnification but with different aperture to prevent overexposure (see text).

2.4.2 Between plant variation

While agroinfiltrating Avr9 and related constructs into *Cf-9* tobacco, it was observed that there was a distinct developmental stage at which the third and fourth fully expanded leaves would no longer develop necrosis in response to Avr9 agroinfiltration. This transition appeared to occur concomitantly with the expansion of the immature inflorescence and opening of the flower buds (over approximately 1 week under the conditions used here).

This transition, and consequently between plant variation of agroinfiltration, was fortuitously demonstrated when identical agroinfiltration experiments were performed on *Cf-9* tobacco plants of identical age that had grown to slightly different developmental stages (Figure 2.3). The unexpanded (Figure 2.3A) and expanded (Figure 2.3B) inflorescences of the two plants are shown in the upper panels and comparable leaf panels agroinfiltrated with Avr9 are shown below. The second fully expanded leaf on plant A responded only weakly to Avr9, while the third leaf responded strongly. At the same time point on plant B however, the second fully expanded leaf did not respond at all (and did not respond even after 15 days, not shown), while the fourth fully expanded leaf responded only weakly after 79 hpi. As shown in the previous section, the fourth fully expanded leaf should respond more strongly than the third, yet this leaf still did not respond as strongly as the third leaf from plant A. This demonstrates the considerable change in the sensitivity of *Cf-9* tobacco plants to Avr9 expressed by agroinfiltration during the developmental transition of the plant to flowering.

As this transition to flowering is very rapid, this experiment was not able to be repeated precisely in the way it is described here. However, there was complete correlation (by visual observation) between the stage of progression of flowering (1 - pre-flowering {with immature inflorescence and flower buds present}; 2 - the transition to flowering {the inflorescence was expanding and flowers beginning to open}; and 3 - flowering {an expanded inflorescence and mature flowers were present}) and reducing activity of agroinfiltrated Avr9. In particular, when Avr9 was agroinfiltrated into equivalent leaves on different plants, high activity was observed in leaves of stage 1 plants on two occasions, decreased activity in stage 2 plants on three occasions, and further decreased activity in stage 3 leaves on more than three occasions (data not shown). This variation

was also consistent with the between leaf (within plant) variation described in Section 2.4.1, with older leaves being less responsive to agroinfiltrated Avr9. Equivalent results were observed when Avr9 variant constructs (in Chapter 3) were infiltrated into Cf-9 tobacco leaves (data not shown).

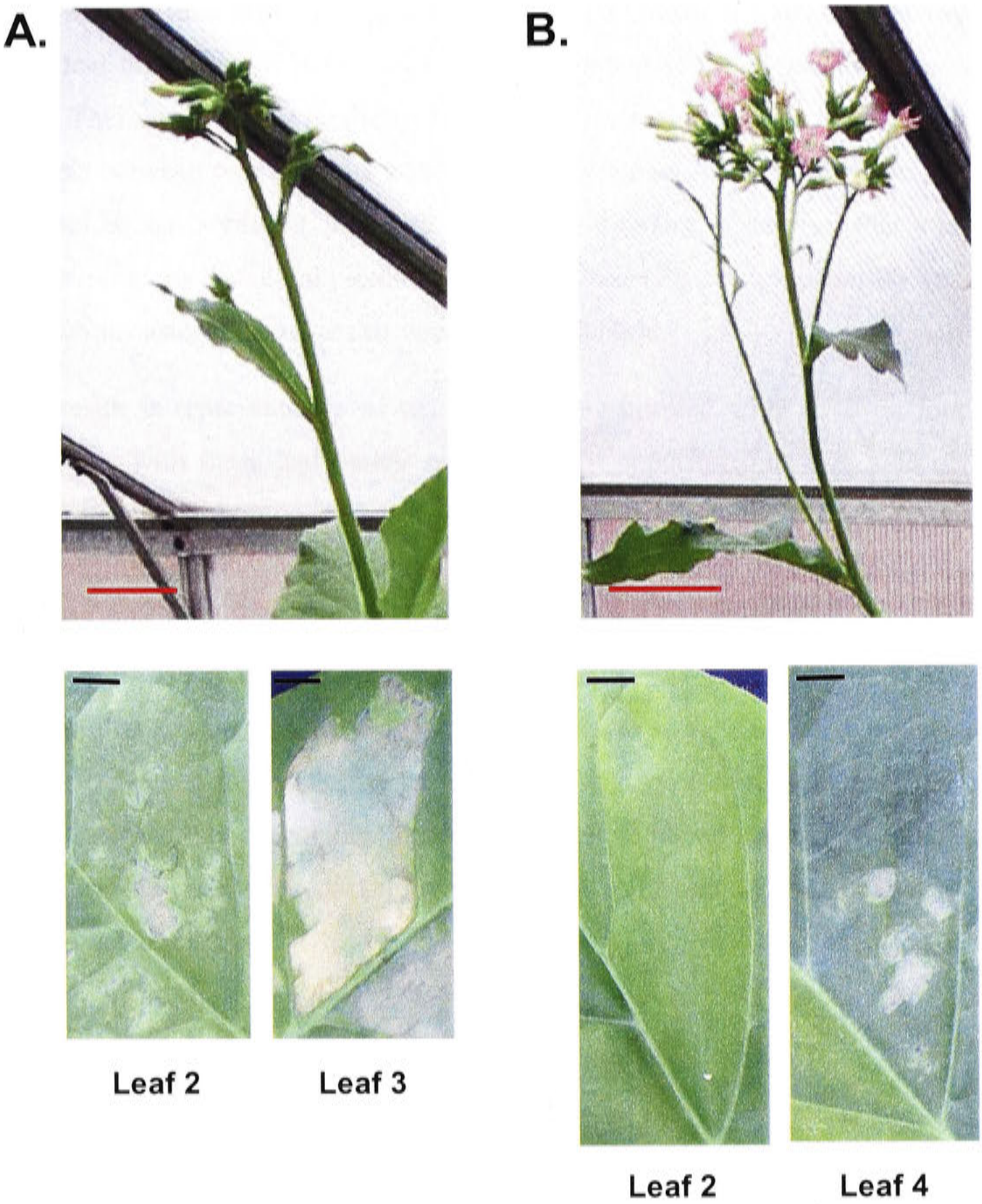

Figure 2.3. Between plant variation of agroinfiltration in *N. tabacum*. *Agrobacterium* containing Avr9 (diluted 50%) was infiltrated into leaf panels of equivalent leaves of two *Cf-9* tobacco plants at different developmental stages, but of identical ages (**A.** and **B.**). Leaf 2 is the second fully expanded leaf from the base of plant A, leaf 3 is the third, and leaf 4 the fourth. Only the half of the leaf panel next to the mid-vein was infiltrated for leaf 4 in B., while other leaf panels were fully infiltrated. Leaf panels are shown 79 hpi and inflorescences are shown at 93 hpi. The black scale bar is 1 cm and the red scale bar is 10 cm.

2.4.3 Within leaf variation

Another potential source of variation in the necrotic response to transiently expressed Avr9 was between different leaf panels. Figure 2.4 shows different leaf panels from the same leaf that were infiltrated with the same preparation of *Agrobacterium* containing Avr9. There was little or no difference between timing of the development of leaf panel necrosis between two opposite and diagonally adjacent leaf panels (panel A compared to panel B). Interestingly, the slight difference in timing of necrosis that was observed between regions distal and proximal to the leaf vein (Figure 2.4, panel B) was observed on other occasions, however this was not reproducible.

This result is representative of ten leaves agroinfiltrated with Avr9 on four separate occasions, with these leaf panels either directly opposite (on either side of the main vein) or diagonally opposite by one leaf panel, as in Figure 2.4. Eight of these leaves showed little or no difference in the timing or extent of necrosis (similar to the figure), whereas two of these leaves had a slight difference in the timing but not extent of necrosis. Equivalent results were observed when Avr9 variant constructs (in Chapter 3) were infiltrated into Cf-9 tobacco leaves (data not shown). These data indicate that little or no difference in the timing or extent of Cf-9/Avr9 dependent necrosis occurs in directly adjacent or diagonally opposite (by one leaf panel) leaf panels, and in turn, that these leaf panels are comparable when using agroinfiltration experiments to study the Cf-9/Avr9 interaction.

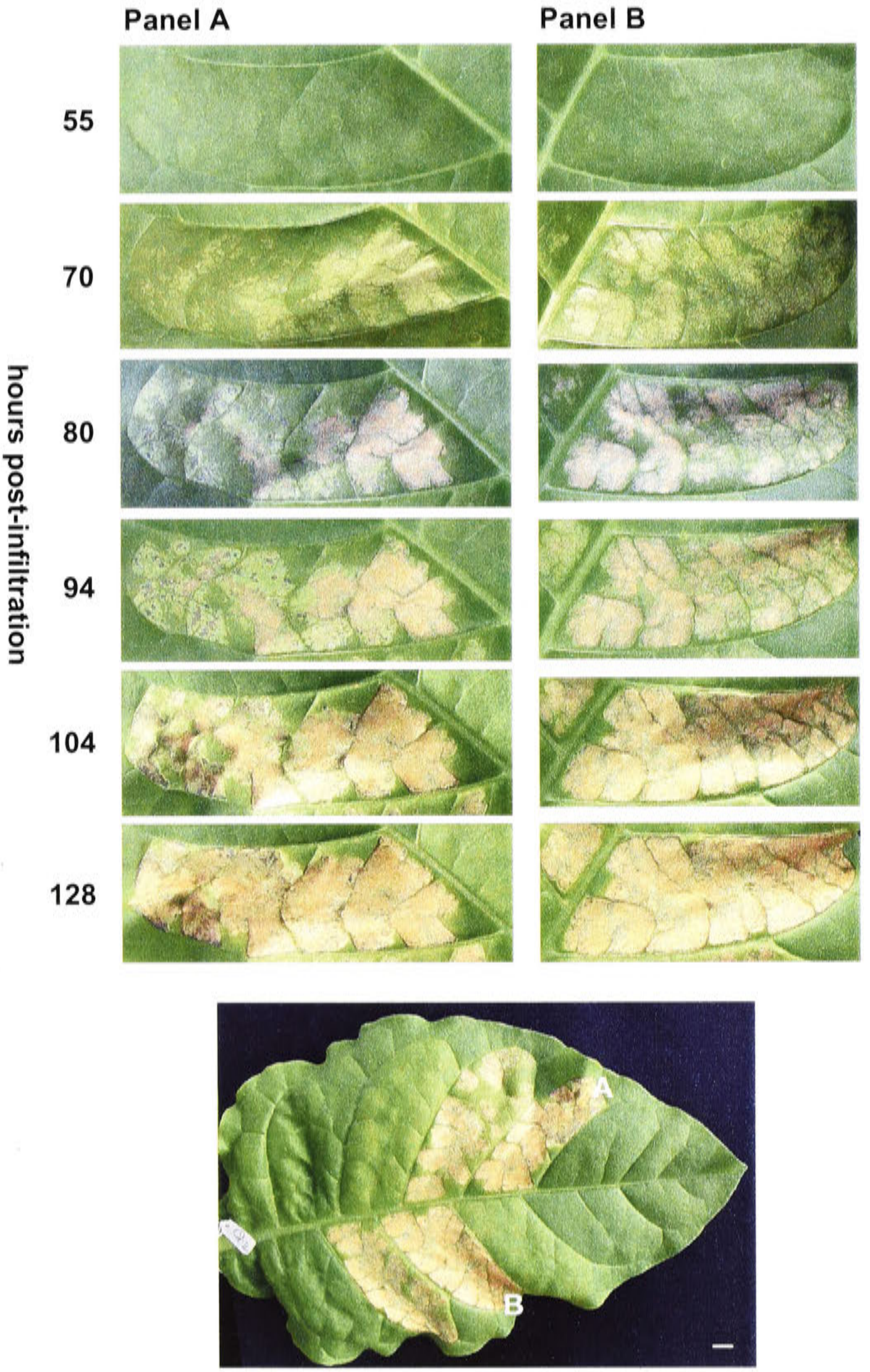

Figure 2.4. Within leaf variation of agroinfiltration in *N. tabacum*. *Agrobacterium* cultures containing Avr9 were infiltrated into different panels (A and B) of the same leaf (whole leaf shown at 128 hpi) of a *Cf-9* tobacco plant, and are shown at a range of intervals after infiltration. Other panels were for an unrelated experiment. The white scale bar is 1 cm.

2.5 DISCUSSION

2.5.1 Variability of the agroinfiltration transient expression system

Agrobacterium-mediated transient expression (agroinfiltration) has previously been utilised for a variety of studies, having been particularly useful for the study of the Cf-9/Avr9 gene-for-gene system (Thomas *et al.* 2000; Van der Hoorn *et al.* 2000; Van der Hoorn *et al.* 2001a). Since this system is relatively new, and since little characterisation of the variability of this method has been published, preliminary investigation of the variability of this method and its suitability for the research presented in Chapter 3 was undertaken.

Potential sources of variation considered in the Cf-9/Avr9 mediated resistance response following agroinfiltration were within leaf, between leaf and between plant variation. When an Avr9 construct was agroinfiltrated into leaves of a range of ages for a single *Cf-9* tobacco plant, a gradient of increasing activity of agroinfiltrated Avr9 was observed from older to younger leaves (Figure 2.1). As most leaf panels in this experiment proceeded to full necrosis, the conclusion is based on the speed at which the different leaves developed necrosis in response to the same suspension of *Agrobacterium* containing an Avr9 construct. This rationale is supported by the fact that the oldest leaf showed a delay in necrosis in response to agroinfiltration with Avr9 as well as ultimately incomplete necrosis (Figure 2.1A). Although this experiment was performed formally only once, these data and the anecdotal evidence presented strongly suggests that this phenomenon is real. However, this experiment would need to be repeated more formally to more clearly characterise this phenomenon.

To determine whether the gradient of activity using the agroinfiltration assay arises from properties of the Cf-9/Avr9 interaction or the agroinfiltration assay system, an equivalent age range *Cf-9* tobacco leaves was infiltrated with IF from transgenic Avr9 tobacco. Contrary to what was observed using agroinfiltration, older leaves were more sensitive to Avr9 peptide, a result not previously reported (Figure 2.4). As this experiment was only repeated on one occasion, these data should only currently be interpreted as indicative of a trend in sensitivity to Avr9 peptide, rather than in any quantitative sense.

Therefore, the gradient of increasing sensitivity of younger leaves to Avr9 agroinfiltration appears to be a product of the agroinfiltration assay system itself. Moreover, this gradient must be steeper than is apparent from the agroinfiltration experiment alone, since it opposes the gradient of *decreasing* sensitivity of younger leaves to Avr9 peptide.

The reason for this agroinfiltration activity gradient is not clear, although two possibilities are apparent. Firstly, this gradient of activity could be a result of developmental regulation of a factor needed for efficient transformation of plant cells. It is known that T-DNA transfer into plant cells is a rate limiting step for *Agrobacterium*-mediated transformation (De Buck *et al.* 2000) and many host factors are necessary for efficient T-DNA transfer (Gelvin 2003; Tzfira and Citovsky 2002; Zambre *et al.* 2003), some of which may be developmentally regulated. Secondly, leaf tissue age-dependent activity of the CaMV35S promoter or protein expression levels could cause reduced transcription in older tissues, although no evidence is apparent to clearly support this possibility.

One approach to test the first possibility could be to introduce the same construct into different tissue types using a different transient expression system, such as microprojectile bombardment. Using this particular method, a marker that can be quantified at low levels, such as the luciferase or GUS (e.g. see Leister *et al.* 1996), would be necessary since only a few cells are typically transformed. If activity did not correlate with tissue type in the same way as the agroinfiltration activity gradient, this would suggest that the ability of *Agrobacterium* to transform cells causes this gradient. Additionally, the CaMV35S promoter could be used to express a marker protein in stable transformants. If a gradient of activity in different aged leaves correlated with the gradient observed using agroinfiltration, this would suggest that promoter activity determines this gradient. Further experiments may be necessary in addition to these to completely resolve this issue, depending upon the results obtained from these suggested experiments.

Since the leaves were arranged at different angles relative to insolation during this experiment (Figure 2.1) it can be concluded that positional effects had little influence on the development of necrosis, although further experimentation would be needed to suggest that there was no effect at all. One possible minor factor could be light intensity,

which may influence the speed of necrosis development through variation in photo-oxidative stress levels.

Variation was also observed between plants, particularly a sharp reduction in the activity of Avr9 by agroinfiltration into *Cf-9* tobacco leaves at the transition to flowering (Figure 2.3; see also comments in associated text). Since *Cf-9* tobacco is more sensitive to infiltrated Avr9 peptide after flowering (unpublished observation), this transition is again probably attributable to the agroinfiltration assay, and may be related to the decreasing activity in older leaves observed in this work (above). It seems probable that the substantial physiological change associated with the transition to flowering could also affect plant factors necessary for efficient transfer of the T-DNA by *Agrobacterium* and/or affect the level of expression driven by the CaMV35S promoter.

Within leaf variation of the activity of Avr9 agroinfiltration was found to be negligible between opposite or diagonally opposite leaf panels, such that these leaf panels could be directly compared with regard to the speed and ultimate extent of necrosis development (Figure 2.4). While these experiments were intended to demonstrate only that opposite and diagonally opposite leaf panels could be compared, it would have been interesting to also determine whether there was a detectable difference between panels distal and proximal to the leaf axil. On two occasions where distant leaf panels on the same leaf were agroinfiltrated with Avr9 (for an unrelated experiment), it appeared that leaf panels distal to the axil were slightly less sensitive to Avr9 agroinfiltration than proximal leaf panels (not shown). However these experiments were not performed to test this possibility, so were not controlled or repeated for this purpose. This could be tested by infiltrating the same *Agrobacterium* suspension containing Avr9 into several (or all) leaf panels from the tip of the leaf to the base on both sides of the leaf. To increase the chance that a differential response is observed over the leaf, two concentrations of Avr9 *Agrobacterium* could be used (e.g. alternating leaf panels infiltrated with cultures at an A_{600} of 0.5 and 0.25).

2.5.2 General comments and further work

Agroinfiltration is certainly a useful tool for rapid analysis of gene constructs in plants, however as the work described here shows, some inherent variability of the assay exists. This variability clearly needs to be accounted for in order to make valid comparisons of

plant responses to infiltrated constructs, and to ensure that sound and objective conclusions can be reached. Due to the considerable variability between leaves and plants, but not within leaves, comparison of multiple constructs within leaves is an ideal approach. Although these sources of variability do not appear to have been discussed in the literature, the fact that agroinfiltration is usually performed in this comparative way on single leaves, especially with the Cf/Avr gene-for-gene systems (Thomas *et al.* 2000; Van der Hoorn *et al.* 2000; see also the introduction to this chapter) suggests that this fact is well recognised.

Therefore, to account for the identified forms of variability in the work described in Chapter 3, pairwise comparisons between control and experimental constructs were made on single leaves, using comparable leaf panels, with repetition on multiple leaves of multiple plants on multiple occasions to ensure reproducibility. One possibly useful implication of this variability, and the consequent need for a pairwise/single leaf experimental design, is that the absolute dosage of *Agrobacterium* is not critical. As long as the *Agrobacterium* dosage of the constructs to be compared on each leaf is identical, the relative development of necrosis between two expressed Avr9 variants can be meaningfully compared. This could potentially be exploited to expand experimental flexibility using this method, perhaps improving throughput by using multiple comparisons or dilutions of each construct on a single leaf, or allowing novel quantitative and statistical analyses of within leaf comparisons.

A further systematic characterisation of this increasingly popular method and its inherent variability would be of clear value to the plant biology and plant genomics research community. One method to do this, in addition to specific suggestions provided in the text above, would be using a well-characterised reporter gene system such as GFP or GUS. This system could be used in a high-throughput manner in 96 well plates, using either anti-GFP antibodies for ELISA (such as those described in Chapter 6 of this thesis) or a substrate fluorescence assay for GUS (Jefferson 1987), for example as used by Hammond-Kosack *et al.* (1994b). Adequate sampling to quantify the sources of variability of this method would be easily achieved and time series experiments would be possible by sampling discs from a leaf panel of interest at each time point.

CHAPTER 3

CAN Cf-9 DETECT AVR9 IN THE ER?

3.1 SUMMARY

KNOWLEDGE of the subcellular location of R proteins is central to an understanding of their function at the cellular level. The discovery of the dilysine motif at the C-terminus of Cf-9 (Jones *et al.* 1994) suggested that this protein might be functional in the endoplasmic reticulum (ER). However, recent studies have produced apparently conflicting results on the subcellular localisation of the Cf-9 protein, suggesting either ER (Benghezal *et al.* 2000) or plasma membrane (PM) localisation (Piedras *et al.* 2000). The research outlined in this chapter aimed to examine this problem using a functional approach; specifically by asking whether Cf-9 can detect Avr9 in the ER. To do this, agroinfiltration was used to compare the Cf-9 mediated response to variants of Avr9 with the 'KDEL' C-terminal ER retention motif or control modifications.

Cf-9 mediated necrosis in response to Avr9-KDEL was delayed when compared to unmodified Avr9. Mutation of this motif to KDDL (a non-retrieved tag, but chemically almost identical to KDEL) abolished this delay, suggesting that retention of the peptide in the ER caused the delay. An S5A mutant of Avr9-KDEL (which destroys the single *N*-glycosylation site while retaining activity) still showed a delay compared to Avr9-S5A, ruling out a role for differential carbohydrate processing in this delay. Dilution series comparisons between Avr9-KDEL and other variants suggested that the KDEL tag reduces activity of Avr9, however no evidence was found to indicate that any portion of the KDEL mediated delay was caused by this reduced activity. Dilution series comparison of Avr9 with Avr9-S5A detected reduced activity of Avr9-S5A, as previously shown using a bioassay (Kooman-Gersmann *et al.* 1997). A slightly delayed necrotic response to Avr9-S5A was sometimes apparent, but this was not clear or reproducible. Quantitative analysis of the temporal development of necrosis was performed on the comparison between Avr9 and Avr9-KDEL, which corroborated the visual observation of the differential response and suggested a delay of approximately

25 hours. Models to explain these results and their implications for Cf-9 function are discussed.

3.2 INTRODUCTION

To further investigate the localisation of functional Cf-9, this project aimed to test whether Cf-9 can respond to Avr9 from the endoplasmic reticulum (ER) by localising Avr9 to the ER. The approach used to achieve this was fusion of a C-terminal ER retention motif, KDEL (single letter amino-acid code), to Avr9 and analysing the Cf-9 dependent response to Avr9-KDEL. Transient expression of constructs was performed using agroinfiltration, as described in the previous chapter. Therefore, as a background to this work, the retention of soluble proteins in the ER by the KDEL/HDEL retrieval system and examples of its experimental manipulation will be considered in detail.

3.2.1 Retrieval and retention of soluble proteins in the lumen of the endoplasmic reticulum

HDEL, KDEL and related motifs

There has been much interest in the mechanisms used by eukaryotic cells to simultaneously secrete an array of proteins while maintaining the proteins necessary for secretory pathway function in the appropriate subcellular compartments. The KDEL and HDEL motifs at the absolute C-terminus were first identified as ER localisation signals, in mammalian and yeast cells respectively, after examination of the primary sequence of several soluble ER resident proteins (Pelham 1989; Pelham 1990). While mammals and yeast have a preference for which signal they use, plants appear to readily use either, depending upon the ER resident protein in question (Hadlington and Denecke 2000).

A number of variants of this signal have been observed (Pelham 1990), and studies on modified signals have found a number of functional, though not necessarily naturally occurring, ER retrieval signals (Andres *et al.* 1990; Andres *et al.* 1991; Denecke *et al.* 1993; Haugejorden *et al.* 1991). The most comprehensive analysis of sorting signals for soluble proteins in plant cells was performed by Denecke *et al.* (1992; 1993) using marker enzymes tagged with the various putative ER retrieval signals in a tobacco cell system. These studies found that tagging with KDEL, HDEL or RDEL resulted in ER

localisation of the marker enzyme, SDEL and KEEL gave only a small amount of retention, and the remaining (KDDL, KDEI and KDEV) resulted in no observable retention of the marker enzyme.

More recently, the H/KDEL variant peptide HDEF was found at the C-terminus of tomato RNase LX and shown to be a functional ER retrieval signal in yeast and plants (Kaletta *et al.* 1998; Lehmann *et al.* 2001). Other variants of the H/KDEL motif have been observed at the C-terminus of predicted barley (HTDEL) and rice (KDEM) cysteine proteases (Chrispeels and Herman 2000; Schmid *et al.* 1999), although no direct functional studies of these proteins have been reported to date.

A number of soluble ER resident proteins in plants have been found to utilise the H/KDEL mediated ER retrieval system, including calreticulin, endoplasmin, protein disulfide isomerase and luminal binding protein (BiP): (Alvim *et al.* 2001; Crofts and Denecke 1998; Denecke 1996; Hadlington and Denecke 2000; Vitale and Denecke 1999). These 'reticuloplasmins' are involved in a range of activities, including disulphide bond formation, chaperone activity to facilitate protein folding, carbohydrate synthesis, glycosylation of glycoproteins and facilitation of stress responses (e.g. Crofts *et al.* 1998; Ellgaard *et al.* 1999; Leborgne-Castel *et al.* 1999; Lerouge *et al.* 1998).

The Auxin-Binding Protein 1 (ABP1), first isolated from maize, was also observed to possess a C-terminal KDEL sequence (Hesse *et al.* 1989; Inohara *et al.* 1989; Tillmann *et al.* 1989). It is intriguing that, while this motif suggests that ABP1 is an ER resident protein, available evidence suggests that it functions from the plasma membrane (see Chapter 7).

The KDEL retrieval system is also utilised by some plant papain-type cysteine proteases in senescing plant tissues. In castor bean (*Ricinus communis*) cotyledons, the cysteine endoprotease proCysEP, which has a C-terminal KDEL sequence, accumulates in ER derived structures known as ricinosomes (Schmid *et al.* 2001). Late during programmed cell death in the senescing cotyledons (Schmid *et al.* 1999), the slightly active pre-pro form of the protease is processed to remove the N-terminal propeptide and C-terminal KDEL motif, substantially increasing its activity (Schmid *et al.* 1998; Schmid *et al.* 2001).

Similarly, a cysteine protease from broad bean cotyledons with a C-terminal KDEL motif (SH-EP) accumulates in an ER derived vesicle (termed 'KV' for KDEL-tailed

cysteine proteinase-accumulating vesicle), and is then released *en masse* to protein storage vacuoles (Toyooka *et al.* 2000). The C-terminus of proSH-EP is cleaved immediately prior to or after leaving the ER, and after progressing toward the protein storage vacuole it is further processed to its active state (Okamoto *et al.* 1999). The authors propose that this is an example of KDEL mediated ER retention serving to regulate the delivery of a protein to its functional site, rather than just maintaining the protein composition of the ER.

Interestingly, the ricinosomes and KV appear to be a generally occurring organelle termed the 'Precursor Protease Vesicles' (Chrispeels and Herman 2000), which is derived from the ER and acts as a storage compartment or for ER to vacuole trafficking.

HDEL/KDEL mediated ER retrieval

The receptor that was predicted to retrieve HDEL bearing proteins from a post-ER compartment back to the ER was identified using a genetic screen in yeast (Hardwick *et al.* 1990; Munro and Pelham 1987; Pelham 1990; Semenza *et al.* 1990). The gene product of one of these ER Retention Defective (ERD) mutants of yeast, ERD2, was clearly shown to be the receptor that retains HDEL bearing luminal proteins in yeast cells (Lewis *et al.* 1990; Pelham 1990; Semenza *et al.* 1990).

ERD2 is a multi-pass transmembrane protein that is a resident of the Golgi apparatus and the ER/Golgi intermediate compartment (ERGIC) (Griffiths *et al.* 1994) and functions by transporting H/KDEL bearing proteins from the Golgi apparatus back to the ER (Lewis and Pelham 1992; Townsley *et al.* 1993). Although ERD2 is present mostly in the *cis*-Golgi network (Griffiths *et al.* 1994), the capacity of this receptor to retrieve H/KDEL bearing proteins extends at least to the *trans*-Golgi network (Miesenbock and Rothman 1995).

The *A. thaliana* ERD2 gene was later isolated and shown to be a functional homologue of the yeast ERD2 gene by complementation of the yeast mutant phenotype (Lee *et al.* 1993). Although it has not been directly demonstrated experimentally in plant cells, it is likely that AtERD2 functions as the H/KDEL receptor in *A. thaliana* (Hadlington and Denecke 2000). The main evidence supporting this is that an AtERD2-GFP fusion protein is localised to the Golgi apparatus in plants and is redistributed to the ER when cells are treated with the fungal metabolite brefeldin A (Boevink *et al.* 1998). A family

of sequences related to ERD2 has been observed in *A. thaliana* (Hadlington and Denecke 2000), although no function is yet known for these predicted proteins.

Other studies of ER retention appear to indicate that mechanisms other than ERD2 mediated retrieval from a post-ER compartment may also contribute to efficient retention of some H/KDEL bearing ER resident proteins (Hammond and Helenius 1995; Pagny *et al.* 1999). In particular, a network of ER resident chaperones including BiP, calreticulin and calnexin has been suggested to aid ER retention (as distinct from retrieval) of many ER residents in mammalian cells (Tatu and Helenius 1997). The fact that BiP and calreticulin are in a complex in plant cells (Crofts *et al.* 1998) is consistent with the existence of this network, but relatively little other evidence for this phenomenon is available for plant systems. One possibility is that ER retention of luminal proteins by incorporation into such a network may be complemented by the H/KDEL retrieval mechanism, which would act to retrieve any ER resident proteins that escape this network (Pagny *et al.* 1999; Tatu and Helenius 1997).

Experimental use of the H/KDEL retrieval mechanism

Of the mechanisms that retain or retrieve secretory proteins in the ER, fusion of a HDEL or KDEL sequence at the C-terminus is the most common approach used to retain heterologous proteins in the ER (e.g. see Pelham 2000). The earliest example of ER retention of a heterologous protein in plant cells was using a KDEL tagged variant of phytohemagglutinin (PHA), a vacuolar protein of the common bean (*Phaseolus vulgaris*, Herman *et al.* 1990). A substantial portion of PHA-KDEL was localised to the ER and nuclear envelope, judged by analysis of carbohydrate forms on the protein and immunocytochemistry, although some escaped retention and progressed to the protein storage vacuole.

Interestingly, a study of the sweet potato root vacuolar storage protein sporamin tagged with HDEL found that the retrieval signal may itself direct proteins that have escaped ER retention to the vacuole, possibly as a quality control mechanism (Gomord *et al.* 1997). This latter study accounted for the possibility that vacuolar targeting may have been the result of native vacuole targeting signals within the protein by deleting the sporamin vacuolar targeting signal. It will be interesting to see whether a clear demonstration of the biological significance of this intriguing phenomenon is reported.

In addition to vacuolar proteins, proteins that are normally secreted (carrot cell wall invertase {Pagny *et al.* 2000}; barley α-amylase {Crofts *et al.* 1999}), and non-secretory proteins (phosphinothricin acetyl transferase {PAT} and neomycin phosphotransferase II, {Denecke *et al.* 1990; Denecke *et al.* 1992}) have also been tagged with H/KDEL or related sequences to study ER retention mechanisms.

When PAT with an N-terminal signal peptide sequence is expressed in tobacco cells it is secreted (Denecke *et al.* 1990). However, when this secreted PAT is tagged at the C-terminus with the HDEL or KDEL motif, the enzyme is prevented from being secreted and accumulates in the ER lumen (Denecke *et al.* 1992). The fact that the non-secretory protein PAT is secreted from cells when translocated into the ER supports the 'bulk flow' model of protein secretion, whereby proteins not actively retained in the ER passively depart by default (Denecke *et al.* 1990). There has been some debate about whether this model or the alternative 'active transport' model (whereby signals for ER export are needed for a protein to be able to leave the ER) best explains the secretion of proteins from eukaryotic cells (Crofts *et al.* 1999; Hong 1998; Phillipson *et al.* 2001; Vitale and Denecke 1999).

Saturation of H/KDEL mediated ER retrieval

It has been noted that it is relatively easy to saturate the HDEL retrieval system in yeast cells (Pelham *et al.* 1988; Pelham 1990; Semenza *et al.* 1990). In mammalian cells retrieval appears to be very efficient for KDEL, so saturation of retrieval does not occur readily (Munro and Pelham 1987; Pelham 2000), while retrieval of HDEL is inefficient or absent in mammalian cells (Pelham *et al.* 1988).

In plants, incomplete ER retention of H/KDEL bearing proteins has been noted on a number of occasions, particularly for heterologous proteins tagged with such motifs. It is important to distinguish between lack of retention and saturation of the retrieval mechanism. In some cases, lack of retention of a heterologously tagged H/KDEL protein could be the result of saturation of the retention mechanism, or alternatively could also be the result of inefficient or ineffective retention of the protein due to an inhibitory sequence context for function of the C-terminal motif. For example, studies have shown that KDEL (Herman *et al.* 1990) or HDEL (Pueyo *et al.* 1995) is not always sufficient for full retention of vacuolar proteins in the ER, allowing some passage of the tagged vacuolar proteins to the vacuoles. It is possible that these results could be

explained by conflicting export signals that direct the protein to the vacuole. These two phenomena (incomplete retention and conflicting export signals) have previously been noted in a range of different contexts (Denecke *et al.* 1992; Munro and Pelham 1987; Pelham *et al.* 1988; Pelham 2000; Phillipson *et al.* 2001; Vitale and Denecke 1999; Zagouras and Rose 1989).

Conversely, a lack of secretion of the H/KDEL protein of interest does not necessarily indicate that no saturation of ER retrieval has occurred. In an early study, transgenic lines expressing up to approximately 1% of total leaf protein as PAT-KDEL and PAT-HDEL were generated to test for the possibility of ER retrieval saturation (Denecke *et al.* 1992). Despite this considerable overexpression, no significant secretion of these proteins from derived protoplasts could be detected after 30 hours (although it is difficult to know how sensitive the experiments were as the data were not presented). This and a related study found evidence that PAT (and its derivatives) were being degraded in a post-ER compartment prior to secretion (Denecke *et al.* 1990; Denecke *et al.* 1992), a finding corroborated by a later study (Phillipson *et al.* 2001).

Two recent studies have provided more detailed insights into the nature and limits of H/KDEL mediated retrieval by saturating retrieval in plant cells. Crofts *et al.* (1999) probed the limits of ER retention of two ER resident proteins, calreticulin and BiP, both of which possess a C-terminal HDEL motif. Tobacco lines expressing calreticulin and BiP with their HDEL motifs deleted (BiPΔHDEL and calΔHDEL) were generated, and it was found that some calΔHDEL, but not BiPΔHDEL, was secreted, indicating that it is competent for ER export. To determine whether secretion of calreticulin could be achieved in the presence of its HDEL signal, calreticulin overexpressing tobacco lines were generated that express up to 100 fold elevated calreticulin levels. In these overproducing lines, calreticulin was found to possess EndoglycosidaseH (EndoH) resistant carbohydrates, indicating that it had passed beyond the *cis*-Golgi apparatus (Crofts *et al.* 1999). This, and the fact that protoplasts from these lines secrete some calreticulin within a 12-hour incubation, clearly indicates that retrieval of this ER resident protein had been saturated (Crofts *et al.* 1999). Further evidence that retrieval saturation has occurred is provided by the fact that these calreticulin-overproducing lines also secrete another ER resident protein, BiP, which would normally be retrieved by the same mechanism (Crofts *et al.* 1999).

Recently, evidence has been published that, although calreticulin lacking its HDEL motif is secreted (Crofts *et al.* 1999), this does not occur readily because a significant portion of it is degraded after leaving the ER (Phillipson *et al.* 2001). This provides some explanation for the extraordinarily high levels of calreticulin overexpression needed to apparently saturate its retrieval (Crofts *et al.* 1999): in other words, saturation is occurring in these overexpressing lines, but is underestimated when secretion is used as a measure for saturation because a significant proportion is degraded in a post-ER compartment prior to being secreted. This highlights a need for caution when using secretion of a protein as a marker for saturation of ER retrieval.

Further strong evidence for saturation of ER retrieval was obtained by Phillipson *et al.* (2001) using a time course analysis of secretion of α-amylase with and without a C-terminal HDEL signal. In a tobacco protoplast transient expression system, secreted amylase was found in the medium almost immediately after transfection. However, while amylase-HDEL activity was rapidly accumulating within the cell, it was not secreted into the medium until around 6-10 hours after transfection (Phillipson *et al.* 2001). Importantly, if the HDEL fusion in this experiment was not fully functional, one would expect amylase-HDEL to be secreted from the beginning of the experiment, but at a lower rate. Therefore, the clear lag time until secretion of the of amylase-HDEL compared to non-retrieved amylase strongly argues that the retention mechanism is: 1) fully functional for the heterologous fusion protein, and; 2) saturated by amylase-HDEL overexpression after around 6 hours (Phillipson *et al.* 2001).

One possible limitation to the interpretation of this experiment is that the natural secretory protein, α-amylase, contains active ER export signals that may lead to an overestimation of the rate of saturation in the abovementioned experiment (Phillipson *et al.* 2001). However, the authors argue that data presented in Figure 6 suggest that the natural secretory protein α-amylase leaves the ER at a similar rate to the ER resident calreticulin with its HDEL motif deleted. If this is true, then this: 1) appears to demonstrate *in vivo* saturation of H/KDEL retention machinery more accurately than previous studies in plant systems; and 2) suggests that α-amylase does not have export signals, and is therefore a good marker for default exit from the secretory pathway.

In summary, it is clear that saturation of the machinery responsible for ER retention of H/KDEL signals can be achieved in plant cells, although this has been clearly

demonstrated on only a few occasions. Furthermore, saturation may occur more readily than previously thought given that some marker proteins (the ER resident calreticulin, and the non-secretory protein PAT) appear to be degraded in a post-ER compartment, leading to underestimation or masking of possible saturation. In this respect, markers that can be shown to be fully secreted, such as the secretory protein amylase (Phillipson *et al.* 2001), may be the most useful to judge the level of saturation occurring in a range of experimental systems.

H/KDEL mediated delivery of toxins to the ER

There have been reports of highly cytotoxic bacterial and plant toxins that are endocytosed and 'reverse secreted' by mammalian cells (Johannes and Goud 1998; Lord and Roberts 1998; Sandvig and van Deurs 1999; Sandvig and van Deurs 2000), including the bacterial toxins *Pseudomonas* exotoxin, and cholera, shiga, diphtheria, anthrax, botulinum and tetanus toxins and the plant toxin ricin. After endocytosis and transportation these toxins are endocytosed and transported via a retrograde secretory pathway to the acidic endosomes or ER, the toxins are translocated into the cytoplasm where they subsequently exert their toxic effect (Lord and Roberts 1998).

Much research has been aimed at determining how these toxins reach their intracellular target compartments, particularly as far into the secretory pathway as the ER. One possible partial explanation was provided by the presence of C-terminal KDEL or KDEL like sequences on some of these toxins (*Pseudomonas* exotoxin {REDLK}, cholera toxin {KDEL} and *E. coli* heat labile toxin {RDEL}). This suggested that some toxins might exploit ERD2-mediated retrograde transport for at least part of their reverse secretion pathway (Jackson *et al.* 1999).

In experiments designed to examine this possibility further, a KDEL signal was fused to the C-terminus of toxins that do not possess such motifs (Johannes *et al.* 1997; Wales *et al.* 1992; Zhan *et al.* 1998), or a related signal was replaced with KDEL (Seetharam *et al.* 1991). This caused an increase in the cytotoxicity of these toxins, implying that ERD2 mediated retrograde transport of these toxins is indeed an important step in their mode of action. This approach also demonstrated a way in which the ultimate effect of these toxins could be enhanced by manipulation of their subcellular localisation.

These experiments thus led to the idea of testing whether Cf-9 could detect Avr9 more or less strongly if Avr9 was directed to the ER using a KDEL motif to provide insight

into the question of subcellular localisation of functional Cf-9. If Cf-9 could function from the ER, then it would be expected that directing accumulation of Avr9 in the ER would hasten or strengthen the response to Avr9. If, alternatively, Cf-9 was functional at the PM, then it would be expected that directing Avr9 to the ER would prevent the response to Avr9.

3.2.2 Aim of this chapter

Conflicting evidence has been published that Cf-9 may function as an ER or PM resident protein. The work described in this chapter aimed to further clarify this issue by testing whether Cf-9 could respond to Avr9 from the ER. Avr9 was localised to the ER by transiently expressing KDEL tagged versions of Avr9 in *Cf-9* tobacco leaves using agroinfiltration. Direct comparison of *Cf-9* dependent necrosis between Avr9 and control variants on single leaves (with repetition) was used to determine the effects of these Avr9 sequence modifications on Cf-9 mediated recognition. Dilution series comparisons between some Avr9 variants were also performed to determine whether the activity of constructs had been perturbed, and to exclude this as a contributor to the differential response by Cf-9 to the Avr9 variants.

3.3 MATERIALS AND METHODS

3.3.1 Plasmid vector construction and mutagenesis

General molecular biology methods were performed according to Appendix 1, except where otherwise stated.

Production of pCBJ231

The plasmid pCBJ231 was used as a progenitor to most plasmids described in this chapter, and was generated as follows. The primers BglII35S and a modified M13 Reverse primer (Table 3.1) were designed and used in combination to amplify the Avr9 expression cassette from pSLJ6201 (Hammond-Kosack *et al.* 1994a) with $Vent_R^{®}$ DNA polymerase (New England Biolabs®). The BglII35S primer anneals at the internal *Bgl*II site of the CaMV35S promoter, which is 284 bp upstream of the 3' *Cla*I site. This was used instead of the M13(-20) primer to amplify the Avr9 cassette as the latter primer

generated a non-target amplification product of 1 kb when used alone with pSLJ6201 as a template.

The amplified 0.9kb fragment was cloned using the Zero Blunt™ PCR cloning kit (Invitrogen™), then excised from the pCR®-Blunt cloning vector as a *Hin*dIII fragment and ligated into *Hin*dIII cut pBluescript SK⁻. A clone with this insert orientated (5'-3') *Sac*I (1574) to *Kpn*I (658) was selected by *Cla*I digestion and designated pCBJ231 (Figure 3.1).

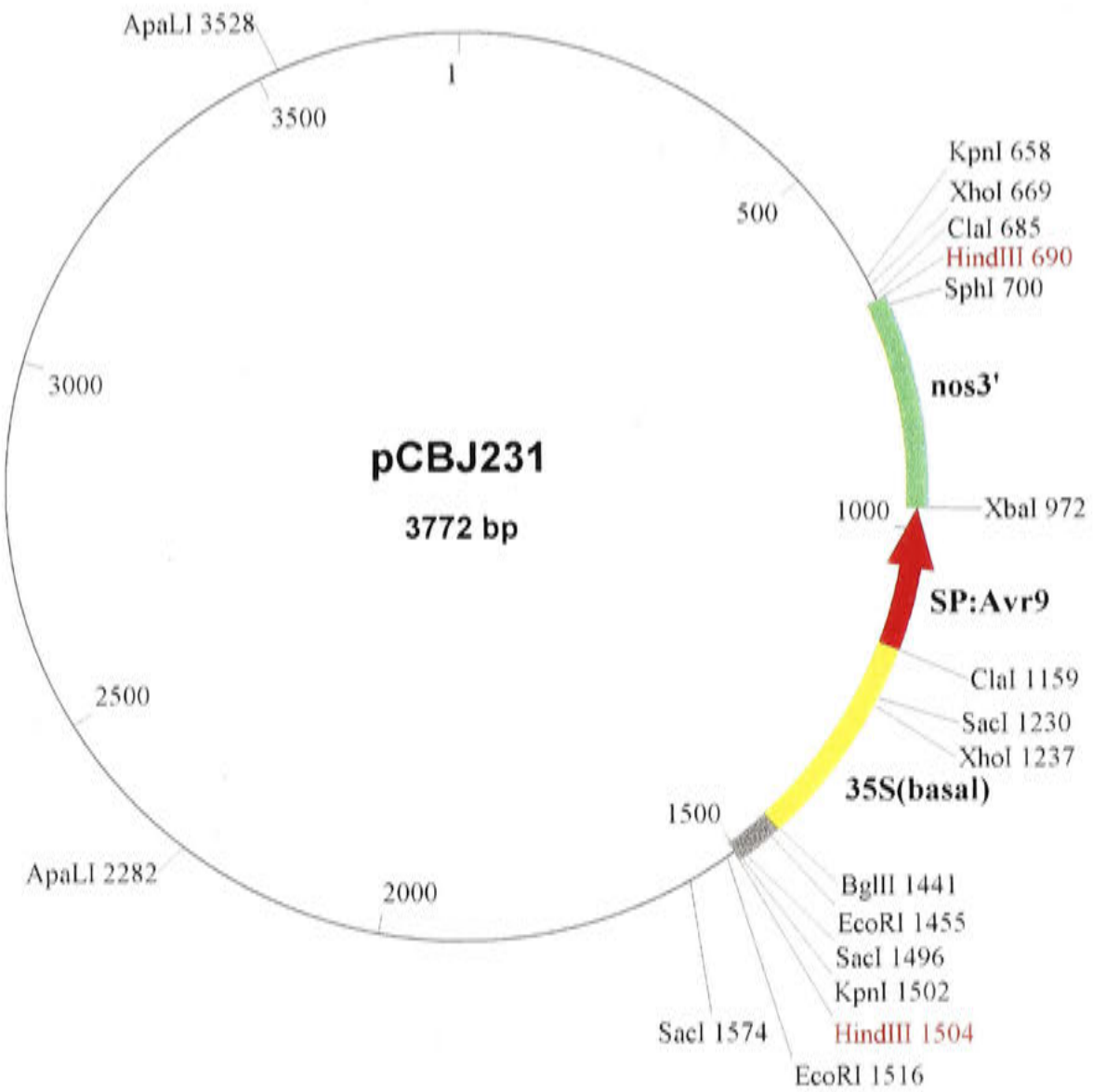

Figure 3.1. Plasmid vector pCBJ231, which contains the CaMV35S basal promoter (yellow), Avr9 with the PR1a signal peptide (red) and the nos3' terminator (green). Selected restriction sites are shown, including the *Hin*dIII sites (red) that this fragment was ligated into (when cloned into pBluescript) and which were used to transfer this fragment into a binary plasmid (see text for details). The grey fragment corresponds to a fragment of pCR-Blunt transferred during construction of pCBJ231.

Table 3.1. PCR primers used in the current work.

Primer name	Primer sequence
ClaIAvr9SP	acaattatcgatgggatttgttctc
modified M13 Reverse primer	caggaaacagctatgaccatg
BglII35S	cgttcaagatctctctgccgacagtg

Production of tagged Avr9 constructs

Avr9 constructs tagged with ER retention motif variants and the S5A mutation were generated by oligonucleotide mediated single stranded DNA mutagenesis essentially as described (Kunkel 1985; Kunkel *et al.* 1987; see the section below). Specific primers were generated for each planned Avr9 variant, each incorporating a unique restriction enzyme cleavage site combination for diagnostic purposes (Table 3.2). Oligonucleotide mutagenesis was performed using single stranded pCBJ231 DNA as a template to generate Avr9-KDEL and Avr9-S5A constructs in the pBluescript backbone, while single stranded pCBJ242 DNA (Avr9-KDEL plasmid, see Table 3.3) was used as the template for Avr9-S5A-KDEL, Avr9-KDDL, Avr9-HDEL and Avr9-HDDL pBluescript plasmids (Table 3.3 and Table 3.4). Each oligonucleotide contained an added restriction enzyme cleavage site to allow diagnostic restriction digestion of resultant clones.

Table 3.2. Sequence of mutagenic oligonucleotides used to generate tagged versions of Avr9. Unique restriction endonuclease cleavage sites ("RE") are underlined, and sequence differences between the oligonucleotide ("primer name") and the ssDNA template (see Table 3.3) are in bold.

Primer name	Primer sequence (5'-3')	RE
Avr9-KDEL	aagctccaatgt**gtgcacaaggacgaactt**tgagatcctctagag	*Apa*LI
plAvr9-S5A	gcctactgtaacagt**gcatgc**acaagagcttttg	*Sph*I
Avr9-KDDL	gtgcacaaggacga**t**ctt**agg**atcctctagagtc	*Bam*HI
Avr9-HDEL	ccaatgtgtgcac**catg**acgaactttgag	*Nla*III
Avr9-HDDL	gctccaatgtgtgcac**catg**acga**t**ctt**agg**atcctctagagtc	*Nla*III & *Bam*HI

Table 3.3. Summary of Avr9 variant expression constructs generated. The ssDNA template/oligonucleotide combination used to generate each Avr9 variant is shown. Oligonucleotide sequences are shown in Table 3.2. The names of the resulting pBluescript and binary plasmid version corresponding to each Avr9 variant are shown.

Avr9 variant name	ssDNA template/oligonucleotide combination	pBluescript version	Binary version
Avr9	n/a	pCBJ231	pCBJ243
Avr9-KDEL	pCBJ231/Avr9-KDEL	pCBJ242	pCBJ244
Avr9-S5A	pCBJ231/plAvr9-S5A	pCBJ245	pCBJ247
Avr9-S5A-KDEL	pCBJ242/plAvr9-S5A	pCBJ246	pCBJ248
Avr9-KDDL	pCBJ242/Avr9-KDDL	pCBJ251	pCBJ254
Avr9-HDEL	pCBJ242/Avr9-HDEL	pCBJ252	pCBJ255
Avr9-HDDL	pCBJ242/Avr9-HDDL	pCBJ253	pCBJ256

Table 3.4. Predicted amino acid sequence of Avr9 variants. Predicted sequence of mature Avr9 variants, generated by oligonucleotide mutagenesis of pCBJ231 or pCBJ242 (see text for details), is shown. Differences relative to mature wildtype Avr9 are shown in bold.

Avr9 variant	Predicted amino acid sequence
Avr9	YCNSSCTRAFDCLGQCGRCDFHKLQCVH
Avr9-KDEL	YCNSSCTRAFDCLGQCGRCDFHKLQCVH**KDEL**
Avr9-S5A	YCNS**A**CTRAFDCLGQCGRCDFHKLQCVH
Avr9-S5A-KDEL	YCNS**A**CTRAFDCLGQCGRCDFHKLQCVH**KDEL**
Avr9-KDDL	YCNSSCTRAFDCLGQCGRCDFHKLQCVH**KDDL**
Avr9-HDEL	YCNSSCTRAFDCLGQCGRCDFHKLQCVH**HDEL**
Avr9-HDDL	YCNSSCTRAFDCLGQCGRCDFHKLQCVH**HDDL**

ssDNA preparation

The plasmid to be mutagenised (pCBJ231 or pCBJ242) was transformed into competent BW313 (*dut*$^-$ *ung*$^-$) *E. coli* cells and selected on LB plates containing 100 μg/ml ampicillin (LBA_{100}). A single colony was used to inoculate 30 ml of pre-warmed (37°C) liquid 2 x YT medium in a 250 ml conical flask containing 50 μg/ml ampicillin and incubated for 30 minutes at 37°C, then 10 μl of M13K07 lysate was added. After further incubation for 2 hours, kanamycin was added to a final concentration of 70 μg/ml and the culture incubated overnight at 37°C with shaking at 250 rpm.

The culture was divided equally into two corex tubes (DuPont), then centrifuged at 5930 x g for 5 minutes. Twelve millilitres of each supernatant was collected, mixed with 3 ml

of 20% PEG-8000/1.5M NaCl in a clean corex tube and incubated at room temperature for 15 minutes. The tubes were then centrifuged at 12 100 x g for 10 minutes and the supernatant discarded. The tubes were re-centrifuged (1088 x g for 2 minutes) and excess supernatant removed using a pipette and discarded. The bacteriophage pellet was resuspended in 1 ml TE, and then transferred to a 1.5 ml eppendorf tube. The corex tube was washed with an additional 200 µl TE and this wash combined with the previously resuspended pellet. The tubes were then centrifuged in a microcentrifuge at 5380 x g for 5 minutes to remove any cell debris.

The supernatant was divided into 2 x 600 µl aliquots, added to 60 µl of 3M NaAc (pH5.2) then extracted successively with an equal volume each of phenol, phenol:chloroform (1:1) and chloroform. ssDNA was precipitated by adding an equal volume of isopropanol and incubating at -20°C for 30 minutes. ssDNA was pelleted by centrifugation for 10 minutes at 23 710 x g at 4°C. The supernatant was discarded and the pellet washed with 70% ethanol, air-dried and resuspend in TE, using approximately 30-50 µl for ssDNA originating from 30 ml of culture supernatant (approximately 100-500 ng/µl). Concentration and integrity of the ssDNA were checked by measuring absorbance at 260nm (A_{260}) and gel electrophoresis on a 0.8% agarose gel. To reduce background plasmid in the ssDNA preparation, double stranded DNA was digested with *Cla*I and *Apa*LI using standard procedures (Appendix 1).

Mutagenic oligonucleotide phosphorylation

The mutagenic oligonucleotide was kinased in a 20 µl reaction containing 100pM oligonucleotide, 1 x ligase buffer (New England Biolabs®), 5 U polynucleotide kinase (New England Biolabs®) then incubated at 37°C for 30-45 minutes. The enzyme was inactivated by incubation at 65°C for 20 minutes.

Annealing of the mutagenic oligonucleotide to ssDNA template

Annealing of the mutagenic oligonucleotide was performed in a 20 µl reaction volume containing 25pmol kinased oligonucleotide, 0.5pmol of ssDNA (~0.5-5 µl) and 1 x Fritz buffer (from an 8 x stock containing 1.5M KCl, 100mM Tris.HCl {pH7.5}). Annealing conditions were adapted specifically for each oligonucleotide, depending upon the predicted annealing and thermal characteristics of the oligonucleotide/template combination, as follows:

For the Avr9-KDEL primer: 96°C, 5 minutes; ramp 0.1°C/second to 70°C; 70°C for 15 minutes; ramp 0.1°C/second to 65°C; 65°C for 10 minutes; ramp 0.2°C/second to 4°C;

For the plAvr9-S5A primer: 96°C, 5 minutes; ramp 0.1°C/second to 64°C; 64°C for 20 minutes; ramp 0.1°C/second to 4°C;

For the Avr9-KDDL and Avr9-HDDL primers: 96°C, 5 minutes; ramp 0.1°C/second to 70°C; 70°C for 10 minutes; ramp 0.1°C/second to 4°C;

For the Avr9-HDEL primer: 96°C, 5 minutes; ramp 0.1°C/second to 67°C; 67°C for 10 minutes; ramp 0.1°C/second to 4°C.

Second strand synthesis

Reactions were then placed on ice and the second strand of DNA synthesised by adding 2.5 µl ligase buffer (10 x), 0.5 µl 3M KCl, 1.3µl 20mM dNTPs, 1 µl Klenow Fragment (1 U) and 0.2 Weiss U of T4 DNA Ligase (New England Biolabs®). Reaction mixtures were then incubated at room temperature (~22°C) for 3-16 hours and transformed into competent *E. coli* (DH5α). Resulting plasmid clones were screened for incorporation of the mutation by restriction digestion of the site introduced into the mutagenic oligonucleotide.

Transfer of constructs to Agrobacterium *binary plasmids*

From each of these pBluescript backbone plasmids, the Avr9 cassette was excised as a *Hin*dIII fragment and ligated into pSLJ7291 (http://www.jic.bbsrc.ac.uk/sainsbury-lab/; Hammond-Kosack *et al.* 1998) binary plasmid cut with *Hin*dIII (Table 3.3; Figure 3.2). Binary plasmids were selected that contained the insert orientated (5'-3') towards the M13(R) priming site (Figure 3.2) by PCR using the ClaIAvr9SP and modified M13(R) primer combination (Table 3.1) and diagnostic restriction digestion of the resultant PCR products where necessary. Avr9 variant plasmids used were therefore identical except for the mutations described. Unless otherwise stated, reference to a plasmid version of Avr9 (i.e. "Avr9-KDEL") indicates the binary plasmid version of the construct or *Agrobacterium* containing the said binary plasmid.

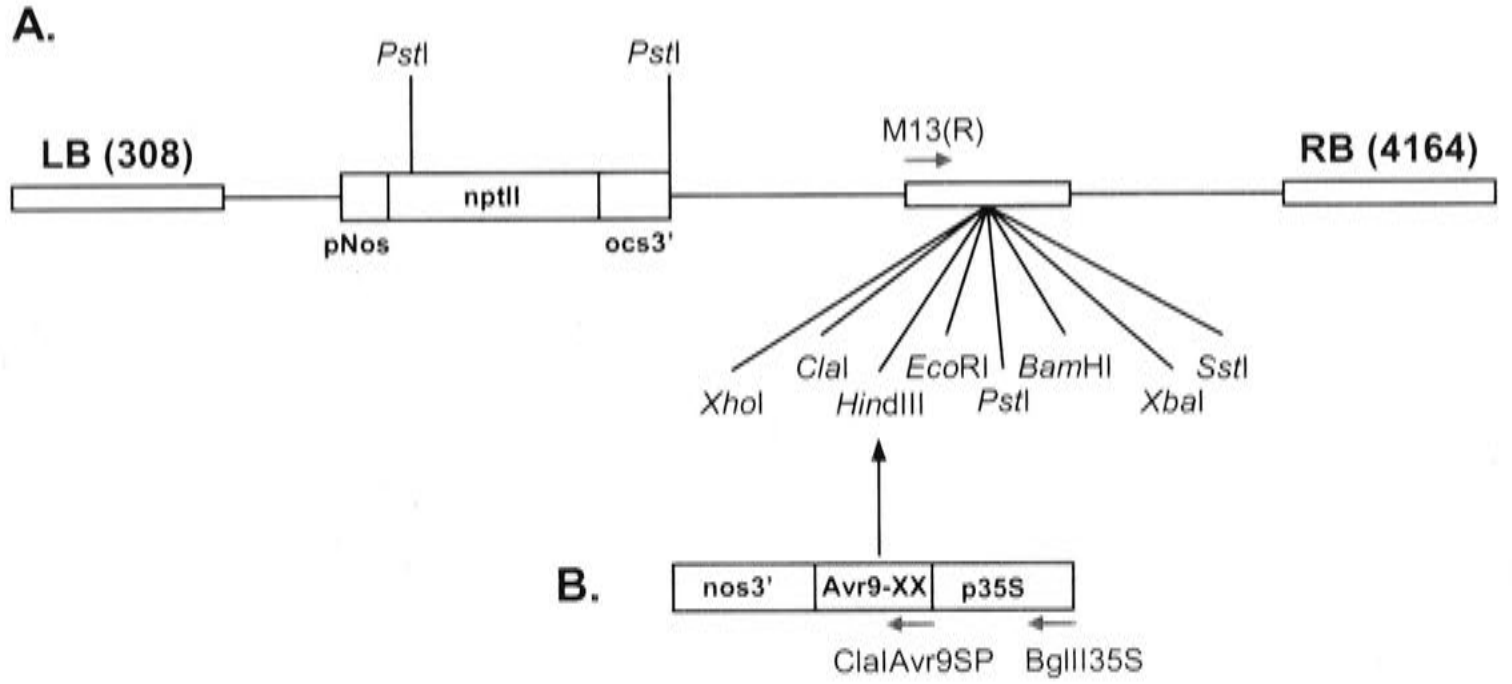

Figure 3.2. A. A map of pSLJ7291 binary plasmid between Left Border (**LB**) and Right Border (**RB**), adapted from the Sainsbury Laboratory website (http://www.jic.bbsrc.ac.uk/sainsbury-lab/). **B.** The location and orientation of the inserted Avr9 variant *Hin*dIII fragments into pSLJ7291 (see text for details). The location and orientation of the M13(R), Cla1Avr9SP and BglII35S primers is indicated by red arrows. Diagram not to scale.

3.3.2 Agroinfiltration

Agroinfiltration was performed as described in Chapter 2 unless otherwise stated. For dilution series experiments, the culture of interest was diluted against GV3101 containing an empty binary plasmid (pSLJ7291) as indicated in the text. Experiments were repeated on at least two independent occasions, using multiple leaves from each of multiple plants on each occasion. The exact number and nature of repetition for each experiment is indicated in the text. The results shown are reproducible and representative except where stated otherwise. On some occasions replicates of these experiments were not successful, as indicated by, for example, necrosis not occurring at all on one leaf, or weakly in one panel with the lowest dilution of *Agrobacterium* only. When this variation in response was attributable to identified sources of variation (e.g. different sensitivity of different leaves, or on plants at the transition to flowering, see Chapter 2), these leaves were discounted as unsuccessful attempts at the experiment.

3.3.3 Quantification and analysis of necrosis

The area of necrosis within each leaf panel of interest and the area of the leaf panel itself were measured using the manual selection feature of SigmaScan® Pro 5 Demo version (SPSS Science™). Whole leaf panels and necrotic regions within the leaf panel were selected manually, and then the area of both measured (pixels) and necrotic area as a percentage of total leaf area calculated. Percent necrosis was plotted against hpi using Microsoft® Excel.

3.4 RESULTS

3.4.1 Pairwise comparison of tagged versions of Avr9 by agroinfiltration

To determine whether Cf-9 can respond to Avr9 from the ER, a number of Avr9 constructs with combinations of ER retention signals and the S5A mutation were generated by single-stranded DNA oligonucleotide mutagenesis, then transferred to *Agrobacterium* (see Materials and Methods). Agroinfiltration of these constructs into *Cf-9* tobacco leaves was used to compare the Cf-9 mediated responses to the encoded Avr9 variants. Comparison of experimental to control Avr9 variants (i.e. pairwise

comparisons) were used within single leaves to exclude the variation between leaves and plants identified in Chapter 2.

Comparison of Avr9 to Avr9-KDEL

To determine the effect of tagging Avr9 with the C-terminal KDEL motif, Avr9-KDEL was compared with Avr9 by agroinfiltration. Necrosis induced by Avr9-KDEL was found to be reproducibly delayed compared to that induced by Avr9 (Figure 3.3). In total, this result was observed on five independent occasions on five different plants. No response was observed when Avr9-KDEL was infiltrated into wildtype tobacco leaves (not shown). The delay in response was quantified in a later experiment (Section 3.4.4).

To determine whether this response was reproducible on multiple leaves of different age and orientations relative to insolation load, this comparison was repeated on multiple leaves on an individual plant. From the same experiment shown in Figure 2.1 (from Chapter 2), it can be seen that the delayed necrosis resulting from Avr9-KDEL relative to Avr9 is repeated for all leaves, regardless of their age and orientation (Figure 3.4). However, when less sensitive (older) leaves are used (e.g. leaf 2), a longer delay is present. Additionally, the reproducible delay (but not the duration of the delay) on these different leaves indicates that the delayed necrosis induced by Avr9-KDEL compared to Avr9 is not dependent on the position of the leaf relative to insolation load or other microhabitat effects. The different activity of agroinfiltrated Avr9 between younger and older leaves (Figure 2.1) is repeated in this experiment by Avr9-KDEL (compare Avr9-KDEL on different leaves, Figure 3.4). Though this particular experiment (Figure 3.4) was performed formally only once, this reduced sensitivity and increased delay of Avr9-KDEL compared to Avr9 on older leaves was observed whenever multiple different aged leaves were used for a comparison (not shown).

The delay between Avr9 and Avr9-KDEL was reduced on younger leaves compared to older leaves, possibly because the higher activity of Avr9 by agroinfiltration in younger leaves (Chapter 2) partially obscures any differential response. For this reason, and because these leaves (the seventh to eighth fully expanded) are moderately difficult to infiltrate without damaging the leaf tissue due to high leaf venation, these leaves were not used for direct comparison experiments unless otherwise indicated. Instead, the third and fourth fully expanded leaves were used as they gave a clear response for both constructs and were easy to infiltrate.

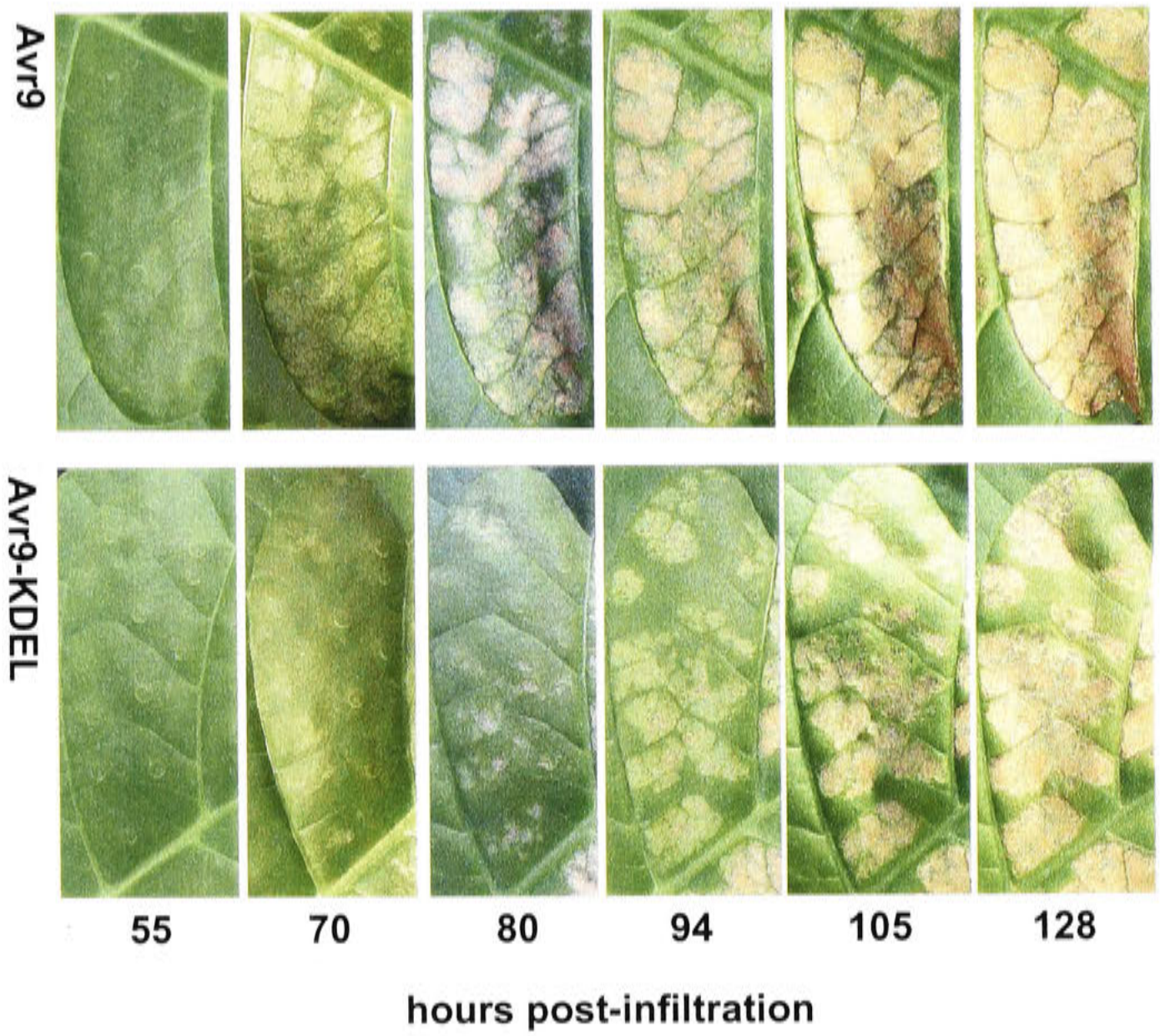

Figure 3.3. Pairwise comparison of Avr9 with Avr9-KDEL by agroinfiltration. *Agrobacterium* containing either construct was infiltrated into the third fully expanded leaf of a *Cf-9* tobacco plant as described in the text. Single comparable leaf panels from the same leaf are shown for each Avr9 variant infiltrated (indicated at the left of the figure) at the time intervals indicated at the bottom of the figure.

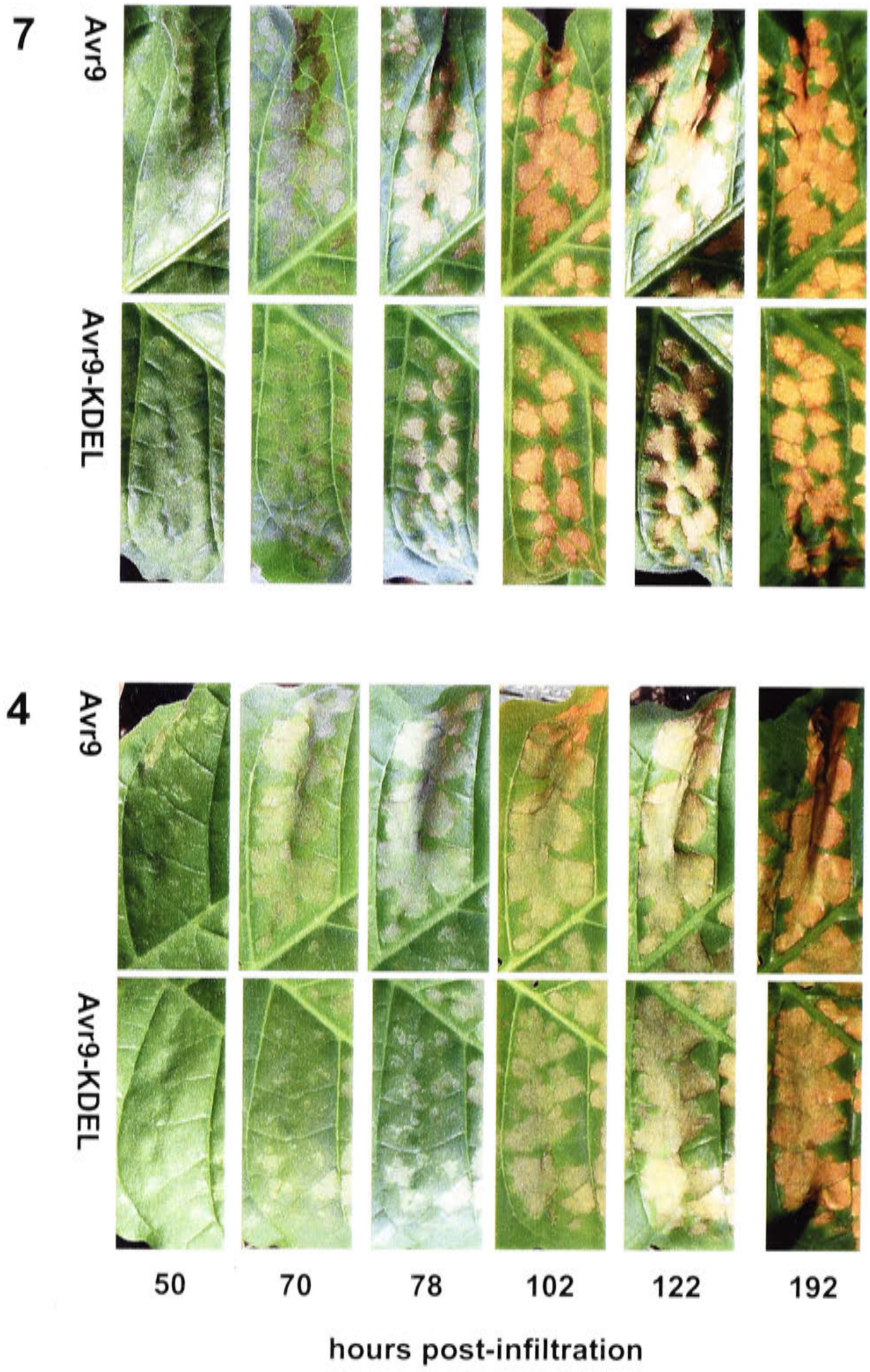

Figure 3.4. Variation of KDEL mediated delay of necrotic response to Avr9 by agroinfiltration in *Cf-9* tobacco leaves. *Agrobacterium* containing Avr9 or Avr9-KDEL was infiltrated into equivalent leaf panels of four *Cf-9* tobacco leaves of different ages (**2**, **3**, **4** and **7** indicate the number of the leaf from the base of the plant). Individual leaf panels are shown for each Avr9 variant infiltrated (indicated at the left of the figure) at the time intervals indicated at the bottom of the figure.

3

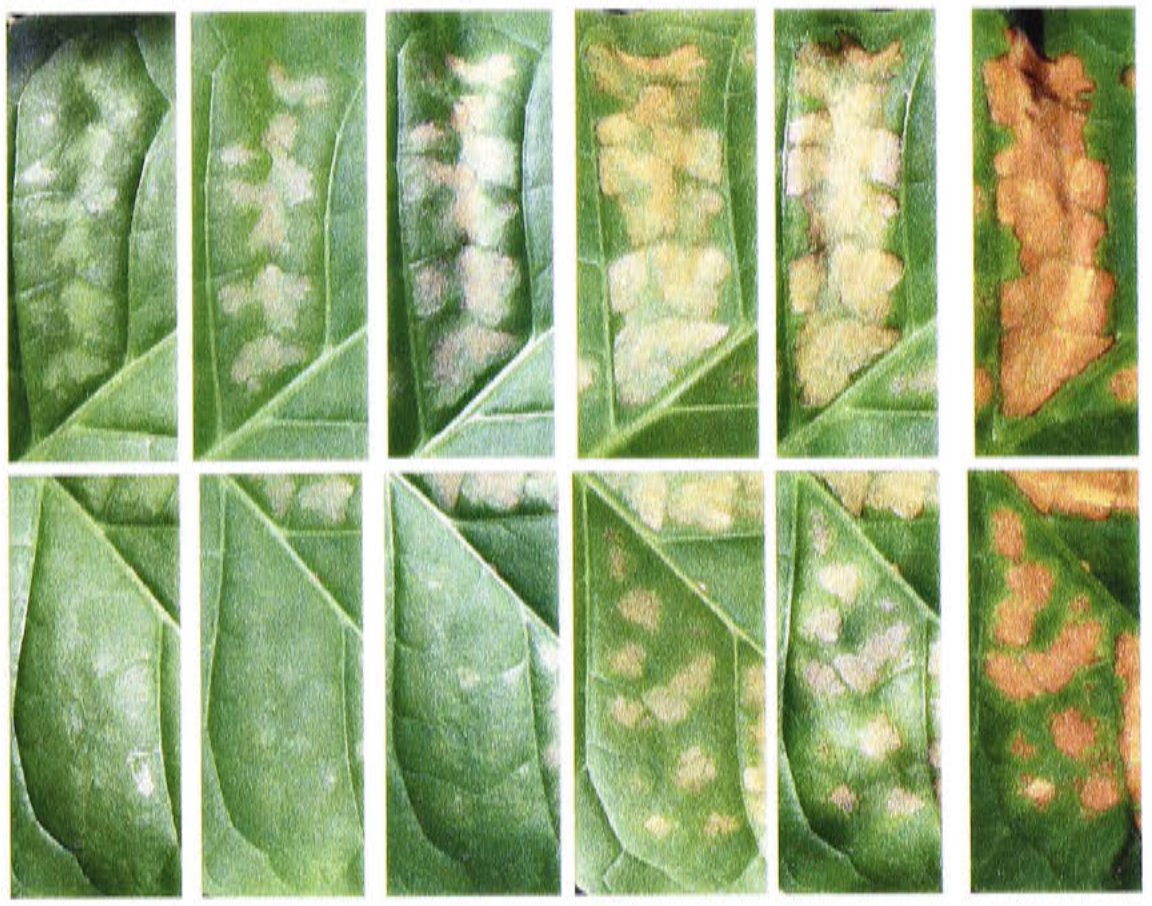
Avr9
Avr9-KDEL

2

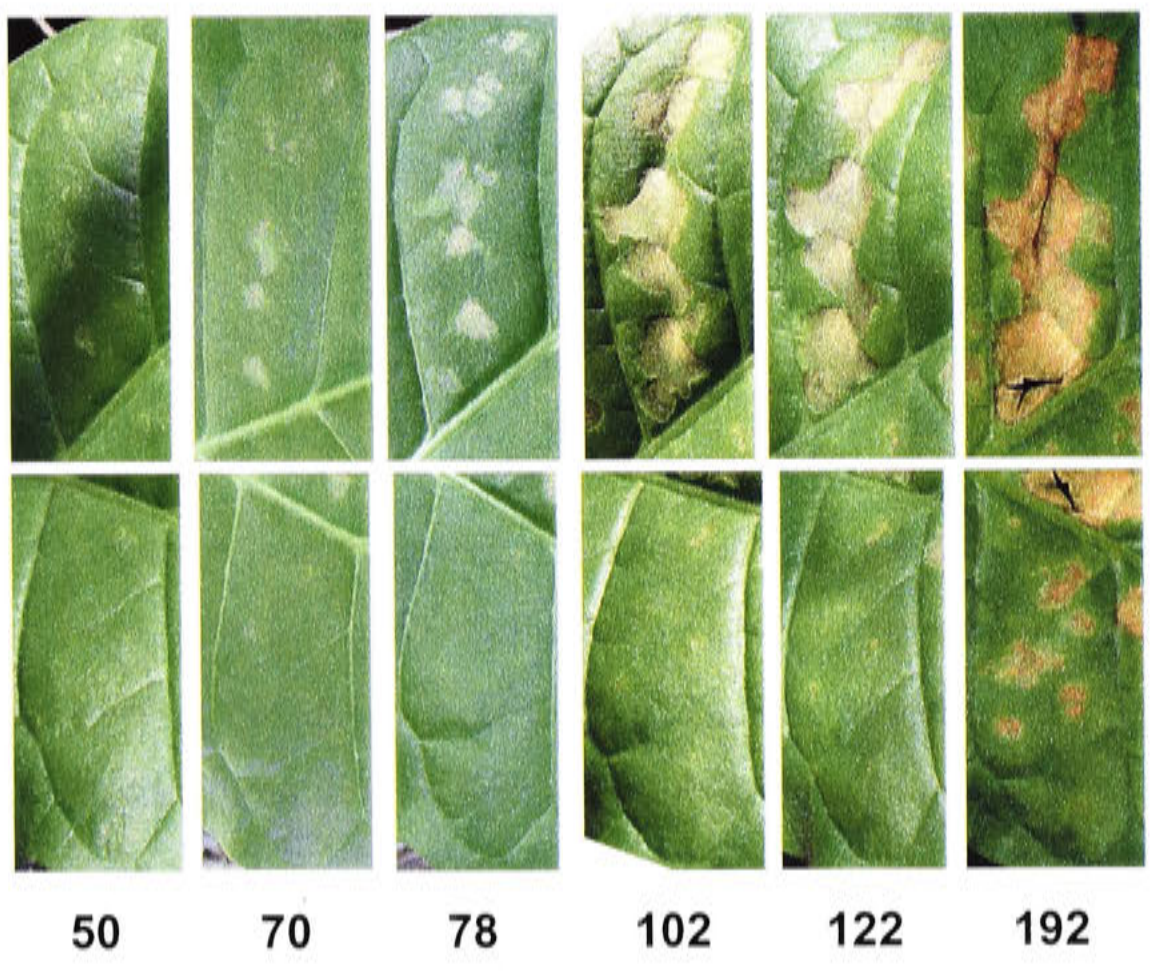
Avr9
Avr9-KDEL
50
70
78
102
122
192
hours post-infiltration

Comparison of Avr9-KDEL to Avr9-KDDL

One possible explanation of the delay of Avr9-KDEL relative to Avr9 is that the KDEL tag disrupts the necrosis inducing activity of Avr9. This would mean that a higher level of Avr9-KDEL would be needed compared to Avr9 in order to induce an equivalent necrotic response. A difference in necrosis inducing activity between Avr genes has previously been observed to cause delayed necrosis using the agroinfiltration system (Van der Hoorn *et al.* 2000; see also the introduction to Chapter 2).

To test this possibility, a version of Avr9 tagged with a variant of the KDEL motif, KDDL, was generated and compared to Avr9-KDEL. The KDDL motif is almost chemically identical to KDEL, yet abolishes KDEL mediated ER retrieval (Denecke *et al.* 1992; Denecke *et al.* 1993). Therefore, this comparison should rule out disruption of Avr9 function by the KDEL motif as a factor contributing to the delayed necrosis.

Development of necrosis as a result of Avr9-KDEL agroinfiltration showed a delay compared to Avr9-KDDL (Figure 3.5), comparable to that observed previously relative to Avr9 (above). In total, this result was observed on two independent occasions on three different plants. This result shows that the delayed necrosis is dependent on the biological activity of the KDEL tag, and strongly implies that ER retrieval of Avr9-KDEL is occurring.

On one occasion this comparison was performed on the younger leaves of two separate plants (one leaf on each plant, being the eighth and ninth fully expanded leaves from the base) instead of the third or fourth (data not shown). Similar to the experiment shown in Figure 3.4, the KDEL mediated delay of necrotic response was not as clearly observed on these younger leaves. However this phenomenon of reduced KDEL mediated delay on younger leaves would need to be confirmed before any firm conclusions were drawn from these data.

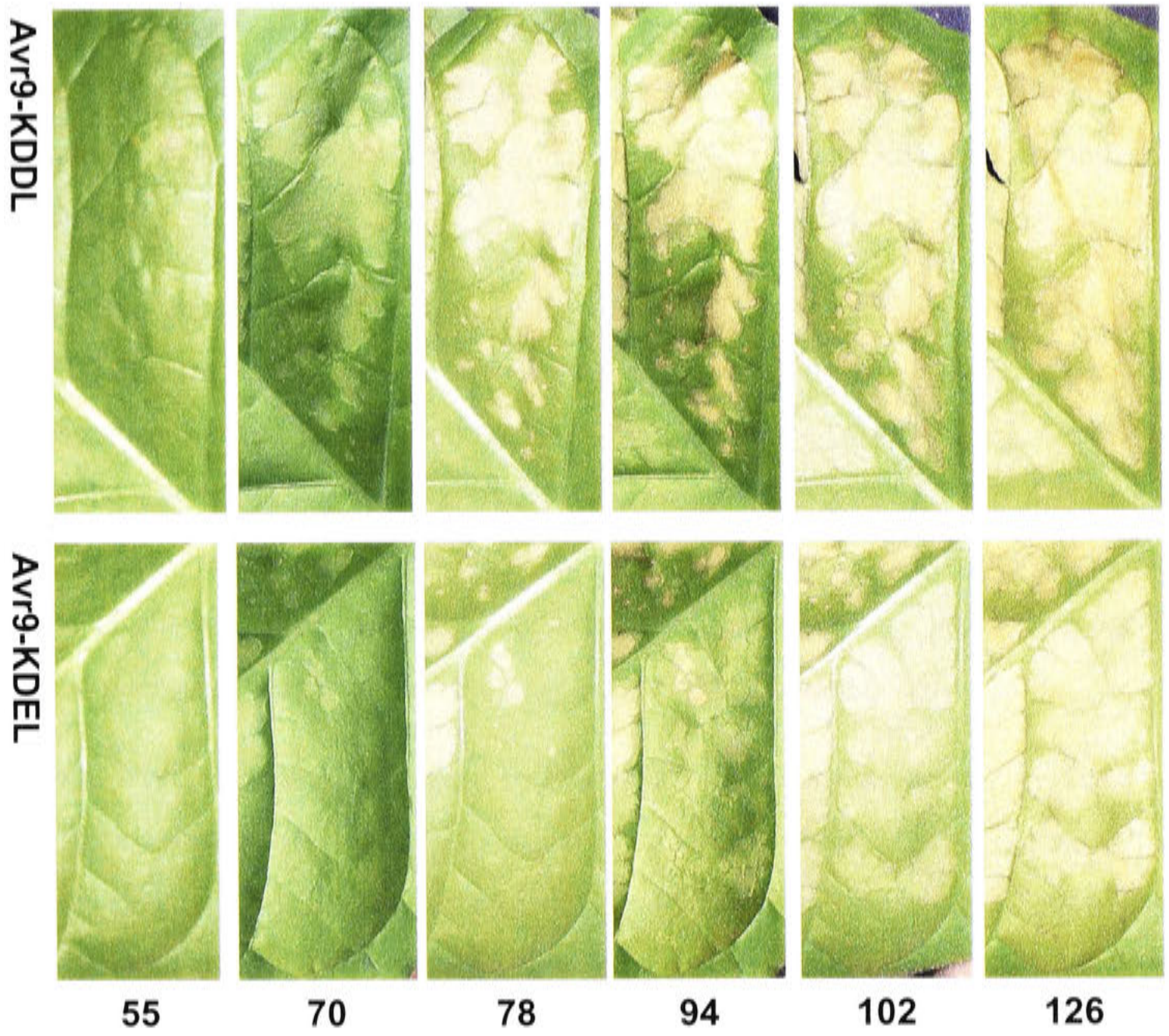

Figure 3.5. Pairwise comparison of Avr9-KDEL with Avr9-KDDL by agroinfiltration. *Agrobacterium* containing either construct was infiltrated into the fourth fully expanded leaf of a *Cf-9* tobacco plant as described in the text. Single comparable leaf panels from the same leaf are shown for each Avr9 variant infiltrated (indicated at the left of the figure) at the time intervals indicated at the bottom of the figure.

Comparison of Avr9-S5A to Avr9-S5A-KDEL

Since Avr9 is known to be glycosylated when expressed in plants (Kooman-Gersmann *et al.* 1998a), it would be expected that while in the ER Avr9 (±KDEL) will possess the 'core' glycan moiety that is transferred to glycoproteins in the ER (Lerouge *et al.* 1998). If Cf-9 was able to respond to Avr9 from the ER, one possible explanation of the KDEL dependent delay of necrosis is that the core glycosylation of Avr9 (±KDEL) in the ER reduces its elicitor activity. This possibility would be consistent with the observed dependence of the delayed necrosis on ER retention (Figure 3.5), as this modification is ER specific.

To test this possibility, S5A mutants of Avr9 and Avr9-KDEL (Avr9-S5A and Avr9-S5A-KDEL respectively) were compared. If the delay results from the core glycosylation in the ER as hypothesised, then this delay of Avr9-KDEL relative to Avr9 should be abolished (or Avr9-S5A-KDEL respond more rapidly) in this comparison. The comparison between Avr9-S5A and Avr9-S5A-KDEL was chosen as it accounted for the slight reduction in activity due to the S5A mutation, which may itself cause delayed necrosis (Kooman-Gersmann *et al.* 1997; see also discussion).

Necrotic development in response to Avr9-S5A-KDEL was delayed, relative to Avr9-S5A, in a comparable manner to the previously observed KDEL dependent delayed necrosis (Figure 3.6). In total, this result was observed on five independent occasions on five different plants. No response was observed to either Avr9-S5A or Avr9-S5A-KDEL when infiltrated into wildtype tobacco (data not shown). Therefore, potential ER specific core glycosylation of Avr9-KDEL while in the ER does not cause the KDEL dependent delayed necrosis observed in previous experiments.

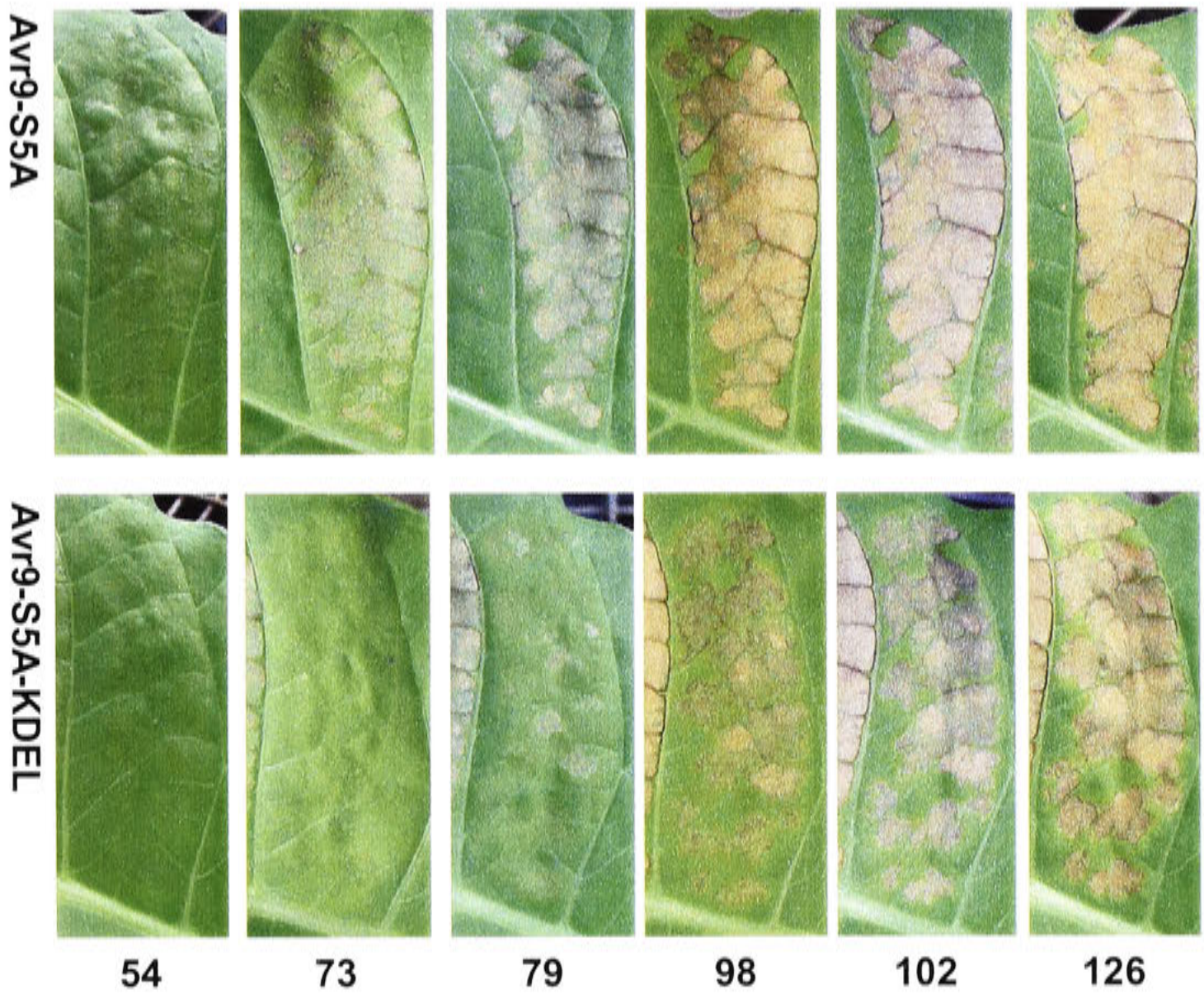

Figure 3.6. Pairwise comparison of Avr9-S5A with Avr9-S5A-KDEL by agroinfiltration. *Agrobacterium* containing either construct was infiltrated into the fifth fully expanded leaf of a *Cf-9* tobacco plant as described in the text. Single comparable leaf panels from the same leaf are shown for each Avr9 variant infiltrated (indicated at the left of the figure) at the time intervals indicated at the bottom of the figure.

3.4.2 Dilution series comparisons of tagged versions of Avr9 by agroinfiltration

Dilution series comparisons, or dose-response analyses, have previously been used with agroinfiltration to assess the relative activities of Cf and Avr variants on single tobacco leaves (see Chapter 2). Experiments above have shown that when a KDEL sequence is fused to the C-terminus of Avr9, a KDEL dependent delay in necrotic response by *Cf-9* tobacco leaves occurs. Although it was shown that this delay is not a result of disruption of Avr9 activity (Avr9-KDEL/Avr9-KDDL comparison, Figure 3.5), it was considered potentially informative to further analyse the relationship between necrosis inducing *activity* of expressed Avr9 variant peptides and the KDEL mediated *delay* in necrosis using dilution series comparisons. Unlike previous experiments, the seventh or eighth fully expanded leaves were typically used for dilution series experiments since they were found to give a more slowly spreading necrosis and more reproducible results for this type of experiment than older leaves.

Dilution series comparisons performed between Avr9 and Avr9-KDEL (Figure 3.7A) showed that the necrotic response to Avr9 was present at a higher dilution than was the case for Avr9-KDEL, suggesting that Avr9-KDEL has a weaker activity than Avr9. This result was observed on two independent occasions using one plant on each (with two leaves on one occasion and one on another). A similar comparison between Avr9-S5A and Avr9-S5A-KDEL (Figure 3.7C) also suggested that the latter variant has weaker activity. However, it should be noted that this latter dilution series comparison (Avr9-S5A and Avr9-S5A-KDEL) was only performed on one occasion (two leaves from one plant), so firm conclusions regarding this comparison can not be drawn.

Significantly, dilution series comparisons between Avr9-KDEL and Avr9-KDDL revealed no clear difference in activity between these two variants (Figure 3.7B). This result was observed on three independent occasions on seven leaves (three were the third or fourth fully expanded and four were the seventh or eighth fully expanded) from six different plants. The slight difference in activity between Avr9-KDEL and Avr9-KDDL in the figure (Figure 3.7B) was not reproducible. It can be concluded therefore, that there is little or no difference in the activity of Avr9-KDEL and Avr9-KDDL using agroinfiltration dilution series comparison, despite KDEL dependent delayed necrosis being observed when these constructs were compared (Figure 3.5).

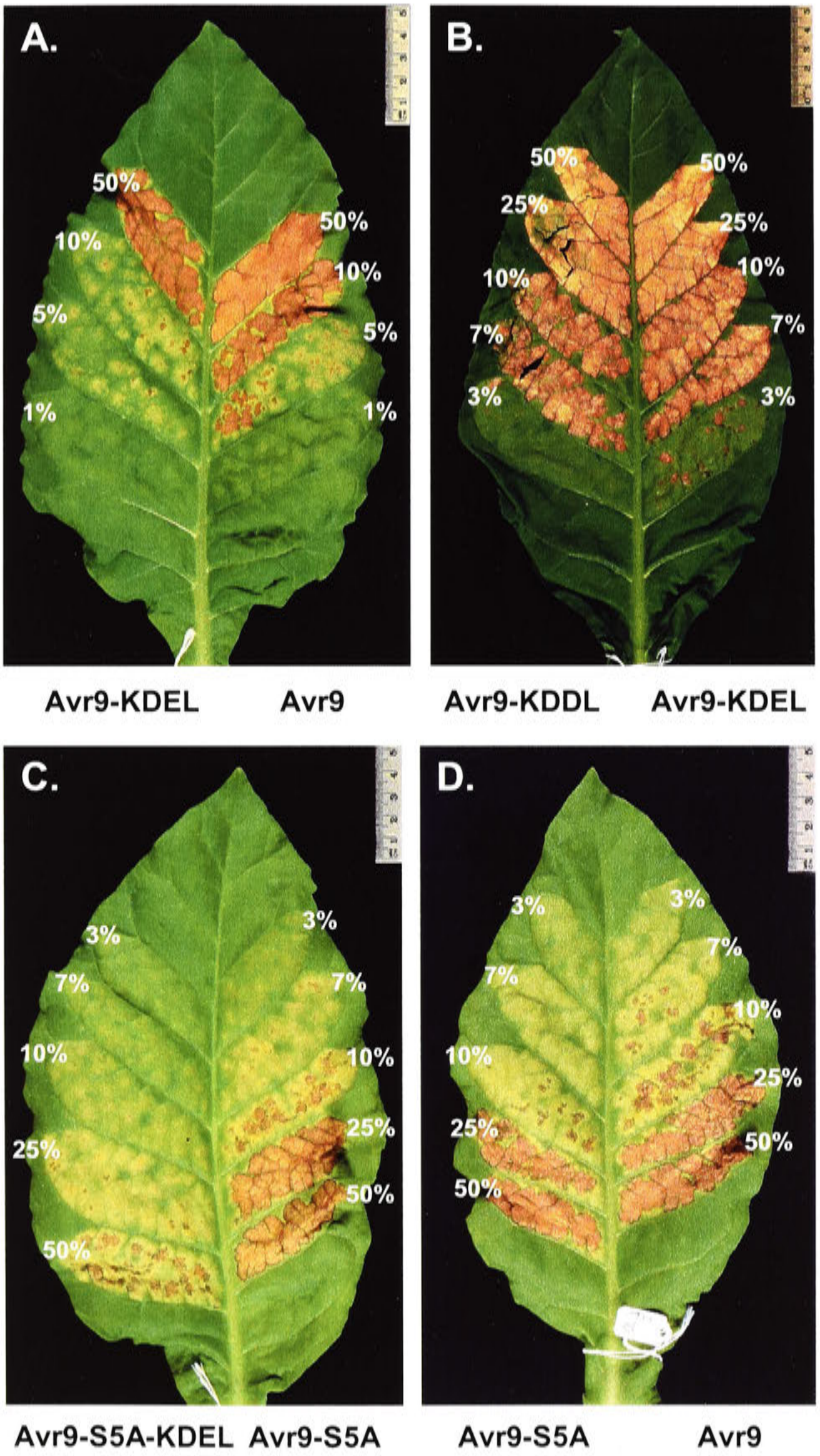

Figure 3.7. Dilution series comparisons of Avr9 variants by agroinfiltration into the seventh fully expanded leaf of *Cf-9* tobacco plants. Avr9 variant identity is indicated at the base of each image on the side of the leaf infiltrated with that variant. Percent of Avr9 variant (diluted against *Agrobacterium* containing empty vector) is indicated next to each leaf panel. **A.** Avr9-KDEL was compared to Avr9 (shown at 7 days post-infiltration {dpi}). **B.** Avr9-KDEL was compared to Avr9-KDDL (shown at 7 dpi). **C.** Avr9-S5A-KDEL was compared to Avr9-S5A (shown at 9 dpi). **D.** Avr9-S5A was compared to Avr9 (shown at 8 dpi). A scale bar is shown for each image.

3.4.3 Comparison of Avr9 to Avr9-S5A

To test the possibility that slightly reduced activity of a version of Avr9 may result in delayed necrosis when compared by agroinfiltration, a comparison was made between Avr9 and Avr9-S5A. The S5A mutant of Avr9 is known to have slightly reduced activity compared to wild type Avr9, as judged by protein bioassays on *Cf-9* tomato (Kooman-Gersmann *et al.* 1997). Therefore, if slightly reduced activity of a variant of Avr9 can cause delayed necrosis in the agroinfiltration assay, this should be apparent in the comparison of Avr9 to Avr9-S5A.

Necrosis induced by Avr9-S5A agroinfiltration into *Cf-9* tobacco leaves was only slightly delayed compared to Avr9 (Figure 3.8). On two occasions, a slight delay of Avr9-S5A was observed, while a repeat leaf on one of these occasions showed no clear delay. On the other occasion the delay was observed (not shown) it was smaller in duration than shown in Figure 3.8. The difference in timing of necrosis induced by Avr9 and Avr9-S5A was therefore never as large as the KDEL dependent delay described in previous experiments. This result suggests that the expected delay of necrosis due to the slightly reduced activity of the Avr9-S5A mutant (Kooman-Gersmann *et al.* 1997; Van der Hoorn *et al.* 2000) is only just detectable in this assay, and increased repetition would be necessary to ensure the validity of such a small difference in response. This in turn suggests that a significant change in activity of an Avr9 variant by agroinfiltration would be necessary to result in substantially delayed necrosis due to reduced activity alone.

Avr9-S5A was then compared to Avr9 by dilution series comparison to determine whether this assay was capable of detecting the slightly reduced necrosis inducing activity of Avr9-S5A directly, rather than indirectly by delayed development of necrosis (Figure 3.7D). Slightly reduced activity of Avr9-S5A compared to Avr9 was observed by dilution series comparison on three independent occasions (on five leaves from five plants). Therefore, the dilution series comparison by agroinfiltration appears to be sensitive enough to detect the difference in Avr9 activity that was previously detected by protein bioassay in *Cf-9* tomato leaves (Kooman-Gersmann *et al.* 1997; Figure 3.7D), but this reduced activity does not generate a clear difference in the timing of necrosis development (Figure 3.8).

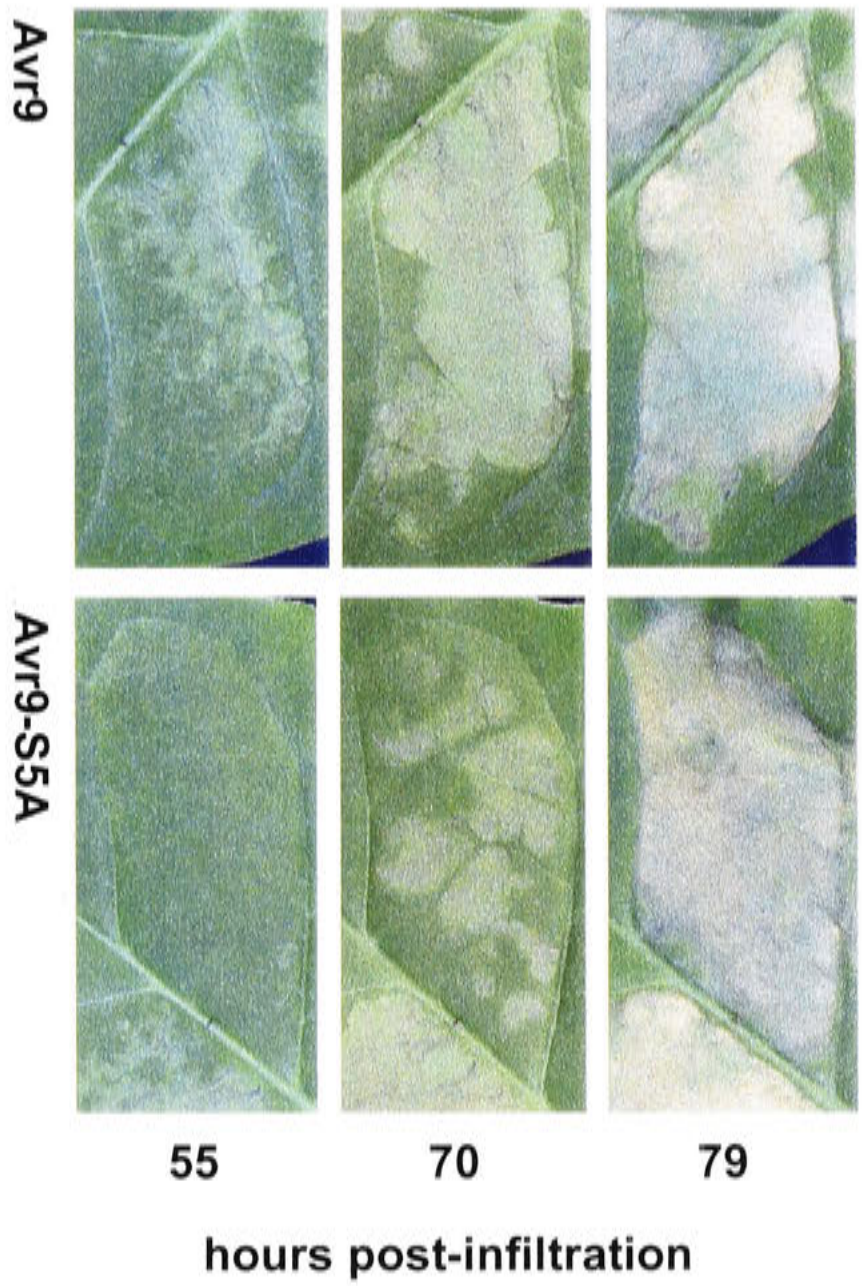

Figure 3.8. Pairwise comparison of Avr9 with Avr9-S5A by agroinfiltration. *Agrobacterium* containing either construct was infiltrated into the third fully expanded leaf of a *Cf-9* tobacco plant as described in the text. Single comparable leaf panels from the same leaf are shown for each Avr9 variant infiltrated (indicated at the left of the figure) at the time intervals indicated at the bottom of the figure.

3.4.4 Quantitative analysis of necrosis development

In an attempt to further dissect the differential temporal development of necrosis caused by the KDEL motif, a quantitative approach was used to analyse the response. It was hoped that this approach would corroborate the visual inspection of the response and be a useful way to observe other trends or make novel insights from the available data. To do this, the percentage of leaf panel area that was necrotic was measured over a time series, and plotted as a function of time for the control and experimental treatment. As discussed in the introduction to Chapter 2, previous quantitative analyses of necrotic responses following agroinfiltration have used a dose-response method, with the temporal development of necrosis only being shown qualitatively. Therefore, the quantitative analysis of temporal development described below is novel for this assay method.

The images from a comparison between Avr9 and Avr9-KDEL, taken at known intervals after infiltration, were chosen for quantitative analysis as these showed the typical KDEL dependent delayed necrotic response of interest. Initially, measurement of the leaf panel area and the percentage of that area that was necrotic was attempted using the threshold functions of Scion Image (release Beta 3b), ImageJ (version 1.24t) and SigmaScan® Pro (version 5). The threshold function allows the program to discriminate between zones of different colour, thus allowing them to be automatically selected by the software and therefore rapidly measured. SigmaScan® Pro had the most capable thresholding function, being able to do this in 24-bit colour (16.7 million colours), whereas the other programs were not so powerful in this respect. Nevertheless, this function was not sufficiently reliable to select necrosis from these images due to the variability in colour of the necrosis compared to the live tissue (i.e. the necrosis is flat light green immediately after tissue collapse, and darker after time had passed) and the variability of incident sunlight, which resulted in significant reflection during high light conditions and dull colours in low light.

Therefore, the manual selection function of SigmaScan® Pro was used to select necrosis and leaf panel area from high resolution 'jpeg' images (2048 x 1536 pixels) taken with a digital camera at each time point of the experiment. The area of the selected necrosis and leaf panel were measured and the percentage necrotic area calculated. Manual

selection of necrosis and leaf panels was found to be a reliable method for measurement of the percent of a leaf panel that was necrotic (Figure 3.9).

The percentage necrosis was determined for two leaves from the same Cf-9 plant (the third and fourth fully expended) each of which had been infiltrated in duplicate with Avr9, Avr9-KDEL and empty vector containing *Agrobacterium*. Percentage necrosis at each time point in response to infiltration of Avr9 or Avr9-KDEL was determined for images taken over a time series, and this data was plotted as percent necrosis against time (Figure 3.10). *Agrobacterium* containing empty vector did not induce necrosis (not shown). The raw data is plotted separately (Figure 3.10A), as well as the mean of percent necrosis ± the standard error of the mean at each time point for Avr9 and Avr9-KDEL treatments (n = 4, Figure 3.10B). This sampling method means that the variability between leaves, leaf panels and data acquisition is accounted for in the standard error values but not the variation between plants.

This analysis clearly supports the previous visual inspection of this same comparison (Figure 3.3), showing the KDEL dependent delay of necrosis of approximately 25 hours, and ultimately weaker necrotic response to Avr9-KDEL relative to Avr9. It should be noted that the low slope of these curves between the x-intercept and the first positive necrosis value for both constructs (Figure 3.10B) is an artefact of the duration between sampling. Visual observation indicates that the necrotic response proceeds evenly and rapidly after initiation, suggesting, by interpolation, that the true x-intercepts would be approximately 40 hpi (Avr9) and 65 hpi (Avr9-KDEL).

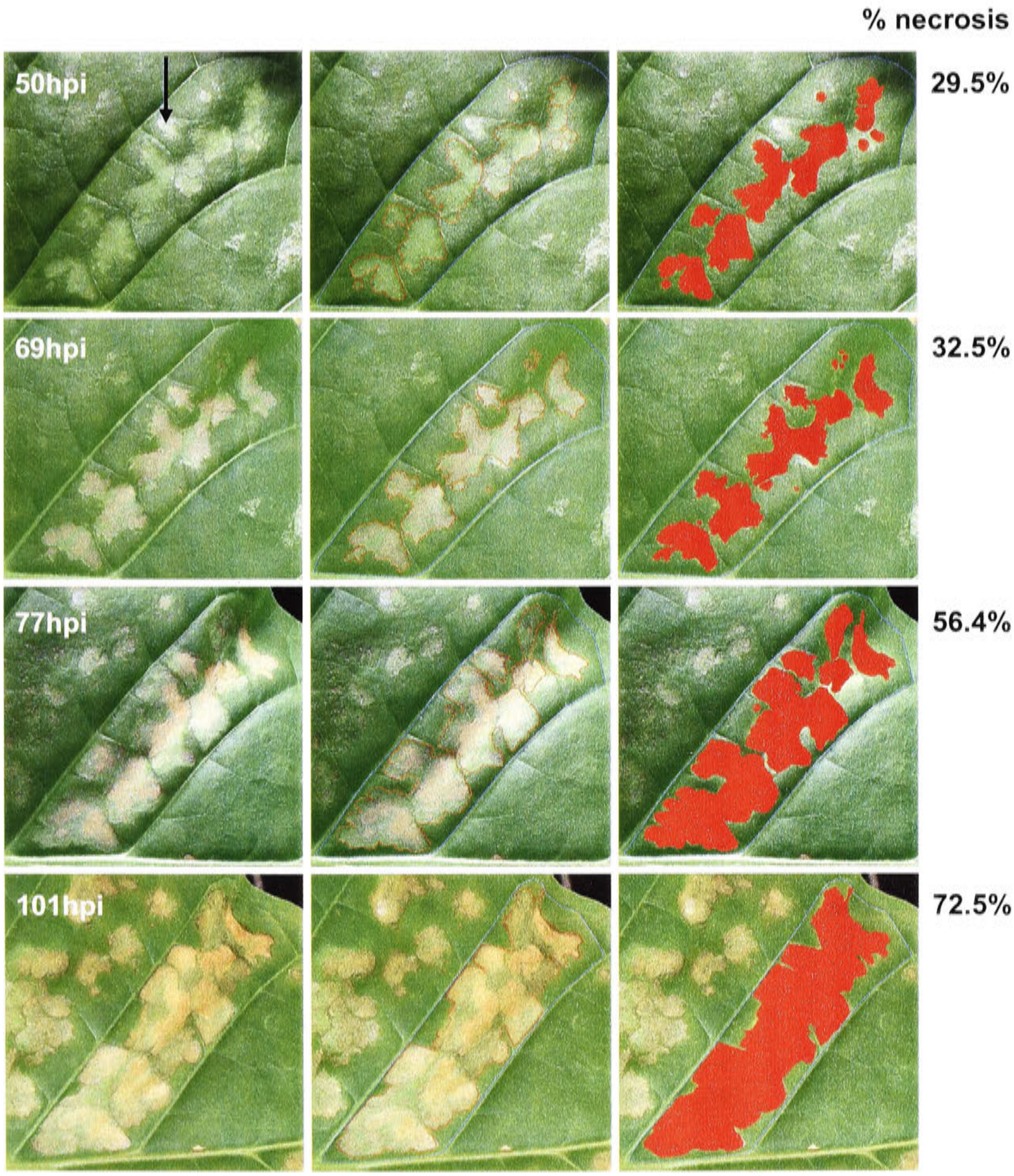

Figure 3.9. Electronic selection of necrosis for quantification of temporal development of necrotic response. The leaf panels shown are the same panel which was infiltrated with Avr9 containing *Agrobacterium* and photographed at the time intervals shown on the left (**hpi**). **A.** shows the leaf panel before selection, **B.** shows the necrosis (red line) and leaf panel (blue line) outlines and **C.** shows the necrotic area filled in (red) so as to determine the percentage of leaf panel area that was necrotic (shown on the right). The spot indicated with the black arrow in the 50 hpi panel was initially mistaken for a dried droplet of *Agrobacterium* preparation, so was not measured.

A.

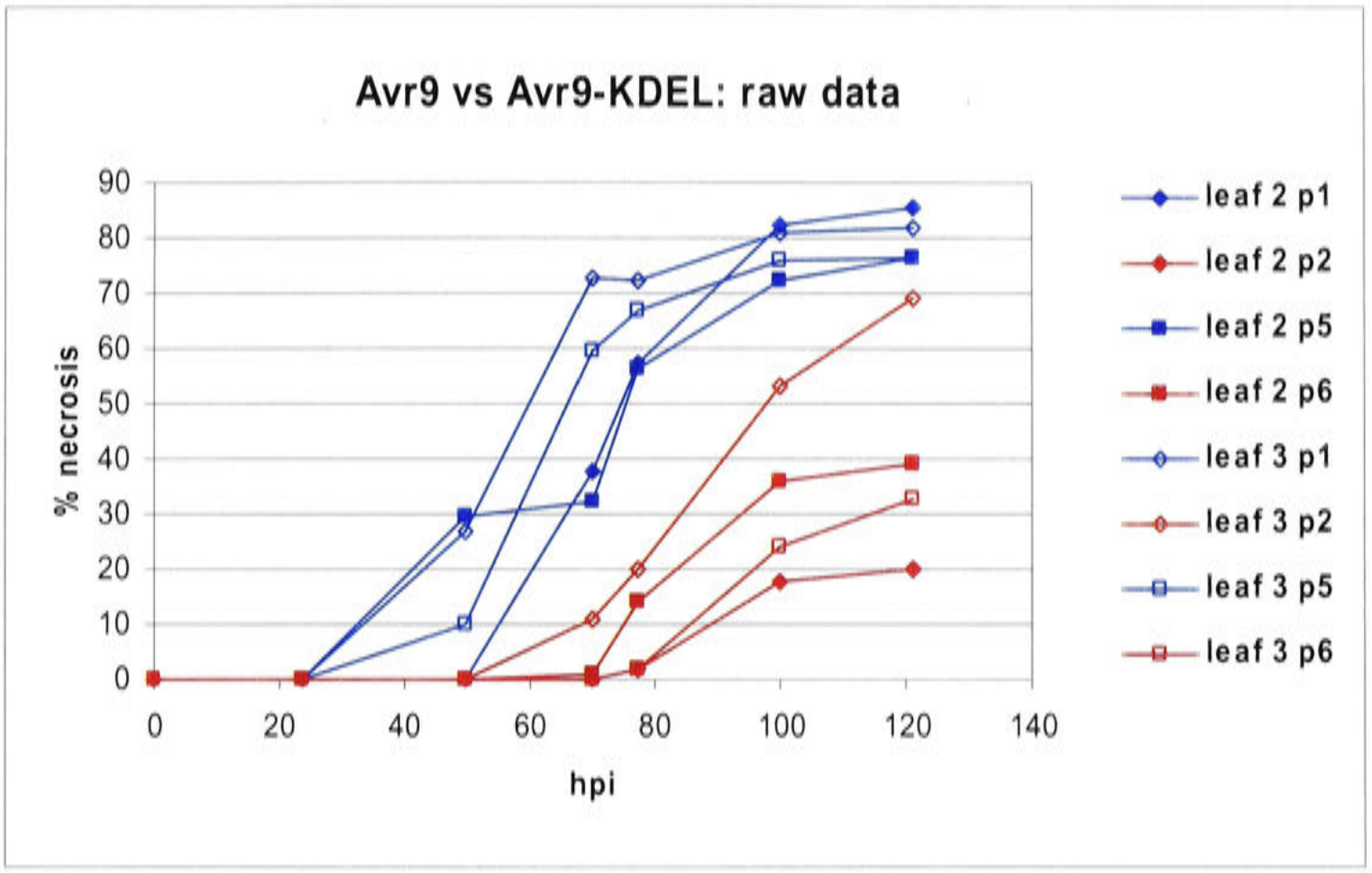

B.

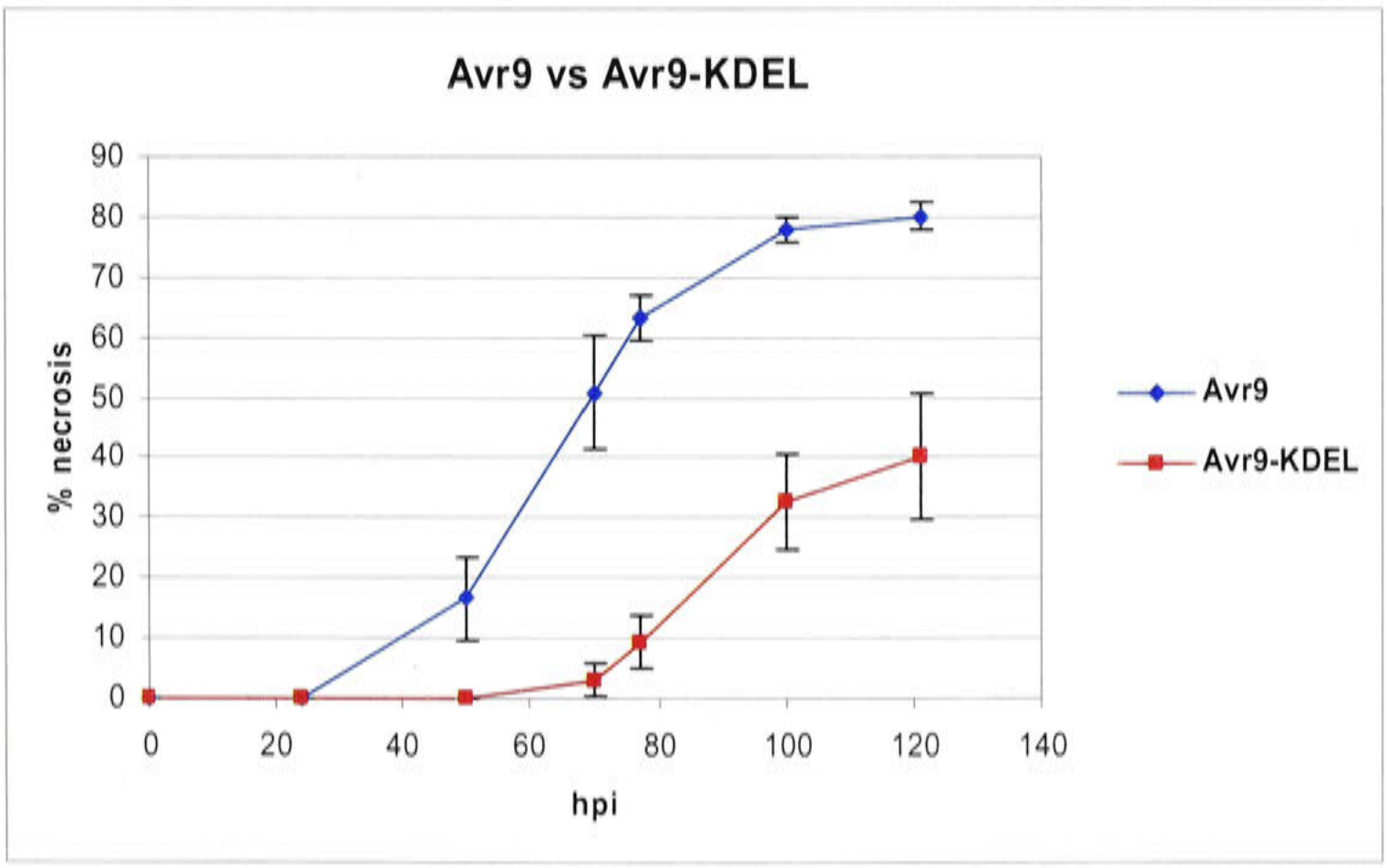

Figure 3.10. Quantitative analysis of the temporal development of necrosis in *N. tabacum*. *Agrobacterium* containing **Avr9** (blue) or **Avr9-KDEL** (red) was infiltrated in duplicate into each of two leaves of *Cf-9* tobacco as described in the text. The percentage of each leaf panel that was necrotic was determined as described, then plotted against hours post-infiltration (hpi) on the x-axis. **A.** The raw data for the two leaves (leaf 2 and 3) is shown: **p1** and **p5** are Avr9 leaf panels and **p2** and **p6** are Avr9-KDEL leaf panels, and empty vector infiltrated panels (which did not respond) are not shown. **B.** The mean (n = 4) and standard error of the mean for each time point is plotted against hpi.

3.5 DISCUSSION

3.5.1 Additional comments on the agroinfiltration assay

Necrosis inducing activity and delayed necrosis

It has been reported that higher activity of Avr4 compared to Avr9 can result in more rapid development of *R* gene specific necrosis using an agroinfiltration assay (Van der Hoorn *et al.* 2000; Chapter 2). An important observation made in that study was that at a dilution corresponding to 50% necrosis inducing activity for both of these constructs there was no difference in the timing of necrosis development, supporting the idea that the observed difference in timing was a result of the difference in activity.

The possibility that reduced activity of an Avr9 variant could cause delayed necrosis was tested in this research using the S5A mutant version of Avr9. This mutant of Avr9 has previously been shown, by dilution series assays of purified peptide, to have slightly reduced necrosis inducing activity compared to Avr9 (Kooman-Gersmann *et al.* 1998a). A dilution series comparison of Avr9 with Avr9-S5A by agroinfiltration detected reduced activity of Avr9-S5A, suggesting that the reported reduced activity can be detected using the agroinfiltration transient expression system (Figure 3.7D). However, only weak evidence was obtained to suggest that this reduced activity translated into any delay of necrotic response (Figure 3.8), although additional repetition may have resolved this.

One possible reason for the observed KDEL dependent delay of necrotic response observed in the experiments described in this chapter was that the KDEL tag disrupted the activity of Avr9. If so, this would have to be a larger reduction in activity than due to the S5A mutation, which caused little delay in necrosis using agroinfiltration (Figure 3.8). The possibility that the KDEL tag may interfere with Avr9 activity is supported by the dilution series comparison between Avr9 and Avr9-KDEL (Figure 3.7A), which indicates that Avr9-KDEL has weaker necrosis inducing ability than Avr9 using this assay.

Therefore, at least some component of the KDEL mediated delay might be attributable to this reduced activity of Avr9-KDEL compared to Avr9. To test this, Avr9-KDEL was compared to Avr9 tagged with KDDL, which is chemically almost identical to KDEL

but does not function as an ER retrieval motif (Figure 3.5). This comparison revealed that while the KDEL dependent delayed necrosis remained, a difference in activity judged by dilution series comparison was not evident between these two constructs (Figure 3.7B). This shows that the KDEL dependent delayed necrosis can be dissociated from the apparent reduction in activity caused by the KDEL tag, strongly suggesting that the KDEL dependent delayed necrosis is due to a factor other than reduced activity of this Avr9 variant. Also, while these data suggest that the KDEL tag does reduce the activity of Avr9, it does not indicate whether or not this results in a delayed necrotic response in the comparison of Avr9 and Avr9-KDEL. The fact that the delayed necrosis of Avr9-KDEL compared with Avr9-KDDL appears similar to that between Avr9 and Avr9-KDEL suggests that the component of the delayed necrosis attributable to the KDEL tag *per se* (i.e. physically rather than its biological activity) is only minor. The biological implications of this comparison are discussed in a later section of this discussion.

This issue could be resolved using tools developed during this work, by comparison of Avr9 with Avr9-KDDL. This would confirm or refute the hypothesis that the KDEL tag reduces Avr9 activity due to its physical presence rather than biological activity, and would determine whether any delay of necrosis results from the tag. This comparison would be informative for future studies using agroinfiltration to investigate the *Cf/Avr* gene-for-gene system as well as studies using proteins fused with KDEL-like ER retention sequences.

Quantitative analysis

The *Cf-9/Avr9* gene-for-gene system has previously been analysed quantitatively using agroinfiltration (Van der Hoorn *et al.* 2000). The approach used in the cited study was a dose-response analysis of *Cf-9/Avr9* and *Cf-4/Avr4* mediated necrosis, obtained by plotting percentage necrosis as a variable against the percentage of the culture containing the construct of interest. Increased activity of the *Cf-4/Avr4* gene pair compared to *Cf-9/Avr9* was observed and found to be attributable to the increased activity of the Avr4 construct using this method. Additionally, the delayed necrotic response of the *Cf-9/Avr9* interaction compared to *Cf-4/Avr4* interaction was represented qualitatively in a similar manner to this study (e.g. Figure 3.3), but no quantification of necrosis or statistical treatment was performed (Van der Hoorn *et al.* 2000).

The work reported in this chapter modified this previously reported analysis, using it to compare variants of a single Avr protein (Avr9 and Avr9-KDEL) by quantification of the temporal development of necrosis (Figure 3.9 and Figure 3.10). The mean value for percent necrosis at each time point (n = 4) for both constructs was plotted ± a standard error of the mean. However, since this experiment used duplicate leaf panels on each of two similar leaves from the one plant, this standard error represents within leaf variation, some between leaf variation and the variation in acquisition of the data, but not between plant variation. It could be suggested that because sampling is not fully independent, the standard error value is not a true value. However, since the comparisons are pairwise comparisons designed to account for the variability that was observed between leaves and between plants (Chapter 2), the standard error value obtained is a good reflection of the variability of the response.

This analysis confirmed previous observations of the KDEL dependent delayed necrosis, and appears to suggest a slower rate of necrosis in response to Avr9-KDEL compared to Avr9. However, further repetition and statistical analysis would be needed to confirm this latter observation. This apparent reduced rate of necrosis development may simply be a result of the ultimately weaker necrotic response to Avr9-KDEL. This could be tested by performing this type of analysis on a comparison between Avr9-KDEL and Avr9-KDDL. Since these Avr9 variants have similar activity as judged by dilution series analysis, any reduced rate of necrosis development would have to be a consequence of KDEL biological function.

One limitation to this approach is the variability of the assay between leaves. This means that a large number of equivalent leaves need to be sampled to resolve relatively minor differences between constructs. The repetition that this would require, in terms of the agroinfiltration assay and the manual (electronic) measurement of necrosis area, is feasible but would be somewhat laborious with larger numbers of repetition. Pilot experiments could be used initially to determine whether this approach would be warranted for a proposed experiment.

3.5.2 KDEL mediated delay of Cf-9 dependent necrosis

In order to determine whether Cf-9 could respond to Avr9 in the ER, Avr9 tagged with an ER retention motif and control Avr9 variants were expressed in *Cf-9* tobacco by

agroinfiltration. Pairwise comparisons between a range of Avr9 variants showed that the biologically active KDEL motif at the C-terminus of Avr9 is sufficient to delay Cf-9 mediated necrosis in tobacco leaves. This was initially shown by a comparison between Avr9 and Avr9-KDEL constructs by agroinfiltration (Figure 3.3). Quantitative analysis of this comparison suggested that the average delay of onset of necrosis was approximately 25 hours (Figure 3.10). When older, less sensitive leaves are used for this experiment, a larger KDEL dependent delay was observed (Figure 3.4), however this is most likely due to the generally reduced activity of these constructs in these older leaves exacerbating the differential response.

One possible cause of this delay was that, while retained in the ER, Avr9 carries the bulky ER specific core glycosylation, which might prevent its recognition in the ER. This hypothesis assumes that ER retention occurs as expected (see below) and that Cf-9 is capable of detecting Avr9 in the ER. The fact that Avr9 appears to be glycosylated when expressed in plants (with a single N-acetyl-hexosamine, Kooman-Gersmann *et al.* 1998a), suggests that while in the ER, this ubiquitous precursor (core) glycosylation must occur to Avr9. The ER specific core glycosylation $Glc_3Man_9GlcNAc_2$ (Ellgaard *et al.* 1999; Lerouge *et al.* 1998) would be a relatively bulky side-chain in relation to Avr9 (28 amino acids), and it is possible that such a structure could disrupt normal recognition of Avr9.

To test this possibility, a comparison was made between Avr9-S5A and Avr9-S5A-KDEL. The KDEL mediated delayed necrosis that was observed in previous experiments was repeated for this comparison, indicating that putative ER specific glycosylation of Avr9 is not preventing a response to Avr9 (±KDEL) in the ER using this assay. This comparison was made rather than, say, a comparison between Avr9-KDEL and Avr9-S5A-KDEL, since it accounted for the reduced activity of Avr9 resulting from the S5A mutation (Kooman-Gersmann *et al.* 1998a). The limited effect of the S5A mutation in the agroinfiltration assay (Figure 3.8) was not known when this experiment was conducted.

However, these comparisons did not exclude the possibility that the delayed necrosis was caused by disruption of Avr9 activity by the KDEL tag. To account for this, an Avr9 variant with a C-terminal KDDL motif was generated and compared to Avr9-KDEL over a time series (Figure 3.5) and by dilution series (Figure 3.7B). The KDDL

motif is almost chemically identical to KDEL yet is not a functional ER retrieval signal (Denecke *et al.* 1992; Denecke *et al.* 1993). Avr9-KDEL showed delayed necrosis compared to Avr9-KDDL (Figure 3.5), however no difference in activity between these constructs was observed by dilution series comparison (Figure 3.7B). This latter comparison suggested that indeed the C-terminal tag had disrupted the activity of Avr9. More importantly, these comparisons demonstrated that the KDEL dependent delayed necrosis is due to the biological activity of the KDEL tag (presumably ER retention), not disruption of Avr9 activity, since an equivalent delay is still present in this experiment. Additionally, this clearly implies that the fusion of the KDEL tag onto Avr9 is functional as an ER retrieval signal.

However, further work would be needed to *directly* demonstrate that ER localisation of KDEL tagged Avr9 is occurring, and could include a combination of Tricine-SDS PAGE (to resolve low molecular weight proteins, Schagger and von Jagow 1987), western blotting (antibodies have been generated against Avr9, Mahe *et al.* 1998; van den Hooven *et al.* 1999), glycosidase digestion and pulse-chase radiolabelling approaches. As glycosylation of Avr9 occurs when expressed in plants (Kooman-Gersmann *et al.* 1998a), it can be assumed that it is core glycosylated while in the ER, though this has not been demonstrated. By probing a western blot of total protein from tobacco leaf tissue expressing Avr9 (±KDEL) with antibodies against Avr9, a proportion should appear as the mature form reported by Kooman-Gersmann *et al.* (1998a), while some should also be present as a larger band corresponding to the expected core glycosylated form. Digestion of these protein extracts with a glycosidase such as PNGase F (which cleaves *N*-linked carbohydrates at the asparagine residue, Calbiochem 2000; Tarentino and Plummer 1994) or EndoH (which cleaves ER type simple glycans such as the ER core glycosylation, Calbiochem 2000; Tarentino and Plummer 1994) would confirm whether any observed larger form of Avr9 was indeed a product of core glycosylation *in planta*. This could then be performed on Avr9 and Avr9-KDEL expressing tissue, and if ER retention of Avr9-KDEL is occurring, the larger band corresponding to core glycosylated Avr9-KDEL should accumulate substantially more than the equivalent Avr9 band (e.g. Pagny *et al.* 2000). The accumulation in the ER could be confirmed using radiolabelling pulse-chase analysis to determine the half-lives of the ER glycoforms of Avr9 (±KDEL) (e.g. Denecke and Vitale 1995; Pagny *et al.* 2000). Alternatively, transmission electron microscopy using

immunogold labelled antibodies or immunofluorescence microscopy could be used to confirm ER localisation of Avr9-KDEL (e.g. Gomord *et al.* 1997; Herman *et al.* 1990). Another approach would be to make a construct encoding GFP fused to Avr9-KDEL and examine localisation using subcellular fractionation or microscopy. However this approach may not offer any strong advantages compared to the above mentioned methods, particularly for kinetic analysis of Avr9-KDEL retention in the ER.

3.5.3 Technical possibility for delayed necrosis

In the results and discussion above, several possibilities for the KDEL dependent delayed necrosis have been considered or excluded, however the question of why the fusion of a C-terminal KDEL tag onto Avr9 causes delayed Cf-9 mediated necrosis remains. One technical explanation of this observation may be that there were differences in the levels of Avr9 variant protein expressed due to differential transcript stability or translation efficiency. This seems unlikely because constructs were identical except for the few base changes introduced to generate the minor amino acid changes between Avr9 variants (see Materials and Methods). Furthermore, in the comparison of Avr9-KDEL with Avr9-KDDL, where the only difference is three bases (one of which leads to a single conservative amino acid substitution) the delay still occurs, strongly suggesting that differential transcript or protein production does not contribute to the differential necrosis. Though probably unnecessary, this could be determined directly using western blotting analysis on tobacco leaf tissue expressing the Avr9 variants by agroinfiltration.

3.5.4 Implications for Cf-9 function

The most likely explanation for the KDEL mediated delay of necrotic response observed in the above experiments is that it arises from the biological properties of the KDEL motif, namely ER retention. This is supported particularly by the comparisons of Avr9-KDEL to Avr9-KDDL, in which the KDEL dependent delay was still observed (Figure 3.5 and Figure 3.7B). There are a number of possible ways to interpret this result, depending upon which model for Cf-9 function (outlined in Chapter 1, Figure 1.2) is used as a hypothetical framework. Broadly speaking, Cf-9 could function in two ways: Model 1 - Cf-9 is involved in detection of Avr9 at the PM, but is retained in the ER temporarily as a quality control mechanism; or Model 2 - Cf-9 functions from the

ER, and Avr9 travels to the ER or initiates signalling from the PM to the ER, to which Cf-9 then responds.

Interpretations based on Model 1 - Cf-9 function at the PM

Based on a model in which Cf-9 functions at the PM, there are a few apparent possible causes of a delayed necrotic response when Avr9 is localised to the ER. Firstly, since expression of the Avr9 variant is driven by the CaMV35S promoter, it is likely that saturation of the retrieval, or incomplete retrieval of KDEL tagged Avr9 is occurring. As discussed in the introduction to this chapter, saturation of the HDEL mediated ER retrieval system has clearly been achieved in tobacco cells using heterologous proteins tagged with HDEL (Phillipson *et al.* 2001) or by overexpression of an endogenous ER resident protein (calreticulin) bearing a C-terminal HDEL sequence (Crofts *et al.* 1999). In this latter study, secretion of calreticulin (indicating saturation of retrieval) was achieved despite the fact that it is degraded in a post-ER compartment (Phillipson *et al.* 2001), indicating that substantial saturation of retrieval had occurred. However, there has been no clear demonstration that the KDEL retrieval system (as *potentially* distinct from the HDEL retrieval system) in plant cells is saturable. While mammals and yeast appear to utilise either KDEL or HDEL mediated retrieval respectively, plants use both readily (Hadlington and Denecke 2000). This, and the fact that plants apparently possess a number of paralogues of the ERD2 retrieval receptor, mean that it can not necessarily be concluded that the KDEL and HDEL retrieval systems of plants are equivalent. It would be interesting to examine the role of these multiple predicted ERD2 proteins in plants – it may be that different paralogues are involved in ER retrieval of KDEL or HDEL bearing proteins, or perhaps that one paralogue has both of these specificities, but has tissue specific expression. Nevertheless, it is reasonable to presume that retrieval of KDEL and HDEL bearing proteins would at least be somewhat similar, including with regard to how easily their retrieval mechanism is saturated.

Therefore, the high level of Avr9-KDEL expression that would be driven by the CaMV35S promoter could saturate the retrieval of Avr9-KDEL. This would allow Avr9-KDEL to progress through the secretory pathway and be secreted into the apoplast, from where the Cf-9 mediated necrotic response could be initiated. If the KDEL fusion to Avr9 was not completely functional, as has been observed for other heterologously tagged proteins (see introduction to this chapter), a similar scenario to this saturation hypothesis would be expected. In particular, incomplete retention would

allow partial, gradual secretion of Avr9-KDEL, resulting in a longer duration before reaching a threshold of Avr9-KDEL in the apoplast sufficient to initiate Cf-9 mediated necrosis. This possibility is supported by work by Zagouras and Rose (1989), who found that addition of a C-terminal KDEL signal to two secretory proteins retarded (but did not prevent) their exit from the ER, which significantly decreased the rate of their secretion (i.e. the half-time for secretion). The fact that secretion of the retrieved protein began almost immediately suggested that this phenomenon was not saturation of ER retrieval but incomplete retention of a heterologously fused KDEL motif (Zagouras and Rose 1989). This suggests that incomplete retention can result in a decreased level and rate of secretion, and is consistent with the hypothesis that partial retention (ineffective retrieval or saturation of retrieval) of Avr9-KDEL delays the necrotic response relative to Avr9, rather than simply preventing any response due to complete retention of Avr9-KDEL.

In plant cells, saturation of HDEL mediated retrieval was observed using α-amylase (a secreted protein) tagged with HDEL (Phillipson *et al.* 2001). Interestingly, no secretion of amylase-HDEL was observed for a period of 6-10 hours after transfection, while secretion was observed for non-retrieved amylase almost immediately. This clearly indicated that saturation of retrieval, but not inefficient retrieval, was causing delayed secretion of amylase-HDEL. Although this system cannot be directly compared to that used in the research described in this chapter, due to the use of different promoters, transient expression systems and marker proteins, this shows that the time required to saturate retrieval can cause delayed secretion of a heterologously tagged molecule. This is also consistent with the hypothesis that partial retention of Avr9-KDEL delays the Cf-9 mediated necrotic response relative to non-retrieved Avr9 variants.

This model of inefficient or saturated retrieval of Avr9-KDEL, and consequent delayed secretion, could be tested in a number of ways. In Chapter 4 of this thesis, a method for detection of Avr9 using MALDI-TOF mass spectrometry from tobacco leaf extracts is described. This method could be used to detect Avr9 or Avr9-KDEL after agroinfiltration into wild type tobacco leaves. At intervals after infiltration, samples of leaf tissue would be taken, extracted as described, and analysed by MALDI-TOF for the appearance of a peak corresponding to the processed form of Avr9 (±KDEL) (i.e. the previously observed form with the single N-acetyl-hexosamine), indicative of escape from ER retrieval. If Avr9-KDEL was escaping ER retention, it would be expected that

the peak corresponding to processed Avr9 would: 1) appear at an earlier time point than the Avr9-KDEL peak (as it would depart the ER more rapidly); and 2) be present at a higher dilution of *Agrobacterium* than the Avr9-KDEL peak (as the latter would likely be completely or mostly retained at lower expression levels).

A better way to determine whether ER retrieval of Avr9-KDEL and subsequent saturation of retrieval was occurring would be to directly observe the conversion of an ER specific glycoform into a non-ER (processed) glycoform upon saturation of retrieval rather than the appearance of a presumably processed form as suggested above. This would strengthen conclusions about ER retention and saturation of retrieval, as it would confirm assumption about ER specific glycoforms of Avr9 (±KDEL). However the MALDI-TOF approach may not observe all glycoforms of Avr9 (±KDEL), since the purification method could select against forms possessing larger carbohydrate side-chains during the acetone precipitation step (see Chapter 4 for details of the purification process). To account for this likely problem, the purification and MALDI-TOF analysis procedures would have to be modified based on empirical investigation.

A good alternative approach to observe whether ER retention and saturation of retention is occurring would be by western blotting and glycosidase digestion analysis (as described in Section 3.5.2) to determine whether characteristic ER or non-ER glycoforms of Avr9-KDEL are present. This method would not only confirm whether ER retention and core glycosylation of Avr9-KDEL occurs, but used in a time-course analysis would also show whether retrieval of Avr9-KDEL is saturated or inefficient. If saturation was occurring this would strongly implicate ER retrieval saturation and subsequent progression of Avr9-KDEL to the PM as the cause for KDEL dependent delayed necrosis. This would therefore support a model in which Cf-9 (or an intermediate component, see below) functions from the PM to detect Avr9 (±KDEL).

A second possible model is that Avr9-KDEL is fully maintained in the ER, with no saturation of retrieval, and some other factor allows departure of Avr9-KDEL from the ER after accumulation in the ER over a period of time, such as cleavage of the C-terminus to remove the KDEL signal. This would be likely to result in much the same necrotic response as would incomplete retrieval or saturation of retrieval, in that the accumulation of expressed Avr9-KDEL in the apoplast would initially be reduced, thus delaying the Cf-9 mediated necrotic response. This could be tested, as with the

possibility of saturation, by carbohydrate analysis to determine whether Avr9 (±KDEL) had left the ER. In addition, MALDI-TOF detection as developed and described in another chapter of this thesis could be used to determine the precise mass of the final form of Avr9 (±KDEL). This method can determine the mass of a peptide this size accurately enough to clearly demonstrate whether or not cleavage of Avr9-KDEL has occurred, and exactly what sequence had been cleaved.

A third possibility that would result in a similar delayed response to Avr9-KDEL is that the KDEL tag could direct molecules that escape the ER to the vacuole. This was observed for a protein that was artificially tagged with the HDEL motif, which was targeted to the vacuole in an HDEL dependent manner when it escaped ER retention (Gomord *et al.* 1997). However, this has not been observed with the KDEL motif, despite equivalent studies having been performed with the KDEL sequence (see introduction to this chapter). Similar studies have observed some vacuolar targeting of a vacuolar protein tagged with KDEL, but this could be the result of residual vacuolar targeting signals (Frigerio *et al.* 2001). If this was occurring to Avr9-KDEL in experiments in this chapter, it would be apparent using carbohydrate analysis only if vacuole specific carbohydrate modifications (Lerouge *et al.* 1998) to Avr9-KDEL could occur. As there is currently no evidence for this, subcellular fractionation to resolve the vacuole and its contents or immunolocalisation microscopy may be useful methods to determine whether any Avr9-KDEL had travelled to the vacuole.

Interpretations based on Model 2 - Cf-9 function in the ER

If Cf-9 was functional and capable of mediating a response to Avr9 in the ER, necrosis in response to Avr9-KDEL might be expected to be stronger and more rapid than that induced by Avr9 using the agroinfiltration assay. Based on a model in which Cf-9 functions in the ER, a few possible explanations of a delayed response to ER retained Avr9 are apparent.

Firstly, Avr9 could be sequestered in the ER by a KDEL specific binding protein, the most obvious candidate being the KDEL receptor protein, ERD2. However, a few lines of evidence suggest that this is unlikely. 1) ERD2 is predominantly a resident of the *cis*-Golgi apparatus and recycles from there to the ER (Boevink *et al.* 1998; Griffiths *et al.* 1994; Lewis and Pelham 1992; Townsley *et al.* 1993), so is unlikely to be capable of significant sequestration of KDEL bearing proteins in the ER. 2) The fact that some of

the ER resident proteins bearing KDEL or HDEL motifs are by far the most abundant proteins of the ER suggests that no other protein would be abundant enough to be involved in specific sequestration of these in the ER (Marquardt *et al.* 1993; Tatu and Helenius 1997). 3) Rapid diffusion of locally expressed BiP (independent of the KDEL tag) was observed in a *Xenopus* oocyte, while PM and ER membrane proteins remained stationary, suggesting that this KDEL bearing ER resident is not anchored to the ER membrane (Ceriotti and Colman 1988). 4) When calreticulin is over-expressed in tobacco cells, causing major dilation of the ER and nuclear envelope (Crofts *et al.* 1999), the calreticulin retained in the ER is distributed throughout the ER lumen, not at the ER membrane where ERD2 would be while in the ER. These factors clearly support a model in which H/KDEL proteins are not bound to H/KDEL specific receptors in the ER, but are retrieved after their departure from the ER (Munro and Pelham 1987; Pagny *et al.* 1999; Pelham *et al.* 1988; Pelham 1989; Pelham 1990; see also introduction to this chapter). One possibility that this model does not account for is the existence of other specific KDEL binding proteins, however since no such proteins other than ERD2 are known and since this receptor appears to fully account for KDEL mediated ER retrieval (Lewis *et al.* 1990; Lewis and Pelham 1992; Semenza *et al.* 1990), this seems unlikely.

A second possibility is that, if Cf-9 did function in the ER, it could be in a different subset of ER than that which the KDEL signal directs soluble retained proteins to. It has been reported that the KDEL and HDEL signals may direct proteins to different subsets of ER (Napier *et al.* 1992). From the data presented, it appears that HDEL retrieved proteins show perinuclear and cortical ER localisation while KDEL proteins show a spotted localisation. However, the authors could not rule out the possibility that the apparent KDEL specific localisation was due to an unusual localisation of the major KDEL bearing protein, the Auxin Binding Protein (ABP1). If this phenomenon is real, it is not certain which of these putative types of ER contains membrane anchored proteins bearing the C-terminal KKXX signal, such as Cf-9 (Benghezal *et al.* 2000; Cosson and Letourneur 1994). The fact that GFP fused to a membrane anchor containing a functional KKXX motif (from Cf-9) co-localised with BiP (an HDEL protein) in the cortical ER of live tobacco cells suggests that 'HDEL ER' and 'KKXX ER' could be equivalent (Benghezal *et al.* 2000).

Some evidence suggests that HDEL and KDEL bearing proteins inhabit similar types of ER was observed in a study that compared an expressed antibody (tagged with the

KDEL motif; an 'artificial reticuloplasmin') with the native HDEL bearing reticuloplasmin, calreticulin (Torres *et al.* 2001). Though the study was primarily aimed at showing different localisation of these proteins in tissue and cell types, the data presented also suggest that these retention motifs may direct proteins to similar types of ER. However, the data do not exclude the possibility that the properties of each given protein could influence localisation, as would be needed to conclusively demonstrate whether or not KDEL and HDEL sequences direct proteins to different types of ER (see below). For example, calreticulin may in part rely upon factors other than the HDEL motif for retention in the ER (see the introduction to this chapter).

Another report has suggested that a slightly different intercellular localisation is determined by the KKXX and KDEL motifs in mammalian cells (Lotti *et al.* 1999). Using the same marker protein, this study reported that the KKXX motif localised the marker protein mostly to the ER-Golgi intermediate compartment and the *cis*-Golgi apparatus, whereas the KDEL version was more localised to the ER. However, this intermediate compartment is not recognised in plant cells (Nebenfuhr and Staehelin 2001; Sanderfoot and Raikhel 1999; Vitale and Denecke 1999), and the demonstration of KKXX in the ER (Benghezal *et al.* 2000) rather than an intermediate compartment, is not consistent with this phenomenon occurring in plant cells.

Further experiments would certainly be needed to confirm whether KDEL, HDEL and KKXX direct proteins to distinct ER subsets. This could include introduction of multiple fluorescent proteins, each bearing different ER retention motifs, into the same cell and observing their respective localisations. Repetition of this approach on multiple cell and tissue types would be interesting to determine if this phenomenon (if repeatable) was wide spread, and would be particularly interesting if such a study revealed tissue specific ER retention.

Preliminary experiments were conducted in this research to test whether the HDEL motif might direct Avr9 to a putatively different form of ER from which Cf-9 could respond. This experiment consisted of a comparison between Avr9-HDEL and Avr9-HDDL (the latter being a non-functional analogue of the HDEL retrieval signal, Denecke *et al.* 1992; Denecke *et al.* 1993). Normal necrosis occurred in response to Avr9-HDDL, but there was no necrosis in response to agroinfiltration of the Avr9-HDEL construct (not shown). However, this experiment was performed on only one

occasion (the result was repeated on four leaves on two plants) and the constructs have not been confirmed by sequencing, preventing any meaningful conclusions. If this result can be confirmed, it could be interpreted in a number of ways and further experimentation would be needed to elucidate the implications of the result.

A model with an intermediate component at the PM

An alternative to interpretations based upon either PM or ER function of Cf-9 above could be that an intermediate step or extra factors exist at the PM. In this model, Cf-9 could be functional in either the PM or ER as described previously, but an upstream component or binding factor is present at the PM. When Avr9 (±KDEL) is expressed co-translationally into the ER, these factors would be absent and recognition would not occur. This model would need to assume that Avr9-KDEL escapes from the ER (see above models) in order to reach the PM and these putative extra components, after which normal recognition could occur. The additional factors could include the Avr9 target protein and/or intermediate proteins required for Cf-9 signalling. One candidate for an intermediate component is the Avr9 High Affinity Binding Site (HABS) that is known to be present on the PM of resistant and susceptible tomato cultivars (Kooman-Gersmann *et al.* 1996).

This model would be more complicated to test, although some indirect approaches may be able to resolve this issue. One possible method would be to conduct more definitive experiments to determine whether Cf-9 is indeed an ER resident protein. Other than optimising previous experiments that showed PM or ER localisation of the bulk of Cf-9 protein (Benghezal *et al.* 2000; Piedras *et al.* 2000), one other approach might be to use a cycloheximide chase (after a radiolabelling pulse) followed by subcellular fractionation, as was used to demonstrate ER localisation of the ethylene receptor in *Arabidopsis* (Chen *et al.* 2002). During cycloheximide incubation no new protein is synthesised, allowing any non-ER resident proteins to depart the ER. Proteins remaining in the ER after a suitable period of incubation are therefore being actively retrieved and are indeed ER resident. Using a system in which Cf-9 was fully functional, ideally under its own promoter, and an appropriate chase time, this approach would most likely demonstrate more clearly whether Cf-9 is a resident of the ER or PM.

Another possible approach would be to determine the fate of Avr9 when it is added exogenously to tobacco suspension cells (the aim of Chapter 4). If Avr9 binds to the

HABS at the PM, as would be expected, and remains there, this might suggest PM function of Cf-9 or initiation of signalling at the PM. If, after binding, Avr9 was subsequently internalised by the cell, this would imply function of Cf-9 within the compartment that Avr9 is transported to. This approach would be complementary to the approach described in this chapter, and is elaborated in Chapter 4.

3.5.5 Summary and general comments

The approach to determine the subcellular localisation of functional Cf-9 used in this work has not generated definitive evidence on this question, and it was not envisioned that it necessarily would. The approach taken was novel in gene-for-gene resistance research, in that ER retention signals and a transient *Agrobacterium*-mediated expression system were utilised to investigate the localisation of a functional R protein. The work in this chapter suggests that KDEL mediated retrieval of Avr9 to the ER delays the necrotic response initiated by Cf-9. From the evidence available in the literature, the simplest model to explain this is one in which Avr9-KDEL retrieval to the ER is eventually saturated, allowing progression to the PM. This model would suggest PM localisation of functional Cf-9 or intermediate components, upstream of the Cf-9, at the PM. Several approaches to further resolve this issue have been outlined. One of these approaches was intended to be performed as described in Chapter 4 of this thesis.

CHAPTER 4

PRODUCTION, PURIFICATION AND MALDI-TOF DETECTION OF AVR9

4.1 SUMMARY

PREVIOUS studies on subcellular localisation of Cf-9 have generated conflicting evidence on whether it is plasma membrane (PM) or endoplasmic reticulum (ER) localised. The previous chapter aimed to investigate this issue by examining whether Cf-9 could respond to ER localised Avr9. The work described in this chapter comprises the development of methods to investigate this same question using a complementary approach.

One hypothesis for Cf-9 function is that it functions from the ER, and detects Avr9 when the latter travels to the ER. If Avr9 does travel to the ER, it would be expected to be glycosylated on its natural N-glycosylation site. To test the hypothesis that Avr9 enters the ER, this work aimed to determine whether Avr9 becomes glycosylated when added exogenously to tobacco cells. Towards this goal, a published purification protocol was adapted for the recovery of Avr9 from crude plant extracts. In particular, the acetone clearance, ion-exchange chromatography (IEC) and C-18 reversed-phase chromatography steps of the purification protocol were adapted for this work. The published method was further developed by testing NaCl elution of Avr9 from IEC resin, using both concentration gradient and batch elution. After gradient elution and C-18 chromatography purification of Avr9 from intercellular washing fluids (IF) of transgenic Avr9 tobacco leaves, most protein in the resulting samples was not Avr9, even though Avr9 activity had been substantially concentrated in the samples. This is consistent with the fact that further purification was needed to isolate relatively pure Avr9 in the published protocol.

In parallel to the adaptation of the purification procedure, a MALDI-TOF mass spectrometry method was developed as a sensitive and accurate method for detection of glycosylation or any other *in vivo* modification to Avr9. MALDI-TOF mass

spectrometry was performed on samples at various stages throughout the purification procedure. A peak of 3394 Da was observed in IF from *Avr9* tobacco plants after acetone clearance and desalting, but not in IF from wildtype tobacco plants. Post-source decay analysis was attempted to independently verify the identity of the peak by its fragmentation pattern, but no degradation products were observed despite a relatively strong peak corresponding to Avr9. IEC purification of samples from *Avr9* tobacco plants significantly improved detection of Avr9 by MALDI-TOF.

To further adapt these methods for the intended experiments, purification and MALDI-TOF analysis was applied to crude leaf tissue extracts from Avr9 tobacco, however only very small amounts of Avr9 were detected in these experiments.

An Avr9 *E. coli* expression system was developed as a potential source of unmodified Avr9 to conduct these experiments. However in preliminary experiments only a limited amount of Avr9 detectable by MALDI-TOF was recovered and functionality of the peptide was not clearly demonstrated. Further work is needed to improve the level of Avr9 recovered from this expression system and to demonstrate its function.

The work presented is discussed with regard to the suitability of these methods for determining whether Avr9 is modified in tobacco cells, further work that could improve these methods and alternative ways to address the initial hypothesis.

4.2 INTRODUCTION

4.2.1 Biological mass spectrometry

Mass spectrometry (MS) is a method whereby a sample of interest is vaporised and ionised, then the resulting ions are accelerated according to their mass/charge (*m/z*) ratio (which is proportional to mass) and detected by a sensitive detector. The methods for ionisation and mass analysis are varied, and some forms of MS are well suited to the analysis of larger molecules found in biological systems due to the 'softer' ionisation methods used, which do not disintegrate the biopolymers of interest. Fast Atom Bombardment was the first ionisation method to allow routine analysis of thermally labile biomolecules of up to a few thousand Daltons (Da) by MS (Griffiths *et al.* 2001). This approach has since largely been superseded in biological research by Electrospray-

Ionisation (ESI) and Matrix-Assisted Laser Desorption/Ionisation (MALDI) methods (Griffiths *et al.* 2001; Yates 1998; see later sections for more detail).

A number of instrument types are available for mass analysis in conjunction with the above ionisation methods. In quadrupole mass spectrometers, ions are separated during transit through an electrical field established between four parallel metal rods (hence quadrupole; Chernushevich *et al.* 2001; Yates 1998). The triple quadrupole mass spectrometer has a series of three quadrupole mass spectrometers; typically the first selects the ion species of interest, the second induces dissociation of the ion and the third analyses the mass of the resulting dissociation products (Siuzdak 1994; Yates 1998). This series of mass spectrometers can be modulated in order to achieve different types of analyses, for example the first can be used to scan for specific structural features and the second to select for a particular *m/z* (Yates 1998). In quadrupole ion trap mass spectrometry, one of the quadrupoles traps the ion species of interest in a three dimensional electric field, allowing further analysis by manipulation of the electrical field (Yates 1998). One advantage of this latter approach is that multiple ion dissociation steps can be used to gain additional structural information about the ion species of interest.

In Time Of Flight (TOF) mass analysers, the ionised sample is accelerated by an electrical field and ions 'fly' to the end a long chamber (the 'flight tube'), where they impact with the ion detector. Since all ions receive the same kinetic energy, the 'flight time' to the detector is proportional to their *m/z*. As MALDI produces mostly singly charged ionic species, the *m/z* corresponds to the molecular mass of the ion.

In tandem MS (MS/MS), multiple mass analyser types are used together in order to generate specific MS capabilities. A well known form of tandem MS used for analysis of biomolecules is quadrupole time of flight mass spectrometry (Q-TOF; Chernushevich *et al.* 2001) although others such as TOF-TOF can be used (Lin *et al.* 2003). The Q-TOF is essentially a triple quadrupole mass spectrometer with the last quadrupole replaced by a TOF analyser (Chernushevich *et al.* 2001), the benefits of which include high sensitivity, resolution and accuracy.

While most of these mass analysis methods are compatible with MALDI and ESI ionised samples, the utility of such combinations depends on the physical and chemical properties of the different ionisation and mass analysis processes (Chernushevich *et al.*

2001; Griffiths *et al.* 2001; Yates 1998). For example, while TOF has always been considered the obvious mass analyser to use with MALDI ionisation, this ionisation method is effectively incompatible with quadrupole mass analysers (Chernushevich *et al.* 2001).

The main types of mass spectrometry amenable to study of biological systems, that have consequently become widely adopted, are ESI-MS (usually in conjunction with a triple quadrupole mass spectrometer) and MALDI-TOF MS (Bakhtiar and Tse 2000; Chaurand *et al.* 1999; Ferguson and Smith 2003; Hop and Bakhtiar 1997), and these methods will be outlined in more detail.

ESI-MS

ESI-MS can detect proteins of up to 100 000 atomic mass units (amu), at concentrations as low as the fempto- to low pico-molar range with an accuracy of ~0.05% (Bakhtiar and Nelson 2000; Bakhtiar and Tse 2000; Ferguson and Smith 2003; Hop and Bakhtiar 1997). The sample of interest is dissolved in the appropriate solvent and introduced into the spectrometer (under a vacuum) through a fine needle, and due to the electrical potential of the needle and solvent evaporation, the sample particularises (Figure 4.1A; Bakhtiar and Tse 2000; Hop and Bakhtiar 1997). Samples ionised by this method can then be mass analysed by acceleration in a strong electrical field and the *m/z* of the molecules in the sample determined. A number of types of mass analysers can be used in conjunction with ESI, including quadrupole and Fourier transform mass spectrometers (a type of ion trap mass spectrometer, see above; Griffiths *et al.* 2001; Hop and Bakhtiar 1997).

Due to the chemistry of the particularisation process, ESI-MS tends to produce multiple-charged analyte species (Bakhtiar and Nelson 2000). Since mass spectrometers measure *m/z* (which is proportional to mass) rather than the mass itself, this results in a series of multiple-charged peaks being detected for any one analyte (Hop and Bakhtiar 1997). The size of each of the multiple peaks can then be used to calculate an accurate mass of the analyte by 'deconvolution'.

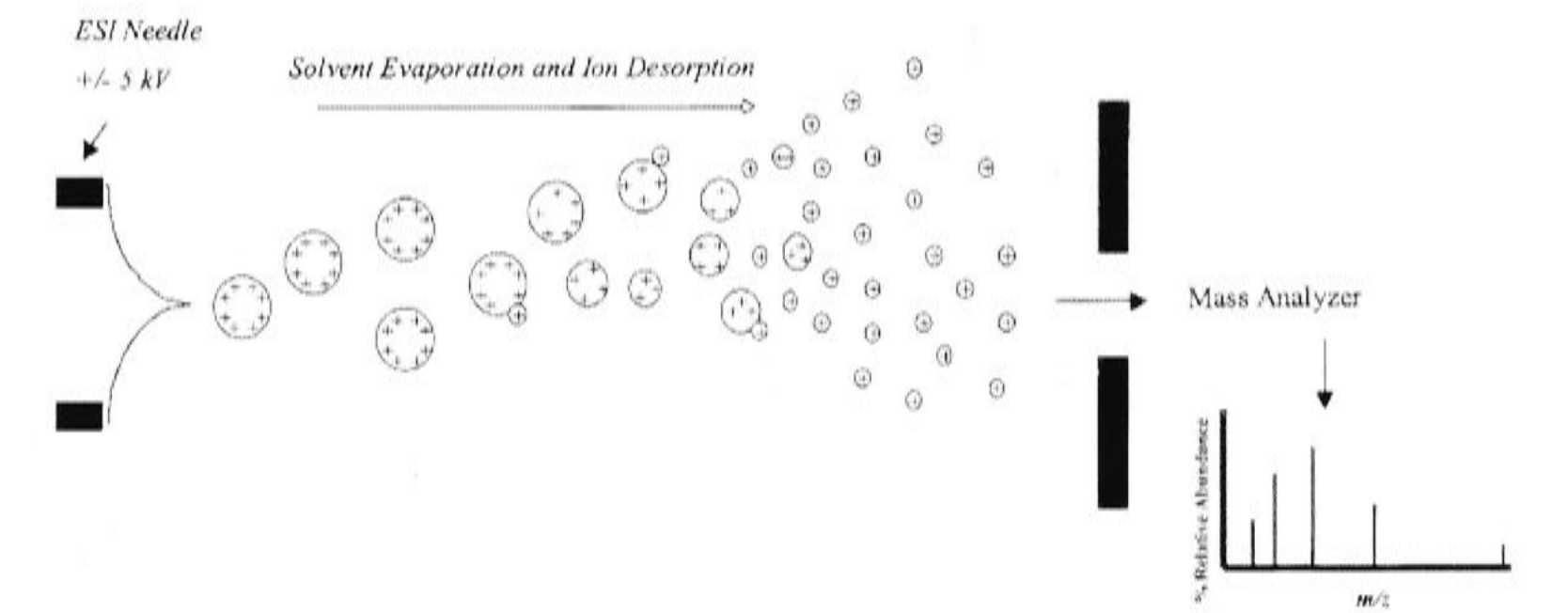

Figure 4.1. Sample ionisation by **A.** Electrospray Ionisation (ESI) and **B.** Matrix-Assisted Laser Desorption/Ionisation (MALDI). After sample ionisation by either method, the ion mixture is extracted into one of multiple types of **mass analyser** (see text for details) for *m/z* analysis. Images were taken from Bakhtiar and Nelson, (2001).

MALDI and MALDI-TOF MS

This section gives an overview of MALDI MS, and unless specifically referenced, general information is taken from a range of sources (Bakhtiar and Nelson 2000; Bakhtiar and Tse 2000; Ferguson and Smith 2003; Hop and Bakhtiar 1997; Micromass 1997). MALDI-TOF MS can detect proteins of up to 1 000 000 amu, and is also sensitive in the fempto- to low pico-molar range and very accurate (≤0.1-0.01%; Bakhtiar and Nelson 2000; Hop and Bakhtiar 1997; Micromass 1997).

The ionisation process used in MALDI MS is assisted by a matrix molecule, which is usually an organic acid that is supplied in excess and co-crystallised with the sample onto the target plate (Bakhtiar and Tse 2000; Hop and Bakhtiar 1997). One consequence of the use of an organic molecule as a matrix is that molecules below ~650 amu cannot be studied using MALDI MS, since this mass range is swamped by non-specific matrix signal and related noise. The co-crystallised matrix/sample on the target plate is ionised by a pulse laser beam (typically a N_2 laser at 337 nm) tuned to the absorption range of the matrix molecule, after which the desorbed/ionised sample is extracted from the chamber by an electrical charge (Figure 4.1B). One advantage of this approach is that extraction of the ionised sample can be delayed (after the laser pulse) which allows a more uniform extraction and thus improved resolution.

In the case of MALDI-TOF mass spectrometry, the sample is extracted into the TOF analyser after ionisation (Figure 4.2A). More modern TOF systems have a reflector device ("reflectron") towards the end of the flight tube, which acts to focus ions and turn them around towards a detector at the other (ion originating) end of the flight tube (Figure 4.2). This focussing by the reflector in combination with the delayed extraction method improves mass resolution considerably compared to linear mass analysers (Chaurand *et al.* 1999).

In addition, the reflector allows analysis of the analyte post-source decay (PSD; Figure 4.2C). Decay during MALDI-TOF MS can occur 'in-source' (i.e. in the ionised sample) or 'post-source' (i.e. in the TOF analyser, during flight). PSD of the analyte of interest can be analysed by 'gating' out all ions except that of interest, then gradually decreasing the energy with which these ions are reflected to their detector (Figure 4.2C). Since only the ion of interest has entered the TOF, only fragmentation products of this peak will be detected. The size of the reflected (smaller) decomposition products can then be used to

determine the fragmentation pattern of the analyte. As protein products often decompose by sequential amino-acid loss, the sequence of peptide fragments can often be determined using the appropriate software (Chaurand *et al.* 1999). Drawbacks to this approach for peptide sequencing are that the resultant spectra are sometimes complicated and therefore difficult to interpret, and that the approach does not work for all proteins (Chaurand *et al.* 1999).

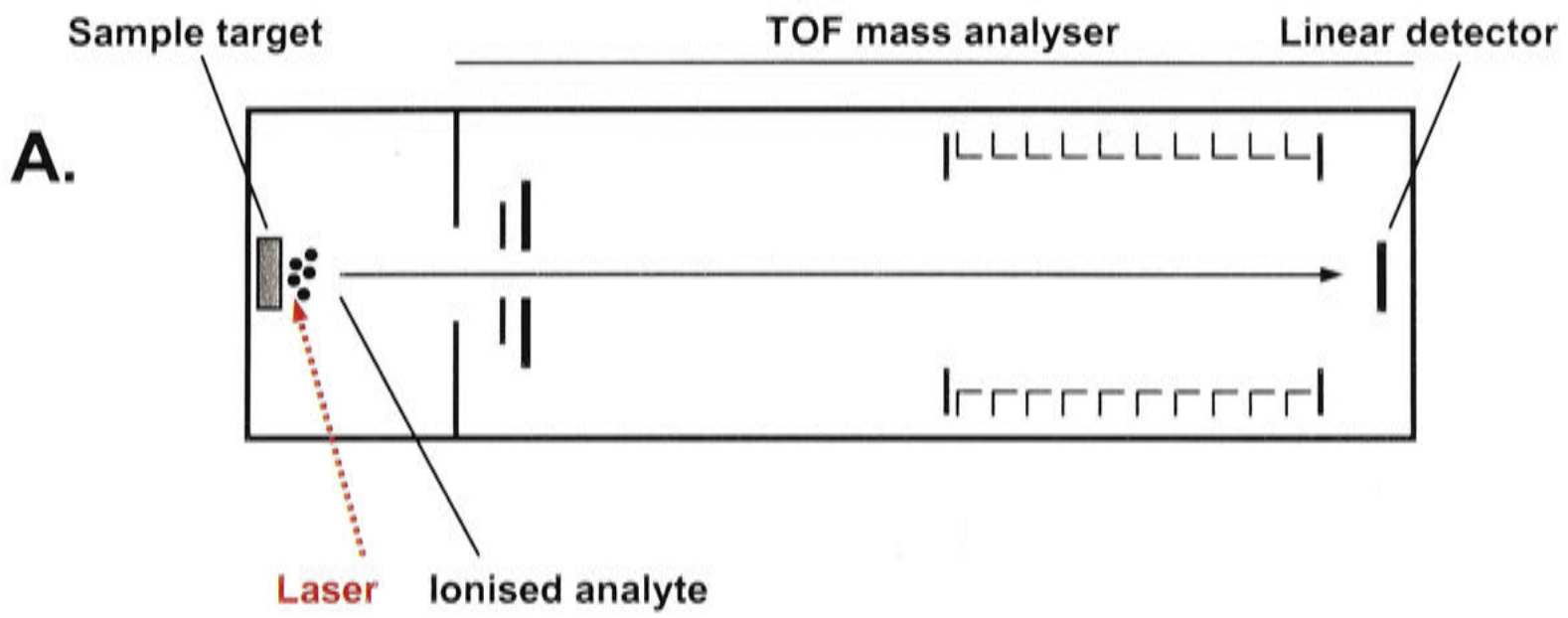

Figure 4.2. MALDI-TOF using: **A.** a linear TOF analyser; and **B.** using a reflector ("reflectron") to 'focus' the sample. The sample molecules are indicated by black dots and other components of the mass spectrometer are labelled (see text for details). **C.** Post-Source Decay (PSD) analysis of the analyte of interest. The molecule (mass range) of interest (yellow) is gated from background molecules of other molecular mass (black) using the ion gate. In reflectron mode, breakdown products of the molecule of interest (red) are detected by the reflectron detector as a molecule of lower mass.

4.2.2 Avr9 biochemistry

Avr9 is a race-specific elicitor from the tomato fungal pathogen *Cladosporium fulvum* (Joosten and de Wit 1999). The predominant 28 amino acid mature form of Avr9 peptide produced during *C. fulvum*/tomato interaction is derived from a 63 amino acid pre-pro-protein (Table 4.1), although intermediate forms of 32, 33 and 34 amino acids are also present during the interaction (Van den Ackerveken *et al.* 1993).

Table 4.1. Sequence variants of the Avr9 peptide. The N-glycosylation site is underlined and the N-terminal tyrosine of the mature 28 amino acid (aa) version of Avr9 is shown in bold.

Peptide sequence	Isoform/Origin	Reference
YCNSSCTRAFDCLGQCGRCDFHKLQCVH	mature 28 aa / infection	(Scholtens-Toma and de Wit 1988)
GVGLD**Y**CNSSCTRAFDCLGQCGRCDFHKLQCVH	33 aa / one partially processed form present during infection	(Van den Ackerveken *et al.* 1993)
MKLSLLSVELALLIATTLPLCWAAALPVGLGVGLD**Y**CNSSCTRAFDCLGQCGRCDFHKLQCVH	63 aa / predicted from cDNA	(van Kan *et al.* 1991)
MGFVLFSQLPSFLLVSTLLLFLVISHSCRA**Y**CNSSCTRAFDCLGQCGRCDFHKLQCVH	PR1aSP:Avr9 / pSLJ6201	(Hammond-Kosack *et al.* 1994a)
MDA**Y**CNSSCTRAFDCLGQCGRCDFHKLQCVH	*E. coli* expressed	(This chapter)

Proton Nuclear Magnetic Resonance spectroscopy (^{1}H-NMR), a method that allows the determination of the nature and context of functional chemical groups, was performed on the 33 aa form of Avr9 in order to elucidate its 2- and 3-dimensional structure (Vervoort *et al.* 1997). This study found strong evidence that Avr9 is a cystine knot peptide, a protein with two disulphide bridges that form a ring with a third disuphide bridge through the ring. The overall structure was found to consist of 3 antiparallel strands that form a rigid β-sheet, very similar to that of the carboxy peptidase inhibitor (Vervoort *et al.* 1997).

More recent studies used *in vitro* synthesis and folding of Avr9 to investigate the kinetics of folding and disulphide bond formation under various conditions (Mahe *et al.* 1998; van den Hooven *et al.* 1999). Approximately 60-70% of the synthesised peptide could be folded into the biologically active form (van den Hooven *et al.* 1999). More

recently, the location of the disulphide bonds in Avr9 was investigated using a combination of partial peptide reduction, HPLC, MALDI-TOF mass spectrometry and peptide sequencing, providing strong evidence that Avr9 is indeed a cystine knot protein (van den Hooven *et al.* 2001).

Analyses of Avr9 and a range of Avr9 mutants have been performed using ESI-MS (Kooman-Gersmann *et al.* 1998a). Avr9 was extracted from transgenic Avr9 tomato, *N. clevelandii* infected with Potato Virus X expressing Avr9 (PVX:Avr9), compatible tomato leaves infected with *C. fulvum* ('wildtype' Avr9) and chemically synthesised variants of Avr9. Wildtype and chemically synthesised variants of Avr9 were observed at the predicted molecular mass (3198 Da; or different for the mutant versions, according to the amino acid change). However in transgenic tomato or PVX:Avr9 infected tobacco, the peak corresponding to Avr9 was observed to be 202 Da larger than predicted. While only the larger peak was present in PVX:Avr9 infected tobacco, both peaks appeared equally in transgenic tomato. Interestingly, the S5A mutant of Avr9, which knocks out the predicted N-glycosylation site on Avr9 (Table 4.1), did not have the extra 202 Da mass, and neither did the wildtype peptide from the infection. These data were interpreted to indicate that Avr9 is glycosylated when expressed in plants, probably by an N-acetyl-glucosamine moiety (Kooman-Gersmann *et al.* 1998a), although it could be any naturally occurring N-acetyl-hexosamine (e.g. N-acetyl-galactosamine, Banks *et al.* 2001).

No reports have since been published about this highly unusual glycosylation pattern on Avr9 when expressed *in planta*, though its significance probably only relates to glycoprotein biology, not Avr9 function. Some suggestions are made in a previous chapter of this thesis for analysing this glycosylation further (see discussion of Chapter 3). Additionally, there have been no reports of mass spectrometry analysis of Avr9 expressed in *N. tabacum*, including the SLJ6201F transgenic Avr9 line used in this thesis and elsewhere (Hammond-Kosack *et al.* 1994a; Hammond-Kosack *et al.* 1998).

4.2.3 Aim of this chapter

Published studies on the subcellular localisation of Cf-9 have generated conflicting evidence on whether it is a PM or ER localised protein (see introductory chapter). In Chapter 3, this issue was considered by localising Avr9 to the ER using KDEL tagged variants of Avr9 expressed by agroinfiltration.

This section aimed to address the question of the localisation of functional Cf-9 by examining the fate of Avr9 peptide. If Cf-9 functions from the ER, then one prediction is that Avr9 travels to the ER. Indeed, a model in which Avr9 is endocytosed and travels to the ER has been mooted previously (Benghezal *et al.* 2000; Joosten and de Wit 1999).

To test this model, the work described in this chapter aimed to determine whether or not Avr9 enters the plant cell. It was intended to take advantage of the natural N-glycosylation site on Avr9, and use its glycosylation as a marker for entry into the ER. This glycosylation could include either the core glycosylation that occurs in the ER, or addition of the 202 Da residue previously observed (above). Alternatively, other unknown modifications may occur to Avr9 if it undergoes retrograde transport.

Similar experiments have been performed in other systems. In an experiment with the ricin toxin from castor bean, trafficking to the ER was observed after endocytosis of the toxin by mammalian cells (Rapak *et al.* 1997). Ricin toxin engineered to contain a glycosylation site was added to cells and shown to subsequently acquire an EndoH sensitive carbohydrate residue, indicating transport to the ER (Rapak *et al.* 1997). A similar study was performed using the bacterial Shiga toxin (Johannes *et al.* 1997), which showed ER-specific glycosylation of this peptide after retrograde transport. In another study, glycosylation of an exogenously added synthetic reporter peptide bearing an N-glycosylation site and KDEL motif was used as a marker for entry into, and retrieval in, the ER (Miesenbock and Rothman 1995).

In the abovementioned experiments, glycosylation was observable by SDS-PAGE as the residues added were quite large. However, there is currently no direct evidence that Avr9 would be glycosylated in the same way when expressed in the ER of plant cells, although this is probably the case. It is also possible that the N-acetyl-hexosamine that appears to be added to Avr9 is a novel glycosylation type, rather than an unusually processed form derived from ER core glycosylation. In any case, this modification would be too small to be detected by SDS-PAGE.

Due to this uncertainty, an alternative approach to detect any possible modification to Avr9 was considered appropriate. MALDI-TOF mass spectrometry was considered suitable for this purpose, as it is highly sensitive, can very accurately determine the mass of a peptide, and can be used to analyse components of complicated mixtures

(Bakhtiar and Nelson 2000; Chong *et al.* 1997; Domin *et al.* 1999; Li *et al.* 2000; Wang *et al.* 1998). This method was chosen over other forms of MS suitable for biomolecules for two main reasons. Firstly, as mentioned, one strength of MALDI-TOF is that it is amendable to analysing analyte mixtures. This was considered necessary in order to detect Avr9 from different semi-pure extracts generated throughout the purification procedures described in this chapter. Secondly, sample analysis by MALDI-TOF is very rapid, thus facilitating analysis of multiple fractions from different purification experiments in a timely manner.

However, prior to performing any experiment intended to detect modifications to Avr9, suitable methods for extraction, purification and MALDI-TOF detection of Avr9 needed to be developed. It was necessary to show that Avr9 could be: 1) extracted (pure or semi-pure) from multiple source materials; and 2) sensitively detected from these extracts by MALDI-TOF mass spectrometry. Most of the work described in this chapter was directed towards these goals, and is therefore developmental in nature. This consisted of the adaptation of a purification procedure from the literature to partially purify Avr9 from transgenic tobacco intercellular washing fluids (IF) and other sources, and the development of a MALDI-TOF procedure to detect Avr9 from samples during the purification procedure.

4.3 MATERIALS, METHODS AND RESULTS

4.3.1 Isolation of IF from SLJ6201F and wildtype tobacco

In order to perform the experiments outlined in this chapter, purified Avr9 protein was required. Initially, published purification methods were applied to samples of IF from transgenic SLJ6201F tobacco plants expressing Avr9, as this was a convenient and plentiful source of functional Avr9. The SLJ6201F tobacco lines express Avr9, under the control of the CaMV35S promoter, with the signal peptide from PR1 fused to the N-terminus to direct secretion of the predicted mature 28 amino acid peptide into the apoplast (Hammond-Kosack *et al.* 1994a).

IF was isolated essentially according to De Wit and Spikman (1982). Briefly, healthy leaves from SLJ6201F plants had their main veins removed, then they were immersed in

deionised water, placed under vacuum and the vacuum released so that water filled the intercellular spaces. Leaves were then blotted dry, cut into strips, gently rolled, placed into syringe barrels and then into centrifuge tubes and centrifuged at 1510 x g for 10 minutes at room temperature. IF was collected and then incubated at 95°C for 10 minutes, frozen, thawed and re-centrifuged to remove additional precipitate, then stored at -20°C. As expected, infiltration of the IF isolated from *Avr9* tobacco into the leaves of *Cf-9* tobacco plants caused *Cf-9* and Avr9 dependent necrosis (Figure 2.2, Chapter 2). In addition to adaptation of Avr9 purification methods, IF was also used as a source of Avr9 for the development of the MALDI-TOF detection method.

4.3.2 Purification and bioassay of Avr9

Acetone clearance of IF

Purification of Avr9 from tobacco Avr9 IF was performed using an adaptation of previously published protocols (Figure 4.3; Honée *et al.* 1995; Kooman-Gersmann *et al.* 1997; Van den Ackerveken *et al.* 1993). IF was cleared by adding an equal volume of acetone to IF from Avr9 and wildtype tobacco, incubated overnight at -20°C. The sample was centrifuged at 1510 x g for 10 minutes at 4°C and the pelleted precipitate discarded. The acetone was removed from the supernatant by rotary evaporation under vacuum in a 50°C water bath. As the rotary evaporation procedure removes some water from the extract in addition to the acetone, samples were typically diluted to a concentration equivalent to, or relative to, the original IF concentration for subsequent experiments (as indicated throughout text).

Acetone-cleared IF from Avr9 or wildtype (control) tobacco plants was infiltrated into *Cf-9* and wildtype tobacco plants (Figure 4.4). The necrotic response in the panels infiltrated with Avr9 after acetone precipitation and rotary evaporation showed that functional Avr9 was recovered by this method, as expected. The lack of response after infiltration of the same extracts into the wildtype leaf showed that the response was Cf-9/Avr9 specific and that any residual components arising from the procedure itself did not elicit necrosis. The stronger response of extracted IF (diluted to the equivalent of its original concentration) compared to un-extracted IF (diluted 20-fold) showed that more than 5% of the original activity was recovered (Figure 4.4). Further work proceeded on the assumption that no substantial losses occurred during this step.

Source

➔ IF – Intercellular Fluid wash

➔ LE – Leaf extract from tobacco

➔ LB – LB medium from *E. coli* culture

↓

Acetone clearance

➔ Acetone precipitate

➔ Recover supernatant, rotary-evaporate

➔ Bioassay to show recovery (IF, Figure 4.4)

➔ MALDI-TOF (IF, n.d., Figure 4.9; and LE, n.d., n.s.)

➔ Centricon desalt (IF, bioassay and MALDI-TOF, Figure 4.10 and Figure 4.11)

↓

Ion-Exchange Chromatography

➔ Binding capacity test (IF, Figure 4.5)

➔ Column binding and NaCl gradient elution (IF, bioassay, Figure 4.6)

➔ Batch elution preliminary test with 100-500mM NaCl (IF, bioassay, Figure 4.7)

➔ Batch elution with 200mM NaP, pH 8.0 (IF, MALDI-TOF, Figure 4.12)

↓

C-18 Reversed-Phase Chromatography

➔ Sep-Pak purification after IEC gradient elution, and bioassay (IF, Figure 4.8)

➔ Ziptip purification after batch elution (200mM NaP), then MALDI-TOF (IF, Figure 4.12; LE, Figure 4.13; LB Figure 4.14).

Figure 4.3. Flow chart summary of Avr9 purification, bioassay and MALDI-TOF analysis experiments described in this chapter. Relevant figures are indicated at the appropriate step. Sources are **IF** (intercellular fluid wash from transgenic Avr9 or wildtype *N. tabacum* leaves), **LE** (whole transgenic Avr9 or wildtype *N. tabacum* leaf extracts) and **LB** (LB culture medium from *E. coli* culture expressing Avr9). **n.d.** is not detected and **n.s.** is not shown.

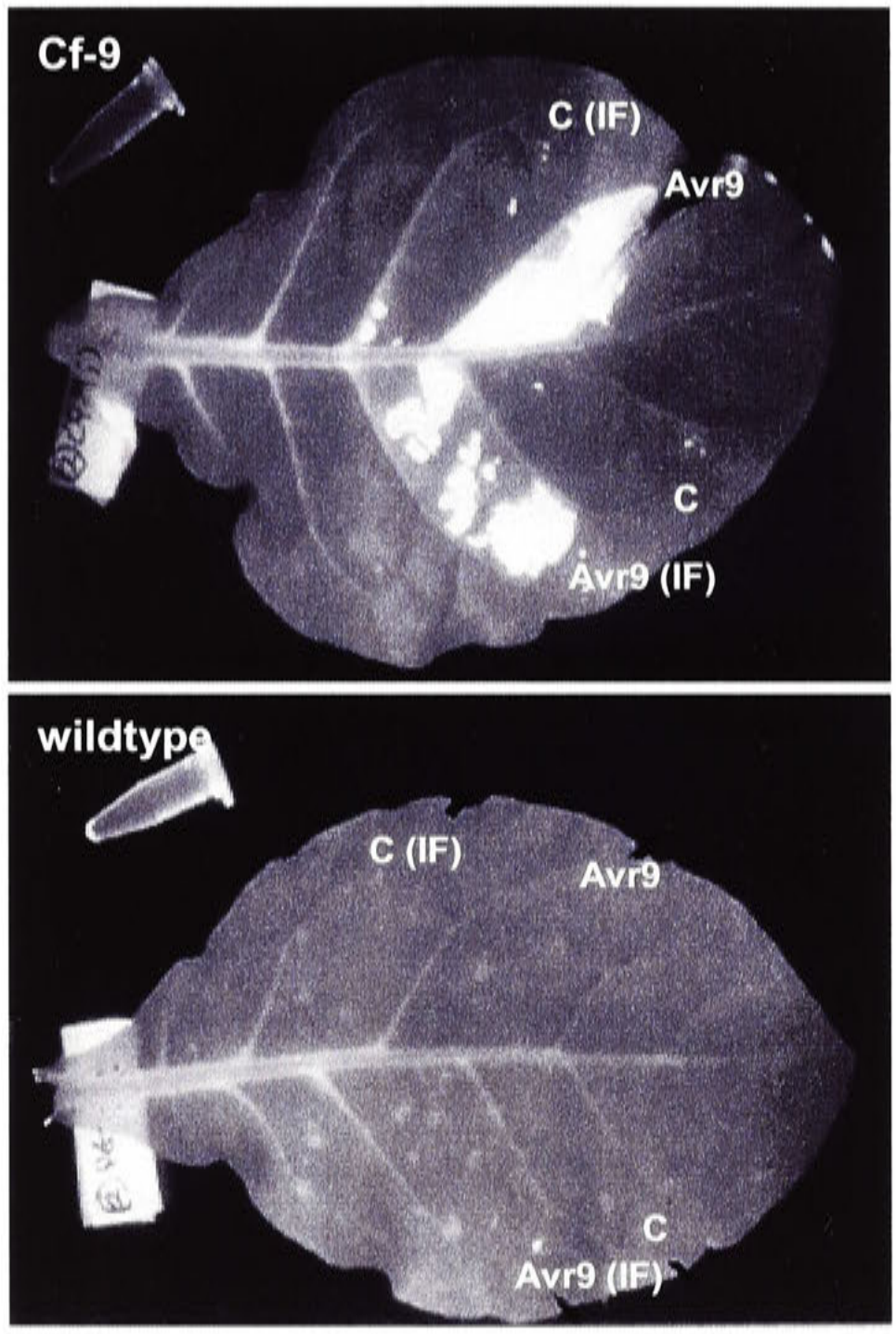

Figure 4.4. Bioassay for Avr9 activity recovered after acetone precipitation and rotary evaporation. Extracts from Avr9 and control IF (**Avr9** and **C** respectively) were infiltrated into **Cf-9** and **wildtype** tobacco leaves as shown. As a positive control, unpurified (i.e. without acetone precipitation and rotary evaporation) Avr9 and control IF (**Avr9 (IF)** and **C (IF)** respectively) were diluted 20-fold and infiltrated into separate leaf panels. Second fully expanded leaves from the base of the plant are shown 7 days post-infiltration under ultra-violet illumination. An eppendorf tube is included as a fluorescence control. Images are under the same magnification but with different apertures to adjust exposure.

Cation-exchange chromatography – resin binding capacity

The next step in the published purification procedure (Honée *et al.* 1995; Kooman-Gersmann *et al.* 1997; Van den Ackerveken *et al.* 1993) was ion-exchange chromatography (IEC) using CM-Sephadex C-25 resin cation-exchange (Pharmacia, Sweden). However, the work described here used an equivalent weak cation exchange resin, Bio-Rex® 70 (100-200 mesh; Bio-Rad), which has a carboxylic acid functional group. Prior to use, the resin was equilibrated with 20mM sodium phosphate (NaP), pH 5.5, according to the manufacturers instructions (Bio-Rad 2003). The resin was used as a 50% (v/v) slurry in this buffer. To ensure efficient purification using this resin, initial experiments were conducted to determine its binding characteristics.

An experiment was conducted to determine how much resin was required to bind a given amount of Avr9 from the semi-purified (acetone-cleared) extract. One hundred microlitres of resin slurry was added to 1, 2.5, and 5 ml of undiluted acetone-cleared IF, to which NaP (1M, pH 5.5) had been added to a final concentration of 20mM, and mixed by inversion at room temperature for 20 minutes. The resin was allowed to settle under gravity for 2 minutes, then a sample of each supernatant was centrifuged at 12 100 x g for 3 minutes to clear residual resin particles and infiltrated into a *Cf-9* tobacco leaf (Figure 4.5). As a control, a sample of the same IF extract was treated in the same way (including addition of NaP), but without addition of resin. Samples were diluted 5-fold with water prior to infiltration, except where indicated otherwise.

The supernatant from the 1 ml binding sample elicited weak necrosis, which was not present when this IF was diluted 5- or 20-fold. The 2.5 and 5 ml binding samples elicited stronger necrosis, with the latter being similar to that of the IF (1:5) and IF (1:20) controls. These results showed that saturation of Avr9 binding to this resin from this extract occurs at a ratio of approximately (or slightly below) 1 ml acetone-cleared IF to 100 µl resin slurry in 20mM NaP (pH 5.5). This value should only be considered approximate, since this experiment (both IEC and bioassay) was performed successfully on only one occasion. However, since this procedure was an adaptation of an existing protocol with an essentially identical resin, this was considered a sufficient demonstration of binding capacity for subsequent use. Therefore, approximately four times more resin than this binding saturation point was used for subsequent experiments (Amersham-Pharmacia 1999).

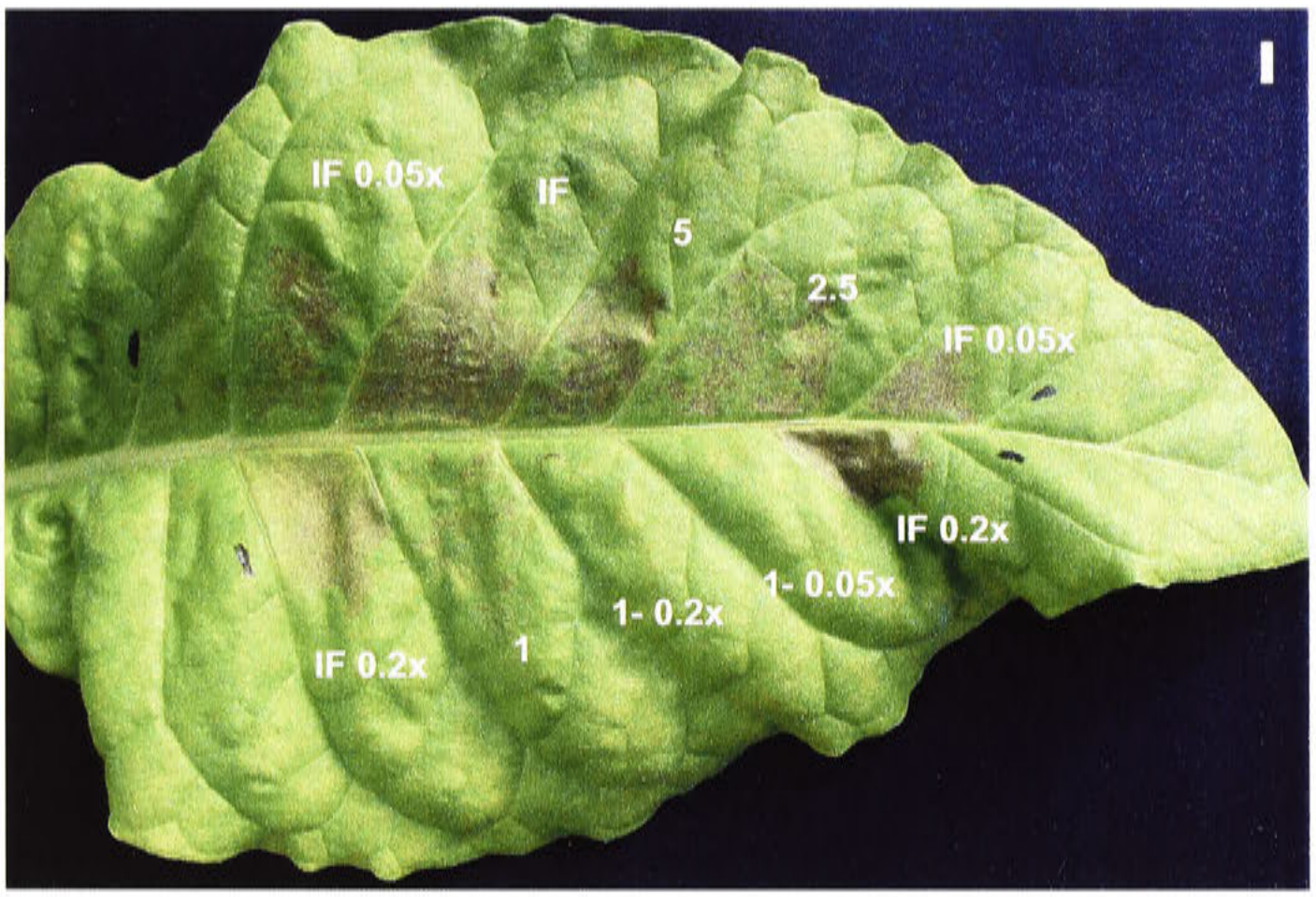

Figure 4.5. Avr9 binding capacity of Bio-Rex 70 resin. Increasing amounts (**1** ml, **2.5** ml and **5** ml) of acetone-cleared IF containing Avr9 was bound to the same amount of Bio-Rex 70 resin (see text). After binding, the supernatant was assayed for Avr9 activity by infiltration into *Cf-9* tobacco leaves. The supernatant from the 1 ml tube was also diluted 5-fold (**1-0.2x)** and 20-fold (**1-0.05x**). For positive controls, the original IF was infiltrated without any treatment (**IF**), or diluted 5-fold (**IF-0.2x)** and 20-fold (**IF-0.05x**). The leaf is shown at 2.5 hpi, with a white 1 cm scale bar.

Cation-exchange chromatography – NaCl column wash and gradient elution

Previously published reports of ion-exchange chromatography used a pH gradient of 20mM NaP (pH 5.5-8) to elute Avr9 from the ion-exchange resin. However, this approach would be relatively slow and generate a large number of fractions because the resin has a strong pH buffering capacity, and swelling of the resin due to the pH change can slow the flow rate when using column chromatography (Amersham-Pharmacia 1999; Bio-Rad).

Initially, this was not a problem when performing batch chromatography elution using 200mM NaP (pH 8.0; which would have eluted material from the resin based on pH and ionic strength), as was used for MALDI-TOF analysis (see Section 4.3.3, Figure 4.12). However, it was decided to test NaCl based methods for elution (in a column or in batch) of Avr9 from the resin as a way to improve the resolution and/or throughput of the ion-exchange chromatography procedure (in this and the next section). In this section, it was decided to test elution of Avr9 from BioRex 70 resin with a 0-1M NaCl gradient (in 20mM NaP, pH 5.5) as a potentially more convenient approach to gradient elution than a 20mm NaP pH gradient. This procedure was performed once each with Avr9 and wildtype IF, and carried out at room temperature.

Ten millilitres of acetone-cleared IF (both Avr9 and wildtype IF) was amended to a final concentration of 20mM NaP (pH 5.5) by adding 1M NaP (pH 5.5), then 20mM NaP was added to a final volume of 15 ml. This was added to a column (6 mm diameter) containing 2 ml of resin slurry, and the effluent collected. The column was washed with 20mM NaP (pH 5.5) under gravity (approximately 0.5-1 ml/minute) until the A_{280} of the effluent returned to baseline (<0.01; approximately 40 ml). A linear gradient of 0 to 1M NaCl was generated and applied using 14 ml each of 20mM NaP (pH 5.5) or 20mM NaP (pH 5.5) + 1M NaCl using a standard gradient maker, with an additional 2 ml of the latter buffer added manually after the gradient had finished. Six 5 ml fractions were collected from the gradient (1-6 = low to high NaCl concentration) and were assayed for Avr9 activity and protein concentration (Figure 4.6). This gradient procedure was performed on one occasion each for Avr9 tobacco IF and wildtype tobacco IF.

Fractions from the Avr9 tobacco IF purification were diluted 5-fold and infiltrated into Cf-9 tobacco leaves and compared to the original acetone-cleared Avr9 tobacco IF and

column flow through (also diluted 5-fold). Some necrosis was induced in response to the third and fourth fractions, suggesting that Avr9 elutes from the resin approximately mid-way through the gradient. Some dying tissue can be observed in the final fraction, which appeared to be due to the high salt concentration in this extract (the concentration after dilution of the fraction for bioassay was 4mM NaP and 200mM NaCl; Figure 4.6A). This possibility is supported by the fact that the dead tissue did not fluoresce significantly under UV illumination (Figure 4.6B), whereas necrosis induced by fractions 3 and 4 did. The effluent collected when acetone-cleared IF was applied to the column ("flow", containing material that was not bound to the column) did not induce necrosis. Additionally, as no control was performed to account for possible quantitative effects of NaCl on the response to Avr9 in the bioassay (i.e. Avr9 plus a range of NaCl concentrations added), no strong conclusion can be drawn about the rate of recovery.

The concentration of total protein in the samples was determined using the maximum sensitivity of the BCA proteins assay method (Pierce), however protein was below 10 μg/ml for all fractions except Avr9 fraction 2 and control fractions 1 and 2, which each contained 15-20 μg/ml total protein. An attempt was made to measure the absorbance of the undiluted fractions at 280 nm (A_{280}) as a measure of total protein in each of the fraction. However, the A_{280} readings were low (between -0.002 and 0.016 for all fractions compared to a 20mM NaP {pH 5.5} blank) and variation was observed between independent measurements of the same fractions, suggesting that the sensitivity limit of the available equipment had been reached (data not shown). Thus, the level of protein in all of these samples is low and no conclusive evidence for the presence of a significant amount of Avr9 protein was observed.

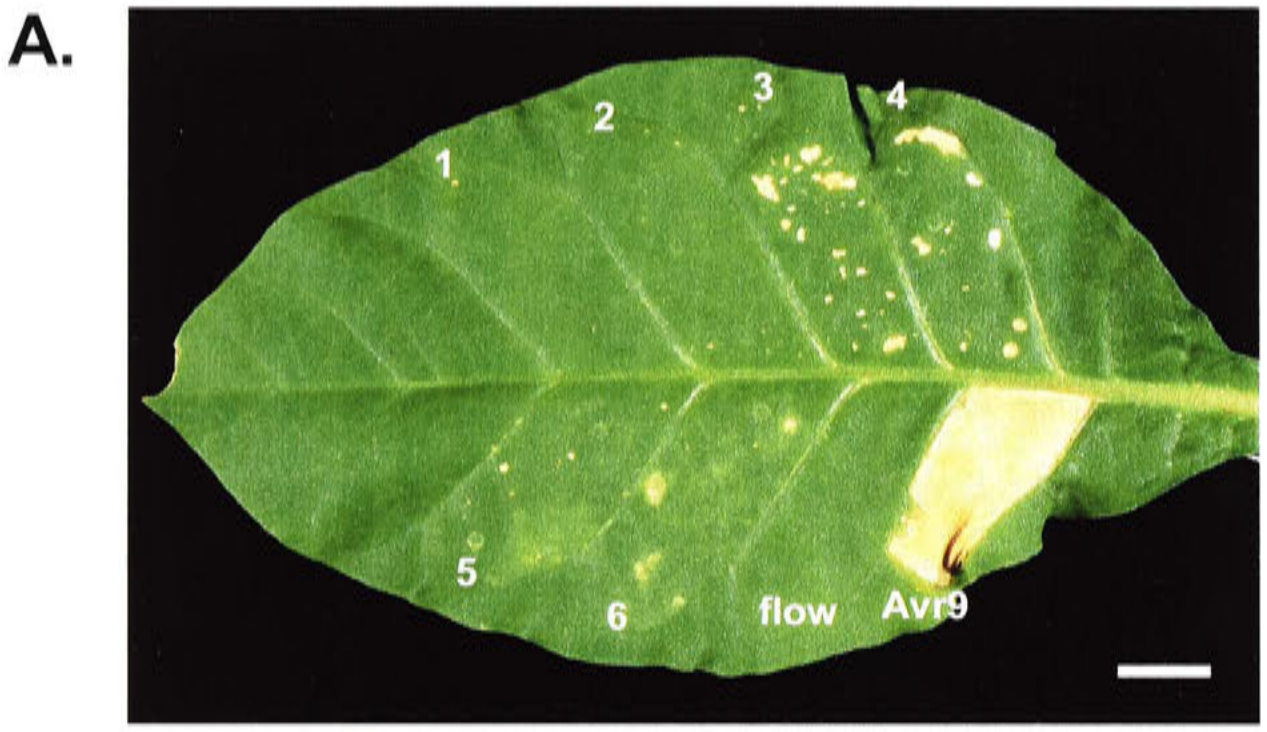

Figure 4.6. Analysis of fractions from a 0-1M NaCl gradient elution of acetone cleared Avr9 or wildtype IF from Bio-Rex 70 cation-exchange resin. The eluate was collected in 6 fractions (**1-6** = low to high NaCl concentration), diluted 5-fold and infiltrated into a *Cf-9* tobacco leaf, which is shown 7 days post-infiltration under visible (**A.**) or ultraviolet (**B.**) illumination. Acetone cleared IF containing **Avr9**, also diluted 5-fold, was included as a positive control, along with the effluent from the sample binding step also diluted 5-fold (**flow**). The white scale bar in A. is 2 cm.

Cation-exchange chromatography – NaCl batch wash and elution

In an attempt to adapt the IEC step for improved throughput, binding, washing and eluting of Avr9 (using NaCl) from the Bio-Rex 70 resin in 'batch' was investigated. Batch chromatography is performed by mixing the resin with the sample, collecting the resin (in this case by sedimentation under gravity), removing the eluate as the supernatant, then repeating these steps with appropriate buffers for washing or elution of the sample.

Since sample binding to the resin in batch had already been investigated (above), a preliminary investigation of a batch NaCl elution step was performed. Several tubes containing 100 µl of resin slurry and 1 ml of acetone-cleared IF containing 20mM NaP (pH 5.5) were prepared, and binding of Avr9 to the resin performed as described previously. The resin was allowed to settle under gravity, the supernatant discarded, and the resin washed by adding 1 ml of 20mM NaP (pH 5.5). After mixing by gentle inversion for 2 minutes, the wash supernatant was discarded. One millilitre of NaP buffer (20mM, pH 5.5) either alone (as a negative control) or containing 100, 200, 300, 400, or 500mM NaCl was then added to each tube and allowed to mix by inversion for 10 minutes. This range of NaCl concentrations was used for this preliminary elution test as it was unknown exactly what concentration would be sufficient to elute Avr9. The tubes were then centrifuged at 12 100 x g for 3 minutes and the supernatant (eluate) collected for bioassay.

The supernatants from the this elution series experiment were diluted 5-fold and infiltrated into a *Cf-9* tobacco leaf along with the original IF diluted 5-fold (0.2x) and 20-fold (0.05x) in water as positive controls to judge the recovery efficiency (Figure 4.7). There was little or no necrotic response from the supernatant of the 20mM NaP negative control elution or the 100mM NaCl elution, indicating that little or no Avr9 is released from the resin in these buffers. A necrotic response of roughly similar intensity was initiated in response to the eluates from the 200-500mM NaCl samples, suggesting that 200mM or more NaCl eluted all elutable Avr9 from this resin under these conditions. No necrosis was present in response to samples eluted with NaP buffer only, indicating that most Avr9 remains bound to the resin. As this experiment (IEC and bioassay) was performed successfully on only one occasion, results should be considered preliminary.

Controls to account for any effects of the NaCl in the samples (i.e. 20-100mM NaCl in Avr9) were not performed as there was not enough space on a single leaf to do this, and this preliminary experiment was not planned to assess recovery. The fact that the 200-500mM samples all induced necrosis suggests that if NaCl did affect the response to Avr9, it would only have a moderate quantitative effect on necrosis induction. Assuming that the NaCl did not significantly affect the bioassay response, these data can be used to derive an approximate recovery rate for Avr9 using this procedure (see discussion). Because samples were infiltrated at a concentration equivalent to their starting initial concentrations, which is equivalent to the 0.2x IF panel, weaker necrosis in eluted sample suggested that not all Avr9 was eluted from the resin even using up to 500mM NaCl. Comparison of the 500mM eluted sample panel to the 0.05x IF panel suggests that less than 25% of Avr9 is elutable from the resin.

Some variability was present between leaf panels, particularly the 400mM and 200mM panels responded slightly stronger than did the 300mM and 500mM panels respectively. Similarly, necrosis of the IF 0.05x panels (distal and proximal panels) was slightly different despite the same extract being infiltrated. This could be due to within leaf effects, either due to slightly differential insolation load or developmental effects. Overall, these results suggest that approximately 200mM NaCl is required to elute Avr9 from this resin under these conditions.

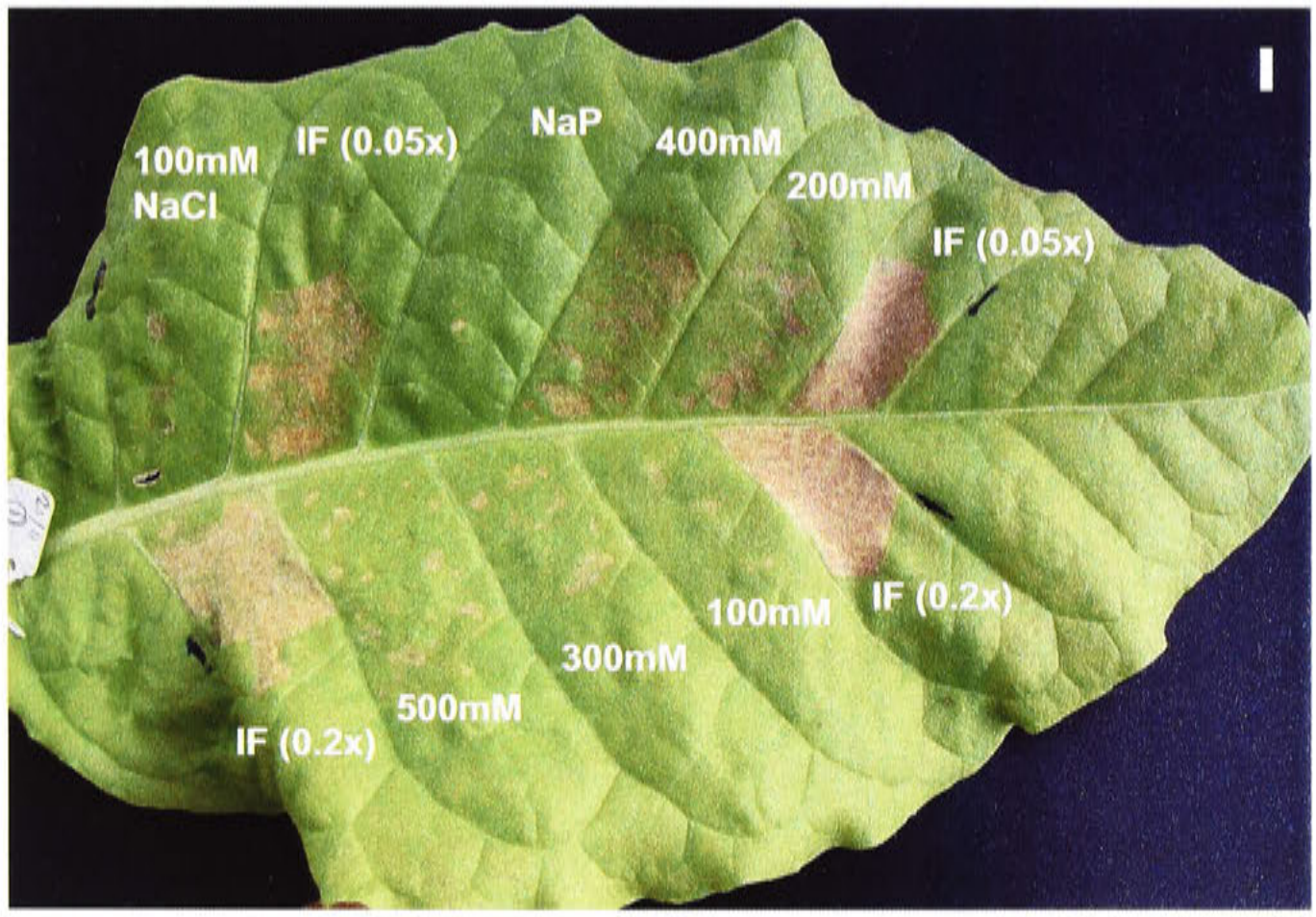

Figure 4.7. Testing of batch elution from Bio-Rex 70 resin using different concentrations of NaCl. Avr9 from acetone cleared IF was bound to the resin as described, then eluted using either 0, **100mM**, **200mM**, **300mM**, **400mM** or **500mM** NaCl in 20mM NaP (pH 5.5). The supernatants (eluates) were diluted 5-fold and infiltrated into a *Cf-9* tobacco leaf, and compared to Avr9 IF diluted 5-fold (**IF (0.2x)**) and 20-fold (**IF (0.05x)**). Negative controls were **100mM NaCl** in 20mM NaP (pH 5.5) buffer, and the negative control 'elution' with 20mM **NaP** only. Leaf panel necrosis is shown at 5 hours post-infiltration. Half leaf panels were infiltrated, and a 1 cm white scale bar is shown.

Reversed-phase chromatography purification

To concentrate and desalt the samples, C-18 cartridges were used for reversed-phase chromatography purification as described previously (Van den Ackerveken *et al.* 1993), with one minor modification. Briefly, fractions 3 and 4 from NaCl gradient eluted Avr9 and wildtype tobacco IF extracts (above) were combined (10 ml total volume for each), amended to a final concentration of 0.1% (v/v) tri-fluoroacetic acid (TFA). Samples were then applied to a C-18 Sep-Pak Plus cartridge with 360 mg of sorbent material (Waters) that had been pre-conditioned with 90% acetonitrile containing 0.1% (v/v) TFA and equilibrated with 0.2% (v/v) TFA (the previously published report used 0.1%). The increased TFA concentration was used to ensure that these crude samples were adequately acidified to maximise binding of the sample to the C-18 matrix (according to manufacturers instructions; previously published methods used relatively pure samples with less potentially pH buffering contaminants). The cartridge was then washed with 4 ml of 0.1% (v/v) TFA and protein eluted with 3 ml of 90% acetonitrile/0.1% (v/v) TFA. The sample volume was reduced under a nitrogen stream at 40°C for 2 hours, and the remaining sample freeze-dried then resuspended in 100 µl filtered 20mM NaP (pH 5.5).

Resultant samples were diluted to various concentrations relative to the original acetone-cleared extracts and tested for Avr9 activity by bioassay (Figure 4.8). Full necrosis was induced in all leaf panels after 27 hours, so the leaf is shown at 2 hpi when a clear differential response was apparent between samples. Comparison of the Avr9 0.05x panel with the C18-A 1x and 0.2x panels suggests that approximate net recovery of Avr9 after ion-exchange chromatography (IEC) and C-18 purification is between 5% and 25%. A significant proportion of this loss probably occurred during the IEC procedure (Figure 4.6; above). The lack of response to the equivalent extract from wildtype IF (C-18W 2x) shows that the response is specific and that properties of the extract arising from either procedure do not cause a necrotic response in this assay. An equivalent result was observed on a duplicate leaf (on a separate plant infiltrated on the same occasion). This experiment shows that Avr9 activity is recovered by the C-18 reversed-phase chromatography procedure, as expected.

The protein concentration in the (undiluted) Avr9 and control extracts after this C-18 purification step was found to be 100 µg/ml and 125 µg/ml respectively, suggesting that most of the protein in these samples was not Avr9.

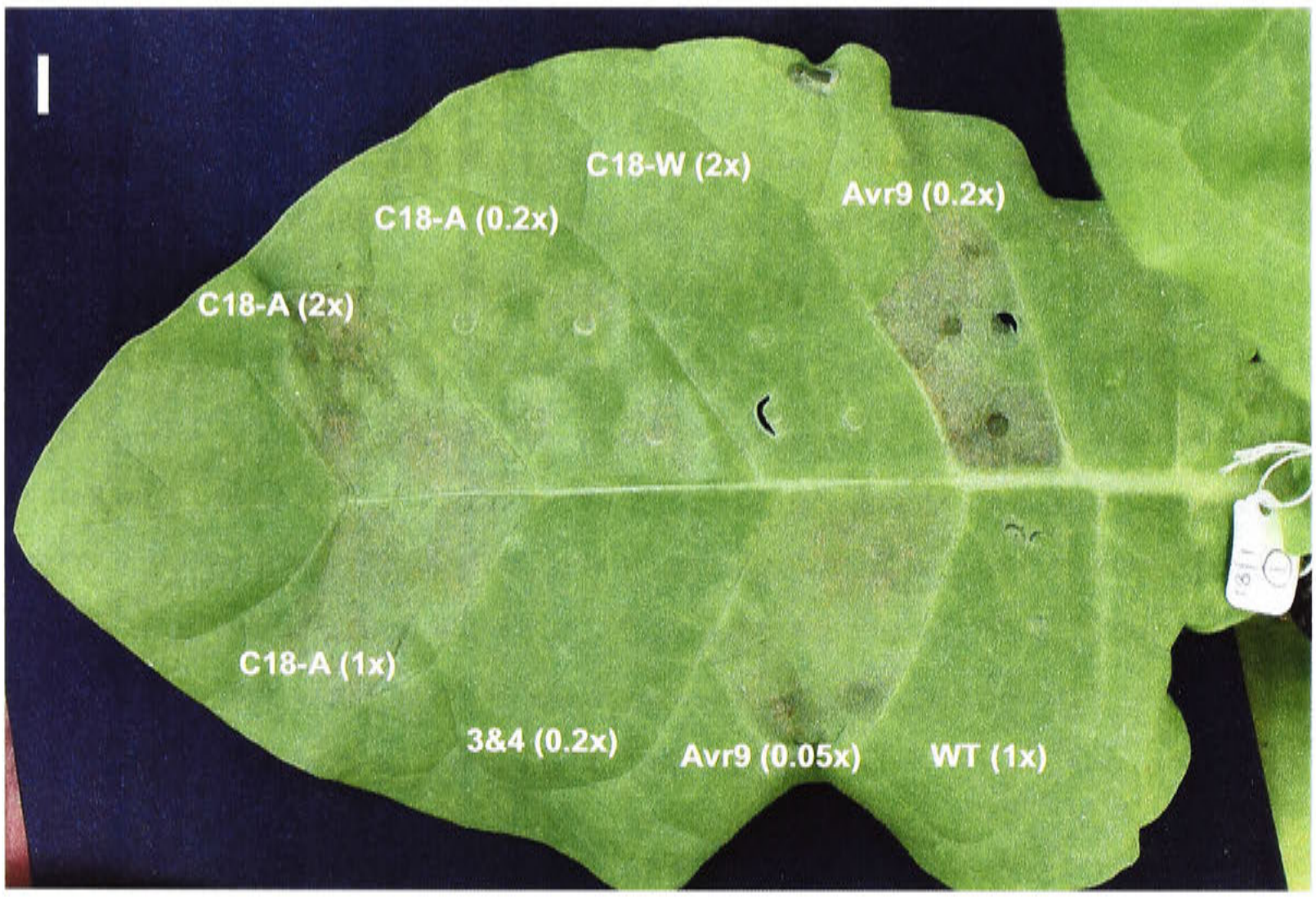

Figure 4.8. Bioassay for recovery of Avr9 after C-18 (Sep-Pak) purification of ion-exchange chromatography purified IF samples. **C18-A** is Avr9 fractions 3 and 4 from the NaCl gradient elution after C-18 cartridge desalting and recovery, diluted with deionised water to various concentrations relative to the original acetone cleared IF (**2x**, **1x**, **0.2x**). For comparison, the acetone cleared **Avr9** IF is infiltrated at **0.2x** and **0.05x** dilutions. Wildtype (control) IF before (**WT 1x**) and after NaCl elution/C-18 purification (**C18-W 2x**) at the original concentration or twice the original concentration respectively. The combined eluted fractions 3 and 4 (**3&4 0.2x**, without C-18 purification) were also infiltrated (but did not respond until after this photo was taken). Since full necrosis occurred in all panels except for WT and C18-W 2x after 27 hours (not shown), the infiltrated leaf is shown at 2 hpi, when a clear differential response was observed. Approximately half of each leaf panel was infiltrated. The white scale bar shown is 1 cm.

4.3.3 MALDI-TOF analysis of Avr9

MALDI-TOF mass spectrometry has been used to determine the mass of many proteins, and it was envisaged that this method could be useful to study modifications of Avr9 (see introduction to this chapter). When this work began, mass spectrometry detection of Avr9 had not been reported using MALDI-TOF, however more recently analysis of Avr9 peptide folding reactions by MALDI-TOF has been reported (van den Hooven *et al.* 2001).

MALDI-TOF was performed using a Micromass TofSpec E MALDI-TOF mass spectrometer according to the manufacturers instructions (Micromass 1997). Unless otherwise stated, samples were prepared by mixing 1 µl of sample with 1 µl of matrix solution (a saturated solution of α-cyano-4-hydroxycinnamic acid, or 'alpha', in a 50/50 mixture of 1% {v/v} aqueous TFA and acetonitrile), then spotting half of this mixture onto a target plate and allowing it to air dry. A range of other published matrix solutions and sample application protocols were tested (Amado *et al.* 1997; Bornsen *et al.* 1997; Chong *et al.* 1997; Cohen and Chait 1996; Kussmann *et al.* 1997; Landry *et al.* 2000; Micromass 1997; Wang *et al.* 1998), however none of these allowed better detection of Avr9 than the above described protocol (not shown).

Avr9 detection was performed in positive reflectron mode at 20 kV operating voltage, and other parameters adjusted as suggested by the manufacturers instructions for each sample as necessary (Micromass 1997). Spectra shown are the average of at least 30 individual spectra (up to 100 when a weak peak was observed). The instrument was calibrated externally using adenocorticotropic hormone (ACTH) as described in the manual. Dr Phil Jackson, of the Research School of Chemistry, Australian National University, performed or assisted with MALDI-TOF detection.

Detection from IF

As MALDI-TOF mass spectrometry has been reported to detect proteins in complex mixtures (see the introduction to this chapter), initial attempts at MALDI-TOF detection of Avr9 were made directly from IF and from acetone-cleared IF. A range of detection parameters were varied in order to detect Avr9, including laser energy, pulse time (time after ionisation that the sample is extracted) and pulse voltage, but no peak of the size corresponding to Avr9 was detected in unpurified IF (Figure 4.9). Based upon previous mass spectrometry of Avr9, this peak was expected at approximately 3390 Da

(Kooman-Gersmann *et al.* 1998a). Additionally, no peak was detected corresponding to half the predicted mass of Avr9 (1695 Da), which might be expected for a double charged ($M + 2^+$) version of Avr9. Nor were peaks present at the expected size of unmodified Avr9 (3189, Kooman-Gersmann *et al.* 1998a) or the corresponding $M + 2^+$ version (1594.5). A range of other peaks were detected, and these were mostly consistent between the Avr9 and wildtype IF extracts (Figure 4.9). As the IF extract is a complicated mixture, it is not known what these peaks might represent, but they are strongly detected components of the mixture. The same experiment was performed on acetone-cleared IF, however no specific peak corresponding to Avr9 was observed (not shown).

A.

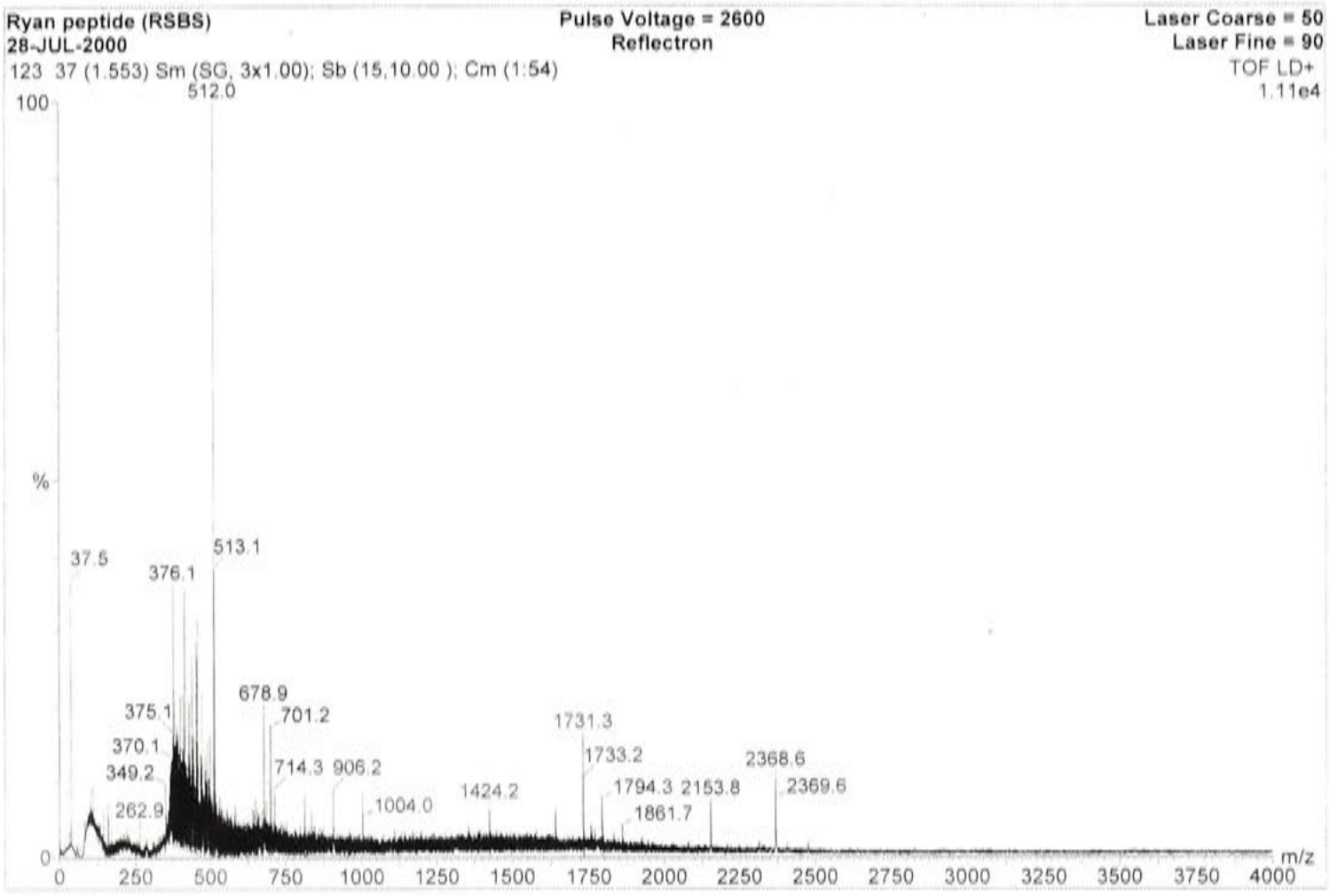

B.

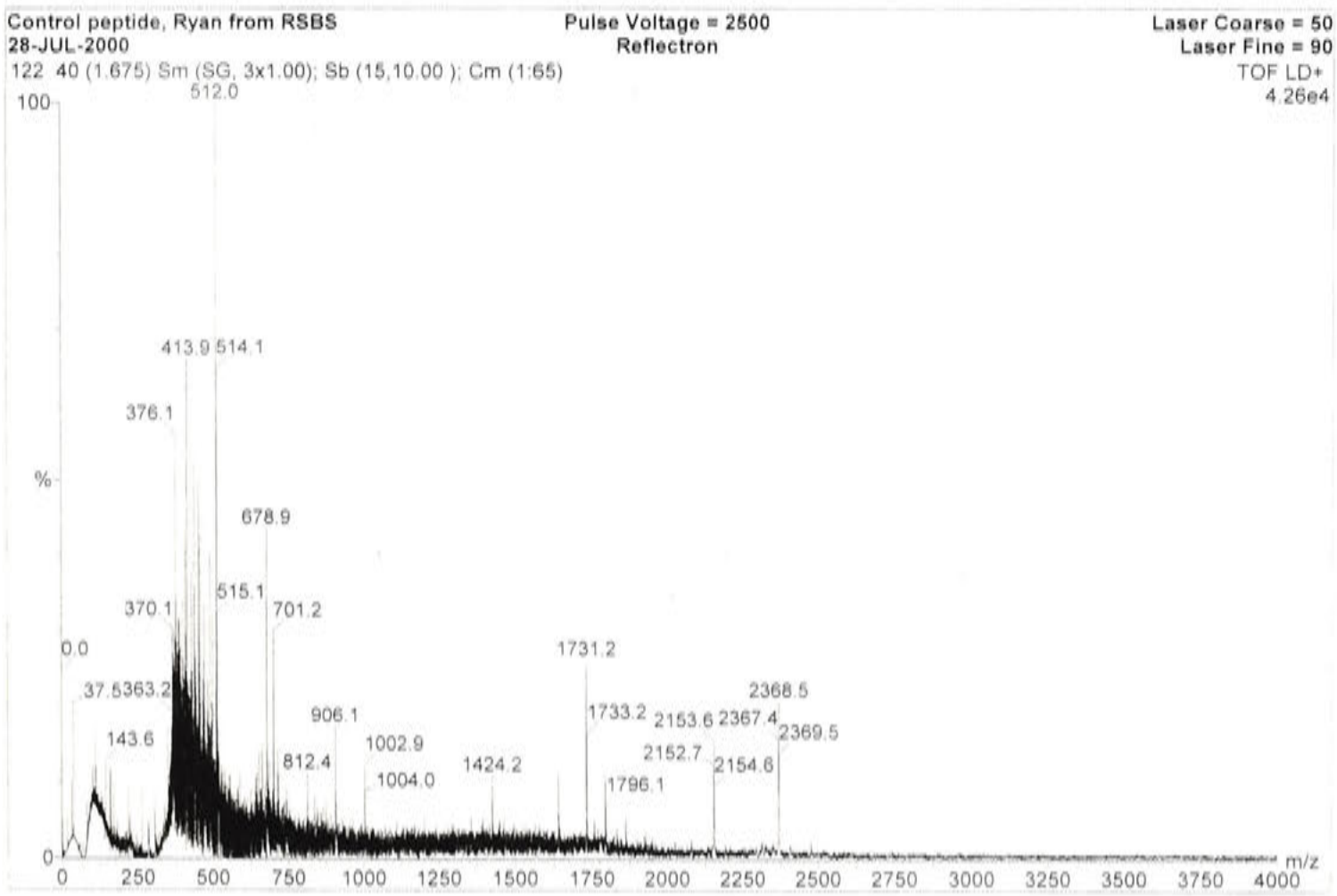

Figure 4.9. MALDI-TOF analysis of crude IF preparations. Mass/charge ratio (*m/z*, equivalent to mass of a singly charged species) is shown on the x-axis and relative peak intensity shown on the y-axis. **A.** shows detection of Avr9 IF and **B.** shows detection of equivalently prepared control (wildtype) IF. MALDI-TOF was performed as described in the text.

Desalting of samples, and detection by bioassay and MALDI-TOF

It was considered likely that one problem with the detection of Avr9 from these relatively crude samples was the presence of a significant quantity of salt or other interfering contaminants. To test this, acetone-cleared IF samples were desalted using Centricon® (Millipore) columns with a nominal molecular weight cut-off of 3000 Da (the lowest available). These columns are an ultrafiltration membrane built into a column unit that can be centrifuged to expedite sample concentration, fractionation and desalting. The molecular weight cut-off for this membrane was not expected to completely retain Avr9 (which was expected to be 3390 Da) but to at least partially do so.

Two hundred microlitres of acetone-cleared Avr9 or wildtype IF that had been concentrated 100-fold (by rotary evaporation) was amended with 300 µl of water, added to the Centricon column and centrifuged at 12 000 x g for 50 minutes at room temperature. The sample that had passed through the membrane (filtrate, approximately 475 µl) was collected, and the remaining fraction in the column ('retentate', approximately 25 µl) washed by refilling the reservoir with 500 µl of water and repeating the centrifugation. The filtrate was again collected (approximately 500 µl) and the wash step repeated, though the filtrate from this last wash was not collected. The retentate was collected by adding water to 200 µl and the first two filtrate fractions combined (theoretically 975 µl).

Resultant fractions were diluted relative to their original concentration (the 1 x acetone-cleared IF sample) and bioassayed by infiltration into *Cf-9* tobacco leaves at different dilutions (Figure 4.10A). The retentate from Avr9 IF showed strong necrosis when infiltrated at 1 x original IF equivalent concentration, while at 0.2 x concentration only weak necrosis surrounding the infiltration sites is evident. The filtrates of the Avr9 IF showed similar necrotic responses at dilutions of 5-fold and 25-fold (0.2 x and 0.04 x) to the undiluted and 5-fold diluted retentate (1 x and 0.2 x) respectively, suggesting that Avr9 is approximately 5 x more concentrated in the filtrate fraction than the retentate fraction. Given that the volume of filtrate in this experiment is almost 1 ml, and the retentate 200 µl, this suggests that more than 95% of Avr9 peptide was lost during this procedure. This value is likely to be higher since the last filtrate fraction was not collected. This desalting experiment was performed on only one occasion.

Retentate fractions from this experiment were analysed on two separate occasions by MALDI-TOF mass spectrometry as described above. A clear peak was observed at 3394 Da in the Avr9 fraction that was not observed in the control fraction (Figure 4.10B and Figure 4.10C). This corresponds very closely to the size of Avr9 previously determined by ESI-MS (3390; Kooman-Gersmann *et al.* 1998a), indicating that this peak is highly likely to be Avr9. Over these and many other experiments using MALDI-TOF detection of fractions from Avr9 and wildtype IF, this peak was never seen in control extracts, but was seen reproducibly in Avr9 extracts when purified sufficiently (as in experiments detailed below). This indicates that Avr9 expressed in the transgenic tobacco line SLJ6201 is the mature form, as expected, and is the same as that expressed in PVX:Avr9 infected *N. clevelandii* (Kooman-Gersmann *et al.* 1998a). A specific 16 Da smaller decay product is apparent from this spectrum, and probably represents the loss of a methyl (CH_4) group.

When the same acetone cleared extracts (either at a concentration equivalent to IF or 100-fold concentrated) were analysed by MALDI-TOF, no 3394 Da peak was detected (above and data not shown respectively). These data suggest that desalting this extract, but not concentrating it, allowed detection of the 3394 Da peak.

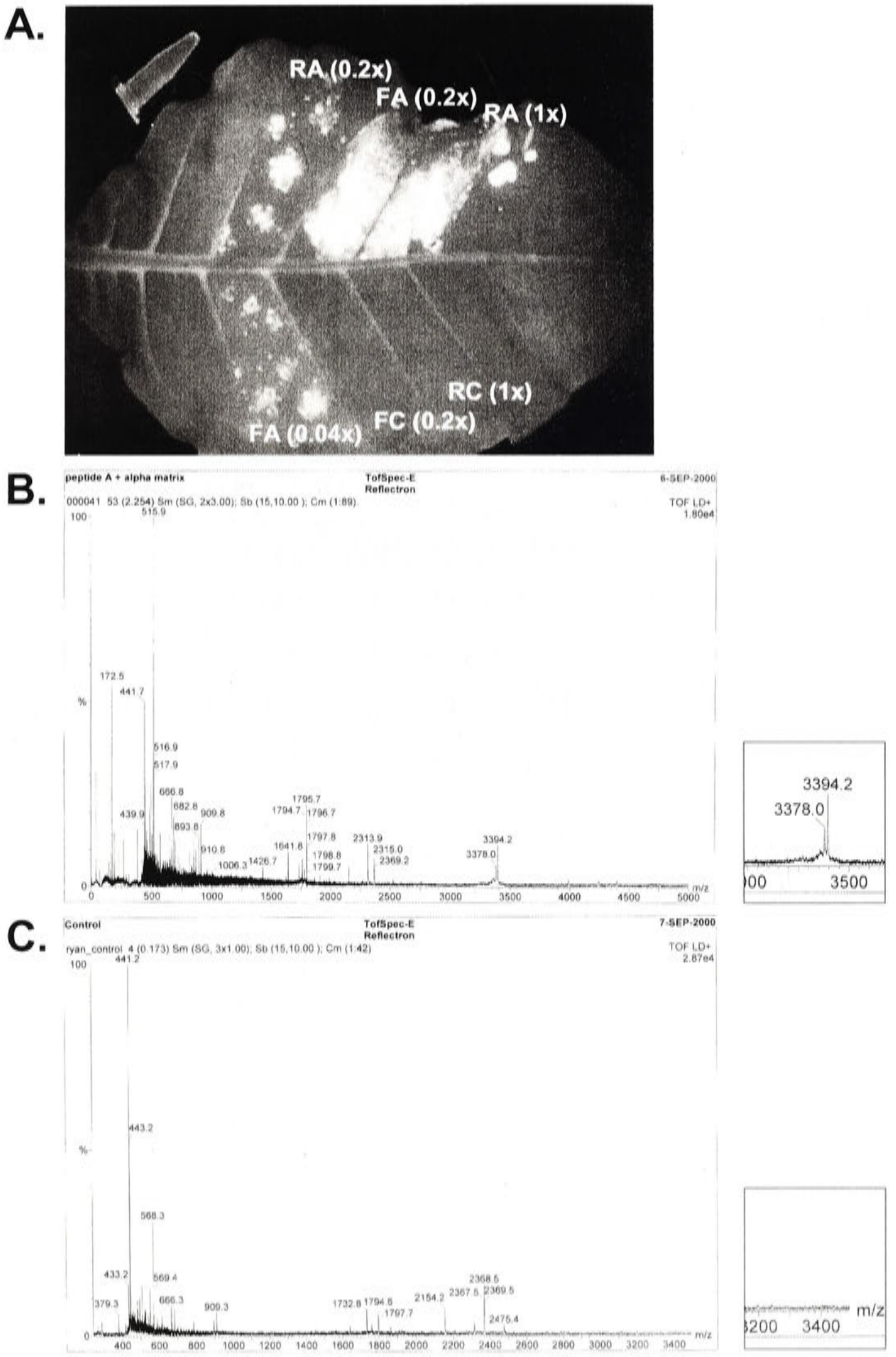

Figure 4.10. Bioassay and MALDI-TOF detection of Avr9 recovered by Centricon column desalting (3000 Da molecular weight cut off) of concentrated, acetone-cleared IF samples. **A.** Shows a bioassay of the various fractions. **RA** and **RC** are the fractions retained ('retentate') in the Centricon column for Avr9 and control IF respectively, while **FA** and **FC** are the flow through ('filtrates') for Avr9 and control IF respectively. The value at each label indicates the concentration factor relative to the original IF extract (**1x**, **0.2x**, **0.04x**). The infiltrated leaf is shown at 4 dpi under ultra-violet illumination. **B.** and **C.** show MALDI-TOF detection of Avr9 and wildtype extracts (retentates only) respectively. The zones corresponding to the 3394 Da peak (B.) in both B. and C. are enlarged to the right of the spectra. Note that the x-axes of B. and C. are not to the same scale.

Analysis of the Avr9 peak

During MALDI-TOF analysis of the Centricon desalted extracts, the mass of Avr9 was resolved to the level of isotopic variants ('isotopic resolution'), as indicated by the series of peaks differing by 1 mass unit each (Figure 4.11A and Figure 4.11B). Isotopic resolution of the Avr9 peak was also achieved on two other occasions using IEC purified Avr9 (desalted by C-18 Ziptip purification, below and data not shown). Post-Source Decay (PSD) analysis was attempted on the 3394 Da peak (after ion gate selection of the peak) in order to independently confirm its identity. This was performed as described in the manufacturers instructions using ACTH as a fragmentation standard (Micromass 1997). As shown in Figure 4.11C, no significant PSD fragments from the 3394 Da peak were observed. Since this is a relatively strong peak, and any decay products should therefore be abundant enough to be readily detected, this suggests that no post-source decay products were generated in the conditions used for the analysis. A few very minor, likely insignificant, peaks were observed (e.g. 1157.9, 1463.8, 1912.8), however these do not appear to correspond to any N-terminal or C-terminal decay products of Avr9.

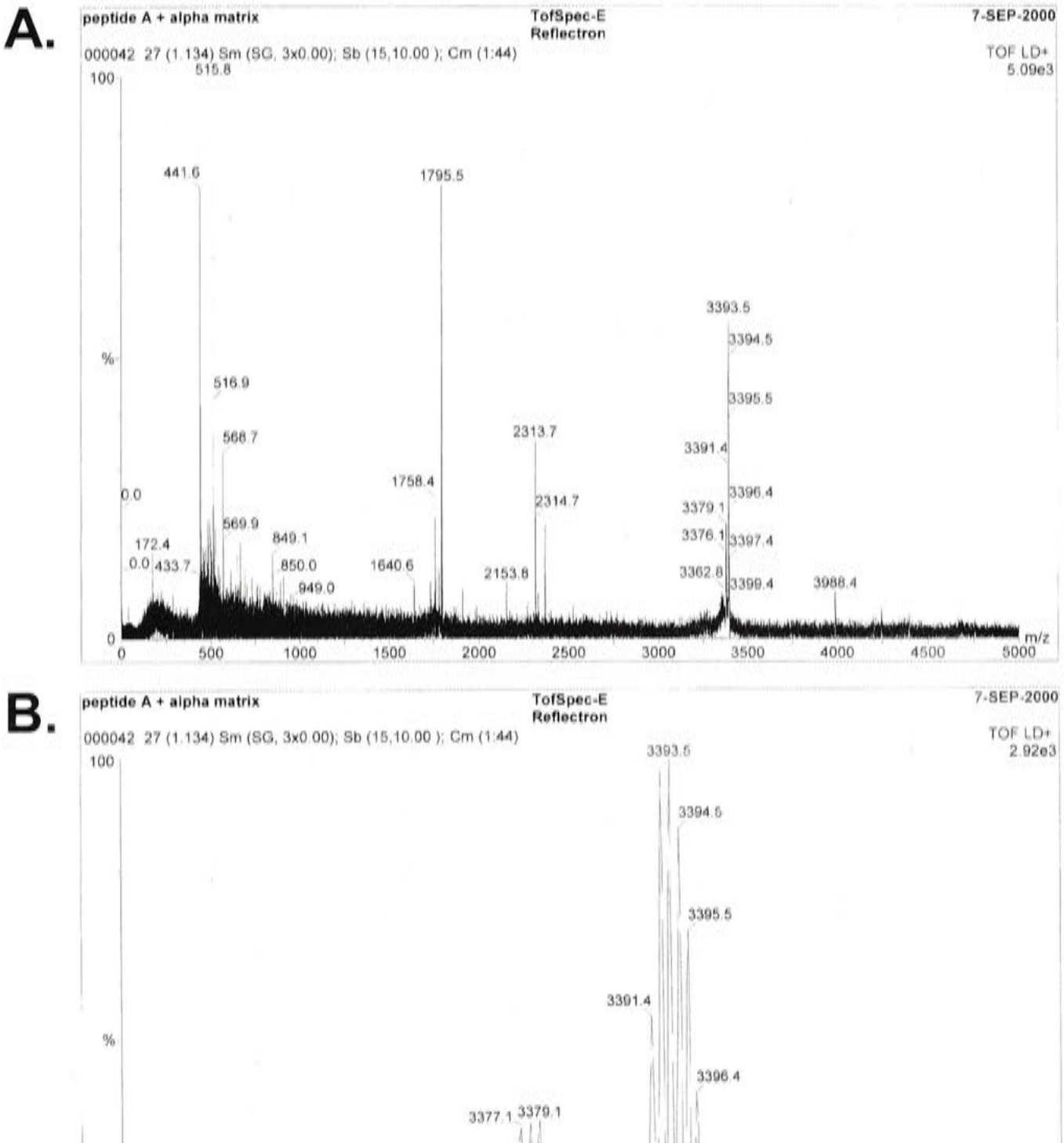

Figure 4.11. MALDI-TOF detection and analysis of Avr9 recovered by centricon column desalting. **A.** The 3394 Da peak predicted to be Avr9 that was chosen for analysis, and **B.** isotopic resolution of this and the neighbouring 3378 Da peak. **C.** A post-source decay spectrum of the Avr9 peak.

Improvements to sample preparation for MALDI-TOF: 'Ziptip' (C-18) and IEC purification

To determine whether detection of Avr9 by MALDI-TOF could be further improved by a simpler desalting procedure than the Centricon method, C-18 purification was performed on acetone-cleared and IEC purified samples. Since MALDI-TOF detection requires only a very small quantity of material, small samples were desalted and concentrated using a C-18 Ziptip® (Millipore), which is a 10 µl pipette tip containing 0.6 µl C-18 matrix. This was performed with the same solutions and procedure as described for the Sep-Pak cartridge C-18 (above), except with modification of scale as follows: preconditioning and equilibration were performed using 10 µl of buffer and the wash step was performed using 100 µl of buffer.

Ziptip purification was performed on 50 µl of acetone-cleared Avr9 or wildtype tobacco IF samples, and the sample eluted from the Ziptip in 10 µl then a portion applied to the target plate as described above. While Avr9 was not detectable directly from acetone-cleared IF samples (Figure 4.9), a weak peak of 3394 Da was detected in the acetone-cleared Avr9 sample (but not wildtype) when purified by Ziptip (two independent occasions, not shown). This suggests that desalting and concentrating these samples is not sufficient to allow clear detection by MALDI, and/or that the concentration of the sample and contaminants (even minus salt) inhibits the detection of Avr9.

To determine whether IEC purification of the acetone-cleared IF allowed better detection of Avr9, acetone-cleared Avr9 IF was purified by batch washing, as described above except with 5 washes in 20 mM NaP (pH 5.5) and elution in 200mM NaP (pH 8.0). This elution method was the approach used prior to conducting the NaCl batch elution experiments outlined above (Figure 4.6 and Figure 4.7). MALDI-TOF detection of this sample after Ziptip purification showed a strong peak of 3394 Da, along with a few satellite peaks (Figure 4.12). Interestingly, a weak peak of ~1697 Da was observed, which may correspond to the $M + 2^{+}$ version of Avr9.

MALDI-TOF detection of Avr9 in this IEC purified, Ziptip purified sample shows a stronger signal (signal to noise ratio) than from the previous Centricon fractionated samples (compare Figure 4.12 to Figure 4.11A and Figure 4.10B). MALDI-TOF analysis was performed on Avr9 from IEC and Ziptip purified IF samples on four separate occasions, and was used as a positive control for MALDI-TOF detection on a

number of subsequent occasions. This demonstrates that the further purification (as distinct from desalting alone) of Avr9 IF significantly increases the detection of Avr9 by MALDI-TOF. Furthermore, since the acetone-cleared IF samples that were purified and concentrated by Ziptip (above) were desalted but not IEC purified, this suggests that the removal of other contaminating components by IEC significantly aided detection by MALDI-TOF.

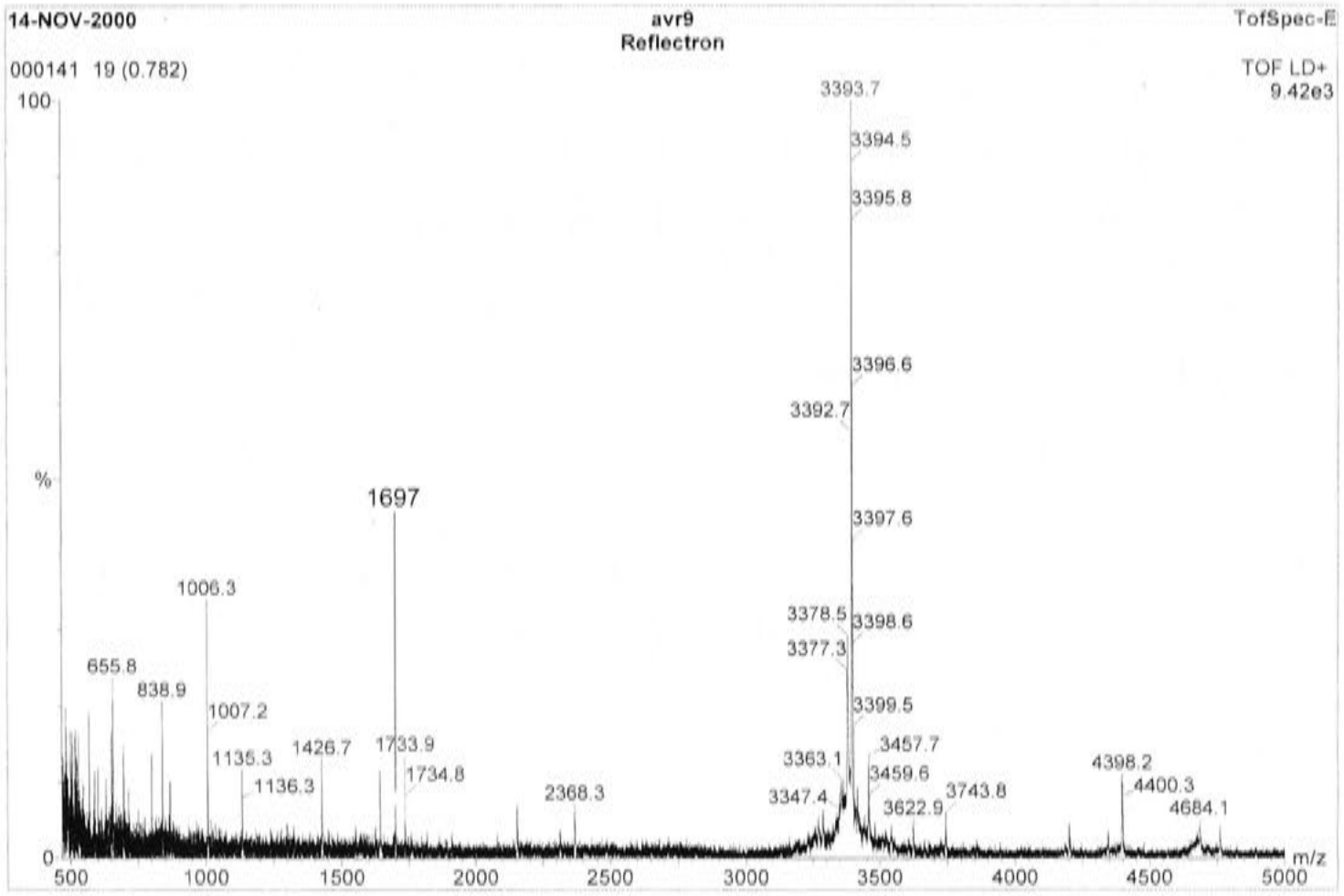

Figure 4.12. MALDI-TOF detection of Avr9 recovered by batch Ion-Exchange Chromatography purification from acetone cleared Avr9 IF. A strong peak of 3394 Da is present, along with some satellite peaks, and a weak peak corresponding to M + 2^+ (1697) is indicated with a red line. Note that the x-axis begins at 500 amu.

MALDI-TOF detection of Avr9 from whole leaf extract

The work described in the chapter ultimately aimed to analyse Avr9 for potential modifications when added exogenously to tobacco cells (initially it was intended to use whole leaves). To detect modifications using MALDI-TOF, it was first necessary to demonstrate that the purification and detection procedures were sufficient to detect Avr9 in whole leaf tissue extracts, rather than IF as was used above. Transgenic tobacco expressing Avr9 (SLJ6201) was used as a source of Avr9 in whole leaf tissue.

Approximately 3 g of leaf tissue was harvested from 6-8 week old SLJ6201 and wildtype tobacco plants and ground on liquid nitrogen. The powdered tissue was resuspended in 5 ml of deionised water per gram of tissue ground, homogenised twice for 30 seconds using an Ultra Turrax TP 18/10 homogeniser (Janke and Kunkel, Staufen, Germany), then incubated in a boiling water bath, acetone precipitated and rotary evaporated as described for IF samples above. A 40 µl sample of each resulting extract was further purified by batch IEC as described above (using 100 µl resin slurry and 200mM NaP {pH 8.0} to elute), Ziptip purification (1/4 of the IEC eluate) and then analysed by MALDI-TOF (Figure 4.13).

Avr9 was not detectable in acetone-cleared whole leaf extracts where Ziptip purification but not IEC purification was used (not shown). When the whole leaf extracts were both IEC and Ziptip purified, a peak of the expected size for Avr9 was weakly detected by MALDI-TOF in the SLJ6201 extract but not the wildtype tobacco extract (Figure 4.13). Enlargements of the equivalent regions of the Avr9 and wildtype spectra suggest that the peak is specific to the Avr9 sample. This peak was detected on one occasion but was not observed on the other occasion that this experiment was performed, so this result should be considered preliminary.

It should be noted that these spectra appear different because the signals below 500 Da are not included in the Avr9 extract (Figure 4.13A), causing the 1733 non-specific peak to be automatically set at 100% intensity rather than the more intense 442 Da peak in the wildtype extract sample (Figure 4.13B).

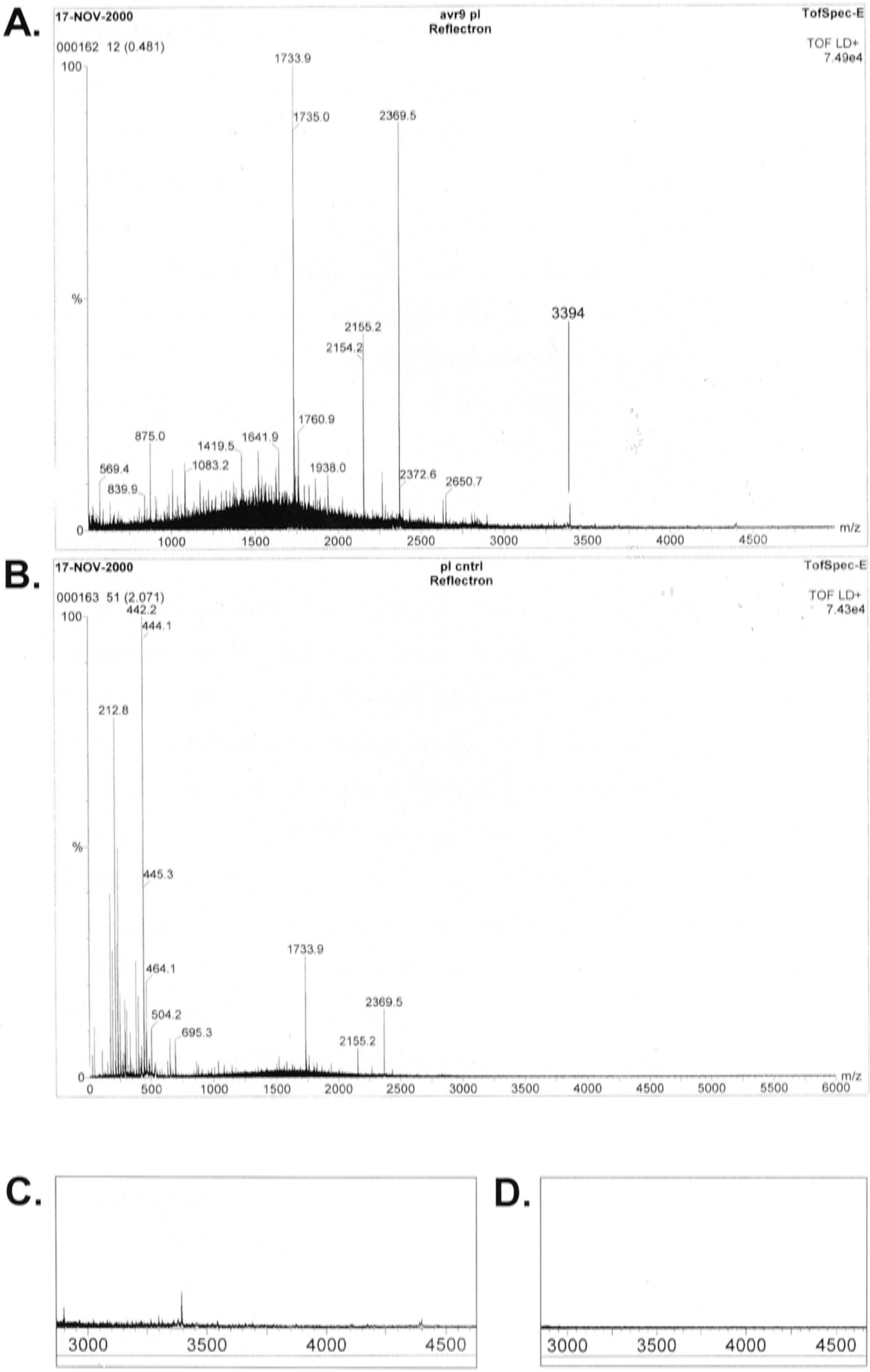

Figure 4.13. MALDI-TOF detection of Avr9 recovered by batch IEC and Ziptip purification of whole tobacco leaf extracts from: **A.** and **C.** SLJ6201 tobacco, **B.** and **D.** wildtype tobacco. Enlargements of regions of the spectra where the 3394 Da peak corresponding to Avr9 is observed are shown in C. and D. with the relative scale of A. and B. maintained).

4.3.4 Heterologous expression of Avr9 in *E. coli*

To determine whether Avr9 enters plant cells, the work described in this chapter ultimately aimed to determine whether Avr9 becomes modified when supplied exogenously to plant cells. Since one possible modification was glycosylation of the NSS motif (amino acids 3-5) of Avr9, a source of Avr9 was needed that did not possess any existing modifications to this motif. Since the predominant form of Avr9 expressed in tobacco is already glycosylated at this site (Kooman-Gersmann *et al.* 1998a), a different source of Avr9 was needed that retained a free and intact N-glycosylation site to determine whether Avr9 is glycosylated when added exogenously. One possibility was to use a glycosidase that could remove the 202 Da glycosyl residue from tobacco Avr9, however none are available that could catalyse such a reaction without destroying the capacity for re-glycosylation.

To solve this problem, Avr9 was expressed in *E. coli* with a bacterial signal peptide using the Novagen pET® expression system. The signal peptide (*pelB*) allows secretion of the protein of interest into the bacterial periplasm or into the medium, which, due to provision of an oxidising environment by shaking and aeration of the culture, should allow relatively efficient folding and disulphide bond formation of Avr9 (Mahe *et al.* 1998). The primers "EcoliAvr9F" (ccatggatgcctactgtaacagttcttg) and "EcoliAvr9R" (aagcttctagaggatctcaatgta), engineered to contain *Nco*I and *Hin*dIII restriction sites respectively (underlined), were used in combination to amplify the mature Avr9 open reading frame from pCBJ231 (see the Materials and Methods section of Chapter 3 for details of this plasmid). The resultant ~100 bp amplified product was cloned into pCR2.1 using the TA Cloning® kit (Invitrogen), excised using *Nco*I and *Hin*dIII, purified from a 2% agarose gel and ligated into pET-22b(+) (Novagen) cut with the same enzymes. The resulting construct (pCBJ237) was confirmed by sequencing, and encodes a protein that is identical to wildtype Avr9 except for three additional amino acids at the N-terminus (Table 4.1). Although this vector encodes a 6-Histidine (6His) tag at the C-terminus of the inserted reading frame, it should not be present on the fusion protein as the normal Avr9 stop codon is included in the construct (after the C-terminal histidine of Avr9).

A preliminary bioassay of the culture medium (LB) of these cells suggested that functional Avr9 was present (not shown). In this bioassay, it was apparent that the LB medium itself contains compounds that elicit necrosis in tobacco leaves, confounding

interpretation of this experiment. Two approaches were used to try to circumvent this problem; firstly batch IEC purification of 50 ml medium of Avr9 expressing and BL21 (negative control) *E. coli* was performed (by the above described batch method, including elution with 200mM NaP, pH 8.0), and secondly the bacterial periplasm was purified as described in the manufacturers instructions (Novagen 2000) as this may have contained more concentrated and pure Avr9. No clear activity was observed in a bioassay of these fractions (not shown).

The resulting supernatant from IEC purification of the LB medium (from both Avr9 and BL21 *E. coli* cultures) was Ziptip purified and analysed by MALDI-TOF as described above. A specific peak of 3508 Da was observed in the Avr9 medium and not in the medium of the same cells lacking a plasmid (BL21 cells; Figure 4.14). The predicted size of the protein produced from this plasmid (Table 4.1), assuming correct cleavage of the signal sequence and no formation of disulphide bonds, is 3512 Da. This indicated that expressed Avr9 was present in the medium, and suggested that some or all of the three disulphide bonds of Avr9 were formed, concurring with the preliminary bioassay evidence.

No further work was undertaken on the expression, purification, bioassay or MALDI-TOF analysis of Avr9 expressed in *E. coli* due to time limitations.

A.

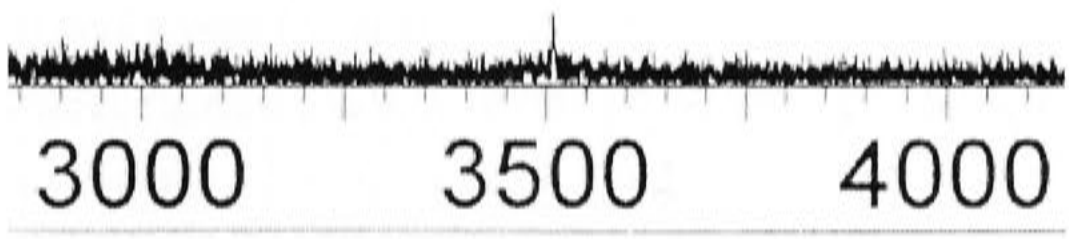

B.

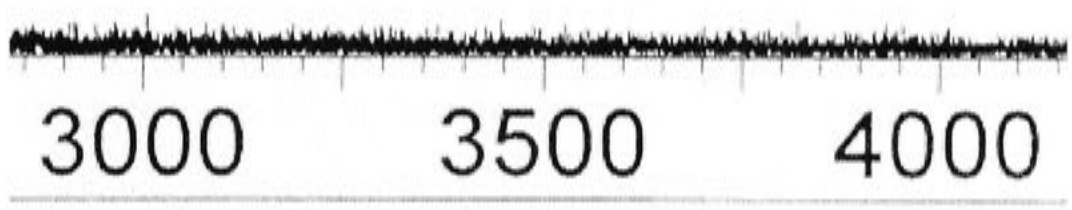

C.

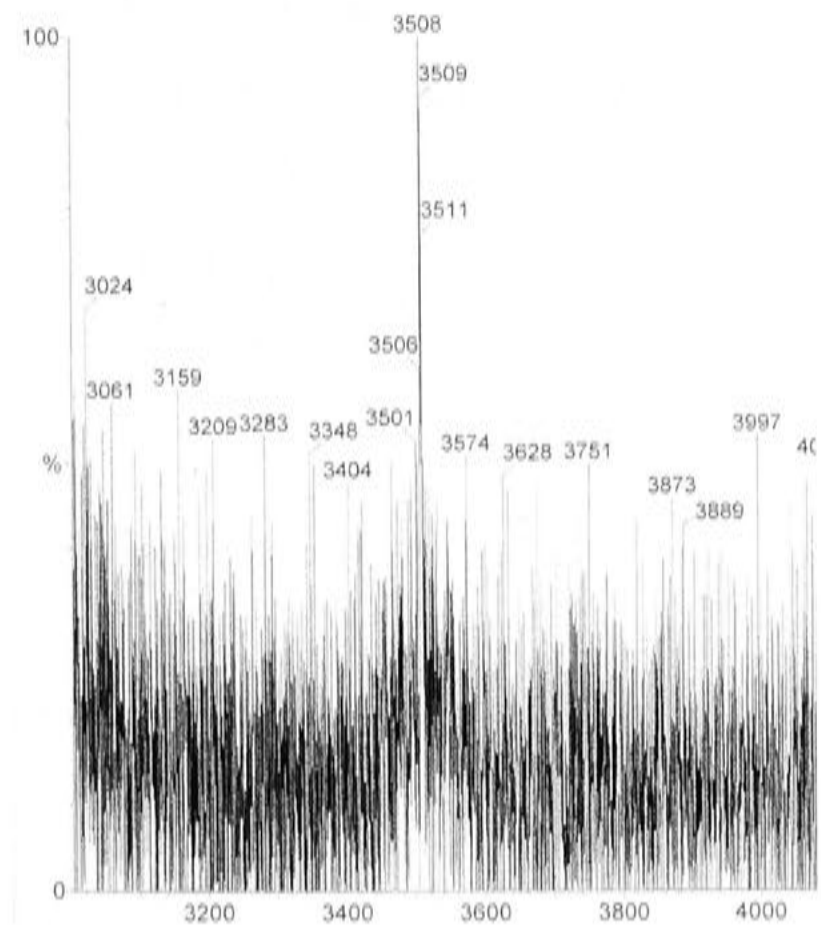

Figure 4.14. MALDI-TOF detection of Avr9 recovered by batch IEC and Ziptip purification from the culture medium of BL21 *E. coli* expressing secreted Avr9 (**A**. and **C.**) and BL21 *E. coli* containing no plasmid (**B.**). An enlargement of the region surrounding the peak from A. is shown in C., with intensity adjusted relative to the 3508 Da peak.

4.4 DISCUSSION

4.4.1 Purification of Avr9

The work described in this chapter aimed to develop tools that would be capable of detecting modifications to Avr9 when supplied exogenously to tobacco cells. MALDI-TOF was chosen as it was a sensitive and accurate method likely to be most useful for the detection of potential modifications to Avr9. A method for purification of Avr9 (from a range of source material) to use in conjunction with subsequent MALDI-TOF analysis of samples was therefore developed by adaptation of previously published methods (Honée *et al.* 1995; Kooman-Gersmann *et al.* 1997; Van den Ackerveken *et al.* 1993). The primary source of Avr9 used for the development of these methods was transgenic SLJ6201F tobacco (*N. tabacum*) expressing Avr9 in the apoplast (Hammond-Kosack *et al.* 1994a), as this was both a convenient and abundant source of functional, mature Avr9 peptide.

As the work described here was primarily intended to establish methods for the purification and analysis of Avr9, it was by nature developmental and consequently experiments demonstrating the procedures were not routinely repeated on more than 1-3 occasions (as indicated in the text). This was not considered critical for a number of the experiments (particularly those not reliant on biological processes) since previously published procedures were being adapted and/or subsequent usage of the methods (either in this chapter or if the work was continued) would highlight any inconsistencies in the techniques.

Cation-exchange chromatography

Previously published Avr9 purification procedures performed Ion-Exchange Chromatography (IEC) using the Pharmacia resin CM-Sephadex C-25, which is a weak cation exchange resin with a carboxylic acid functional group (Amersham-Pharmacia 1999). However, an equivalent IEC resin (Bio-Rex 70, Bio-Rad) which had the same functional group was already available and was used instead. Nevertheless, it was appropriate that experiments were first conducted to ensure that it performed in the expected manner and to determine an Avr9 binding capacity from the relevant source material.

The previously published protocols for the purification of Avr9 used a pH gradient of 20mM NaP (pH 5.5-8.0) to elute Avr9 from a column. However, this approach would have been problematic (though not unachievable) as the resin is a strong pH buffer, and because of resin swelling that results from changing the pH of the buffer (Amersham-Pharmacia 1999; Bio-Rad 2003). To account for these factors, initial IEC purification experiments (in particular for the MALDI-TOF detection experiments) were conducted using batch washing, and subsequent batch elution with 200mM NaP (pH 8.0). In an attempt to improve the resolution and/or throughput of the IEC step, preliminary investigations of NaCl elution of Avr9 from the resin in batch or with a linear gradient were conducted. These methods were tested empirically, since no report of NaCl elution of Avr9 from an ion-exchange resin had been published previously.

Gradient elution was tested using a linear gradient of 0-1M NaCl in 20mM NaP (pH 5.5) to elute Avr9 from a Bio-Rex 70 column. One limitation to this experiment, particularly with regard to determining what NaCl concentration was required to elute Avr9, was that the slope and integrity of the gradient was not able to be confirmed (by measurement of fraction conductivity) due to limitations in the conductivity range of the available conductivity meter. This was not pursued further as this approach was not subsequently considered to be of sufficient value to the envisaged outcomes and available timeframe of this chapter to warrant this. In any case, the gradients formed were probably satisfactory as NaCl gradients are generally considered to be routine and reproducible (Amersham-Pharmacia 1999).

The eluted fractions containing Avr9 activity and the equivalent wildtype extracts were concentrated and desalted by C-18 cartridge reversed-phase chromatography (C-18), freeze dried and, after dissolution at 100 x higher concentration, the protein concentration was determined. The Avr9 and wildtype extracts contained 100 and 125 µg/ml protein respectively, suggesting that most of the protein in these fractions was not Avr9. These results indicate that further purification would be required to obtain pure Avr9 (though this was not the aim of the work described here), as expected judging from the published literature on Avr9 purification (Honée *et al.* 1995; Kooman-Gersmann *et al.* 1997; Van den Ackerveken *et al.* 1993).

There are a few ways in which this procedure could be further developed. One improvement would be to collect smaller fractions, say 2-3 ml, to improve the

resolution of this procedure. This was not done initially as the experiment described was intended only as a preliminary study to determine whether this approach may be of value. Using smaller fractions would probably act to obtain similar quantities of Avr9 in a smaller volume with less contaminating protein components. Another possibility would be to use a 0-0.5M NaCl gradient to elute Avr9, which would also act to improve the resolution of this procedure. Alternatively, as the primary purpose of this IEC step was to remove a large proportion of contaminants, it may be most useful left as is and/or performed in batch as a large scale 'clean up' step for significant quantities of source material. This would complement the next step in the published protocol (after C-18 chromatography), High Performance Liquid Chromatography purification, which has high resolution and requires a relatively clean sample.

Recovery estimation

One limitation to the bioassays of the NaCl batch and gradient eluted fractions (Figure 4.6 and Figure 4.7) is that the recovery could not be assessed due to the lack of NaCl containing positive controls. These were not performed as space on the leaf was limiting and because quantitative effects of buffer components were not intended to be investigated in this first instance. The quantitative effects of buffer components (particularly salts) on the Avr9 bioassay in *Cf-9* tobacco leaves have not previously been reported, so it is not clear whether the variable salt levels influence the response. The results of these experiments suggested (without the benefit of the specified controls) that either Avr9 was lost during the procedure or that the NaCl in the samples reduced the intensity of the response to Avr9 in the bioassay.

The possibility that NaCl inhibits the Avr9 bioassay could be further investigated by adding increasing amounts of NaCl to aliquots of the same IF extract (up to the maximum tolerated by the leaf tissue), infiltrating these extracts into tobacco leaves and observing the strength of necrotic response. To observe a relatively minor difference in response using such an approach, it may be necessary to use only just enough Avr9 to initiate necrosis and add increasing amounts of NaCl to the samples. A better approach may be to infiltrate a series of two-fold dilutions of Avr9 IF with and without NaCl (say 100mM), or any other compound of interest. Any differences in the necrosis inducing activity would be apparent as a difference in the dilution at which the leaf tissue responds to the IF.

The reversed-phase chromatography (C-18) purification of the fractions resulting from the column purification experiment suggested that the recovery after the combined IEC and C-18 procedures was between 5-25% of Avr9 from acetone-cleared IF (Figure 4.8). This is approximately comparable to the recovery estimated for the batch NaCl IEC purification procedure (<25%), although this latter experiment lacked the appropriate NaCl containing control to confirm this estimation.

If increasing NaCl concentration in the samples did not affect the response to Avr9, this would suggest that a considerable proportion of Avr9 was lost during the procedure, in concurrence with the bioassay of the C-18 recovered samples. Since little activity was detected in the flow through from the column, indicating that most if not all Avr9 bound to the column initially, this suggests that the loss of Avr9 may be due to irreversible binding of some Avr9 to the resin. Alternatively, it is possible that a very small portion of Avr9 was continuously lost from the resin during the washing procedure and/or at a low level in the other NaCl eluted fractions, such that the main peak of Avr9 activity was reduced. Further work would be necessary to determine which of these possibilities is more likely. These could be tested by recovering Avr9 from all wash fractions from the column (using C-18 chromatography) and testing this and eluted fractions in a semi-quantitative bioassay (for example using appropriate dilution series comparisons to control samples).

4.4.2 MALDI-TOF analysis of Avr9

MALDI-TOF MS was decided upon as a method to analyse potential modifications to Avr9 because of its high sensitivity, reported ability to detect proteins from a mixture and the relative ease of use. At the beginning these experiments, MALDI-TOF had not been used to detect Avr9, however it has subsequently been used to monitor the folding of pure Avr9 protein (van den Hooven *et al.* 2001). The method used in this paper used the same matrix (alpha) in an almost identical solvent mix (50/50/1 acetonitrile/water/TFA, compared to 50/50/0.5 in this chapter) using broadly the same MALDI-TOF conditions (positive reflector mode with external calibration; no other details were reported). This supports the finding in this chapter that these conditions were suitable for detection of Avr9.

However, the detection of Avr9 from a known solution containing only pure Avr9 would be more routine that detecting it from semi-purified extracts, as was attempted in

this chapter. Although MALDI-TOF can detect proteins from complicated mixtures (Bakhtiar and Nelson 2000; Chong *et al.* 1997; Domin *et al.* 1999; Li *et al.* 2000; Wang *et al.* 1998) it is not to be expected that every protein could be detected from every mixture. Nevertheless, attempts were made to detect Avr9 directly from IF and acetone-cleared IF and, perhaps unsurprisingly, no peaks corresponding to the expected size of Avr9 were observed.

As salt is known to cause problems with MALDI-TOF mass spectrometry (Micromass 1997), acetone-cleared IF samples were desalted using a Centricon ultrafiltration column (molecular weight cut-off of 3000 Da). A bioassay for Avr9 activity of this fractionation procedure showed that most of the Avr9 from the sample (>95%) was lost. This is not surprising, since the specified molecular weight cut-off is nominal, and typically one would use a cut-off value significantly below the molecular weight of the protein of interest to retain the majority of the sample. For fractionation of a protein the size of Avr9, a 1000 Da cut-off would have been more appropriate, however the 3000 Da cut-off column was the smallest available ultrafiltration column and the yield was not paramount for this experiment.

MALDI-TOF analysis of these desalted samples revealed a relatively strong signal at 3394 Da in the Avr9 IF extracts that was never observed in the wildtype IF extracts, indicating that this peak is Avr9. This peak was resolved to the level of isotopic variants (single atomic mass units), indicating the high level of precision of this method at this molecular weight. Previous mass spectrometry analysis (using ESI-MS) had determined a mass of tobacco (*N. clevelandii*) expressed Avr9 to be 3390 Da. The difference is most likely due to the different types of MS used, probably arising from error associated with the calibration of the instruments or the calculation (deconvolution) of the mass of the peptide from several *m/z* peaks generated during ESI-MS (Hop and Bakhtiar 1997).

This is the first time Avr9 expressed in *N. tabacum* has been detected using mass spectrometry, and also the first time that the presence of the correctly expressed and processed form has been demonstrated in the SLJ6201 transgenic line by a method other than bioactivity. Also, this result confirms the previous result (Kooman-Gersmann *et al.* 1998a) that Avr9 expressed in tobacco is 202 Da larger than predicted from amino-acid sequence alone, a mass difference ascribed to the presence of an N-acetyl-glucosamine residue (Kooman-Gersmann *et al.* 1998a). In the MS analysis of Avr9 here the mass of

Avr9 was determined to be 3394 Da, which is 206 Da higher than that predicted from amino-acid sequence alone, however the significance of this difference is not clear.

The strength of this peak was expected to have been sufficient to perform a post-source decay (PSD) analysis of the analyte. PSD analyses the size of degradation products of a peak of interest, which can allow determination of peptide sequence in many cases (see introduction to this chapter). This approach was attempted in the hope that it would independently confirm the identity of the 3394 Da peak as Avr9. However, no specific PSD products of the peak were observed, consistent with the fact that this approach is not amenable to all proteins (Chaurand *et al.* 1999).

One reason for the lack of success with PSD analysis of Avr9 may be that the active peptide has a very robust tertiary structure. This possibility could be tested by reducing the three disulphide bridges prior to MALDI-TOF analysis. On one occasion, an attempt was made to reduce Avr9 using β-mercaptoethanol (250mM, 80°C, 10 minutes), but a 6 amu shift in the size of the peak indicative of reduction of the three disulphide bonds was not observed (data not shown). A subsequently published report on the structure of Avr9 and its disulphide suggests that harsher chemical treatment may have been necessary to reduce these bonds (van den Hooven *et al.* 2001).

Performing the MALDI-TOF detection on the IEC purified Avr9 (after C-18 purification by Ziptip) gave a stronger peak than from acetone-cleared and desalted IF. Despite the fact that MALDI-TOF MS can analyse a mixture of proteins, purer samples do result in improved MALDI-TOF signals (Micromass 1997). This is supported by supporting the observation that IEC purified and desalted Avr9 gave a better signal than the desalted IF. It is probably for this reason that MALDI-TOF analysis of complex samples is usually used as a 'profiling' tool, rather than for analysis of a particular analyte of interest (Chong *et al.* 1997; Domin *et al.* 1999; Wang *et al.* 1998), unless the analyte is a major component of the mixture (Chong *et al.* 1997).

4.4.3 Towards an experimental outcome

The development of the purification and MALDI-TOF detection methods was aimed at providing tools to determine whether Avr9 is modified, in particular by glycosylation, when added exogenously to plant cells. In pursuance of this goal, the above purification and MALDI-TOF detection methods (that were developed using IF extracts) were

applied to extracts from whole leaf tissue. Avr9 was much less detectable by MALDI-TOF from these extracts than it was from IF extracts. It is not clear whether this was due to reduced levels of Avr9 being extracted or whether sensitivity was reduced due to the higher abundance of contaminating proteins in the whole leaf extract. Further development of the purification method is therefore probably necessary to purify Avr9 from plant tissue to an adequate level for the detection of Avr9 and any variants using MALDI-TOF.

Another drawback of this experimental approach to the biological question is that it assumes that modified forms of Avr9 would also be extractable using this protocol. There are two main problems with this assumption. Firstly, the acetone clearance step could select against proteins with large carbohydrate moieties because of the usually low solubility of carbohydrates in acetone. Secondly, the putative modification could change the pI of Avr9, which may affect the efficiency of the IEC purification step. One possible way to account for these possibilities in the first instance would be to use SDS PAGE and western blotting of plant tissue expressing Avr9 (as outlined in the discussion of Chapter 3) to determine whether or not core ER glycosylation of Avr9 does occur. If this did occur, western blotting would be an adequate approach to determine whether this modification also occurred on exogenously added Avr9, and the above described methods would not need to be further refined. If core ER glycosylation did not occur, further modification of the purification method would be needed. However, the possibility that the methods might select against variants of Avr9 would be difficult to exclude in the absence of prior knowledge of the modifications, making this approach problematic.

Further towards the ultimate aim of these experiments, expression of Avr9 in *E. coli* was investigated as a clean and plentiful source of Avr9 with an unmodified N-glycosylation site. Preliminary bioassay analysis suggested that functional Avr9 was probably produced. However, this bioassay needs to be repeated using either a minimal culture medium (that does not elicit necrosis in tobacco) or with an improved IEC purification step to remove elicitors from the medium. This latter approach was attempted once, but no bioassay response was observed (not shown).

MALDI-TOF analysis of IEC purified *E. coli* Avr9 detected a significant but faint peak 4 Da (amu) smaller than the predicted size of the expressed peptide with all cysteine residues reduced. While this difference is only 4 amu, not 6 that would be expected if all

three disulphide bonds had formed, it seems most likely that this peak represents fully folded and oxidised Avr9 rather than that with one disulphide bond reduced, for the following reasons. Firstly, studies on Avr9 folding have shown that the primary sequence of Avr9 contains sufficient information for complete folding to a functional form (van den Hooven *et al.* 1999). In particular, the method for folding of synthesised Avr9 involves simply stirring a solution of the peptide at room temperature to allow oxidation of the peptide (Mahe *et al.* 1998), suggesting that any Avr9 present in the medium of *E. coli* expressing this peptide will be fully oxidised. Secondly, the preliminary evidence for Avr9 activity in the culture medium by bioassay, while not conclusive on its own, is consistent with the presence of active (and therefore fully oxidised) Avr9.

The work on this avenue for Avr9 production has not proceeded further due to time constraints, although the further development of such a resource would be useful in at least the following ways. This method could be adapted to allow expression of Avr9 in a minimal medium so that subsequent purification would be considerably simpler than from plant IF extract. Also, the use of an *E. coli* expression system allows the rapid production of protein from a large culture, so the quantity of source material would not be limiting. A large culture volume in combination with batch IEC as the initial purification and concentration step would thus allow large quantities of pure, functional Avr9 to be produced relatively quickly and easily.

4.4.4 General comments and further work

This work has described the adaptation of a published Avr9 purification protocol and the development of a method for MALDI-TOF detection for Avr9 from different extracts. An expression system that has the potential to produce useful quantities of pure, functional Avr9 has also been developed, although further development is required to demonstrate its utility. While the initially intended experiments have not been conducted, significant progress towards achieving this goal has been made. Furthermore, these tools could be useful for other aspects of this project or any other investigation of the Avr9 protein. For example, one possible way to use these methods to monitor Avr9 variant expression is outlined in the discussion of Chapter 3.

Another approach to determining whether Avr9 enters the cell when added exogenously could be attempted using the tools developed here. An experimental approach could be

to label Avr9 with a fluorescent dye, then add it to a suspension culture of wildtype *N. tabacum* cells. Using confocal microscopy to monitor the localisation of fluorescence, it should be apparent whether or not Avr9 is internalised by the cells. If it does not enter the cell, it should at least bind to the high affinity binding site for Avr9 on the PM (Kooman-Gersmann *et al.* 1996), which would be of interest in itself. A dye that would be useful would be an amine reactive conjugate of the Alexa-Fluor® series from Molecular Probes, which are available in standard absorption/emission ranges. The advantages of using this system would be the high photostability, good water solubility and function over a wide pH range (Probes 2003). Functional Avr9 purified from the *E. coli* expression system partially developed in this work would be a good source of for these experiments if developed further. The labelling procedure could be monitored by MALDI-TOF as developed here, to ensure single labelling (e.g. Lu and Zenobi 1999), while modifications to the chemistry of the labelling (Hentz *et al.* 1997) could be used to selectively label Avr9 in a way that does not disrupt bioactivity (Kooman-Gersmann *et al.* 1997).

CHAPTER 5

NO EVIDENCE FOR Cf-9 FUNCTION IN WHEAT

5.1 SUMMARY

THERE is considerable interest in the possibility of transferring *R* genes between species and between broader taxonomic groupings. This chapter describes work that aimed to determine whether the *Cf-9* resistance gene from tomato could function in wheat to recognise Avr9 and elicit a disease resistance like response. After an unsuccessful attempt to generate transgenic *Cf-9* and *Avr9* wheat, a transient microparticle bombardment assay was used to determine whether *Cf-9* could function in wheat. Plasmids encoding GFP tagged Cf-9 with a wheat α-amylase signal peptide (wheat Cf-9) as well as an Avr9/GUS plasmid were generated for this assay. Comparisons of bombardments of the Avr9/GUS plasmid alone or in combination with the wheat Cf-9 plasmid revealed no difference in the number of cells expressing GUS (a marker for cell vitality), indicating that the Cf-9/Avr9 plasmid combination did not induce cell death in this assay. Quantification and statistical analysis of the results revealed no statistically significant differences between the Avr9 and Cf-9/Avr9 treatments. Confocal microscopy analysis showed that the wheat Cf-9 construct was being expressed, and that the protein had perinuclear and cytoplasmic localisation, but provided no strong evidence for or against ER localisation of the protein. Together, these data suggest that Cf-9 does not function effectively in wheat.

5.2 INTRODUCTION

5.2.1 *R* gene transfer to heterologous species

Prior to their molecular isolation, *R* genes could only be transferred between sexually compatible species or species that could otherwise be hybridised. However, the molecular cloning of many *R* genes has paved way for the use of transgenic technology

to transfer these genes between species that cannot be hybridised. There are some instances where inter-generic or inter-specific transfer of *R* genes has been found to confer resistance to pathogens carrying the appropriate *Avr* genes. The tomato *R* gene for resistance to *Pseudomonas syringae* (*P. s.*) pv *tomato* strains carrying the *avrPto* gene was found to confer resistance of *N. tabacum* (Thilmony *et al.* 1995) and *N. benthamiana* (Rommens *et al.* 1995) to *P. s.* pv *tabaci* strains to which the *avrPto* gene had been transferred. Likewise, the tobacco *N* gene for resistance to tobacco mosaic virus was found to confer resistance of tomato plants to this pathogen (Whitham *et al.* 1996). The *Bs2* resistance gene, which confers resistance of pepper to *X. campestris* pv *vesicatoria* with the *avrBs2* gene, was also found to confer resistance of tomato to this same bacterium (Tai *et al.* 1999).

These studies were possible because the pathogens in question were able to successfully infect the heterologous species in which the *R* gene was tested, however this is not always the case. To circumvent this host range limitation, a number of studies have tested *R* gene function (but not the ability to confer a resistance specificity) by combining the *R* and *Avr* genes or gene products in the same plant, then observing gene-for-gene specific induction of responses, typically necrosis. For example, the *Cf-9* gene was shown to function in tobacco (*N. tabacum*) and potato by infiltrating Avr9 IF into leaves of transgenic *Cf-9* lines, which resulted in a *Cf-9/Avr9* dependent necrotic response in both species (Hammond-Kosack *et al.* 1998). Additionally, tobacco seedling death (or lack of seedling germination) was observed when both the transgenes were inherited from a *Cf-9* x *Avr9* cross.

An alternative approach often used is to co-express *R* and *Avr* genes using a transient expression system such as agroinfiltration. One example found that *Cf-9* and *Cf-4* were functional in a range of solanaceous species (*Nicotiana* species and *Petunia*) by co-expressing these genes and the corresponding *Avr* genes and observing gene-for-gene specific necrosis (Van der Hoorn *et al.* 2000).

5.2.2 The limits of *R* gene function?

While the *Bs2* gene was found to function in other genera in the Solanaceae, by both pathogen resistance and *R/Avr* co-expression tests, it did not function using the co-expression test in *Arabidopsis*, turnip, cucumber and broccoli (Tai *et al.* 1999). This observation led the authors to suggest that *R* genes may exhibit restricted taxonomic

functionality (RTF), specifically within the plant family boundary. It is difficult to ascertain how many cloned *R* genes have been found not to function in heterologous species, particularly across family boundaries, but negative results noted include *RPS2* (transferred from *Arabidopsis* to tomato; Tai *et al.* 1999), *Cf-9* (transferred from tomato to lettuce, lupin, pea and flax; Van der Hoorn *et al.* 2000) and *Cf-4* (from tomato to lupine, pea and flax; Van der Hoorn *et al.* 2000). One limitation of these data is that there are many possible technical and biological explanations for these negative results.

However there are also examples where *R* genes have been shown to function across family boundaries using the *R*/*Avr* gene co-expression method. Using agroinfiltration, the *Cf-4* gene, but not *Cf-9*, was shown to elicit necrosis when co-expressed with *Avr4* in lettuce (Van der Hoorn *et al.* 2000). Also, it has been noted that *Cf-9* apparently functions in *Arabidopsis*, judging by specific seedling death when *Cf-9* and *Avr9* transgenic lines are crossed (K. Hammond-Kosack, pers. comm. in Kooman-Gersmann *et al.* 1998b), although it did not respond to relatively high levels of infiltrated Avr9 peptide (6 μM; Kooman-Gersmann *et al.* 1998b). It should be noted, however, that this result has not subsequently been published.

The *Cf-9* and *Avr9* interaction has been shown to activate low level defence responses in transgenic *Brassica napus* containing both genes, although no death of seedlings containing both transgenes was observed (Hennin *et al.* 2001b). Interestingly, in *B. napus* lines containing *Cf-9* and *Avr9*, the activated defence responses conferred increased resistance to *Leptosphaeria maculans*. This moderate increase in resistance, based upon a laboratory assay, was observed at 7 and 10 days post-inoculation (dpi), but not at 14 dpi or thereafter (Hennin *et al.* 2001b). A similar result was observed when a *Cf-9 B. napus* leaf was infiltrated with IF containing Avr9 prior to infection (Hennin *et al.* 2001b).

This study was taken further by investigating whether moderate induction of resistance response using the *Cf-9*/*Avr9* combination would confer resistance to other fungal pathogens (Hennin *et al.* 2002). Infiltration of Avr9 IF below a cell death inducing threshold into *Cf-9 B. napus* leaves was sufficient to increase resistance to *L. maculans* and *Sclerotinia sclerotiorum* around the Avr9 injection site, while only systemic resistance to *Erysiphe polygoni* was induced in this experiment. In another study, injection of Avr9 at the infection site at a level sufficient to induce necrosis was shown

to inhibit *E. polygoni* but promote the spread of the necrotrophic pathogen *S. sclerotiorum* on *Cf-9 B. napus* (Hennin *et al.* 2001a).

Although the levels of resistance measured in these studies do not appear strong, and further work would be needed to determine whether this would be meaningful in the field, it is interesting that a resistance gene from tomato against a non-pathogen of *Brassica* (*C. fulvum*) can induce resistance to fungal pathogens of *Brassica*. This suggests that although specific resistance genes may confer resistance only to one race of a pathogen, they may be able to induce endogenous defence mechanisms that are effective against a broader range of pathogens.

More recently, the function of the unique *Arabidopsis R* genes *RPW8.1* and *RPW8.2* (Xiao *et al.* 2001) was tested in three species from the Solanaceae. These genes confer broad-spectrum resistance of *Arabidopsis* to powdery mildew fungi (*E. cichoracearum*, *E. orontii*, *E. cruciferarum* and *Oidium lycopersici*; Xiao *et al.* 2001). Since these pathogens can infect members of the Solanaceae as well as *Arabidopsis*, these resistance genes were ideal to assess whether a resistance specificity could be transferred across a family boundary. Transformation of *N. tabacum* and *N. benthamiana* with the *RPW8.1* and *RPW8.2* genes resulted in increased resistance to *E. orontii* and *O. lycopersici* (*N. tabacum*), and to *E. cichoracearum* (*N. benthamiana*), while transgenic tomato plants remained susceptible to these three pathogens (Xiao *et al.* 2003).

This latter study is significant because it is an example of a resistance specificity associated with a particular *R* gene, rather than just the ability of the *R* gene to induce defence responses, being transferred across a family boundary. However, this should be noted in the context of this *R* gene class so far being structurally and functionally unique. The extent to which the RTF of other *R* genes, particularly members of the abundant NBS-LRR class, can be overcome remains to be determined.

5.2.3 What causes RTF?

The available reports considered above suggest that *R* gene functionality can usually be transferred between species or genera, but that the family boundary can only be crossed occasionally. An important question relating to the transfer of *R* genes between species is the reason/s for RTF, and whether and how they can be overcome. Relatively little is known, or has been hypothesised, about what limits the function of *R* genes in

heterologous species. A widely posited explanation is that *R* gene functionality in heterologous species is restricted by the similarity of signalling pathways leading to defence response activation (Hennin *et al.* 2001b; Hulbert *et al.* 2001; Rommens *et al.* 1995; Thilmony *et al.* 1995). One hypothesis put forward to explain the difference of *RPW8.1* and *RPW8.2* function between tobacco and tomato, that could be used to explain RTF, is that the heterologous species may lack a component for *R* gene-dependent pathogen perception (Xiao *et al.* 2003).

One possible reason for RTF of R proteins that are predicted to be membrane anchored, such as the Cf proteins (Benghezal *et al.* 2000; Piedras *et al.* 2000) or Xa21 (Song *et al.* 1995, is that their signal peptide may not direct efficient translocation of the protein across the ER membrane during translation. This was observed with the Cf-9 signal peptide in *Arabidopsis*, a problem remedied by re-engineering the protein with a signal peptide from *Arabidopsis* (Benghezal *et al.* 2000). Lack of membrane translocation of the Cf-9 protein in *Arabidopsis* may be the cause of the reduced response of *Cf-9 Arabidopsis* to Avr9 peptide noted previously (Kooman-Gersmann *et al.* 1998b).

Hypotheses to explain RTF are discussed further in Chapter 7 of this thesis (the general discussion) along with further consideration of the possible causes of this phenomenon and a model that considers RTF in light of the guard hypothesis.

5.2.4 Aim of this chapter

The work described in this chapter aimed to determine whether the *Cf-9* resistance gene from tomato could initiate a resistance response to co-expressed *Avr9* in wheat. If function of *Cf-9* in this heterologous species could be demonstrated, it could potentially be utilised to engineer a non-specific form of disease resistance known as genetically-engineered acquired resistance ('GEAR', Hammond-Kosack *et al.* 1998; Jones *et al.* 1995). This involves generating a plant that contains *Cf-9* tagged (and inactivated) with a *Dissociation* transposable element (*Ds*), constitutively expressed *Avr9* and a stable source of *Activator* transposase (*sAc*). When somatic excision of the *Ds* element occurs (in a small proportion of cells), *Cf-9* function is restored and *Avr9* recognition occurs, resulting in localised death and systemic activation of defence responses. In tomato, this has been shown to confer increased resistance to a range of pathogens (Jones *et al.* 1995), and if *Cf-9* functioned in wheat, a similar outcome could be engineered in wheat. In support of this approach, the maize *Ac/Ds* system has been shown to function in

wheat (Takumi *et al.* 1999), which should therefore function to activate *Cf-9* in somatic cells in the same way as it does in tomato. Additionally, it has been shown that the *Cf-9/Avr9* combination in *B. napus* can induce defences against *Brassica* diseases (above; Hennin *et al.* 2001b; Hennin *et al.* 2002), suggesting that if *Cf-9* could be activated in wheat, increased resistance to wheat diseases may be possible.

In further support of this possibility, wheat and rice are known to have genes with similar sequence motifs and analogous structures to *Cf-9*. Searching of the National Center for Biotechnology Information (NCBI) non-redundant database using blastp and psi-blast reveals a number of sequences with similarity to Cf-9 in both wheat and rice. In wheat, structural and sequence similarity of the AWJL proteins to Cf-9 has previously been described (Jones and Jones 1997). More recently a number of other homologues of the *AWJL* genes have since been placed in Genbank (*WM 1* genes; Whitford, R. Sutton T., Dong, C., Able, J., Wolters, P. and Langridge, P. unpubl., 2004), which also exhibit significant similarity to *Cf-9*. A significantly larger number of predicted proteins similar to Cf-9 are detected by blast analysis of the rice genome, though further analysis of these would be required to ascertain to what extent they were structurally similar to Cf-9. The observation of such genes in wheat and rice is consistent with the possibility that appropriate signal transduction machinery may exist in cereals to allow function of Cf-9, though does not constitute evidence that Cf-9 would function in these species.

Therefore, to test whether Cf-9 can recognise Avr9 in wheat, a *R/Avr* gene co-expression approach was adopted. Initially it was planned to generate and inter-cross stable transgenic *Cf-9* and *Avr9* wheat lines and examine progeny for seedling death or low level responses indicative of Cf-9 activation, such as increased cell death, lesions or activation of defence related gene expression. As the stable transformation attempt was unsuccessful, a transient assay based upon co-expression of *Cf-9*, *Avr9* and a marker gene (*uidA*; encoding β-glucuronidase {GUS}) by particle bombardment was conducted. This approach was based upon previous methods that used a reduction of marker gene expression in cells expressing both the *R* and *Avr* genes as an indicator of cell death, and therefore *R* gene function (Jia *et al.* 2000; Mindrinos *et al.* 1994). To ensure correct localisation of the expressed Cf-9 protein, it was engineered with a new signal peptide to ensure correct localisation of the protein to improve the likelihood of it functioning in wheat.

In this assay, a plasmid containing *Avr9* and *uidA* was bombarded alone or in combination with a *Cf-9* plasmid into wheat leaves, and resulting leaf sections examined for a *Cf-9*-dependent reduction in cells expressing the marker gene. Statistical analysis was performed on the experimental data from the co-bombardment experiments to ensure that conclusions were statistically sound. To demonstrate that Cf-9 protein was being produced as expected, confocal microscopy was performed on onion seedlings bombarded with the *Cf-9* construct (which has an N-terminal GFP tag).

Evidence obtained using this approach suggests that Cf-9 does not function in wheat, although this is not conclusive. The limitations of the data and basis of conclusions are discussed, along with potential approaches to further this work.

5.3 MATERIALS AND METHODS

5.3.1 Plasmid construction

pCBJ236 – Wheat Cf-9

The plasmid pCBJ236 contains a chimeric gene encoding a wheat α-amylase signal peptide, an N-terminal GFP fusion, the *Cf-9* coding region and the *Cf-9* 3' untranslated region (Figure 5.1), and was generated as follows. The primers 5'WheatSP (atcgatgggcaagcactctgctactct) and 3'WheatSP (gaattcagcctgtgctaagctggag) were used in combination to amplify the approximately 80 bp fragment corresponding to the amylase signal peptide (National Center for Biotechnology Information, USA, accession CAA29252) from *Triticum aestivum* cv Veery5 genomic DNA. The PCR product was cloned using a TA cloning kit (Invitrogen), then excised using the *Cla*I and *Eco*RI restriction enzyme cleavage sites that were engineered into the 5'WheatSP and 3'WheatSP primers, respectively (underlined). The resulting fragment was used in a three-way ligation in combination with pBluescript (SK$^-$) cut with *Cla*I and *Xba*I and the ~800 bp *Eco*RI-*Xba*I fragment from pCBJ92. This last fragment corresponds to the 5' end of the GFP fragment of mGFP5 (*Eco*RI to *Nco*I; Siemering *et al.* 1996) and the remainder of the GFP coding sequence from pCBJ4 (*Nco*I to *Xba*I; Benghezal *et al.* 2000). The resulting wheat signal peptide:GFP fusion plasmid (pCBJ234) was confirmed by sequencing. The signal peptide:GFP fragment was excised as an ~800 bp *Cla*I-*Xba*I fragment and used in a three-way ligation with the 2.9 kb *Xba*I-*Bam*HI

fragment from pCBJ92 (the Cf-9 fragment, which is equivalent to the same fragment from pCBJ5; Benghezal *et al.* 2000) and the 2.9 kb *Cla*I-*Bam*HI fragment from pCBJ80 (which corresponds to the 'dark' pBluescript KS^+ vector; Jones *et al.* 1992), resulting in pCBJ235. The junctions and 5' and 3' ends of this construct were confirmed by sequencing.

The 3.7 kb *Cla*I-*Bam*HI fragment corresponding to the wheat signal peptide:GFP:Cf-9 fragment was excised from pCBJ235 and ligated into pSLJ10122 cut with *Cla*I and *Bam*HI, resulting in pCBJ236. The plasmid pSLJ10122 corresponds to the CaMV35S promoter with the tobacco mosaic virus omega leader as a 1413 bp *Eco*RI-*Cla*I fragment in pUC119. This last step (resulting in pCBJ236) was kindly performed by Dr Daigo Takemoto, of the Research School of Biological Sciences, Australian National University, Canberra, Australia. The resulting construct was confirmed by sequencing, and encodes a wheat α-amylase signal peptide:GFP:Cf-9 fusion under the control of a CaMV35S promoter (Figure 5.1).

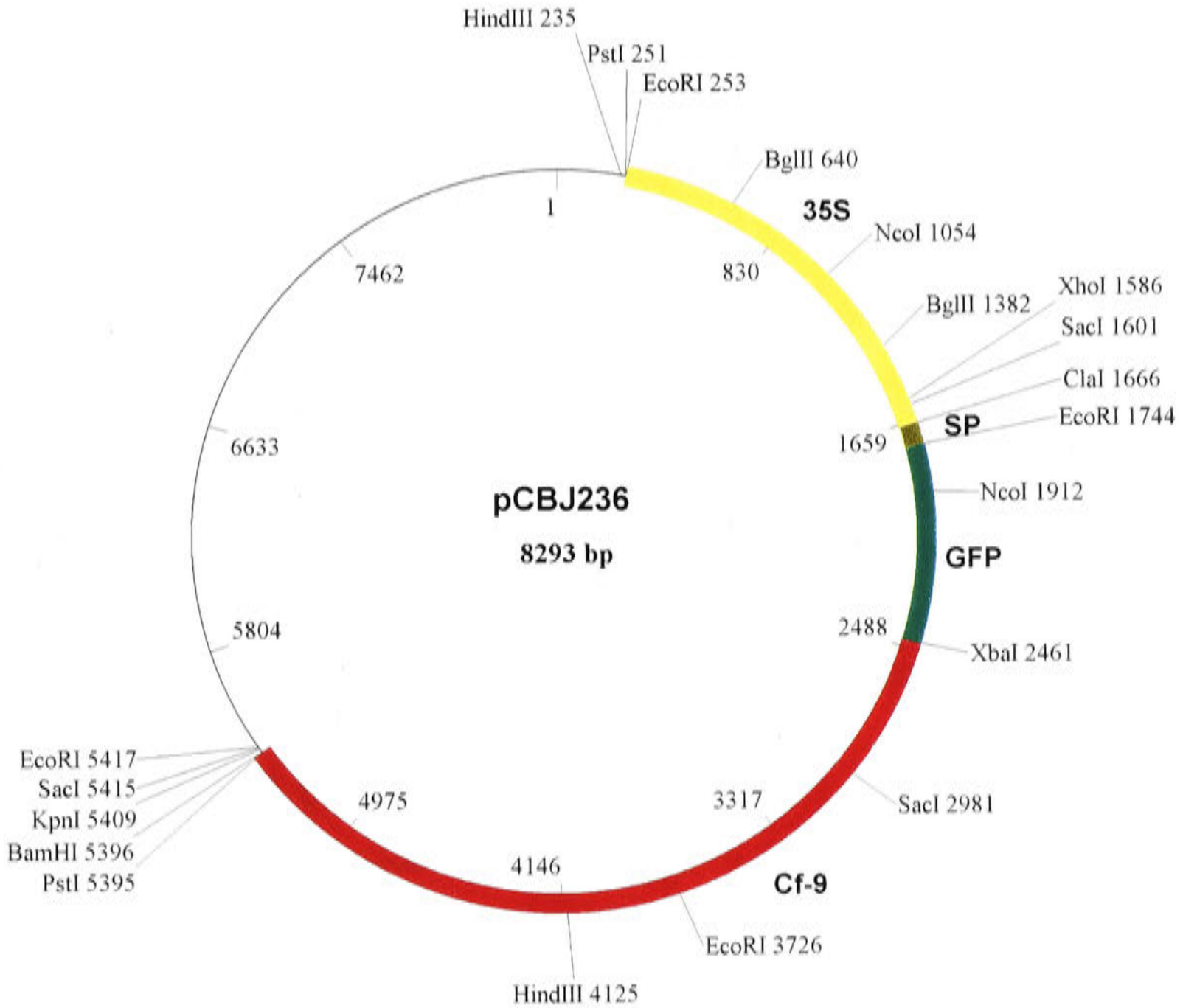

Figure 5.1. Plasmid vector pCBJ236, which contains the CaMV35S promoter (yellow) controlling the expression of a recombinant protein consisting of (N to C terminal) a wheat α-amylase signal peptide (**SP**, brown), Green Fluorescent Protein (**GFP**, green) and **Cf-9** (red; including the Cf-9 3' untranslated region) fusion protein in a pUC119 backbone.

pCBJ263 – Avr9/GUS plasmid

The plasmid pAHC25 contains the *uidA* (which encodes the GUS enzyme) and the *BAR* genes both under the control of the maize polyubiquitin (Ubi) promoter (Christensen and Quail 1996). To generate a single plasmid that encodes Avr9 and Ubi:GUS, the ~4 kb *Sph*I fragment from pAHC25 (corresponding to the full Ubi:GUS cassette) was excised and ligated into pCBJ231 (Avr9 in pBluescript, see Chapter 3) cut with *Sph*I, resulting in pCBJ263 (not shown). The clone selected for use contained the Ubi:GUS and CaMV35S:Avr9 constructs in the same orientation.

Other plasmids

The plasmid pCBJ96 was generated by Dr Mohammed Benghezal (unpublished). Briefly, it consists of the full length *Cf-9* gene with the *Arabidopsis* chitinase signal peptide and a GFP fusion between the signal peptide and B domain of *Cf-9*, under the control of the CaMV35S promoter in the binary vector pSLJ755I5. The control GFP-HDEL plasmid used was pBIN-mGFP5-ER (Haseloff *et al.* 1997; Siemering *et al.* 1996; see also http://www.plantsci.cam.ac.uk/Haseloff/IndexGFP.html), which is known to be present in the ER of onion cells (Collings *et al.* 2000).

5.3.2 Plant culture

Cultivar Veery5 wheat seeds were sterilised by first incubating seeds in 80% ethanol for 1 minute, draining, then incubating for 10 minutes in 10% (v/v) Domestos (Lever Rexona), then washing 4 times with 15 ml of autoclaved deionised water. Seeds were then germinated in vented culture flasks containing MS salts (pH 6.0) supplemented with 1% sucrose and 0.8% agar. Seedlings were germinated under 16/8 hour day/night cycle at approximately 24°C and used for microprojectile bombardment when 9-11 days old.

Onion seedlings (*Allium cepa* cv Gladalan Brown, Yates, Australia) were germinated on moistened tissue paper in sealed Petri-dishes in the dark at room temperature (approximately 23°C), and used 4-5 days after germination.

5.3.3 Microprojectile co-bombardment assay

Microprojectile bombardment was performed using modifications of previously described methods (Schweizer *et al.* 1999; Weeks *et al.* 1993), as follows.

Particle preparation

For each particle coating reaction, 1.8 mg of 1 μm gold particles (Bio-Rad) were mixed with 50 μl of 2.5M $CaCl_2$, 20 μl 0.1M spermidine (for multiple coating reactions, this mixture was made in bulk and aliquotted accordingly). Three microlitres (400 ng) of each plasmid was then added to each particle coating reaction, vortexed at high speed for 3 minutes and incubated on ice for 5 minutes. After centrifugation at 8 400 x g for 10 seconds, the supernatant was removed and 250 μl of 100% ethanol was added. The samples were vortexed for 1 minute, the centrifugation repeated, and the supernatant removed. The pelleted particles were resuspended by vortexing in 100 μl of 100% ethanol, and 10 μl of this mixture used for bombardment.

Bombardment, GUS staining and statistical analysis

The leaf blades of wheat seedlings, germinated as described above, were cut into ~6-15 mm long sections with a sharp scalpel blade ready for bombardment. Groups of 3-6 segments were placed close together on the centre of Petri-dishes containing MS salts (pH 6.0) and 0.8% agar. The open Petri-dish with the leaf samples was placed on the second (from the bottom) target shelf for bombardment (9 cm from the microcarrier disk stopping screen). Bombardments were performed using the Bio-Rad PDS-1000/He system, using 1100 psi rupture disks and a chamber vacuum of 25 inches of Hg. Onion seedlings were bombarded in groups of approximately 20 in the same way.

After microprojectile bombardment, Petri-dishes were closed and sealed using parafilm, and the leaf segments incubated for 2 days under the same conditions that the seedlings were germinated. Wheat leaf segments were then stained for GUS activity according to Schweizer *et al.* (1999), while onion seedlings were used for confocal microscopy as described below.

One-way analysis of variance was performed by Dr Jeff Wood, of the Statistical Consulting Unit, at the Australian National University, Canberra, Australia, using GenStat Release 6.1. Experiments were quantified as described in the text.

5.3.4 Confocal microscopy

Onion seedling epidermal cells were examined for GFP fluorescence using the Leica SP2 (Leica, Wetzlar, Germany) confocal microscope system with the assistance of Darryl Webb, of the Plant Cell Biology group, Research School of Biological Sciences,

Australian National University, Canberra, Australia. Samples were excited at 488 nm with an argon laser and fluorescence emission measured at 500-570 nm. All cells shown were viewed using a 20X numerical aperture 0.70 water immersion lens, and the line average used is given in figure legends. Other conditions and details are indicated in the text where necessary.

5.4 RESULTS

5.4.1 Stable transformation attempt

Initially, it was intended to generate stable transformed lines of wheat containing the *Cf-9* or *Avr9* transgenes, cross these lines and check for indications of Cf-9 function, such as seedling death or resistance response activation as has been used previously (Hammond-Kosack *et al.* 1998; Hennin *et al.* 2001b; Jones *et al.* 1994). The plasmids used for this transformation attempt were pSLJ6201 (CaMV35S:Avr9 in a binary vector plasmid; Hammond-Kosack *et al.* 1994a), and pCBJ96 (CaMV35S:GFP:Cf-9 in a binary vector plasmid; M. Benghezal, unpubl., described above). This work was performed by Drs Ryan Whitford and Chong-Mei Dong in the laboratory of Professor Horst Lörz, University of Hamburg, Germany using the method described by Becker *et al.* (1994).

GFP fluorescence was observed for some Cf-9 calli when viewed under a dissecting microscope and illuminated with 488 nm wavelength light. The subcellular localisation of resulting protein could not be interpreted under the low magnification of the available fluorescence microscope. While regenerating calli were recovered from both the Cf-9 and Avr9 transformation attempts, no mature plants were recovered from either (R. Whitford, C-M. Dong and P. Langridge unpubl.).

5.4.2 Re-engineering of plasmids

One problem with the particle bombardment stable transformation approach is likely to have been a low transformation efficiency for large plasmids (Taylor and Fauquet 2002) such as the binary vector plasmids pSLJ6201 and pCBJ96 (~25 kb), especially considering that the wheat transformation process is relatively inefficient (1.2% of bombarded immature embryos, Becker *et al.* 1994). Therefore, plasmids that contained

complete *Cf-9* and *Avr9* cassettes in a small plasmid backbone such as pBluescript or pUC were generated for more efficient stable transformation, although ultimately they were only used for the bombardment assay.

It has previously been observed that the native Cf-9 signal peptide does not direct efficient translocation of the protein into the ER in *Arabidopsis* (Benghezal *et al.* 2000), suggesting that a functional signal peptide is critical for Cf-9 localisation and therefore function. It was therefore decided to re-engineer the GFP:Cf-9 plasmid with an endogenous wheat signal peptide (from α-amylase) to ensure correct subcellular localisation of the protein when expressed in wheat. GFP tagged Cf-9 was chosen for this study to allow visualisation of the resulting protein by microscopy or by western blotting. Cf-9 tagged at the N-terminus with GFP has previously been shown to function in tomato to recognise Avr9 (D. A. Jones, unpubl.), indicating that this tag does not disrupt Cf-9 function. The desired plasmid, 'wheat Cf-9' (α-amylase SP:GFP:Cf-9 under CaMV35S promoter) was therefore generated as described in Section 5.3.1, see Figure 5.1).

The plasmid pCBJ231 (derived from pSLJ6201 as described in Chapter 3) contains Avr9 fused to the signal peptide from tobacco pathogenesis related protein 1a (PR1a), which is known to function in tomato and tobacco (Hammond-Kosack *et al.* 1994a), under the control of the CaMV35S promoter. A GUS expression cassette under the control of the maize ubiquitin promoter was cloned into pCBJ231 in order to generate the Avr9/GUS plasmid, pCBJ263 (see Materials and Methods).

5.4.3 Co-bombardment assay for Cf-9 function

To test whether Cf-9 can function in wheat to confer recognition to Avr9, and elicit subsequent cell death, a biolistic co-bombardment approach was employed that was similar to previously described approaches (Jia *et al.* 2000; Mindrinos *et al.* 1994). In essence, gold particles coated with a marker gene along with one or both *R* and *Avr* genes are bombarded into target tissue. If the *R* gene is functional, *R*/*Avr* dependent cell death will occur and reduce the number of cells expressing the marker gene.

If Cf-9 functions in wheat, co-bombardment of the plasmids wheat Cf-9 and Avr9/GUS should result in cell death, and therefore the absence of GUS expression, whereas Avr9/GUS alone should result in numerous cells expressing GUS. Previous studies have

shown that introducing two plasmids on the same batch of particles in this way gives around 73% co-expression of the plasmids of interest in bombarded wheat leaf tissue (Schweizer *et al.* 1999). Therefore, if wheat-Cf-9 functions in wheat to recognise Avr9 and initiate cell death, it would be expected that ~73% less GUS expressing cells be observed in the Avr9/GUS + Cf-9 bombardment than from Avr9/GUS bombardment alone. That fact that such a result has been observed in an equivalent study (Jia *et al.* 2000) supports this expectation.

Segments of wheat leaf were bombarded with 1 μm gold particles coated with either Avr9/GUS + pBluescript (the latter to equalise the amount of DNA coated onto the particles) or Avr9/GUS + wheat Cf-9 as described in Section 5.3.3. After 48 hours, leaf samples were stained for GUS activity, cleared with ethanol and viewed under a dissecting microscope with illumination from below. No clear difference in the number of cells expressing GUS was observed, as shown by the representative leaf samples in Figure 5.2, although some variation was observed between leaf segments (see below). This experiment was repeated on three independent occasions. On one occasion, one bombardment for each plasmid combination (Avr9/GUS + pBluescript and Avr9/GUS + wheat Cf-9) was performed, and on the two other occasions two bombardments were performed for each plasmid combination. On these latter two occasions, each plasmid combination was prepared using a different particle binding reaction to account for this known source of variability (Southgate *et al.* 1995). Therefore, this represents five repetitions of this experiment on three separate occasions. On all occasions, either four or five leaf segments were bombarded for each plasmid combination (see Appendix 3 for the raw data). The lack of difference between the two treatments was observed over all repetitions.

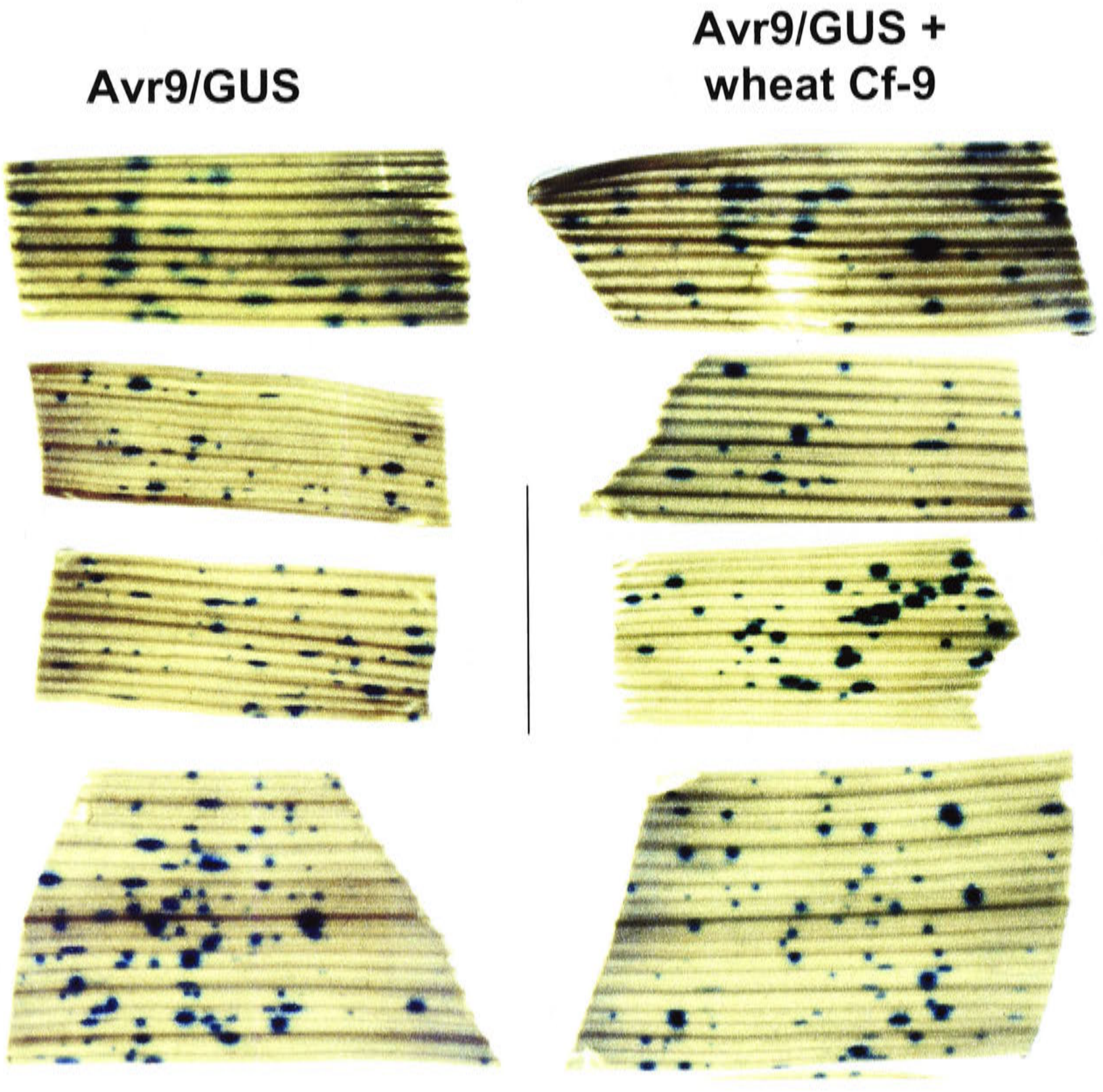

Figure 5.2. Microprojectile bombardment of pCBJ263 (**Avr9/GUS**) or pCBJ263 and pCBJ236 combined (**Avr9/GUS + wheat Cf-9**) into wheat seedling leaf segments, followed by GUS staining. Representative leaf segments of comparable sizes are shown for Avr9/GUS and Avr9/GUS + wheat Cf-9 bombardments. The scale bar shown between the columns of leaf segments is 5 mm.

5.4.4 Quantification and statistical analysis

While visual inspection does not reveal an obvious difference between the Avr9/GUS and Avr9/GUS + wheat Cf-9 bombardments, it is possible that minor, quantitative differences occurred between the treatments. To account for this possibility, these experiments were quantified by measuring leaf segment area and the number of GUS transformed cells per unit area for each leaf segment for subsequent statistical analysis. In total, this represented 24 leaf segments bombarded with Avr9/GUS + pBluescript coated particles ("Avr9") and 23 segments with Avr9/GUS + wheat Cf-9 coated particles ("Avr9/Cf-9"). The area of the leaf segments was measured from photographs using Image J (National Institute of Health, USA) image analysis software, and GUS positive cells were counted manually. Any leaf segments with less than six GUS positive cells were removed from the data set as unrepresentative, leaving 18 Avr9 (six removed) and 19 Avr9/Cf-9 (four removed) segments (see Appendix 3 for the raw data).

One-way analysis of variance was performed on the number of GUS positive cells per cm^2 between Avr9 and Avr9/Cf-9 leaf segments. No significant difference was found between these treatments ($F = 0.71$, 1,36 d.f. $P = 0.41$) with means (± standard error) of 72.4 (± 9.2) and 63.1 (± 6.4) transformed cells per cm^2 respectively. Logarithmic transformation of the variables did not alter this result ($F = 0.1$, 1,36 d.f. $P = 0.75$).

During visual observation of a number of bombardment experiments, it was noticed that there appeared to be both very strongly GUS stained cells and weakly GUS stained cells on each leaf, piece regardless of which particles they were bombarded with (e.g. see Figure 5.2). These weakly stained GUS cells could have expressed a small amount of GUS after particle bombardment, but then died due to the stress of particle bombardment or the assay conditions (Mindrinos *et al.* 1994; see also the discussion of this chapter). If this is the case, this could be caused or exacerbated by a weak Cf-9/Avr9 interaction, which would increase the proportion of these weak GUS cells.

To test this hypothesis, the number of weak and strong GUS expressing cells for each leaf segment was counted manually (using an arbitrary distinction between the cell types, see discussion) for analysis of the ratio of weak/strong GUS expressing cells. If the Cf-9/Avr9 interaction increases the proportion of weak GUS expressing cells, this ratio should increase compared to the Avr9 bombardment control. To determine if this was the case, a one-way analysis of variance was performed on the weak/strong GUS

cell ratio within each leaf. As this is a within leaf ratio, this should normalise between leaf variation. However, this analysis did not reveal a significant difference between the Avr9 and Avr9/Cf-9 bombardment treatments ($F = 0.64$, 1,36 d.f. $P = 0.43$), with mean ratios of 2.00 and 1.66 respectively.

Collectively, these data (Sections 5.4.3 and 5.4.4) do not provide evidence that wheat Cf-9 initiates cell death in response to Avr9 in this assay (see discussion).

5.4.5 Confocal microscopy imaging of wheat-Cf-9 expression

To determine whether the wheat Cf-9 protein was expressed and whether the expressed protein was correctly localised, onion seedlings were bombarded with pCBJ236 and analysed by confocal microscopy. Based on studies of Cf-9 in tobacco (Benghezal *et al.* 2000; Piedras *et al.* 2000), it was expected that wheat Cf-9 would be localised to the ER or PM when expressed in onion cells. Wheat seedlings were not used as the leaves and coleoptile were strongly autofluorescent under the conditions used for GFP imaging, despite having been germinated in the dark (not shown). In addition to wheat Cf-9, a GFP-HDEL encoding plasmid (see Materials and Methods) was bombarded as a control for ER localisation. Two days after bombardment, segments of hypocotyl were cut from the seedlings and examined for GFP fluorescence by confocal microscopy.

Fluorescence corresponding to GFP was observed in a number of separate epidermal cells on different seedlings, as expected. Five separate cells bombarded with wheat Cf-9 were analysed by confocal microscopy. While examining fluorescent cells in tissue samples with excitation at 488 nm, some material was observed that fluoresced between 500 and 570 nm but did not appear to be cell localised. To confirm that the fluorescent cells observed were indeed fluorescing in a GFP specific manner, and to exclude the other material, spectral analysis was performed on one fluorescent cell and a nearby region of fluorescent material (Figure 5.3).

The same optical section was excited with the 488 nm laser, and emission intensity measured at wavelengths over a range from 495 to 575 nm in 5 nm windows. The three regions of interest (ROI 1-3) of the fluorescent cell were compared to a nearby fluorescent region (ROI 4; Figure 5.3A). A plot of nominal intensity against emission wavelength shows that ROIs 1-3 have a strong emission peak at approximately 511 nm

(Figure 5.3B). This and the shape of the emission spectrum are essentially identical to that previously reported for the Class 2 phenolate anion varieties of GFP (Tsien 1998), as was used in this study, clearly indicating that this is indeed GFP fluorescence (Figure 5.3B). This indicated that the wheat Cf-9 fusion protein (or at the least part containing the GFP fusion) is being expressed. However, ROI 4 emission does not peak at this wavelength and has a long flat emission spectrum, indicating that it is non-specific fluorescence.

Another representative cell bombarded with wheat Cf-9 is shown in Figure 5.4A. In this and the previous figure (and all cells expressing this construct that were examined), cells showed perinuclear and cytoplasmic localisation of GFP fluorescence, with large non-fluorescent regions that probably correspond to the vacuole (V) and the nucleus (N). It could not be determined whether any fluorescence corresponded to the PM due to the strong cytoplasmic fluorescence. To determine whether fluorescence was potentially consistent with ER localisation in this cell type, onion seedlings were bombarded in the same way with the GFP-HDEL plasmid as a control for ER localisation and analysed by confocal microscopy. A similar localisation of fluorescence was observed in the one cell transformed with this construct that was examined, however no structures clearly indicative of the ER were observed (Figure 5.4B). The nucleus and vacuole were observed in the GFP-HDEL cell as in cells transformed with wheat Cf-9, however structures that were probably trans-vacuolar strands (TVS) of cytoplasm were also observed. Similar structures were also observed in some images of wheat Cf-9 expressing cells, though these were not as clear as in this GFP-HDEL cell (not shown).

It is not clear from these images whether wheat Cf-9 fluorescence is cytoplasmic only, or is partially localised to the ER (including peri-nuclear ER). The GFP-HDEL cell imaged under slightly lower magnification also did not show fluorescence that distinctly indicated ER localisation, although only one GFP-HDEL cell was analysed in detail. However, since the images shown for the wheat Cf-9 and GFP-HDEL cells are optical sections through approximately the middle of the cells, this approach is unlikely to visualise cortical ER (ER around the periphery of the cell under the PM). Cells expressing these constructs were therefore analysed by optical sectioning to clarify the localisation of the expressed proteins (below).

A.

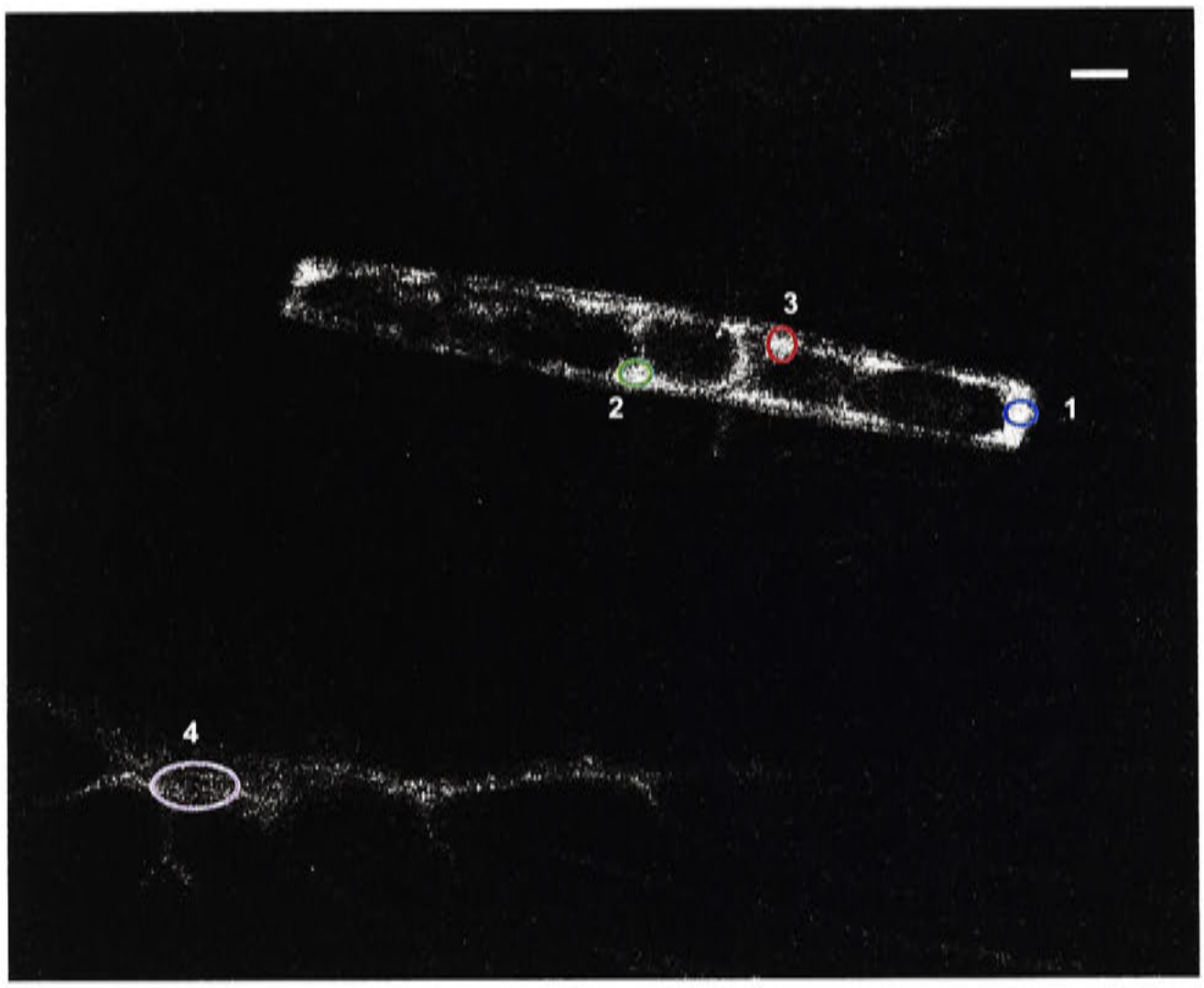

B.

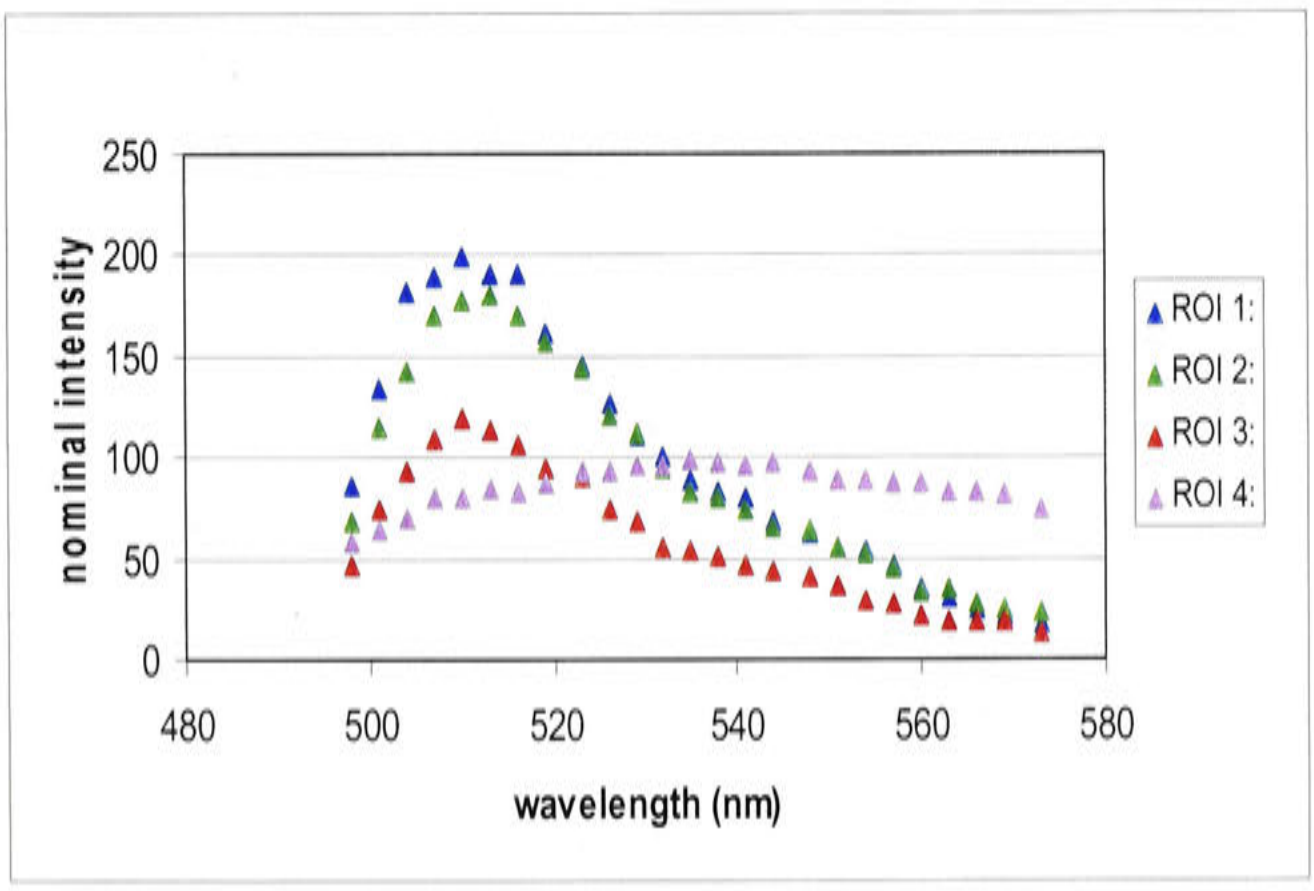

Figure 5.3. Spectral analysis of a fluorescent onion epidermal cell bombarded with pCBJ236 (wheat Cf-9) and a nearby autofluorescent region. Using confocal microscopy, a single optical section of the same region was illuminated under 488 nm light and 25 individual emission spectra collected between 495 and 575 nm. Four regions of interest (ROI) were selected for analysis (**A. ROI 1-4**, blue, green, red and purple circles respectively). Nominal emission intensity (on an 8 bit scale) at each window was plotted against the wavelength for each ROI (**B**). The scale bar shown is 10 μm and the line average used was 4.

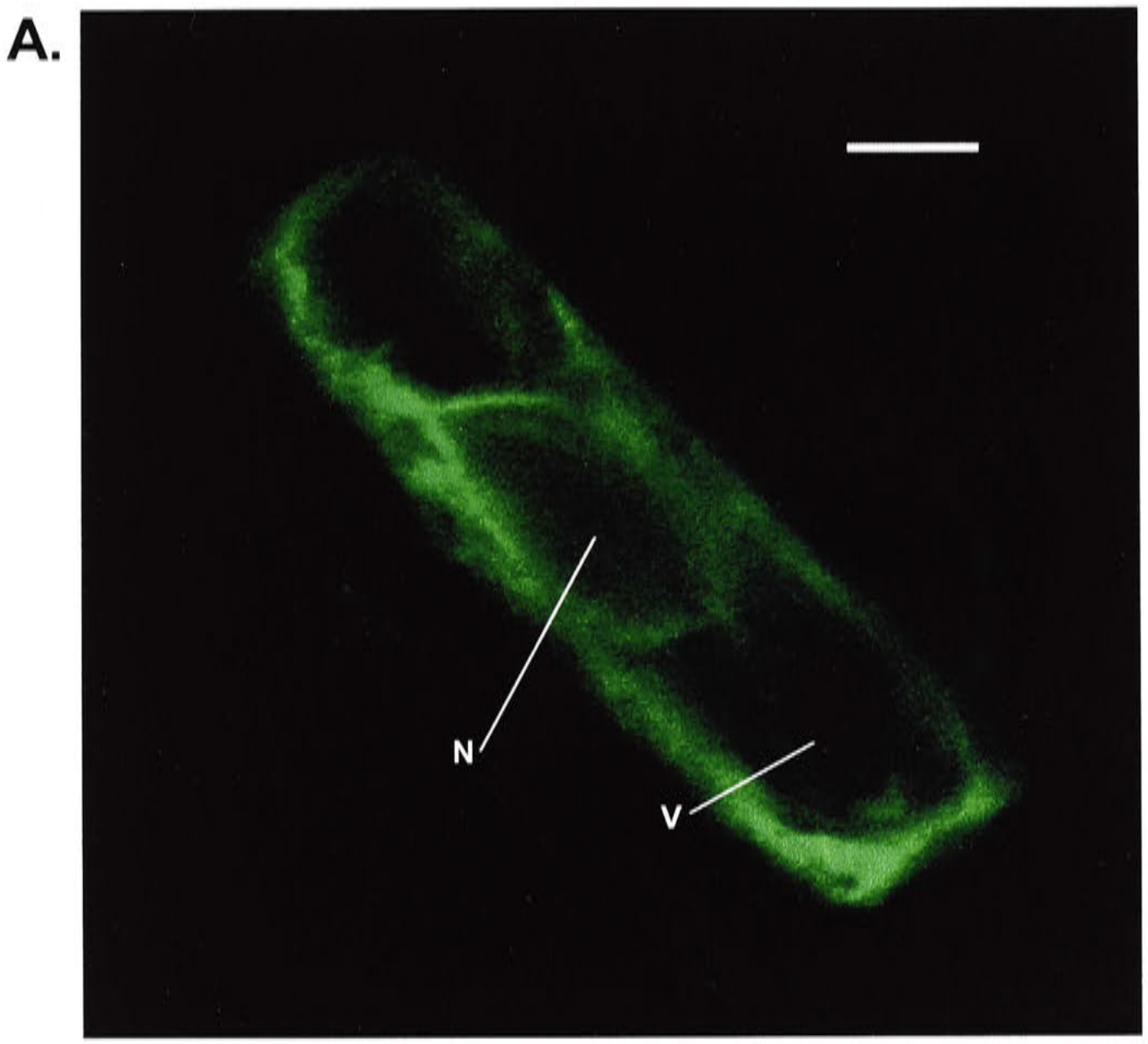

Figure 5.4. Visualisation of wheat Cf-9 (pCBJ236) (**A**) and GFP-HDEL (**B**) expression in onion epidermal cells by confocal microscopy. Cells were imaged for GFP fluorescence 2 days after microprojectile bombardment with the indicated constructs as described in the text. Both images are single optical sections midway through each cell. Nuclei (**N**), vacuoles (**V**) and a transvacuolar strand (**TVS**) are indicated. The scale bars are 10 μm, and the line average for both images was 16.

A series of 650 nm sections was taken through a wheat Cf-9 expressing cell (different to those above) from approximately the cell wall towards the centre of the cell (Figure 5.5). Again, cytoplasmic and perinuclear fluorescence is present, and the nucleus and vacuoles are apparent. No structures typical of cortical ER in this cell type (Scott *et al.* 1999) were observed in this experiment. Interestingly, a weakly fenestrated pattern of fluorescence was observed in the cytoplasm, possibly suggesting that the fluorescence is either ER localised (possibly in an unusual form of ER, see discussion), or cytosol localised and excluded from small bodies in the cytosol. Additionally, it is interesting that little or no fluorescent signal is arising from within the nucleus while fluorescence is apparent in the nuclear envelope. This suggests that the protein is either ER localised (predominantly perinuclear, since no cortical ER was clearly observed), and/or cytoplasmically localised and too large to pass freely through the nuclear pores. This z-series sectioning analysis was performed on three wheat Cf-9 expressing cells, and the perinuclear and cytoplasmic labelling (but not within the vacuole or nucleus) was consistently observed. However, since only the cell shown in Figure 5.5 was imaged at this higher magnification, it is not known whether this fenestrated fluorescence is reproducible in multiple cells or cell types.

To determine whether ER fluorescence might be visible under these conditions, z-series sectioning (1 μm sections) was performed on a GFP-HDEL expressing cell (the same cell shown in Figure 5.4B). However, no structures similar to cortical ER were present, although the cytoplasmic and perinuclear fluorescence, vacuole and nucleus were apparent in sections further into the cell (Figure 5.6). Enlargement of the images in this figure does not reveal any further structures, since the full resolution of the images is shown. This was the only GFP-HDEL cell on which z-series sectioning was performed.

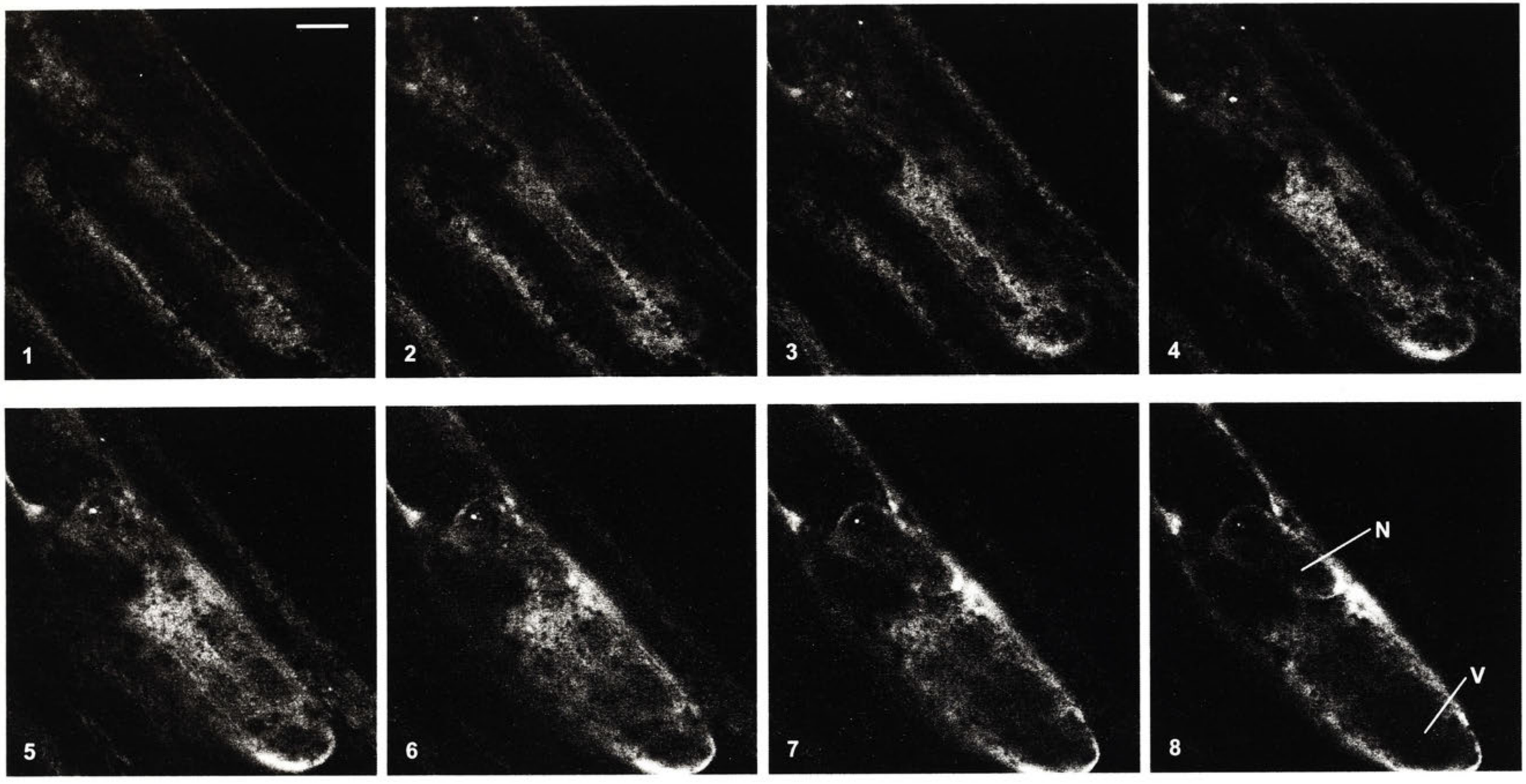

Figure 5.5. Z-series optical sectioning of an onion epidermal cell expressing wheat Cf-9 (pCBJ236) by confocal microscopy. Images 1 to 8 are a series of 650 nm sections starting approximately from the cell wall and progressing into the cell. Other conditions are as described in the text. The nucleus (**N**) and vacuole (**V**) are indicated. The scale bar shown (for all images) is 10 μm and the line average used was 8.

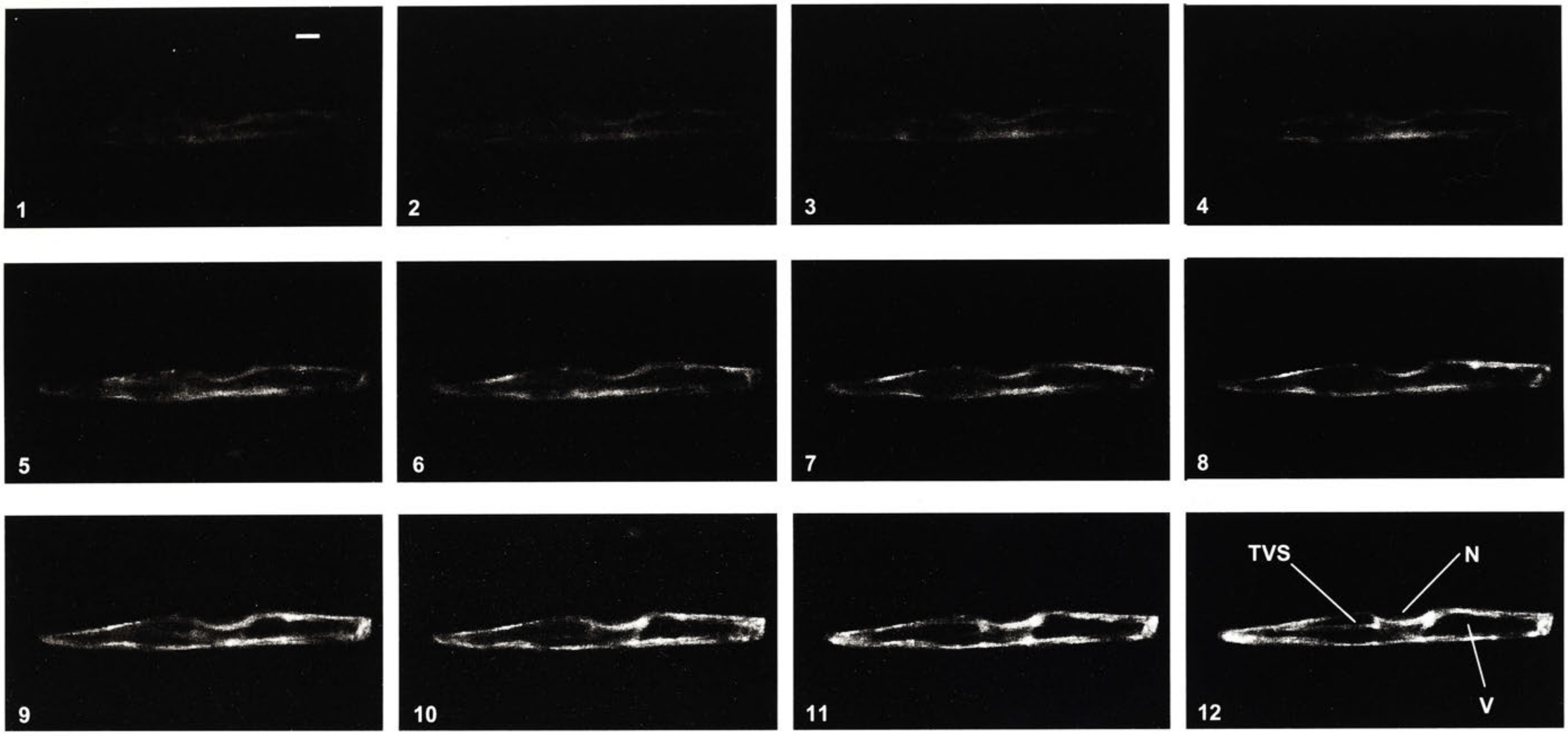

Figure 5.6. Z-series optical sectioning of an onion epidermal cell expressing GFP-HDEL by confocal microscopy. Images **1 to 12** are a series of 1 µm sections starting approximately from the cell wall and progressing into the cell. Other conditions are as described in the text. The nucleus (**N**), vacuole (**V**) and a transvacuolar strand (**TVS**) are indicated. The scale bar shown (for all images) is 10 µm and the line average used was 16.

5.5 DISCUSSION

5.5.1 Stable transformation attempt

This chapter describes work that aimed to test whether the *Cf-9* resistance gene from tomato could function in the monocotyledonous crop species *Triticum aestivum*. The first step planned towards this goal was to generate stable *Cf-9* and *Avr9* wheat transformants, and to cross these lines and check for seedling death or other phenotypes indicative of *Cf-9* activation in the presence of *Avr9*.

However the attempted transformation procedure was not successful, despite a number of regenerating calli being recovered from both Cf-9 and Avr9 transformations, no mature plants were recovered. It was concluded that the large plasmid size was a probable cause of the lack of stable transformants generated by the bombardment procedure, since wheat transformation is relatively inefficient in any case (1.2% of bombarded immature embryos, Becker *et al.* 1994) and large plasmids are known to be more problematic for stable transformation in general (Taylor and Fauquet 2002). To circumvent this problem, GFP:Cf-9 and Avr9 constructs were generated in small cloning vectors rather than the large binary vector plasmids. These plasmids were initially intended for stable transformation but were ultimately used for the bombardment experiments described in the chapter.

5.5.2 Co-bombardment assay for Cf-9 function

Re-engineering of plasmids

Previous work had shown that the native Cf-9 signal peptide did not direct efficient translocation of proteins across the ER membrane (Benghezal *et al.* 2000), suggesting that the Cf-9 signal peptide may have limited function in heterologous species. Based on this evidence, Cf-9 was re-engineered with the wheat α-amylase signal peptide to ensure correct localisation of the bulk of expressed protein in wheat cells. To generate a suitable Avr9/GUS construct, a fragment containing *uidA* under the control of the maize polyubiquitin promoter was cloned into the Avr9 plasmid generated earlier in this thesis (pCBJ231, Chapter 3).

As there was no evidence that the PR1a signal peptide fused to Avr9 in this plasmid would not function in heterologous species, it was retained with the expectation that it

would mediate sufficient translocation of Avr9 to the ER in wheat. However, no evidence was obtained in the work described here to demonstrate that this signal peptide was functional in wheat. To test for production of functional Avr9 in wheat it was planned to use stable Avr9 lines generated from a second stable transformation attempt that was initiated by collaborators (not shown). Potential approaches to demonstrate whether functional, and therefore properly translocated and processed, Avr9 was produced in wheat are discussed below.

Quantification and statistical analysis of co-bombardment assay

To account for minor, quantitative differences in the number of GUS expressing cells, and thus the possibility of a low level of wheat Cf-9 function in this system, the data resulting from the co-bombardment experiments were quantified and analysed statistically. Quantification of the number of GUS positive cells per cm^2 of leaf tissue and analysis of Avr9/GUS and Avr9/GUS + wheat Cf-9 treatments by one-way analysis of variance did not reveal a statistically significant difference between the treatments.

A small proportion of data from unrepresentative leaf segments was removed prior to the analysis of the data (Appendix 3). This would not affect the results as it was a small proportion of segments, an approximately equal number were taken from both treatments and the segments removed were clearly not representative (as indicated by the low number of GUS positive cells, probably as a result of these leaf segments being outside the range of the region bombarded efficiently).

It was noticed that bombarded leaf segments appeared to have a proportion of cells that express a small amount of GUS distinct from those expressing a large amount of GUS (Figure 5.2). This heterogeneous expression of a bombarded marker has been reported previously (Schweizer *et al.* 2000), although the authors did not make any comments on this observation. This phenomenon could be the result of some marker expression being achieved immediately after the cells are bombarded but, as bombardment kills some cells (Mindrinos *et al.* 1994), high levels of the marker do not accumulate in a proportion of the cells due to their subsequent death. Alternatively, the different level of expression could due to different cell types present in wheat leaf epidermis (Schweizer *et al.* 1999), which may express the marker promoter at a different strength, or accumulate a different total level of GUS enzyme. However this assumes these different

cell types are physiologically as well as morphologically distinct, and it is not clear to what extent this is true.

Further histological analysis would be needed to determine which cell types are being transformed, and this would need to be performed before any questions of physiological differences between cell types were considered. In this context it is important to note that the GUS stained spots observed in the experiments conducted here are quite large (relative to a single cell) because the colourless intermediate of the GUS staining reaction (the indoxyl derivative of X-Gluc) is soluble and diffuses outwards from the cell prior to oxidation to form the characteristic insoluble blue precipitate (Jefferson 1987). To determine which cell type is transformed, this would need to be reduced by optimising the staining procedure, for example by reducing the concentration of X-Gluc, the duration of staining, and/or increasing the concentration of the oxidative catalyst (Jefferson 1987).

It was attempted to utilise this weak GUS expressing cell phenomenon to test for wheat Cf-9 function, by testing whether the wheat Cf-9/Avr9 interaction increased the proportion of weak GUS cells relative to strong GUS cells. However, no statistically significant difference was observed between the control and test treatments. The data for this analysis was collected by making an arbitrary, within leaf, distinction between weak and strong GUS expressing cells. This approach could potentially be improved by using specific criteria for making the distinction, such as GUS spot size, shape and level of colour saturation, however care would need to be taken to ensure that this was done consistently across numerous leaves. However the absence of evidence that an *R/Avr* interaction affects this phenomenon means that this possibility is currently conjecture, and may be of limited use.

Expression and functional analyses of Avr9 expressed in wheat

One specific limitation to the experimental approach used here is that while evidence for wheat Cf-9 protein expression was obtained by confocal microscopy, no evidence for expression of functional Avr9 was obtained. To determine whether functional Avr9 was produced, the Avr9 construct would need to be expressed in wheat cells in such a way as to generate enough protein for detection, ideally using a transgenic Avr9 wheat line. This was intended following a second stable transformation attempt, however this was not able to be completed by collaborators in sufficient time for these experiments to

be performed. Alternatively, recently developed *Agrobacterium*-mediated transient expression methods for wheat could be useful to express sufficient amounts of Avr9 in wheat for analysis (Amoah *et al.* 2001; Khanna and Daggard 2003; Weir *et al.* 2001).

Avr9 from these systems could be analysed using either western blot analysis, an Avr9 bioassay in *Cf-9* tobacco or the purification and MALDI-TOF detection methods developed in Chapter 4 of this thesis. The MALDI-TOF approach would have the advantage that it could detect small amounts of Avr9, though it requires relatively pure samples and might need some validation or improvement prior to use in this way. The western blot analysis approach would be technically more straight forward, though antibodies against Avr9 would first need to be acquired or developed (Mahe *et al.* 1998). The bioassay approach would have the advantage that a semi-pure extract could be used (providing that the contaminants do not induce necrosis), and that a clear demonstration of biological function could be obtained, however a larger quantity of Avr9 would be needed for this approach.

These experiments could also demonstrate whether Avr9 had been properly processed, and thus whether the PR1a signal peptide was functional in wheat. If the bioassay approach detected biologically active Avr9 (especially if extracted from IF), this would clearly demonstrate that the signal peptide was functional since this requires folding in the ER. Additionally, if MALDI-TOF analysis of extracted IF or whole leaf tissue (as described in Chapter 4) detected a peak corresponding to mature, processed Avr9 (3394 Da), this would indicate that the signal peptide was functional, as it would need to be translocated across the ER membrane and cleaved for this processed form of Avr9 to be present (Alberts *et al.* 1994).

Limitations and improvements to the co-bombardment assay

There are also some general limitations to this transient bombardment approach that need consideration, particularly with regard to interpretation of negative results. Firstly, this approach is only likely to give a clear result when a relatively strong *R* gene mediated response occurs. If wheat Cf-9 functioned only weakly in wheat, as did Cf-9 when introduced into *B. napus* (Hennin *et al.* 2001b), then it might not be expected to induce a cell death response and consequently would not significantly reduce the number of cells expressing the GUS marker. This could be overcome in the following ways. One would be to use the originally planned approach for this work, that being to

generate stable *Cf-9* and *Avr9* lines, cross these lines and examine them for subtle effects (in the absence of seedling death) such as low level cell death or defence response gene activation. Another way to account for this possibility, based on a co-bombardment assay, would be to normalise the assay using a transformation control such as luciferase (Luc, Leister *et al.* 1996). The control marker is coated onto separate particles so that its activity indicates transformation efficiency. The activity of the marker of interest (the vital marker) is then expressed relative to transformation marker, so as to normalise between leaf variation. This approach gives standardised quantitative data and is therefore able to detect more subtle differences in *R* gene activation, which may be sufficient to determine whether wheat Cf-9 functions at a low level in this wheat cell transient system. However, this latter approach may not detect sub-cell death inducing activation of Cf-9 (or R proteins generally). One approach to account for this might be to fuse a marker gene to the promoter of a gene activated by the *R* the gene dependent response (e.g. Stintzi *et al.* 1993; Tornero *et al.* 1996), although this would require further work to demonstrate this approach in a co-bombardment assay system.

Secondly, this assay assumes that the *R* gene in question will function in the tissue and environmental conditions used for the assay. It may be that wheat Cf-9 can only function or detect Avr9 in certain tissue or cell types or under certain environmental conditions, such as low humidity or high light intensity. It is difficult to control for these factors in the absence of a positive response of the tissue tested. One possibility would be to use a similar approach with leaves of tobacco seedlings, although this approach would only demonstrate that the assay works in principle (in tobacco), not that it could work in wheat leaf tissue. In any case, this control would have been valuable in providing further strength to any conclusions drawn from the negative data obtained from the bombardment assays described in this chapter.

Another positive control that could be used would be a wheat *R* gene known to induce a cell death response, and either a co-expressed *Avr* gene or, since no wheat specific *Avr* genes from wheat pathogens appear to have been isolated, co-inoculation with an avirulent pathogen. This could perhaps use the MLA6 gene from barley, which is known to function in wheat (Halterman *et al.* 2001).

Thirdly, without the separate transformation control suggested above, the variability between individual leaves (even within a single bombardment) cannot be normalised,

thus reducing the strength of any statistical analysis of the quantified results. In this chapter, the GUS positive cells per cm^2 varied from 1.5 to 139 (in the raw data, Appendix 3). When there is clear function of the *R* gene being tested, the lack of this normalisation control would not be a significant problem (as in Jia *et al.* 2000; Mindrinos *et al.* 1994), however in cases where function results in only a low proportion of cell death or a resistance response without cell death, other analyses would be needed. The variability could be normalised by using a bombardment control such as Luc and normalising GUS expression against this, or using a pathogen induced promoter fused to a marker (see above). Alternatively, the use of stable transgenic lines would avoid this problem.

5.5.3 Confocal microscopy

The N-terminal GFP tag on the predicted wheat Cf-9 protein allowed confocal microscopy to be used to examine whether the fusion protein was expressed and correctly localised in the transient bombardment system. Onion hypocotyl epidermal cells were chosen for this study as this is a convenient model for microscopy (Scott *et al.* 1999). Onion is also a monocotyledonous species, so is probably more closely related to wheat than dicotyledonous models.

The spectral properties of the onion cell fluorescence were analysed, confirming that the expected form of GFP was being expressed and that other fluorescent material was non-specific (Figure 5.3). Single optical sections of onion cells expressing wheat Cf-9 showed cytoplasmic and peri-nuclear, but not vacuolar or nuclear, fluorescence corresponding to GFP. To determine the subcellular localisation of the fluorescence, z-series optical sectioning of a single onion cell expressing wheat Cf-9 was performed at higher magnification (although only on one occasion at this magnification; Figure 5.5). This supported the previous conclusion about cytoplasmic and peri-nuclear localisation, but did not provide any clear evidence for ER localisation. In addition, the fluorescence in the cytoplasm prevented any conclusions being drawn on whether any protein is localised to the PM. If wheat Cf-9 was present in the cortical ER, fluorescence would be expected to be visible under this magnification (by comparison to Figure 2 from Scott *et al.* 1999). This could indicate that there is little wheat Cf-9 protein in the cortical ER, and that much of the protein is present in the cytoplasm and/or in the peri-nuclear ER.

Also, since the level of fluorescence in this cell is quite low (the detector gain was high; 9.89), any protein in the cortical ER may not be visible.

By comparison of the wheat Cf-9 cell images to other papers that have examined ER in onion cells, it is clear that this does not appear to be the distinctive network of cortical ER typically seen in these cells (Knebel *et al.* 1990; Lichtscheidl and Url 1990; Scott *et al.* 1999). Some fenestrated fluorescence was observed in this z-series of optical sections, which may have been ER that was not clearly observed due to the low intensity of the GFP fluorescence. Alternatively, the fenestrated fluorescence could be the result of exclusion of cytosolic (soluble) GFP fluorescence from vesicles or bodies in the cytoplasm. Another possibility is that the fenestrated pattern could be unusual forms of ER, such as the developmental stage specific 'perforated sheets' of cortical ER observed by Ridge *et al.* (1999), that was not clear due to the low intensity of the fluorescence.

It is also noteworthy that no transvacuolar strands were observed in this higher magnification z-series experiment (Figure 5.5). However only eight 650 nm optical sections were taken from the cell wall into the cell, and consequently the final section is only 5.2 μm into the cell (with the vacuole only just apparent in final sections). It is thus not surprising that no transvacuolar strands were visible as these would only be likely to be visible in optical sections deeper into the vacuole (Emans *et al.* 2002).

The issue of wheat Cf-9 localisation (by confocal microscopy) could be resolved by improving the sensitivity of GFP fluorescence detection by optimising the imaging system, or alternatively using a more sensitive detection method, such as immunofluorescence. This latter approach would allow the co-labelling of a known ER resident protein such as BiP, and any co-localisation of the wheat Cf-9 (labelled with an anti-GFP antibody, such as that generated in Chapter 6) with BiP would indicate that wheat Cf-9 is ER localised.

One interesting observation in all wheat Cf-9 expressing cells observed is that fluorescence is mostly excluded from the nucleus. This suggests that either most of the protein is translocated across the ER membrane (so cannot diffuse into the nucleus) or that any cytoplasmic protein cannot diffuse through the nuclear pores. It has previously been shown that GFP (28 kDa) can diffuse freely from the cytoplasm into the nucleus, whereas relatively little GFP dimer and trimer could do so (von Arnim *et al.* 1998),

consistent with the previously estimated nuclear pore size exclusion limit for free diffusion of ~40-60 kDa (Görlich and Mattaj 1996). This would suggest that any cytoplasmic wheat Cf-9 protein is larger than this limit, and therefore that at least a significant proportion of the predicted 123 kDa protein (without glycosylation) is being produced.

To confirm that the full length GFP:Cf-9 protein is being produced would require further experiments, probably western immunoblotting analysis. This could be done using the anti-GFP antibodies produced as described in Chapter 6 of this thesis, although the sensitivity of these antibodies for such an experiment would first have to be confirmed. This approach, however, would need stable transgenic lines containing the wheat Cf-9 construct, or alternatively could use a transient expression method based on *Agrobacterium* (Khanna and Daggard 2003; Weir *et al.* 2001) so that a detectable quantity of protein could be analysed. Testing for glycosylation of wheat Cf-9 (by western and glycosidase digestion analysis) could be used to determine what proportion of the protein is translocated into the ER, since such modifications are specific to the secretory pathway. Alternatively, membrane bound and soluble proteins could be separated and analysed by western immunoblot. Membrane anchored wheat Cf-9 protein would almost certainly be full length, since the trans-membrane domain is at the C-terminus of this protein.

In any case, the evidence presented here suggests that a significant proportion of the wheat Cf-9 expressed in this system is present in the cytoplasm (probably including a significant quantity that is soluble in the cytosol) but not the vacuoles or nucleus. The data do not support a strong conclusion on whether or not any proportion of the protein is present in the ER (or PM). Also, it is important to note the possibility that the localisation of the wheat Cf-9 protein in onion cells may not be representative of the same protein in wheat. This is because, although onion and wheat are both monocotyledonous, they are only distantly related, and the wheat signal peptide used (from α-amylase) may not function properly in onion cells. This would not apply to the GFP-HDEL protein expressed from the control plasmid used in these experiments as it has previously been demonstrated to localise to the ER in onion cells, indicating that its signal peptide is functional (Collings *et al.* 2000). Further work would be needed to clarify the localisation (in particular whether it is membrane anchored) of the wheat Cf-9 protein expressed in wheat cells. Western immunoblot analysis as described above

would be sufficient to determine whether Cf-9 was membrane anchored, however alternative approaches would be necessary to determine whether it was PM or ER localised (see Chapter 3).

5.5.4 Summary and further work

In summary, a bombardment assay for Cf-9 function in wheat provides no evidence for Cf-9 mediated recognition of Avr9 in this species, suggesting that Cf-9 does not function strongly in wheat. However, the data presented are not definitive, and some limitations to this transient assay approach are noted. Suggestions are provided on how this approach could be modified to improve the sensitivity and increase the possibility that differences between the Cf-9 and Avr9/Cf-9 treatments could be detected if they were present. However, this approach would require significant further development, and would not be assured of an outcome.

A better alternative to this transient method would be the originally intended approach of generating stable transgenic *Cf-9* and *Avr9* wheat lines. This is particularly so in light of the more recent availability of improved particle bombardment methods for stable transformation of wheat (e.g. Pellegrineschi *et al.* 2002) and increasing numbers of *Agrobacterium*-mediated stable transformation methods (Khanna and Daggard 2003; Wu *et al.* 2003). Generation of transgenic lines would also allow tests for more subtle induction of defence responses such as defence gene activation (without cell death), low level cell death or sensitivity to infiltrated Avr9 peptide, similar to the study of transgenic *B. rapa* by Hennin *et al.* (2001b).

CHAPTER 6

GENERATION OF ANTI-GFP ANTIBODIES

6.1 INTRODUCTION

ANTIBODIES that recognise a specific protein of interest are a powerful laboratory tool, allowing detection and analysis by methods such as western (protein gel blot) analysis, Enzyme-Linked Immunosorbent Assay (ELISA) and immunoprecipitation (Harlow and Lane 1988). Antibodies against common marker sequences such as GFP or the triple hemagglutinin or triple myc epitope tags are particularly useful, as they can detect any marker or fusion protein engineered with this sequence.

A project planned at an early stage of this PhD thesis was to determine whether the Cf-9 and Avr9 proteins interacted physically using an immunoprecipitation approach with GFP tagged Cf-9. It was decided to generate monoclonal antibodies for this approach 'in-house' (rather than purchase them commercially) so that the purchase cost of this critical tool would not limit the progress of the project. However, a significant effort to determine whether Cf-9 and Avr9 interact physically (Luderer *et al.* 2001) was published during this project and found no evidence for a direct interaction between these proteins, so the project did not proceed beyond the preparation and preliminary analysis of a monoclonal anti-GFP antibody.

This chapter describes the production of an *E. coli* expression vector for 6-histidine tagged GFP (6His:GFP) and subsequent purification of native and denatured GFP. Purified native 6His:GFP was then used to generate mouse monoclonal antibodies against GFP (with technical assistance). Potential uses and limitations of this resource are discussed.

6.2 MATERIALS, METHODS AND RESULTS

6.2.1 Generation and purification of 6His-tagged GFP

The pQE *E. coli* expression system (Qiagen, California, USA) was chosen as an expression system to generate 6His:GFP. The 6His tag allows rapid purification of the fusion protein using nickel affinity chromatography. To generate a plasmid encoding 6His:GFP, the GFP cassette from pCBJ8 was excised with *Xba*I, gel purified, the ends filled in using *Pfu* DNA polymerase (Stratagene, California, USA) and ligated into pQE31 cut with *Sma*I. This cassette is identical to that from pCBJ4 (Benghezal *et al.* 2000). A positive clone was selected based upon the ability of the *E. coli* colony (DH5α) to fluoresce under a portable UV transilluminator, and the plasmid confirmed by restriction digestion with *Nco*I and named pCBJ188.

E. coli (DH5α) expressing 6His:GFP was grown to early stationary phase at 37°C in a 2 litre culture of 2 x YT containing 50 μg/ml ampicillin with shaking at approximately 200 rpm. Affinity purification of 6His:GFP on a Ni-NTA nickel column was then performed using the described native (protocol 5) and denaturing (protocol 7) methods (Qiagen 1992) with some minor modifications as outlined below.

For native 6His:GFP preparation, each gram (wet weight) of pelleted cells was resuspended in 2 ml of modified sonication buffer (50 mM NaP pH 8.0, 400 mM NaCl) containing 1 mg/ml lysozyme and incubated on ice for 30 minutes. Triton X-100 was added to a final concentration of 0.2%, the cells mixed gently, and the cell debris pelleted by centrifugation at 10 000 x g for 20 minutes at 4°C. The supernatant was collected, 6 ml of 50% Ni-NTA resin slurry was added and the mixture incubated at 4°C for 15 minutes with gentle inversion. The resin was then washed with sonication buffer in 15 ml batches until the A_{280} of the supernatant was below 0.01, then transferred to a column (20 mm diameter). Washing was continued (in the column) with wash buffer (50 mM NaP pH 6.0, 500mM NaCl, 10% glycerol) until the A_{280} was below 0.01. The 6His:GFP was eluted using 250mM imidazole in wash buffer, then fluorescent green/yellow (under ambient light) fractions combined and dialysed overnight against PBS (phosphate buffered saline; according to Sambrook *et al.* 1989).

The native 6His:GFP purification procedure was performed on two separate occasions, yielding 12 mg of purified protein on one occasion and 3 mg on another. An SDS polyacrylamide gel of a typical native purification procedure is shown in Figure 6.1A. The majority of the protein in the extract was present in a strong band of approximately 32 kDa, although there was also a faint and/or poorly resolved band approximately 2 kDa larger. The predicted size of the 6His:GFP protein is 30 kDa, suggesting a slight difference between the predicted and apparent molecular weight of the expressed protein (see discussion). A negative control purification was not used as the intense yellow/green fluorescence of the sample (bound to the resin or after elution) under ambient light indicated that a large quantity of 6His:GFP was present. The majority of protein in the extract is therefore likely to be 6His:GFP.

Denaturing preparation of 6His:GFP was performed essentially according to the manual (protocol 7; Qiagen 1992) except for the elution step, on three separate occasions. Briefly, the procedure involved lysing cells by stirring in buffer A (6M guanidinium HCl {GuHCl}, 0.1M NaP, 10mM Tris-HCl pH 8.0) for one hour, binding to 4 ml of 50% resin slurry and batch washing in buffer A (5 x 15 ml). The resin was loaded onto a column, washed sequentially with buffer B (8M urea, 0.1M NaP, 10mM Tris-HCl pH 8.0) and buffer C (same as B except pH 6.3) each until the A_{280} of the flow through was below 0.01, then eluted in 15 ml of buffer C containing 250 mM imidazole. An example of 6His:GFP purified this way is shown in Figure 6.1B. This shows the typical outcome of denaturing preparation of 6His:GFP, specifically the higher yield of protein with little background of contaminating proteins (compare Figure 6.1A, lane 6 {10 µl sample of 9 ml eluate loaded} to Figure 6.1B, GFP lane {5 µl sample of 15 ml eluate loaded}, both of which were stained using the same coomassie brilliant blue staining protocol). Similar to the native GFP extracts, the predominant band appeared slightly above the predicted 30 kDa molecular mass for 6His:GFP, and (when less protein was loaded, not shown), an additional less-resolved minor band of approximately 2 kDa higher mass was observed.

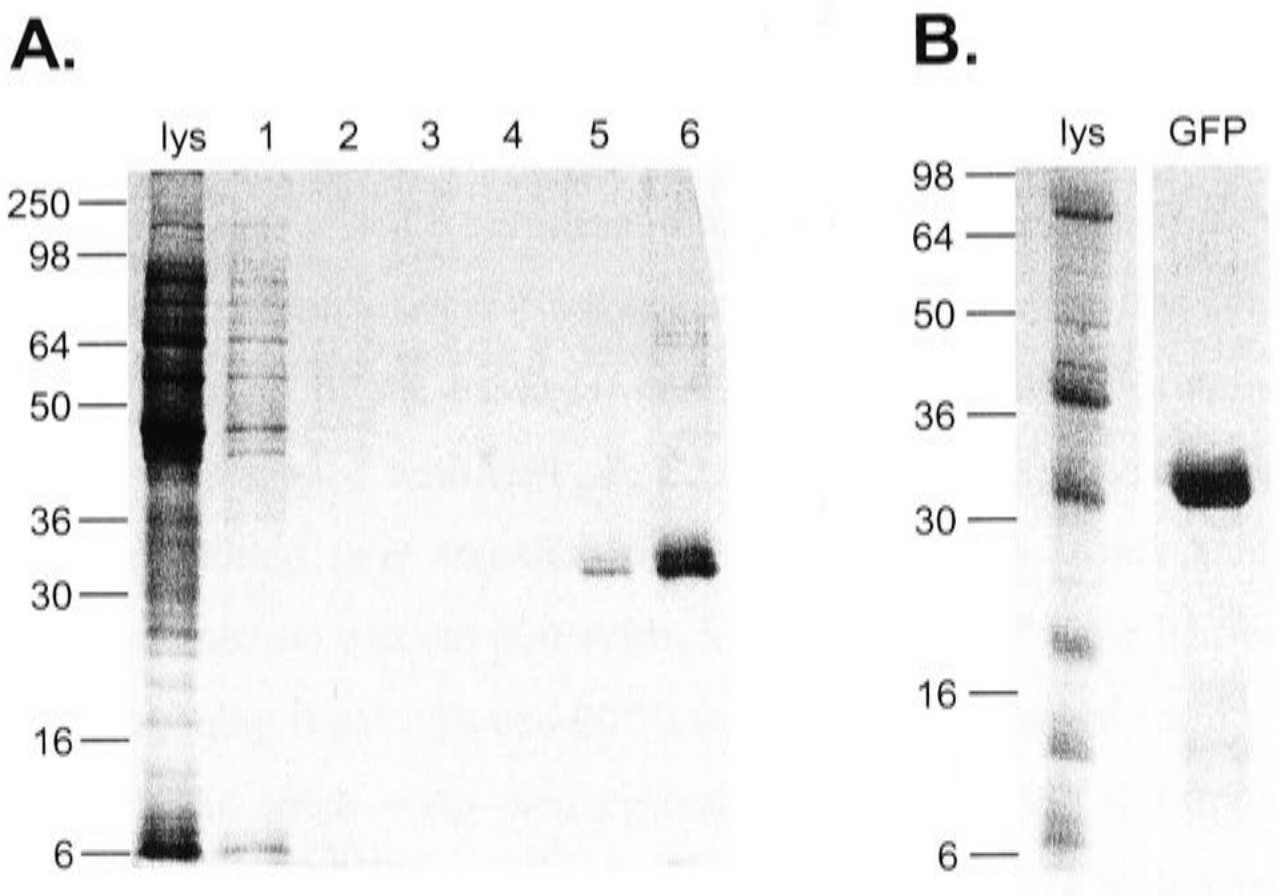

Figure 6.1. Coomassie-stained 12% SDS-PAGE gels of extracts of affinity-purified 6His:GFP. The position of molecular mass markers is indicated to the left. **A.** Native purification of 6His:GFP. Lanes on the gel are the bacterial lysate supernatant after binding of 6His:GFP with the nickel affinity resin (**lys**, 10 µl loaded), sequential batch washes (lane **1-4**, 10 µl of each wash), and lane **5** and **6** are 2 and 10 µl samples of the 9 ml 6His:GFP eluate (corresponding to 0.68 and 3.4 µg protein, respectively). **B.** Denaturing purification of 6His:GFP. The first lane is total cell lysate (**lys**) and the second is 5 µl of the 15 ml 6His:GFP eluate (**GFP**). The black line indicates that these are non-adjacent lanes of the same gel.

6.2.2 Immunisation and monoclonal antibody production

Purified native 6His:GFP was then used to generate mouse monoclonal antibodies against GFP. Parts of the monoclonal antibody production procedure were performed by Jan Elliott of the Plant Cell Biology group, Research School of Biological Sciences, Australian National University, Australia, as specified throughout the text. Jan Elliott immunised two mice (with 100 μg each of purified native 6His:GFP and Freunds adjuvent), followed by four booster injections (identical to the immunisation) at fortnightly intervals using standard procedures (Coligan *et al.* 1994).

Mouse blood serum was tested by western immunoblot (performed by me) to determine whether an immune response to GFP had occurred. Briefly, baculovirus culture medium (4 μl of a 1:10 dilution of the medium) containing a GFP fusion protein (fused to a maize mitotic cyclin tagged with GFP, P. C. L. John, unpubl.) was separated by 12% SDS-PAGE and blotted (wet transfer) to PVDF membrane (Amersham-Pharmacia) overnight. The membrane was cut into strips, blocked with 4-5% low fat milk powder in PBST (PBS containing 0.05% Tween-20™) for 1 hour and washed for 5 minutes three times in PBST. The strips were then probed with serum from the immunised mice diluted 1000 fold in PBST for 1 hour, washed again, incubated with goat anti-mouse IgG peroxidase (1:5000; Sigma), washed and detected using the ECL™ kit according to manufacturers instructions (Amersham-Pharmacia, Uppsala, Sweden; Figure 6.2A).

Strong bands were present in the baculovirus culture supernatants containing GFP-cyclin but not in supernatant from negative control cultures containing only the empty vector (after 1 minute exposure; Figure 6.2A). Since the blots were exposed and treated identically except for the mouse serum used, the stronger bands present on the blot probed with serum from one of the two mice compared to the other (GFP 2) indicates that there was a stronger immune response in this mouse. When exposed for 15 minutes, a band of approximately 65-70 kDa and a number of minor bands were observed in only the GFP-cyclin lanes, possibly representing the full-length version and some intermediate degradation products of the expected fusion protein respectively (not shown). The absence of any bands in the control extract (lacking GFP) indicates that the bands observed are GFP specific. A separate membrane blotted with GFP-cyclin and control baculovirus extract that was not probed with a primary antibody is also shown as

a negative control (Figure 6.2A, after 15 minutes exposure). The lack of bands indicates that the bands are dependent upon the primary antibody from the mouse serum.

The mouse with the stronger response against GFP was used for production of monoclonal antibodies, using standard procedures, performed by Jan Elliott (Coligan *et al.* 1994). Spleen cells were isolated, cells fused and hybridoma cultures generated. Eight hundred and sixty four hybridoma lines were screened by ELISA for the ability to detect native GFP, most of which was performed by me essentially as described (the 'indirect method', Coligan *et al.* 1994). Briefly, 50 µl of purified native 6His:GFP (diluted to 10 µg/ml) was coated onto the wells of 96 well Immulon® ELISA plates (Thermo Labsystems, Vantaa, USA), washed three times with PBST and probed with hybridoma culture supernatant. Plates were washed, incubated with biotinylated sheep anti-mouse immunoglobulin antibody (1:300; Amersham-Pharmacia) then washed again. The wells were then incubated with streptavidin horse-radish peroxidase (1:500; Amersham-Pharmacia), and detection was performed using ABTS (2,2'-azino-bis(3-ethylbenzthiazoline-6-sulfonic acid) substrate (2mM, with 5.5 g/L citric acid and 7.1 g/L sodium citrate, pH 4.5) with 0.03% H_2O_2 freshly added. Reactions were stopped with 300mM NaF and quantified by measuring absorbance at 405 nm with a plate reading spectrophotometer.

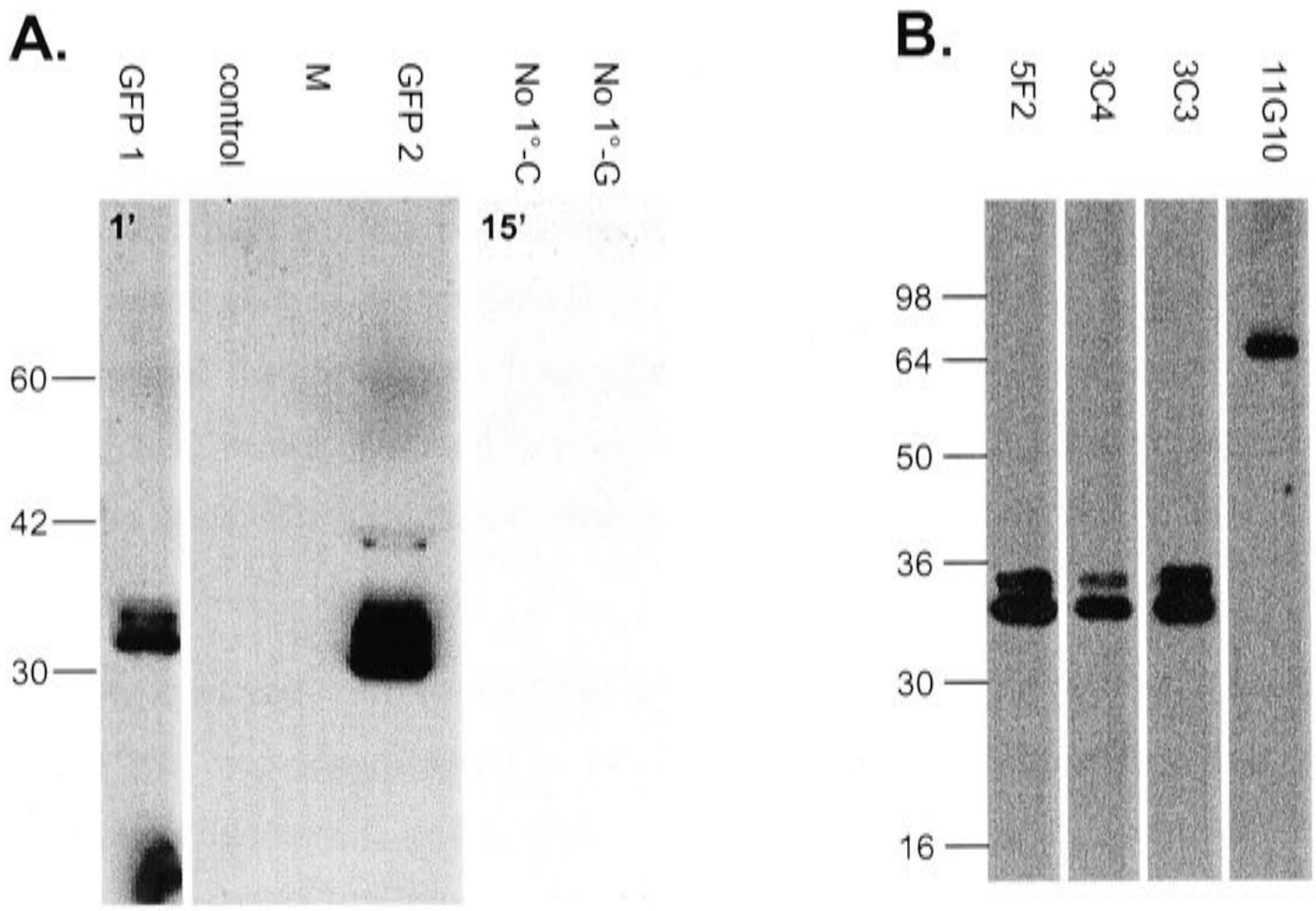

Figure 6.2. A. Testing of mouse blood serum from the two immunised mice for polyclonal antibodies against GFP. A western blot of baculovirus-infected insect-cell culture supernatant containing GFP-cyclin (predicted full-length molecular mass approximately 65 kDa, **GFP**) or supernatant of a baculovirus culture expressing an empty vector (**control**). The **GFP 1** and **GFP 2** membrane strips were blotted with the same amount of protein (from the same gel) but probed with serum from two different mice immunised with GFP. The control extract was probed with both sera, but is only shown for GFP 2 serum, since no bands were detected with either. Another membrane strip is shown that was treated identically except the mouse serum omitted (i.e. a no primary antibody control on GFP-cyclin extract {**No 1°-G**} and control extract {**No 1°-C**}), except the blot was exposed for 15 minutes (**15'**). The difference in background colour of the two blots is an artefact of scanning. Non-adjacent lanes of the same gel are separated by white. **B.** The same baculovirus extract containing GFP-cyclin was separated in a single well 12% SDS polyacrylamide gel and blotted to PVDF membrane. Thin strips of membrane were probed with the supernatants from the 17 hybridoma lines that were positive by ELISA screening. Membrane strips are shown for the four antibodies that detected a band in the fusion protein extract (all strips are from the same gel, shown adjacent to each other). No bands other than those shown were present. See text for comment on the band in lane 11G10. The marker (**M**) sizes are shown on the left of the gels.

From the hybridomas screened, 17 were recovered that strongly detected GFP by ELISA. Clonal lines were isolated by limiting dilution and further tested for the ability to detect GFP on a western blot by probing strips of PVDF membrane blotted with GFP-cyclin as above (Figure 6.2B). The same bands that were detected using the serum samples were detected when blots were probed with the hybridoma culture supernatant (undiluted, but freeze dried and resuspended in PBST) from three of the 17 ELISA positive cell lines (Figure 6.2B). One of the cell lines detected a protein from the baculovirus extract of approximately 70 kDa (11G10). Interestingly, when these strips were exposed for 15 minutes (instead of only 1 as in the figure shown), this latter antibody also weakly detected one of the lower molecular weight GFP-cyclin bands, while the other three antibodies also weakly detected the larger 70 kDa band (not shown).

The isotype of the three monoclonal antibodies that recognised GFP by ELISA and western blot was determined (by Jan Elliott) using the Mouse Isotyping Kit from Amersham-Pharmacia (Uppsala, Sweden). Antibodies 3C3 and 5F2 were determined to be IgG_1 isotype and 3C4 was an IgM isotype.

6.3 DISCUSSION

6.3.1 6His:GFP purification

Six-histidine tagged GFP was produced in an *E. coli* expression system and subsequently purified using both native and denaturing nickel affinity chromatography protocols. Both procedures reliably produced useful quantities of relatively pure 6His:GFP protein. The denaturing protocol typically gave a greater yield and slightly improved purity compared to the native purification protocol, judging by SDS-PAGE. The increased yield of the denaturing was most likely due to the solubilisation of 6His:GFP protein aggregates ('inclusion bodies'), which would have accumulated in cells due to constitutive expression from the plasmid in the *E. coli* DH5α strain used (Baneyx 1999; Qiagen 1992).

When the purified GFP protein extract was examined by SDS-PAGE, there was a strong band of approximately 32 kDa and a weaker, less resolved band of around 33-34 kDa. Although the fusion protein was predicted to be 30 kDa, the phenomenon of higher

apparent molecular mass of 6-histidine fusion proteins has been noted (Qiagen 1992), and probably explains the observation in this case. However it is not clear whether both of these bands are 6His:GFP, and if so why there is a doublet instead of a single band. This may also be due to a proportion of the protein running aberrantly by SDS-PAGE due to the 6-histidine tag. Alternatively, the major (smaller) band could be a degradation product and the larger band the full-length version. If the smaller band is a degradation product, this could be the result of imidazole in the sample (which can cause hydrolysis of acid labile bonds at high temperatures, Qiagen 1992). However, this seems unlikely since samples were prepared for SDS-PAGE at 37°C instead of boiling, as recommended to prevent imidazole mediated cleavage (Qiagen 1992). The presence of this additional band, even if a contaminating protein, was not considered important as ultimately monoclonal antibodies were each to be tested against an independent source of GFP.

6.3.2 Anti-GFP antibody generation

Purified native GFP was used to immunise two mice for the production of monoclonal antibodies. Serum from both mice detected a GFP-cyclin fusion protein from a baculovirus expression system culture medium, indicating that antibodies against GFP were present in both mice. The bands were absent from the vector-only control lane and when the primary antibody was omitted, indicating that the detected bands were indeed the GFP-cyclin fusion protein (Figure 6.2A). The mouse with the strongest immune response to GFP was chosen to generate monoclonal antibodies. Of the 864 hybridomas screened by ELISA, 17 were found to strongly detect GFP, three of which also detected the GFP-cyclin fusion protein by western blot. One monoclonal antibody detected what appeared to be a non-specific band of 65-70 kDa from the GFP baculovirus extract. The fact that a band of this size was observed on the blots probed with the three other monoclonal antibodies when overexposed, and that a similar band was present on blots of the same protein probed with mouse serum could indicate that this band is a variant of the GFP-cyclin fusion protein, possibly the full length protein. However, no negative control extract was probed with each of these monoclonal antibodies, so it is not clear whether this 65-70 kDa band is a non-specific protein in the baculovirus extract or is the variant of the GFP-cyclin fusion protein observed when probed with mouse serum. This issue could be resolved by probing blots of baculovirus supernatant from the empty vector expressing control cell line with each of the monoclonal antibodies.

Although the level of GFP protein in the baculovirus extract was not quantified, it was noticeably fluorescent under ambient light, suggesting that it was abundant in this extract. The facts that undiluted hybridoma medium (containing the monoclonal antibody) was being used to probe blots, and that the sensitive ECL method was being used for detection, mean that it cannot necessarily be concluded that these antibodies are highly sensitive for western blotting. Further characterisation would be needed to determine the sensitivity of these antibodies more accurately. This could be done by probing a blot of a series of known amounts of pure GFP protein (such as that generated here) using a constant amount of antibody. Alternatively, similar amounts of GFP could be blotted and probed with a range of dilutions of the test antibody and a commercially available antibody for comparison.

One possible reason for the strong response of these GFP antibodies by ELISA but not by western blot is that hybridomas were initially screened by ELISA against native GFP, which may have selected against antibodies that can detect denatured forms of GFP sensitively (as would be needed for sensitive SDS-PAGE immunoblotting). This hypothesis could be tested by performing ELISA on the same GFP extract, using native and denatured (e.g. by heat treatment) samples of the extract. A reduction in the sensitivity of detection of the denatured GFP by the antibody would support this idea. This possibility could be accounted for by screening hybridoma cell lines with both denatured and native GFP by ELISA. Alternatively, if an antibody that is highly sensitive by western immunoblot was desired, cell lines could be screened initially using this method. While this would be more laborious, it would be more likely to yield an antibody that detects blotted GFP very sensitively. One way to improve the throughput of this method would be to combine five or more hybridoma supernatants at the preliminary screen to probe thin strips of membrane blotted with GFP.

Although possibly of limited sensitivity for western blotting, these anti-GFP antibodies are likely to be useful for techniques that detect native GFP, such as immunoprecipitation and ELISA. In support of this, immunoprecipitation was performed successfully by Dr Magdalena Weingartner, of the University of Vienna, Austria, using the 3C3 antibody generated here (Appendix 4).

6.3.3 Further work

Although the development of a monoclonal antibody was originally intended for use to investigate whether Cf-9 and Avr9 proteins interacted physically, it could still be useful for investigation of a similar question. The question of Cf-9/Avr9 direct interaction was examined by Luderer *et al.* (2001) using a number of approaches, finding no evidence for an interaction. However, the possibility that Cf-9 and Avr9 were present in a complex *in vivo* during an interaction was not examined. This would be an interesting question to test, and the antibodies generated in this chapter could be used to pursue an immunoprecipitation approach similar to that used by Leister *et al.* (2000). In this case, immunoprecipitation of epitope tagged RPS2 (an *Arabidopsis* R protein) co-immunoprecipitated AvrRpt2 (the corresponding Avr protein) in a complex of proteins from radiolabelled leaf protoplasts.

It was apparent that the low abundance of the proteins of interest was a significant limitation to the Leister *et al.* (2000) study, and this could also be the case for an equivalent study with Cf-9/Avr9. A suitable experimental system for this experiment would therefore first need to be developed and validated. One way to do this would be to introduce GFP:Cf-9 under its native promoter (to exclude overexpression dependent artefacts) in a tobacco suspension cell system and immunoprecipitate radiolabelled GFP-Cf-9 and associated proteins (± Avr9) using the GFP antibody. Cf-9 has been shown to function in a tobacco suspension system previously (Piedras *et al.* 1998), and since Cf-9 cells can respond to added Avr9 after 5 minutes, but do not die even after 15-20 hours (de Jong *et al.* 2000; Piedras *et al.* 1998), it would be expected that Cf-9 and Avr9 have the potential to co-exist in any complex for at least some time. As a preliminary experiment, of interest in itself, it would need to be determined whether and for how long Cf-9 is present during the interaction. As rapid Avr dependent R protein degradation has been observed previously for the *Arabidopsis* resistance protein RPM1, Boyes *et al.* 1998), this possibility would need to be evaluated for the Cf-9 system so that an appropriate time frame for the immunoprecipitation experiment could be used.

One possible limitation to this approach is that it may be difficult to get adequately high specific activity of labelling for Avr9 due to its small size (28 amino acids). One way to circumvent this problem, which would also reduce the background radiolabelling (and therefore increase the sensitivity) of the method used by Leister *et al.* (2000) might be to

separately express, purify and radiolabel Avr9 and add this exogenously to non-radioactive (cold) GFP:Cf-9 tobacco cell suspension cultures. This would allow longer exposure times of resulting cell extracts, and would thus be more likely to detect smaller quantities of protein. This could be done using the Avr9 *E. coli* expression system partially developed in Chapter 4 of this thesis. Modifications suggested in that chapter would allow expression of Avr9 with relatively little background contaminating protein. Labelled Avr9 could be produced *in vivo* (with ^{35}S-cysteine, since Avr9 contains six cysteine residues) or *in vitro* by purification of cold Avr9 then labelling with ^{125}I as performed previously (Kooman-Gersmann *et al.* 1996). This latter approach would have the advantage of the strong signal produced by this isotope. With such an approach, cold GFP:Cf-9 could be immunoprecipitated from a suspension culture with little or no radioactive background, and consequently radiolabelled Avr9 would probably be sensitively detected. Clearly however, this approach would need some development.

Another possible approach would be to make use of the MADLI-TOF method for Avr9 developed in Chapter 4 to analyse GFP:Cf-9 ± Avr9 immunoprecipitates. Since an immunoprecipitated protein complex would be a relatively pure mixture, this approach may allow highly-sensitive detection of Avr9 without the need for radiolabelling. However, the sensitivity of this approach would also first need to be tested, which could be done by spiking Cf-9 immunoprecipitates with known quantities of purified Avr9 then analysing these mixtures by MALDI-TOF.

Other potential uses of the antibodies generated in this chapter, in particular for potential further work outlined in other parts of this thesis, are outlined in the general discussion (Chapter 7).

CHAPTER 7

GENERAL DISCUSSION

Analysis of models for Cf-9 function

THE work described in this thesis was based on two broad models for Cf-9 function, described in Chapter 1. In Model 1, Cf-9 functions at the PM, with ER retrieval probably acting as a quality control mechanism. In Model 2, Cf-9 functions in the ER and either Avr9 travels to the ER or initiates signalling from the PM to the ER.

There are precedents for such models in other biological systems. An example similar to Model 1 is the immunoglobulin E high affinity receptor in mammalian cells (Letourneur *et al.* 1995). The KKXX ER retrieval motif of this protein has been shown to be functional, but is masked in assembled complexes, allowing them to depart the ER (Letourneur *et al.* 1995). In plant systems, Model 1 is best exemplified by the Auxin Binding Protein 1 (ABP1; Timpte 2001). While ABP1 contains a C-terminal ER retention signal for soluble proteins (KDEL) and is mostly localised to the ER (around 99%; Henderson *et al.* 1997), a range of available evidence suggests that it functions at the PM where only a small proportion is present (Diekmann *et al.* 1995; Henderson *et al.* 1997; Jones and Herman 1993; Napier 1997; Timpte 2001).

An example similar to Model 2 is the Major Histocompatibility Complex 1 (MHC1) protein, which binds peptide fragments in the ER and transports these to the PM for presentation to cytotoxic T-cells (Alberts *et al.* 1994). It has been shown that specific MHC1 binding peptides added to mammalian cell cultures were delivered to their corresponding MHC1 receptors in the ER within five minutes, and that this was not due to MHC1 endocytosis from the PM, but another unidentified delivery mechanism (Day *et al.* 1997). This example demonstrates in principle that an exogenous peptide molecule can be rapidly delivered from the PM to a receptor molecule located in the ER. A similarly rapid transportation pathway would probably be necessary if Cf-9 functioned in a similar way, as it has been shown (in tobacco cell suspension cultures) to respond to Avr9 in around 5 minutes (Piedras *et al.* 1998), although this might be slower in whole leaves. Also similar to Model 2 are the bacterial and plant toxins that are endocytosed

and transported to the ER of mammalian cells (e.g. ricin toxin and shiga toxin), as outlined in the introduction to Chapter 3.

The alternative scenario for Model 2 (Avr9 dependent signal, but not Avr9, transmitted from the PM to the ER) raises the further question of what mechanism/s could allow rapid transduction of a signal from the PM to the ER. An example of ligand dependent signalling from the PM to the ER is the stimulation of MHC1 export from the ER by insulin (Malide *et al.* 2001). This presumably is initiated by the insulin receptor on the PM, and this signalling has been shown to occur through a pathway involving phosphatidyl-inositol-3-kinase, which may then modulate ER to Golgi-apparatus transport (Malide *et al.* 2001).

Another interesting example of a plant receptor that is a resident of the ER is the ethylene receptor (Chen *et al.* 2002). Although this is a receptor of a small gaseous molecule, which could diffuse easily through (and within) cell membranes as well as the aqueous phase, this example indicates that it is possible and advantageous to have a key receptor molecule present in the ER. This implies that mechanisms and signalling pathways are present in, and involving, the ER that would allow activation by ligand (ethylene) interaction to be transmitted into downstream signals and cellular responses.

Though these examples do not constitute an argument for localisation of Cf-9 in either the PM or the ER, they at least demonstrate that the two models of Cf-9 function presented here are biologically feasible. However, there would need to be a functional basis for either model. In the case of Model 1 (PM function of Cf-9) this is clear: as *C. fulvum* apparently does not penetrate the PM during infection and secretes Avr9 into the apoplast (Joosten and de Wit 1999; Lazarovits and Higgins 1976), localisation of functional Cf-9 at the PM would be ideal for rapid detection of the avirulent pathogen. On the other hand, Model 2 would need to postulate additional steps to the interaction, particularly entry of Avr9 into the cell (Benghezal *et al.* 2000) or induction of PM to ER signalling by Avr9.

Clear evidence for entry of pathogenicity/virulence factors into cells utilising the bacterial Type III secretion system is available for bacterial disease model systems (Büttner and Bonas 2002). However, while it seems likely that fungal pathogens would manipulate internal components of the plant cell during pathogenesis, little clear evidence for the direct transfer of fungal virulence factors into the host cell is apparent.

One possible piece of evidence that implies that some fungal pathogens may transfer proteins into the host cytoplasm is available from the rice/rice blast fungus interaction (Jia *et al.* 2000). The rice resistance gene product Pi-ta, predicted to be a cytoplasmic protein, induces resistance responses after physical interaction with the cognate rice blast avirulence gene product AVR-Pita (Jia *et al.* 2000). Additionally, a resistance response was triggered after expression of the mature AVR-Pita protein with its native signal peptide in plant cells, but not when ten amino acids from the N-terminus were deleted. This latter observation could mean that the AVR-Pita protein needs to be secreted from the plant cell prior to eliciting Pi-ta dependent responses, although could be a result of disruption of the avirulence activity of this protein.

One additional line of evidence for transfer of fungal proteins into the plant cytoplasm is that R proteins conferring resistance to some fungal (and oomycete) pathogens are predicted to be cytosolic (Dangl and Jones 2001). However one possibility that could account for this is that these R proteins may be part of transmembrane complexes and trigger resistance from the cytosol in response to pathogenic factors interacting with these complexes in the apoplast.

Functional analyses of Cf-9

As a way to test which of these two models of Cf-9 function more closely resembles its function, experiments presented in Chapter 3 of this thesis tested whether Cf-9 could function in the ER by localising Avr9 to the ER and examining the Cf-9 dependent necrotic response. While not definitive on their own, the data obtained using this approach seem most easily interpreted to indicate that either 1) Cf-9, or 2) an intermediate step upstream of Cf-9 (independent of Cf-9 localisation), is present at the PM.

If the first suggestion was true, this could indicate that Cf-9 functions in a similar manner to that previously suggested (Benghezal *et al.* 2000; Piedras *et al.* 2000; Van der Hoorn *et al.* 2001b), whereby Cf-9 is initially ER retained, but assembled/functional complexes are released from the ER to the PM. This could be similar to ABP1, whereby most Cf-9 is ER localised, and a small amount is functional at the PM. Delivery of a Cf-9 complex from the ER to the PM could be a passive, unregulated process, whereby Cf-9 complexes are released at a constant rate, or alternatively could be an active, regulated process in which delivery of the complex is regulated positively or negatively. An

example analogous to this latter suggestion is the MHC1 protein in rat adipose tissue, which is initially ER localised, then rapidly and specifically exported from the ER to the PM after stimulation of the cell with insulin (Malide *et al.* 2001). If Cf-9 were to function in this way, delivery of a Cf-9 complex could be regulated by Avr9 stimulation or possibly other factors in the complex.

If the second suggestion reflected Cf-9 function (i.e. an intermediate, upstream step at the PM), this would not provide clear evidence for either PM or ER localisation of Cf-9. If there was an intermediate step at the PM and Cf-9 was also PM localised, the above possibilities (i.e. for regulated delivery of Cf-9 from the ER to the PM) would still hold. Indeed part of the complex assembled in the ER could be involved in the intermediate step at the PM. Alternatively, if there was an intermediate step at the PM, and Cf-9 was ER localised, this might indicate that the intermediate component(s) was involved in transducing an Avr9-dependent signal or Avr9 itself to the ER (i.e. Model 2, as outlined above).

Both of these scenarios would in turn raise questions about the nature of the intermediate component. One possible candidate for a putative intermediate component is the High Affinity Binding Site (HABS) for Avr9 identified on the PM of solanaceous plants (Kooman-Gersmann *et al.* 1996). If HABS binding is an intermediate step in Cf-9/Avr9 interaction, it may be part of the virulence function of Avr9, and if interpreted using the guard hypothesis, might also be the pathogenicity target of Avr9 that is guarded by Cf-9.

To test one of these models of Cf-9 function, experiments were planned in Chapter 4 to determine whether Avr9 enters plant cells, in particular the ER. If Cf-9 did function in the ER, then Avr9 would be expected to either travel to the ER or initiate a signal from the PM to the ER. The experiments planned in Chapter 4 were expected to confirm or exclude the first of these possibilities, however they would not have excluded the second if Avr9 was not observed to enter the cell. Although these experiments were not ultimately performed, significant progress towards this goal was achieved in the development of a repertoire of suitable tools, and possible experimental strategies were suggested.

A key question relating to R protein function is how broadly these proteins can function taxonomically and what limits their function in heterologous species. The first issue was

central to the studies in Chapter 5, which attempted to determine whether Cf-9 could function in the monocotyledonous crop species, wheat. Using a microprojectile co-bombardment approach with a purpose-engineered Cf-9 construct for wheat expression, no evidence was found for Cf-9 mediated recognition of Avr9, although some limitations to the approach were noted.

If Cf-9 was found to be functional in wheat, using this or another approach, it may have been possible to engineer a form of non-specific disease resistance known as Genetically Engineered Acquired Resistance (Hammond-Kosack *et al.* 1998). If this (or any other) approach was used to engineer resistance in wheat (or any other crop), laboratory and field studies would still be necessary to determine whether a useful degree of resistance could be obtained in a cropping situation. In particular, it would be important to demonstrate that the induced resistance mechanisms are efficacious against significant disease/s and are not associated with loss of other important traits, particularly yield (Brown 2002).

RTF and the 'guard' hypothesis

'Restricted Taxonomic Functionality' (RTF) of *R* genes has been proposed as a general phenomenon to describe the limited taxonomic range over which these genes appear to retain function (Tai *et al.* 1999). The reasons for RTF are not clear, and relatively little consideration has been given to this topic (see Chapter 5 for details). One hypothesis is that the breadth of functionality of *R* genes is restricted by the similarity of signalling pathways leading to defence response activation (Hennin *et al.* 2001b; Hulbert *et al.* 2001; Rommens *et al.* 1995; Thilmony *et al.* 1995; Xiao *et al.* 2003).

The emerging 'guard' hypothesis for R protein function (Dangl and Jones 2001; Dixon *et al.* 2000; McDowell and Woffenden 2003; van der Biezen and Jones 1998) may be a useful framework within which to interpret RTF. The guard hypothesis posits that the R protein monitors, or guards, a specific host protein that is a pathogenicity target (PT), and elicits defence responses when a specific pathogen interacts with the PT in some way (see introductory chapter). Using this model, a key determinant of whether an R protein functions in a heterologous species must be the degree of conservation of the 'guardee' between those species (in addition to downstream signalling components), an idea only very recently suggested (McDowell and Woffenden 2003). The level of PT conservation would thus determine whether or not the heterologous R and Avr proteins

would interact with it, and consequently whether downstream signalling in the heterologous host could be induced (Figure 7.1).

This could potentially explain the result of functional tests of Cf-4 and Cf-9 in lettuce, in which Cf-4 functioned to recognise Avr4, but Cf-9 did not function to detect Avr9 in the same species (Van der Hoorn *et al.* 2000). Since these proteins have identical C-termini, which are presumed to be involved in activation of signalling rather than recognition of Avr proteins (Jones and Jones 1997; Thomas *et al.* 1997), if one of these proteins was active in lettuce due to the conservation of signalling components, then it would be expected that the other be functional. Using the model in Figure 7.1, it may be that the Cf-4 guardee is present and sufficiently conserved in lettuce for Cf-4 and Avr4 to recognise it, while the Cf-9 guardee is absent or divergent (Van der Hoorn *et al.* 2000).

Since very little is currently known about these putative PT/guardee molecules (if the guard hypothesis is an accurate model for R protein function), this model could explain the variable success and lack of apparent pattern to the ability of R proteins to function in heterologous hosts. Further evidence for or against these models might be obtained by investigating gene-for-gene resistance systems in which a putative PT/guardee has been identified (e.g. RIN4 {Mackey *et al.* 2002}, Pto {Kim *et al.* 2002; van der Biezen and Jones 1998}, At-RSH1 {van der Biezen *et al.* 2000} and TIP {Ren *et al.* 2000}). Possible tests include analysis of sequence divergence of the guardee between divergent species, particularly between those for which *R* gene function in one species had been demonstrated and not another, and transferring the combination of R, Avr and PT genes to the heterologous species. However, such experiments would be subject to many factors that could generate negative results, and should only be undertaken with this in mind.

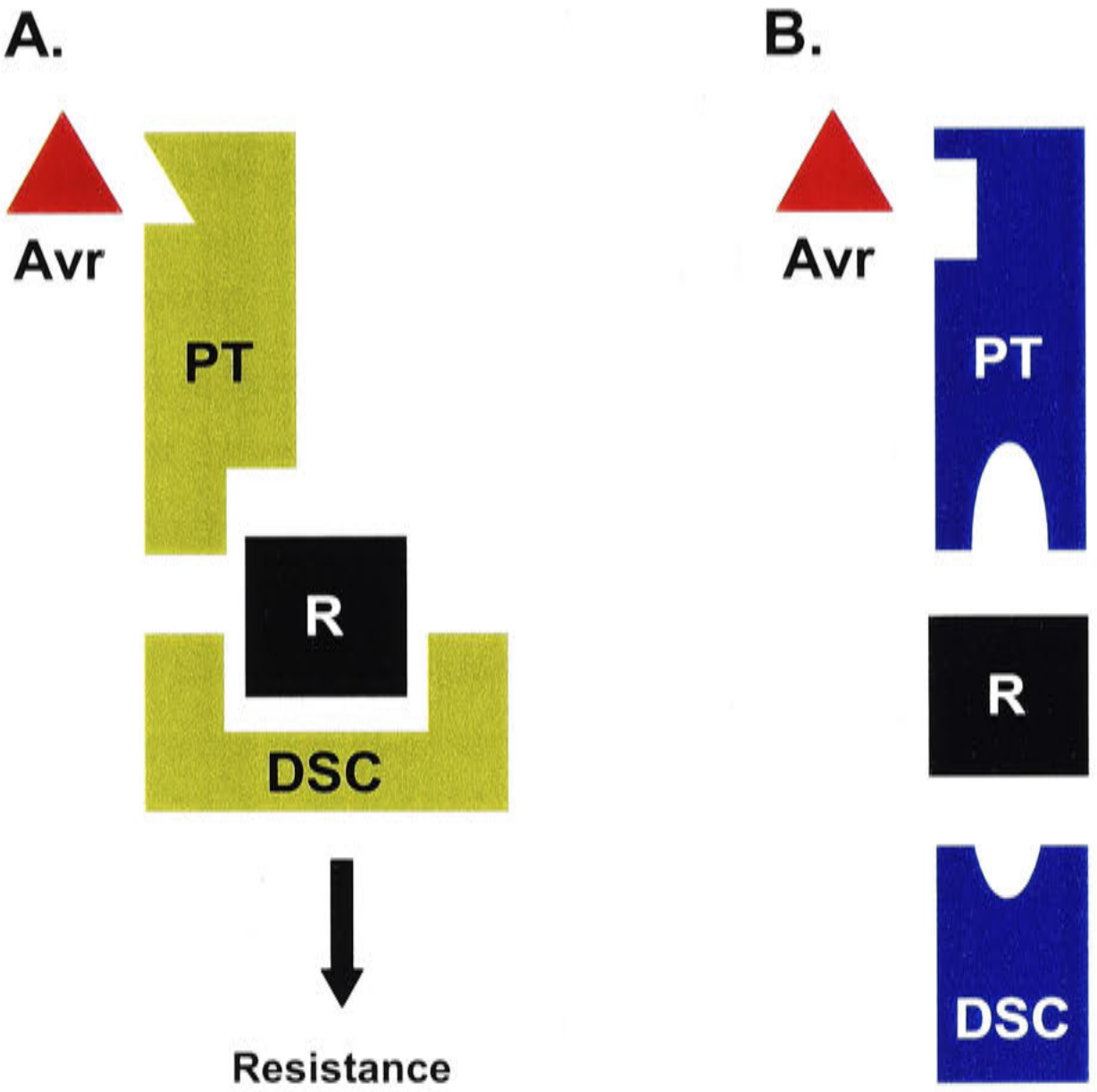

Figure 7.1. An hypothesis for Restricted Taxonomic Functionality (RTF) of R proteins using the guard hypothesis as a framework. **A.** In the native host plant, the avirulence protein interacts with the pathogenicity target (**PT**) for virulence function, and the host **R** protein responds by activating **resistance** mechanisms via downstream signalling components (**DSC**). **B.** In the heterologous species, the homologous **PT** has not co-evolved with the R and Avr proteins being tested or is absent, and thus does not interact appropriately with these proteins in divergent species. Additionally, the test R protein may not interact appropriately with the heterologous host DSC. Consequently, no activation of resistance mechanisms occurs when the R/Avr combination is co-expressed in that divergent species.

In general, this proposed model for RTF is very broad, and may be of only limited value for making specific predictions or hypotheses. Instead, it is perhaps better considered a potential framework in which RTF could be analysed. For example, one thing that this model suggests, or perhaps confirms, is that the limitation of our current understanding of R and Avr protein interaction with host proteins is the key impediment to the use of gene-for-gene systems in heterologous species, for both the investigation of plant disease resistance and for application of this knowledge to crop design.

Concluding remarks

This thesis has considered a few key issues relating to the function of the Cf-9 resistance protein at the cellular and molecular (biochemical) level. A novel approach was taken to investigate the function of Cf-9 at the cellular level, which contributed to a currently unresolved issue in the literature of this field. Further experiments were planned that would have further clarified the questions on Cf-9 function outlined here, and significant progress was made towards this goal in the form of development of experimental tools. The continuation of aspects of this work, as outlined in the relevant sections, would contribute further to this rapidly evolving and significant field of research.

APPENDICES

APPENDIX 1

General molecular biology

All molecular biology methods were performed according to manufacturers instructions where relevant or Sambrook *et al.* (1989) unless stated otherwise. All enzymes were purchased from New England Biolabs (Massachusetts, USA) and all chemicals from Sigma-Aldrich unless stated otherwise.

Plasmid DNA 'minipreps' were performed as described (Sambrook *et al.* 1989) with the following modifications. All centrifugation steps were performed at room temperature (~22°C) instead of 4°C, except where low yields were expected; the lysozyme-Tris solution was amended with 0.1 mg/ml RNase and stored at -20°C; resulting pellets of plasmid DNA were resuspended in 25 µl of TE (10 mM Tris, 1 mM EDTA, pH 8.0), and 0.5-2.0 µl of this preparation was used in a digest of 10-20 µl, depending upon the experiment.

Polymerase Chain Reaction (PCR) was performed using a PTC-200 Peltier Thermal Cycler (MJ Research, Boston, USA) using Sigma REDTaq™, according to the manufacturers instructions or as indicated in the text.

APPENDIX 2

Growth media recipes

All media were used as liquid or solidified with 1.5% (w/v) agar for solid media.

LB

Tryptone	10 g/L
Yeast extract	5 g/L
NaCl	10 g/L

2 x YT

Tryptone	16 g/L
Yeast extract	10 g/L
NaCl	10 g/L

YEP

Peptone	10 g/L
Yeast extract	10 g/L
NaCl	5 g/L

MinA

5 x MinA salts	200 ml/L
1M $MgSO_4$	1 ml/L
20% glucose	5 ml/L

- 5 x MinA salts included (per 100 ml) 5.25 g K_2HPO_4, 2.25 g KH_2PO_4, 0.5 g $(NH_4)SO_4$ and 0.25 g tri-sodium citrate.$2H_2O$.

- 1 L of MinA was prepared by separately autoclaving 500 ml containing salts (all except $MgSO_4$) and 500 ml containing 3% agar, mixing these while still hot, then adding separately autoclaved $MgSO_4$ and filter sterilised glucose.

APPENDIX 3

Table 1. Quantification of co-bombardment experiments to determine whether Cf-9 functions in wheat, as described in Chapter 5. The raw data for each leaf segment is presented (with a reference number) including values used for the analyses described in Chapter 5 (labelled). Leaf segments that were excluded as unrepresentative are highlighted in grey.

Leaf segment reference	Combination (Avr or R/Avr)	Leaf segment area (cm^2)	Strong GUS	Weak GUS	Total GUS	Weak / strong ratio	GUS/cm^2
020517_1	Avr	0.2	1	0	1	0	5.0
020517_2	Avr	0.32	23	5	28	0.217	87.5
020517_3	Avr	0.32	9	5	14	0.556	43.8
020517_4	Avr	0.37	7	12	19	1.71	51.4
020517_5	Avr	1.31	2	0	2	0	1.5
020523_B2&3_1	Avr	0.27	17	15	32	0.882	118.5
020523_B2&3_2	Avr	0.41	18	21	39	1.17	95.1
020523_B2&3_3	Avr	0.17	10	8	18	0.800	105.9
020523_B2&3_4	Avr	0.26	13	23	36	1.77	138.5
020523_B2&3_5	Avr	0.51	30	40	70	1.33	137.3
020523_B2&3_6	Avr	0.17	0	3	3	0	17.7
020523_B4&5_1	Avr	0.16	7	9	16	1.29	100.0
020523_B4&5_2	Avr	0.25	5	19	24	3.80	96.0
020523_B4&5_3	Avr	0.3	5	19	24	3.80	80.0
020523_B4&5_4	Avr	0.18	4	7	11	1.75	61.1
020523_B4&5_5	Avr	0.22	1	2	3	2.00	13.6
020606_B1&2_1	Avr	0.59	6	12	18	2.00	30.5
020606_B1&2_2	Avr	0.34	4	4	8	1.00	23.5
020606_B1&2_3	Avr	0.34	2	14	16	7.00	47.1
020606_B1&2_4	Avr	0.27	0	5	5	0	18.5
020606_B3&4_1	Avr	0.41	4	10	14	2.50	34.2
020606_B3&4_2	Avr	0.35	3	9	12	3.00	34.3
020606_B3&4_3	Avr	0.53	4	6	10	1.50	18.9
020606_B3&4_4	Avr	0.33	1	5	6	5.00	18.2
020517_6	R/Avr	0.28	12	8	20	0.667	71.4
020517_7	R/Avr	0.29	13	9	22	0.692	75.9
020517_8	R/Avr	0.35	5	8	13	1.60	37.1
020517_9	R/Avr	0.39	21	11	32	0.524	82.1
020517_10	R/Avr	0.37	14	13	27	0.929	73.0
020523_B2&3_7	R/Avr	0.29	6	16	22	2.67	75.9
020523_B2&3_8	R/Avr	0.6	20	40	60	2.00	100.0
020523_B2&3_9	R/Avr	0.26	4	6	10	1.50	38.5
020523_B2&3_10	R/Avr	0.29	8	18	26	2.25	89.7

Leaf segment reference	Combination (Avr or R/Avr)	Leaf segment area (cm^2)	Strong GUS	Weak GUS	Total GUS	Weak / strong ratio	GUS/cm^2
020523_B2&3_11	R/Avr	0.4	7	10	17	1.43	42.5
020523_B4&5_6	R/Avr	0.35	9	14	23	1.56	65.7
020523_B4&5_7	R/Avr	0.29	12	4	16	0.333	55.2
020523_B4&5_8	R/Avr	0.28	17	21	38	1.24	135.7
020523_B4&5_9	R/Avr	0.23	5	5	10	1.00	43.5
020523_B4&5_10	R/Avr	0.37	7	14	21	2.00	56.8
020606_B1&2_5	R/Avr	0.33	0	1	1	0	3.0
020606_B1&2_6	R/Avr	0.37	1	3	4	3.00	10.8
020606_B1&2_7	R/Avr	0.39	1	2	3	2.00	7.7
020606_B1&2_8	R/Avr	0.31	2	8	10	4.00	32.3
020606_B3&4_5	R/Avr	0.44	4	9	13	2.25	29.6
020606_B3&4_6	R/Avr	0.44	7	19	26	2.71	59.1
020606_B3&4_7	R/Avr	0.35	1	1	2	1.00	5.7
020606_B3&4_8	R/Avr	0.36	4	9	13	2.25	36.1

APPENDIX 4

A.

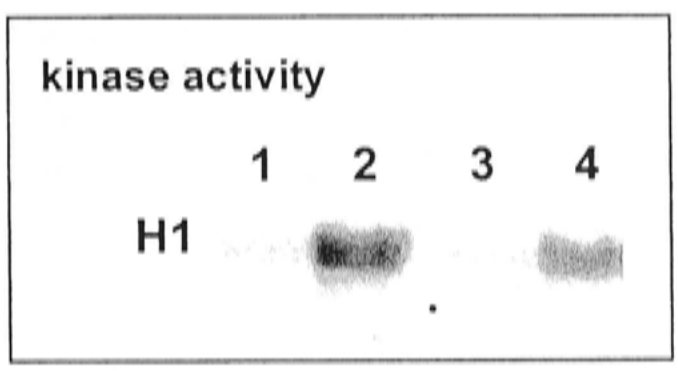

B.

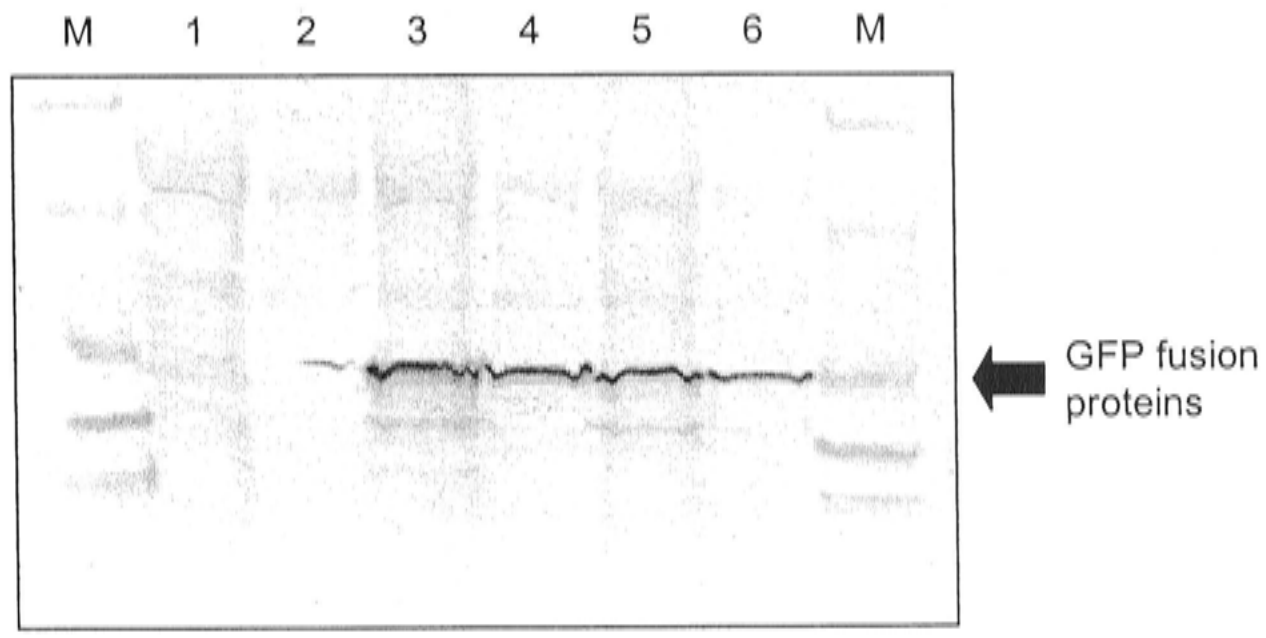

Appendix 4. Experiments performed by other researchers using the 3C3 mouse anti-GFP monoclonal antibody generated in Chapter 6. **A.** Immunoprecipitation of a Cdc2-GFP fusion protein from tobacco cell suspension culture total protein using 3C3 (data kindly provided by Dr Magdalena Weingartner, University of Vienna, Austria), with a subsequent kinase assay by histone phosphorylation shown. Lane **1** and **3** is extracts from cells expressing GFP only (500 μg and 200 μg total protein respectively) and lane **2** and **4** is Cdc2-GFP (500μg and 200 μg total protein respectively). The strong bands in lanes 2 and 4 indicates the kinase activity of GFP-Cdc2 has been immunoprecipitated by 3C3. **B.** A western blot of total protein extracted from *N. benthamiana* plants 16 days after inoculation with tobacco mosaic virus based viral vectors expressing two GFP fusions proteins (data kindly provided by Dr Dianne Webster, CSIRO, Adelaide, Australia) probed with 3C3 (diluted 1/200). **M** indicates lanes with a marker, lanes **1** and **2** are 20 μl and 5 μl of infected control tobacco extract respectively, lanes **3** and **4** are 20 μl and 5 μl of GFP fusion protein 1, lanes **5** and **6** are 20 μl and 5 μl of GFP fusion protein 2. The GFP fusion proteins are indicated at the right of the blot.

REFERENCES

Alberts, B., Bray, D., Lewis, J., Raff, M., Roberts, K. and Watson, J. D. (1994). Molecular Biology of the Cell, Garland Publishing, Inc., New York & London.

Alvim, F. C., Carolino, S. M. B., Cascardo, J. C. M., Nunes, C. C., Martinez, C. A., Otoni, W. C. and Fontes, E. P. B. (2001). Enhanced accumulation of BiP in transgenic plants confers tolerance to water stress. Plant Physiology **126**: 1042-1054.

Amado, F. M. L., Graca Santana-Marques, M., Ferrer-Correia, A. J. and Tomer, K. B. (1997). Analysis of peptide and protein samples containing surfactants by MALDI-MS. Analytical Chemistry **69**: 1102-1106.

Amersham-Pharmacia (1999). Ion Exchange Chromatography - Principles and Methods, Amersham-Pharmacia Biotech. 18-1114-21 Edition AA.

Amoah, B. K., Wu, H., Sparks, C. and Jones, H. D. (2001). Factors influencing *Agrobacterium*-mediated transient expression of *uidA* in wheat inflorescence tissue. Journal of Experimental Botany **52**: 1135-1142.

Andres, D., Dickerson, I. and Dixon, J. (1990). Variants of the carboxyl-terminal KDEL sequence direct intracellular retention. Journal of Biological Chemistry **265**: 5952-5955.

Andres, D., Rhodes, J., Meisel, R. and Dixon, J. (1991). Characterization of the carboxyl-terminal sequences responsible for protein retention in the endoplasmic reticulum. Journal of Biological Chemistry **266**: 14277-14282.

Askerlund, P., Laurent, P., Nakagawa, H. and Kader, J.-C. (1991). NADH-Ferricyanide reductase of leaf plasma membranes. Plant Physiology **95**: 6-13.

Axtell, M. J. and Staskawicz, B. J. (2003). Initiation of *RPS2*-specified disease resistance in *Arabidopsis* is coupled to the AvrRpt2-directed elimination of RIN4. Cell **112**: 369-377.

Bakhtiar, R. and Nelson, R. W. (2000). Electrospray ionization and matrix-assisted laser desorption ionization mass spectrometry. Emerging technologies in biomedical sciences. Biochemical Pharmacology **59**: 891-905.

Bakhtiar, R. and Tse, F. L. S. (2000). Biological mass spectrometry: a primer. Mutagenesis **15**: 415-430.

Baneyx, F. (1999). Recombinant protein expression in *Escherichia coli*. Current Opinion in Biotechnology **10**: 411-421.

Banks, D. J., Jurat-Fuentes, J. L., Dean, D. H. and Adang, M. J. (2001). *Bacillus thuringiensis* Cry1Ac and Cry1Fa δ-endotoxin binding to a novel 110 kDa aminopeptidase in *Heliothis virescens* is not *N*-acetylgalactosamine mediated. Insect Biochemistry and Molecular Biology **31**: 909-918.

Batoko, H., Zheng, H.-Q., Hawes, C. and Moore, I. (2000). A Rab1 GTPase is required for transport between the endoplasmic reticulum and Golgi apparatus and for normal Golgi movement in plants. The Plant Cell **12**: 2201-2217.

Becker, D., Brettschneider, R. and Lörz, H. (1994). Fertile transgenic wheat from microprojectile bombardment of scutellar tissue. The Plant Journal **5**: 299-307.

Bendahmane, A., Querci, M., Kanyuka, K. and Baulcombe, D. C. (2000). *Agrobacterium* transient expression system as a tool for the isolation of disease resistance genes: application to the *Rx2* locus in potato. The Plant Journal **21**: 73-81.

Benghezal, M., Wasteneys, G. O. and Jones, D. A. (2000). The C-terminal dilysine motif confers endoplasmic reticulum localization to Type I membrane proteins in plants. The Plant Cell **12**: 1179-1201.

Bent, A. F., Kunkel, B. N., Dahlbeck, D., Brown, K. L., Schmidt, R., Giraudat, J., Leung, J. and Staskawicz, B. J. (1994). *RPS2* of *Arabidopsis thaliana*: a leucine-rich repeat class of plant disease resistance genes. Science **265**: 1856-1860.

Bio-Rad (2003). Bio-Rex weakly acidic cation exchange resin: instruction manual. Bio-Rad Laboratories, California, USA. LIT-206 Rev B, Bulletin 9163.

Boevink, P., Oparka, K., Santa Cruz, S., Martin, B., Betteridge, A. and Hawes, C. (1998). Stacks on tracks: the plant Golgi apparatus traffics on an actin/ER network. The Plant Journal **15**: 441-447.

Bornsen, K. O., Gass, M. A., Bruin, G. J., von Adrichem, J. H., Biro, M. C., Kresbach, G. M. and Ehrat, M. (1997). Influence of solvents and detergents on matrix-assisted laser desorption/ionization mass spectrometry measurements of proteins and oligonucleotides. Rapid Communications in Mass Spectrometry **11**: 603-609.

Boyes, D. C., Nam, J. and Dangl, J. L. (1998). The *Arabidopsis thaliana* RPM1 disease resistance gene product is a peripheral plasma membrane protein that is degraded coincident with the hypersensitive response. Proceedings of the National Academy of Sciences USA **95**: 15849-15854.

Brown, J. K. M. (2002). Yield penalties of disease resistance in crops. Current Opinion in Plant Biology **5**: 339-344.

Büttner, D. and Bonas, U. (2002). Getting across - bacterial type III effector proteins on their way to the plant cell. EMBO Journal **21**: 5313-5322.

Calbiochem (2000). Glycobiology catalog and technical resource. Calbiochem, La Jolla, California.

Ceriotti, A. and Colman, A. (1988). Binding to membrane proteins within the endoplasmic reticulum cannot explain the retention of the glucose-regulated protein GRP78 in *Xenopus* oocytes. EMBO Journal **7**: 633-638.

Chaurand, P., Luetzenkirchen, F. and Spengler, B. (1999). Peptide and protein identification by matrix-assisted laser desorption ionization (MALDI) and MALDI-post-source decay time-of-flight mass spectrometry. Journal of the American Society for Mass Spectrometry **10**: 91-103.

Chen, Y.-F., Randlett, M. D., Findell, J. L. and Schaller, G. E. (2002). Localization of the ethylene receptor ETR1 to the endoplasmic reticulum of *Arabidopsis*. Journal of Biological Chemistry **277**: 19861-19866.

Chernushevich, I. V., Loboda, A. V. and Thomson, B. A. (2001). An introduction to quadrupole-time-of-flight mass spectrometry. Journal of Mass Spectrometry **36**: 849-865.

Chong, B. E., Wall, D. B., Lubman, D. M. and Flynn, S. J. (1997). Rapid profiling of *E. coli* proteins up to 500 kDa from whole cell lysates using matrix-assisted laser desorption/ionization time-of- flight mass spectrometry. Rapid Communications in Mass Spectrometry **11**: 1900-1908.

Chrispeels, M. J. and Herman, E. M. (2000). Endoplasmic reticulum-derived compartments function in storage and as mediators of vacuolar remodeling via a new type of organelle, precursor protease vesicles. Plant Physiology **123**: 1227-1234.

Christensen, A. H. and Quail, P. H. (1996). Ubiquitin promoter-based vectors for high-level expression of selectable and/or screenable marker genes in monocotyledonous plants. Transgenic Research **5**: 213-218.

Cohen, S. L. and Chait, B. T. (1996). Influence of matrix solution conditions on the MALDI-MS analysis of peptides and proteins. Analytical Chemistry **68**: 31-37.

Coligan, J. E., Kruisbeck, A. M., Margulies, D. A., Shevach, E. M. and Strober, W., Eds. (1994). Current Protocols in Immunology. John Wiley and Sons, Inc., New Jersey.

Collings, D. A., Carter, C. N., Rink, J. C., Scott, A. C., Wyatt, S. E. and Allen, N. S. (2000). Plant nuclei can contain extensive grooves and invaginations. The Plant Cell **12**: 2425-2439.

Cosson, P. and Letourneur, F. (1994). Coatomer interaction with di-lysine endoplasmic reticulum retention motifs. Science **263**: 1629-1631.

Crofts, A. J. and Denecke, J. (1998). Calreticulin and celnexin in plants. Trends in Plant Science **3**: 396-399.

Crofts, A. J., Leborgne-Castel, N., Pesca, M., Vitale, A. and Denecke, J. (1998). BiP and calreticulin form an abundant complex that is independent of endoplasmic reticulum stress. The Plant Cell **10**: 813-823.

Crofts, A. J., Leborgne-Castel, N., Hillmer, S., Robinson, D. G., Phillipson, B., Carlsson, L. E., Ashford, D. A. and Denecke, J. (1999). Saturation of the endoplasmic reticulum retention machinery reveals anterograde bulk flow. The Plant Cell **11**: 2233-2247.

Dangl, J. L. and Jones, J. D. G. (2001). Plant pathogens and integrated defence responses to infection. Nature **411**: 826-833.

Day, P. M., Yewdell, J. W., Porgador, A., Germain, R. N. and Bennink, J. R. (1997). Direct delivery of exogenous MHC class I molecule-binding oligopeptides to the endoplasmic reticulum of viable cells. Proceedings of the National Academy of Sciences USA **94**: 8064-8069.

De Buck, S., De Wilde, C., Van Montagu, M. and Depicker, A. (2000). Determination of the T-DNA transfer and the T-DNA integration frequencies upon cocultivation of *Arabidopsis thaliana* root explants. Molecular Plant-Microbe Interactions **13**: 658-665.

de Jong, C. F., Honée, G., Joosten, M. H. A. J. and de Wit, P. J. G. M. (2000). Early defence responses induced by AVR9 and mutant analogues in tobacco cell suspensions expressing the *Cf-9* resistance gene. Physiological and Molecular Plant Pathology **56**: 169-177.

de Wit, P. J. G. M. and Spikman, G. (1982). Evidence for the occurrence of race and cultivar-specific elicitors of necrosis in intercellular fluids of compatible interactions of *Cladosporium fulvum* and tomato. Physiological Plant Pathology **21**: 1-11.

Denecke, J., Botterman, J. and Deblaere, R. (1990). Protein secretion in plant cells can occur via a default pathway. The Plant Cell **2**: 51-59.

Denecke, J., De Rycke, R. and Botterman, J. (1992). Plant and mammalian sorting signals for protein retention in the endoplasmic reticulum contain a conserved epitope. EMBO Journal **11**: 2345-2355.

Denecke, J., Ek, B., Caspers, M., Sinjorgo, K. M. and Palva, E. T. (1993). Analysis of sorting signals responsible for the accumulation of soluble reticuloplasmins in the plant endoplasmic reticulum. Journal of Experimental Botany **44 Suppl**: 213-221.

Denecke, J. and Vitale, A. (1995). The use of protoplasts to study protein synthesis and transport by the plant endomembrane system. Methods in Cell Biology **50**: 335-348.

Denecke, J. (1996). Soluble endoplasmic reticulum resident proteins and their function in protein synthesis and transport. Plant Physiology and Biochemistry **34**: 197-205.

Deslandes, L., Olivier, J., Peeters, N., Xin Feng, D., Khounlotham, M., Boucher, C., Somssich, I., Genin, S. and Marco, Y. (2003). Physical interaction between RRS1-R, a protein conferring resistance to bacterial wilt, and PopP2, a type III effector targeted to the plant nucleus. Proceedings of the National Academy of Sciences USA **100**: 8024-8029.

Diekmann, W., Venis, M. A. and Robinson, D. G. (1995). Auxins induce clustering of the auxin-binding protein at the surface of maize coleoptile protoplasts. Proceedings of the National Academy of Sciences USA **92**: 3425-3429.

Dixon, M. S., Jones, D. A., Keddie, J. S., Thomas, C. M., Harrison, K. and Jones, J. D. G. (1996). The tomato *Cf-2* disease resistance locus comprises two functional genes encoding leucine-rich repeat proteins. Cell **84**: 451-459.

Dixon, M. S., Hatzixanthis, K., Jones, D. A., Harrison, K. and Jones, J. D. G. (1998). The tomato *Cf-5* disease resistance gene and six homologs show pronounced allelic variation in leucine-rich repeat copy number. The Plant Cell **10**: 1915-1925.

Dixon, M. S., Golstein, C., Thomas, C. M., Van Der Biezen, E. A. and Jones, J. D. G. (2000). Genetic complexity of pathogen perception by plants: the example of *Rcr3*, a tomato gene required specifically by *Cf-2*. Proceedings of the National Academy of Sciences USA **97**: 8807-8814.

Domin, M. A., Welham, K. J. and Ashton, D. S. (1999). The effect of solvent and matrix combinations on the analysis of bacteria by matrix-assisted laser desorption/ionisation time-of-flight mass spectrometry. Rapid Communications in Mass Spectrometry **13**: 222-226.

Ellgaard, L., Molinari, M. and Helenius, A. (1999). Setting the standards: quality control in the secretory pathway. Science **286**: 1882-1888.

Ellis, J., Dodds, P. and Pryor, T. (2000). The generation of plant disease resistance gene specificities. Trends in Plant Science **5**: 373-379.

Ellis, J. G. and Jones, D. A. (2003). Plant disease resistance genes. Humana Press Inc, Totowa, New Jersey.

Emans, N., Zimmermann, S. and Fischer, R. (2002). Uptake of a fluorescent marker in plant cells is sensitive to brefeldin A and wortmannin. The Plant Cell **14**: 71-86.

Ferguson, P. L. and Smith, R. D. (2003). Proteome analysis by mass spectrometry. Annual Review of Biophysics and Biomolecular Structure: 110601.141854.

Flor, H. H. (1971). Current status of the gene-for-gene concept. Annual Review of Phytopathology **9**: 275-296.

Frigerio, L., Pastres, A., Prada, A. and Vitale, A. (2001). Influence of KDEL on the fate of trimeric or assembly-defective phaseolin: selective use of an alternative route to vacuoles. The Plant Cell **13**: 1109-1126.

Gelvin, S. B. (2003). *Agrobacterium*-mediated plant transformation: the biology behind the "gene-jockeying" tool. Microbiology and Molecular Biology Reviews **67**: 16-37.

Gomord, V., Denmat, L. A., Fitchette-Laine, A. C., Satiat-Jeunemaitre, B., Hawes, C. and Faye, L. (1997). The C-terminal HDEL sequence is sufficient for retention of secretory proteins in the endoplasmic reticulum (ER) but promotes vacuolar targeting of proteins that escape the ER. The Plant Journal **11**: 313-325.

Görlich, D. and Mattaj, I. W. (1996). Nucleocytoplasmic transport. Science **271**: 1513-1519.

Grant, M. R., Godiard, L., Straube, E., Ashfield, T., Lewald, J., Sattler, A., Innes, R. W. and Dangl, J. L. (1995). Structure of the *Arabidopsis RPM1* gene enabling dual specificity disease resistance. Science **269**: 843-846.

Griffiths, G., Ericsson, M., Krijnse-Locker, J., Nilsson, T., Goud, B., Soling, H., Tang, B., Wong, S. and Hong, W. (1994). Localization of the Lys, Asp, Glu, Leu tetrapeptide receptor to the Golgi complex and the intermediate compartment in mammalian cells. Journal of Cell Biology **127**: 1557-1574.

Griffiths, W. J., Jonsson, A. P., Liu, S., Rai, D. K. and Wang, Y. (2001). Electrospray and tandem mass spectrometry in biochemistry. Biochemical Journal **355**: 545-561.

Hadlington, J. L. and Denecke, J. (2000). Sorting of soluble proteins in the secretory pathway of plants. Current Opinion in Plant Biology **3**: 461-468.

Halterman, D., Zhou, F., Wei, F., Wise, R. P. and Schulze-Lefert, P. (2001). The MLA6 coiled-coil, NBS-LRR protein confers *AvrMla6*-dependent resistance specificity to *Blumeria graminis* f. sp. *hordei* in barley and wheat. The Plant Journal **25**: 335-348.

Hammond, C. and Helenius, A. (1995). Quality control in the secretory pathway. Current Opinion in Cell Biology **7**: 523-529.

Hammond-Kosack, K. E., Harrison, K. and Jones, J. D. G. (1994a). Developmentally regulated cell death on expression of the fungal avirulence gene *Avr9* in tomato seedlings carrying the disease-resistance gene *Cf-9*. Proceedings of the National Academy of Sciences USA **91**: 10445-10449.

Hammond-Kosack, K. E., Jones, D. A. and Jones, J. D. G. (1994b). Identification of 2 genes required in tomato for full *Cf-9*-dependent resistance to *Cladosporium fulvum*. The Plant Cell **6**: 361-374.

Hammond-Kosack, K. E. and Jones, J. D. G. (1994). Incomplete dominance of tomato *Cf* genes for resistance to *Cladosporium fulvum*. Molecular Plant-Microbe Interactions **7**: 58-70.

Hammond-Kosack, K. E., Tang, S., Harrison, K. and Jones, J. D. G. (1998). The tomato *Cf-9* disease resistance gene functions in tobacco and potato to confer responsiveness to the fungal avirulence gene product Avr9. The Plant Cell **10**: 1251-1266.

Hardwick, K. G., Lewis, M. J., Semenza, J., Dean, N. and Pelham, H. R. (1990). ERD1, a yeast gene required for the retention of luminal endoplasmic reticulum proteins, affects glycoprotein processing in the Golgi apparatus. EMBO Journal **9**: 623-630.

Harlow, E. and Lane, D., Eds. (1988). Antibodies: A laboratory manual. Cold Spring Harbor Laboratory, New York.

Haseloff, J., Siemering, K. R., Prasher, D. C. and Hodge, S. (1997). Removal of a cryptic intron and subcellular localization of green fluorescent protein are required to mark transgenic *Arabidopsis* plants brightly. Proceedings of the National Academy of Sciences USA **94**: 2122-2127.

Haugejorden, S., Srinivasan, M. and Green, M. (1991). Analysis of the retention signals of two resident luminal endoplasmic reticulum proteins by *in vitro* mutagenesis. Journal of Biological Chemistry **266**: 6015-6018.

Henderson, J., Bauly, J. M., Ashford, D. A., Oliver, S. C., Hawes, C. R., Lazarus, C. M., Venis, M. A. and Napier, R. M. (1997). Retention of maize auxin-binding protein in the endoplasmic reticulum: quantifying escape and the role of auxin. Planta **202**: 313-323.

Hennin, C., Diederichsen, E. and Höfte, M. (2001a). Local and systemic resistance to fungal pathogens triggered by an AVR9-mediated hypersensitive response in tomato and oilseed rape carrying the *Cf-9* resistance gene. Physiological and Molecular Plant Pathology **59**: 287-295.

Hennin, C., Höfte, M. and Diederichsen, E. (2001b). Functional expression of *Cf9* and *Avr9* genes in *Brassica napus* induces enhanced resistance to *Leptosphaeria maculans*. Molecular Plant-Microbe Interactions **14**: 1075-1085.

Hennin, C., Diederichsen, E. and Höfte, M. (2002). Resistance to fungal pathogens triggered by the *Cf9-Avr9* response in tomato and oilseed rape in the absence of hypersensitive cell death. Molecular Plant Pathology **3**: 31-41.

Hentz, N. G., Richardson, J. M., Sportsman, J. R., Daijo, J. and Sittampalam, G. S. (1997). Synthesis and characterization of insulin-fluorescein derivatives for bioanalytical applications. Analytical Chemistry **69**: 4994-5000.

Herman, E. M., Tague, B. W., Hoffmann, L. M., Kjemtrup, S. E. and Chrispeels, M. J. (1990). Retention of phytohemagglutinin with carboxyterminal tetrapeptide KDEL in the nuclear envelope and the endoplasmic reticulum. Planta **182**: 305-312.

Hesse, T., Feldwisch, J., Balshusemann, D., Bauw, G., Puype, M., Vandekerckhove, J., Lobler, M., Klambt, D., Schell, J. and Palme, K. (1989). Molecular cloning and structural analysis of a gene from *Zea mays* (L.) coding for a putative receptor for the plant hormone auxin. EMBO Journal **8**: 2453-2461.

Honée, G., Melchers, L. S., Vleeshouwers, V. G., van Roekel, J. S. and de Wit, P. J. G. M. (1995). Production of the AVR9 elicitor from the fungal pathogen *Cladosporium fulvum* in transgenic tobacco and tomato plants. Plant Molecular Biology **29**: 909-920.

Hong, W. (1998). Protein transport from the endoplasmic reticulum to the Golgi apparatus. Journal of Cell Science **111**: 2831-2839.

Hop, C. E. C. A. and Bakhtiar, R. (1997). An introduction to Electrospray Ionization and Matrix-Assisted Laser Desorption/Ionization Mass Spectrometry: essential tools in a modern biotechnology environment. Biospectroscopy **3**: 259-280.

Hulbert, S. H., Webb, C. A., Smith, S. M. and Sun, Q. (2001). Resistance gene complexes: evolution and utilization. Annual Review of Phytopathology **39**: 285-312.

Inohara, N., Shimomura, S., Fukui, T. and Futai, M. (1989). Auxin-binding protein located in the endoplasmic reticulum of maize shoots: molecular cloning and complete primary structure. Proceedings of the National Academy of Sciences USA **86**: 3564-3568.

Jackson, M. E., Simpson, J. C., Girod, A., Pepperkok, R., Roberts, L. M. and Lord, J. M. (1999). The KDEL retrieval system is exploited by *Pseudomonas* exotoxin A, but not by Shiga-like toxin-1, during retrograde transport from the Golgi complex to the endoplasmic reticulum. Journal of Cell Science **112**: 467-475.

Janssen, B. J. and Gardner, R. C. (1990). Localized transient expression of GUS in leaf discs following cocultivation with *Agrobacterium*. Plant Molecular Biology **14**: 61-72.

Jefferson, R. A. (1987). Assaying chimeric genes in plants: the GUS gene fusion system. Plant Molecular Biology Reporter **5**: 387-405.

Jia, Y., McAdams, S. A., Bryan, G. T., Hershey, H. P. and Valent, B. (2000). Direct interaction of resistance gene and avirulence gene products confers rice blast resistance. EMBO Journal **19**: 4004-4014.

Johannes, L., Tenza, D., Antony, C. and Goud, B. (1997). Retrograde transport of KDEL-bearing B-fragment of Shiga toxin. Journal of Biological Chemistry **272**: 19554-19561.

Johannes, L. and Goud, B. (1998). Surfing on a retrograde wave: how does Shiga toxin reach the endoplasmic reticulum? Trends in Cell Biology **8**: 158-162.

Johansen, L. K. and Carrington, J. C. (2001). Silencing on the spot. Induction and suppression of RNA silencing in the *Agrobacterium*-mediated transient expression system. Plant Physiology **126**: 930-938.

Jones, A. M. and Herman, E. M. (1993). KDEL-containing auxin-binding protein is secreted to the plasma membrane and cell wall. Plant Physiology **101**: 595-606.

Jones, D. A., Thomas, C. M., Hammond-Kosack, K. E., Balint-Kurti, P. J. and Jones, J. D. G. (1994). Isolation of the tomato *Cf-9* gene for resistance to *Cladosporium fulvum* by transposon tagging. Science **266**: 789-793.

Jones, D. A., Hammond-Kosack, K. E. and Jones, J. D. G. (1995). Method of introducing pathogen resistance in plants. Patent Number WO9531564.

Jones, D. A. and Jones, J. D. G. (1997). The role of leucine-rich repeat proteins in plant defences. Advances in Botanical Research **24**: 89-167.

Jones, J. D. G., Shlumukov, L., Carland, F., English, J., Scofield, S. R., Bishop, G. J. and Harrison, K. (1992). Effective vectors for transformation, expression of heterologous genes, and assaying transposon excision in transgenic plants. Transgenic Research **1**: 285-297.

Joosten, M. H. A. J. and de Wit, P. J. G. M. (1999). The tomato-*Cladosporium fulvum* interaction: A versatile experimental system to study plant-pathogen interactions. Annual Review of Phytopathology **37**: 335-367.

Kaletta, K., Kunze, I., Kunze, G. and Kock, M. (1998). The peptide HDEF as a new retention signal is necessary and sufficient to direct proteins to the endoplasmic reticulum. FEBS Letters **434**: 377-381.

Kapila, J., Derycke, R., Vanmontagu, M. and Angenon, G. (1997). An *Agrobacterium*-mediated transient gene expression system for intact leaves. Plant Science **122**: 101-108.

Khanna, H. K. and Daggard, G. E. (2003). *Agrobacterium tumefaciens*-mediated transformation of wheat using a superbinary vector and polyamine-supplemented regeneration medium. Plant Cell Reports **21**: 429-436.

Kim, Y. J., Lin, N.-C. and Martin, G. B. (2002). Two distinct *Pseudomonas* effector proteins interact with the Pto kinase and activate plant immunity. Cell **109**: 589-598.

Knebel, W., Quader, H. and Schnepf, E. (1990). Mobile and immobile endoplasmic reticulum in onion bulb epidermis cells: short- and long-term observations with a confocal laser scanning microscope. European Journal of Cell Biology **52**: 328-340.

Kooman-Gersmann, M., Honée, G., Bonnema, G. and de Wit, P. J. G. M. (1996). A high-affinity binding site for the Avr9 peptide elicitor of *Cladosporium fulvum* is present on plasma membranes of tomato and other solanaceous plants. The Plant Cell **8**: 929-938.

Kooman-Gersmann, M., Vogelsang, R., Hoogendijk, E. C. and de Wit, P. J. G. M. (1997). Assignment of amino acid residues of the AVR9 peptide of *Cladosporium fulvum* that determine elicitor activity. Molecular Plant-Microbe Interactions **10**: 821-829.

Kooman-Gersmann, M., Vogelsang, R., Vossen, P., van den Hooven, H. W., Mahe, E., Honée, G. and de Wit, P. J. G. M. (1998a). Correlation between binding affinity and necrosis-inducing activity of mutant AVR9 peptide elicitors. Plant Physiology **117**: 609-618.

Kooman-Gersmann, M., Weide, R., Honée, G., Saijun, T., Hammond-Kosack, K. E., Jones, J. D. G. and de Wit, P. J. G. M. (1998b). The *Cf-9* resistance gene nor its homologues are required for high affinity binding of the Avr9 elicitor of *Cladosporium fulvum*. PhD thesis, Agricultural University Wageningen, Netherlands.

Kunkel, T. A. (1985). Rapid and efficient site-specific mutagenesis without phenotypic selection. Proceedings of the National Academy of Sciences USA **82**: 488-492.

Kunkel, T. A., Roberts, J. D. and Zakour, R. A. (1987). Rapid and efficient site-specific mutagenesis without phenotypic selection. Methods in Enzymology **154**: 367-382.

Kussmann, M., Nordhoff, E., Rahbek-Nielsen, H., Haebel, S., Rossel-Larsen, M., Jakobsen, L., Gobom, J., Mirgorodskaya, E., Kroll-Kristensen, A., Palm, L. and Roepstorff, P. (1997). Matrix-assisted Laser Desorption/Ionization Mass Spectrometry sample preparation techniques designed for various peptide and protein analytes. Journal of Mass Spectrometry **32**: 593-601.

Landry, F., Lombardo, C. R. and Smith, J. W. (2000). A method for application of samples to matrix-assisted laser desorption ionization time-of-flight targets that enhances peptide detection. Analytical Biochemistry **279**: 1-8.

Lazarovits, G. and Higgins, V. J. (1976). Ultrastructure of susceptible, resistant, and immune reactions of tomato to races of *Cladosporuim fulvum*. Canadian Journal of Botany **54**: 235-249.

Leborgne-Castel, N., Jelitto-Van Dooren, E. P. W. M., Crofts, A. J. and Denecke, J. (1999). Overexpression of BiP in tobacco alleviates endoplasmic reticulum stress. The Plant Cell **11**: 459-469.

Lee, H. I., Gal, S., Newman, T. C. and Raikhel, N. V. (1993). The *Arabidopsis* endoplasmic reticulum retention receptor functions in yeast. Proceedings of the National Academy of Sciences USA **90**: 11433-11437.

Lehmann, K., Hause, B., Altmann, D. and Kock, M. (2001). Tomato ribonuclease LX with the functional endoplasmic reticulum retention motif HDEF is expressed during programmed cell death processes, including xylem differentiation, germination, and senescence. Plant Physiology **127**: 436-449.

Leister, R. T., Ausubel, F. M. and Katagiri, F. (1996). Molecular recognition of pathogen attack occurs inside of plant cells in plant disease resistance specified by the *Arabidopsis* genes *RPS2* and *RPM1*. Proceedings of the National Academy of Sciences USA **93**: 15497-15502.

Leister, R. T. and Katagiri, F. (2000). A resistance gene product of the nucleotide binding site - leucine rich repeats class can form a complex with bacterial avirulence proteins *in vivo*. The Plant Journal **22**: 345-354.

Lerouge, P., Cabanes-Macheteau, M., Rayon, C., Fischette-Laine, A. C., Gomord, V. and Faye, L. (1998). N-glycoprotein biosynthesis in plants: recent developments and future trends. Plant Molecular Biology **38**: 31-48.

Letourneur, F., Hennecke, S., Demolliere, C. and Cosson, P. (1995). Steric masking of a dilysine endoplasmic reticulum retention motif during assembly of the human high affinity receptor for immunoglobulin E. Journal of Cell Biology **129**: 971-978.

Lewis, M. J., Sweet, D. J. and Pelham, H. R. (1990). The ERD2 gene determines the specificity of the luminal ER protein retention system. Cell **61**: 1359-1363.

Lewis, M. J. and Pelham, H. R. (1992). Ligand-induced redistribution of a human KDEL receptor from the Golgi complex to the endoplasmic reticulum. Cell **68**: 353-364.

Li, L., Garden, R. W. and Sweedler, J. V. (2000). Single-cell MALDI: a new tool for direct peptide profiling. Trends in Biotechnology **18**: 151-160.

Lichtscheidl, I. K. and Url, W. G. (1990). Organization and dynamics of cortical endoplasmic reticulum in inner epidermal cells of onion bulb scales. Protoplasma **157**: 203-215.

Lin, D., Tabb, D. L. and Yates, I., John R. (2003). Large-scale protein identification using mass spectrometry. Biochimica et Biophysica Acta **1646**: 1-10.

Loh, Y. T., Zhou, J. and Martin, G. B. (1998). The myristylation motif of Pto is not required for disease resistance. Molecular Plant-Microbe Interactions **11**: 572-576.

Lord, J. M. and Roberts, L. M. (1998). Retrograde transport: going against the flow. Current Biology **8**: R56-58.

Lotti, L. V., Mottola, G., Torrisi, M. R. and Bonatti, S. (1999). A different intracellular distribution of a single reporter protein is determined at steady state by KKXX or KDEL retrieval signals. Journal of Biological Chemistry **274**: 10413-10420.

Lu, J. and Zenobi, R. (1999). Matrix-assisted laser desorption/ionization time-of-flight mass spectrometry for identifying the composition of labeled proteins. Analytical Biochemistry **269**: 312-316.

Lucas, J. A. (1998). Plant Pathology and Plant Pathogens. Blackwell Science, United Kingdom.

Luderer, R., Rivas, S., Nurnberger, T., Mattei, B., Van den Hooven, H. W., Van der Hoorn, R. A. L., Romeis, T., Wehrfritz, J. M., Blume, B., Nennstiel, D., Zuidema, D., Vervoort, J., De Lorenzo, G., Jones, J. D. G., de Wit, P. J. G. M. and Joosten, M. H. A. J. (2001). No evidence for binding between resistance gene product Cf-9 of tomato and avirulence gene product AVR9 of *Cladosporium fulvum*. Molecular Plant-Microbe Interactions **14**: 867-876.

Mackey, D., Holt, B. F., Wiig, A. and Dangl, J. L. (2002). RIN4 interacts with *Pseudomonas syringae* type III effector molecules and is required for RPM1-mediated resistance in *Arabidopsis*. Cell **108**: 743-754.

Mackey, D., Belkhadir, Y., Alonso, J. M., Ecker, J. R. and Dangl, J. L. (2003). *Arabidopsis* RIN4 is a target of the type III virulence effector AvrRpt2 and modulates RPS2-mediated resistance. Cell **112**: 379-389.

Mahe, E., Vossen, P., Van den Hooven, H. W., Le-Nguyen, D., Vervoort, J. and de Wit, P. J. G. M. (1998). Solid-phase synthesis, conformational analysis, and biological activity of AVR9 elicitor peptides of the fungal tomato pathogen *Cladosporium fulvum*. Journal of Peptide Research **52**: 482-494.

Malide, D., Yewdell, J. W., Bennink, J. R. and Cushman, S. W. (2001). The export of major histocompatibility complex class 1 molecules from the endoplasmic reticulum of rat brown adipose cells is acutely stimulated by insulin. Molecular Biology of the Cell **12**: 101-114.

Marquardt, T., Hebert, D. and Helenius, A. (1993). Post-translational folding of influenza hemagglutinin in isolated endoplasmic reticulum-derived microsomes. Journal of Biological Chemistry **268**: 19618-19625.

Martin, G. B., Brommonschenkel, S. H., Chunwongse, J., Frary, A., Ganal, M. W., Spivey, R., Wu, T., Earle, E. D. and Tanksley, S. D. (1993). Map-based cloning of a protein kinase gene conferring disease resistance in tomato. Science **262**: 1432-1436.

McDowell, J. M. and Woffenden, B. J. (2003). Plant disease resistance genes: recent insights and potential applications. Trends in Biotechnology **21**: 178-183.

Micromass (1997). TofSpec E & SE Operator Manual. Micromass, United Kingdom. Issue 4 - Code Number 6666446.

Miesenbock, G. and Rothman, J. E. (1995). The capacity to retrieve escaped ER proteins extends to the trans-most cisterna of the Golgi stack. Journal of Cell Biology **129**: 309-319.

Mindrinos, M., Katagiri, F., Yu, G. L. and Ausubel, F. M. (1994). The *A. thaliana* disease resistance gene *RPS2* encodes a protein containing a nucleotide-binding site and leucine-rich repeats. Cell **78**: 1089-1099.

Molecular Probes, (2003). Molecular Probes Catalogue. Ninth edition.

Munro, S. and Pelham, H. R. (1987). A C-terminal signal prevents secretion of luminal ER proteins. Cell **48**: 899-907.

Napier, R. M., Fowke, L. C., Hawes, C., Lewis, M. and Pelham, H. R. (1992). Immunological evidence that plants use both HDEL and KDEL for targeting proteins to the endoplasmic reticulum. Journal of Cell Science **102**: 261-271.

Napier, R. M. (1997). Trafficking of the auxin-binding protein. Trends in Plant Science **2**: 251-255.

Nebenfuhr, A. and Staehelin, L. A. (2001). Mobile factories: Golgi dynamics in plant cells. Trends in Plant Science **6**: 160-167.

Novagen (2000). The pET system manual. TB055 9th Edition 05/00.

Okamoto, T., Minamikawa, T., Edward, G., Vakharia, V., Herman, E. and Okomoto, T. (1999). Posttranslational removal of the carboxyl-terminal KDEL of the cysteine protease SH-EP occurs prior to maturation of the enzyme. Journal of Biological Chemistry **274**: 11390-11398.

Pagny, S., Lerouge, P., Faye, L. and Gomord, V. (1999). Signals and mechanisms for protein retention in the endoplasmic reticulum. Journal of Experimental Botany **50**: 157-164.

Pagny, S., Cabanes-Macheteau, M., Gillikin, J. W., Leborgne-Castel, N., Lerouge, P., Boston, R. S., Faye, L. and Gomord, V. (2000). Protein recycling from the Golgi apparatus to the endoplasmic reticulum in plants and its minor contribution to calreticulin retention. The Plant Cell **12**: 739-755.

Palanichelvam, K. and Schoelz, J. E. (2002). A comparative analysis of the avirulence and translational transactivator functions of gene VI of Cauliflower mosaic virus. Virology **293**: 225-233.

Pelham, H. R., Hardwick, K. G. and Lewis, M. J. (1988). Sorting of soluble ER proteins in yeast. EMBO Journal **7**: 1757-1762.

Pelham, H. R. (1989). The selectivity of secretion: protein sorting in the endoplasmic reticulum. Biochemical Society Transactions **17**: 795-802.

Pelham, H. R. (1990). The retention signal for soluble proteins of the endoplasmic reticulum. Trends in Biochemical Sciences **15**: 483-486.

Pelham, H. R. (2000). Using sorting signals to retain proteins in endoplasmic reticulum. Methods in Enzymology **327**: 279-283.

Pellegrineschi, A., Noguera, L. M., Skovmand, B., Brito, R. M., Velazquez, L., Salgado, M. M., Hernandez, R., Warburton, M. and Hoisington, D. (2002). Identification of highly transformable wheat genotypes for mass production of fertile transgenic plants. Genome **45**: 421-430.

Phillipson, B. A., Pimpl, P., da Silva, L. L., Crofts, A. J., Taylor, J. P., Movafeghi, A., Robinson, D. G. and Denecke, J. (2001). Secretory bulk flow of soluble proteins is efficient and COPII dependent. The Plant Cell **13**: 2005-2020.

Piedras, P., Hammond-Kosack, K. E., Harrison, K. and Jones, J. D. G. (1998). Rapid, *Cf-9*- and Avr9-dependent production of active oxygen species in tobacco suspension cultures. Molecular Plant-Microbe Interactions **11**: 1155-1166.

Piedras, P., Rivas, S., Droge, S., Hillmer, S. and Jones, J. D. G. (2000). Functional, c-myc-tagged Cf-9 resistance gene products are plasma-membrane localized and glycosylated. The Plant Journal **21**: 529-536.

Pueyo, J. J., Chrispeels, M. J. and Herman, E. M. (1995). Degradation of transport-competent destabilized phaseolin with a signal for retention in the endoplasmic reticulum occurs in the vacuole. Planta **196**: 586-596.

Qiagen (1992). The QIA*expressionist*. Qiagen, California. Summer 1992, Second Edition.

Rapak, A., Falnes, P. O. and Olsnes, S. (1997). Retrograde transport of mutant ricin to the endoplasmic reticulum with subsequent translocation to cytosol. Proceedings of the National Academy of Sciences USA **94**: 3783-3788.

Ren, T., Qu, F. and Morris, T. J. (2000). *HRT* gene function requires interaction between a NAC protein and viral capsid protein to confer resistance to turnip crinkle virus. The Plant Cell **12**: 1917-1925.

Ridge, R. W., Uozumi, Y., Plazinski, J., Hurley, U. A. and Williamson, R. E. (1999). Developmental transitions and dynamics of the cortical ER of *Arabidopsis* cells seen with green fluorescent protein. Plant and Cell Physiology **40**: 1253-1261.

Rivas, S., Romeis, T. and Jones, J. D. G. (2002). The Cf-9 disease resistance protein is present in an ~420-kilodalton heteromultimeric membrane-associated complex at one molecule per complex. The Plant Cell **14**: 689-702.

Rommens, C. M., Salmeron, J. M., Oldroyd, G. E. and Staskawicz, B. J. (1995). Intergeneric transfer and functional expression of the tomato disease resistance gene *Pto*. The Plant Cell **7**: 1537-1544.

Rossi, L., Escudero, J., Hohn, B. and Tinland, B. (1993). Efficient and sensitive assay for T-DNA-dependent transient gene expression. Plant Molecular Biology Reporter **11**: 220-229.

Salmeron, J. M., Oldroyd, G. E., Rommens, C. M., Scofield, S. R., Kim, H. S., Lavelle, D. T., Dahlbeck, D. and Staskawicz, B. J. (1996). Tomato *Prf* is a member of the leucine-rich repeat class of plant disease resistance genes and lies embedded within the *Pto* kinase gene cluster. Cell **86**: 123-133.

Sambrook, J., Frisch, E. F. and Maniatis, T. (1989). Molecular Cloning: A laboratory manual, Cold Spring Harbor Laboratory Press, New York.

Sanderfoot, A. A. and Raikhel, N. V. (1999). The specificity of vesicle trafficking: coat proteins and SNAREs. The Plant Cell **11**: 629-641.

Sandvig, K. and van Deurs, B. (1999). Endocytosis and intracellular transport of ricin: recent discoveries. FEBS Letters **452**: 67-70.

Sandvig, K. and van Deurs, B. (2000). Entry of ricin and Shiga toxin into cells: molecular mechanisms and medical perspectives. EMBO Journal **19**: 5943-5950.

Schagger, H. and von Jagow, G. (1987). Tricine-sodium dodecyl sulfate-polyacrylamide gel electrophoresis for the separation of proteins in the range from 1 to 100 kDa. Analytical Biochemistry **166**: 368-379.

Schmid, M., Simpson, D., Kalousek, F. and Gietl, C. (1998). A cysteine endopeptidase with a C-terminal KDEL motif isolated from castor bean endosperm is a marker enzyme for the ricinosome, a putative lytic compartment. Planta **206**: 466-475.

Schmid, M., Simpson, D. and Gietl, C. (1999). Programmed cell death in castor bean endosperm is associated with the accumulation and release of a cysteine endopeptidase from ricinosomes. Proceedings of the National Academy of Sciences USA **96**: 14159-14164.

Schmid, M., Simpson, D. J., Sarioglu, H., Lottspeich, F. and Gietl, C. (2001). The ricinosomes of senescing plant tissue bud from the endoplasmic reticulum. Proceedings of the National Academy of Sciences USA **98**: 5353-5358.

Schob, H., Kunz, C. and Meins, F., Jr. (1997). Silencing of transgenes introduced into leaves by agroinfiltration: a simple, rapid method for investigating sequence requirements for gene silencing. Molecular and General Genetics **256**: 581-585.

Scholtens-Toma, I. M. J. and de Wit, P. J. G. M. (1988). Purification and primary structure of a necrosis-inducing peptide from the apoplastic fluids of tomato infected with *Cladosporium fulvum* (syn. *Fulvia fulva*). Physiological and Molecular Plant Pathology **33**: 59-67.

Schweizer, P., Pokorny, J., Abderhalden, O. and Dudler, R. (1999). A transient assay system for the functional assessment of defense-related genes in wheat. Molecular Plant-Microbe Interactions **12**: 647-654.

Schweizer, P., Pokorny, J., Schulze-Lefert, P. and Dudler, R. (2000). Double-stranded RNA interferes with gene function at the single-cell level in cereals. The Plant Journal **24**: 895-903.

Scofield, S. R., Tobias, C. M., Rathjen, J. P., Chang, J. H., Lavelle, D. T., Michelmore, R. W. and Staskawicz, B. J. (1996). Molecular basis of gene-for-gene specificity in bacterial speck disease of tomato. Science **274**: 2063-2065.

Scott, A., Wyatt, S., Tsou, P. L., Robertson, D. and Allen, N. S. (1999). Model system for plant cell biology: GFP imaging in living onion epidermal cells. BioTechniques **26**: 1125, 1128-1132.

Seetharam, S., Chaudhary, V. K., FitzGerald, D. and Pastan, I. (1991). Increased cytotoxic activity of *Pseudomonas* exotoxin and two chimeric toxins ending in KDEL. Journal of Biological Chemistry **266**: 17376-17381.

Semenza, J. C., Hardwick, K. G., Dean, N. and Pelham, H. R. (1990). ERD2, a yeast gene required for the receptor-mediated retrieval of luminal ER proteins from the secretory pathway. Cell **61**: 1349-1357.

Shenkman, M., Ehrlich, M. and Lederkremer, G. Z. (2000). Masking of an endoplasmic reticulum retention signal by its presence in the two subunits of the asialoglycoprotein receptor. Journal of Biological Chemistry **275**: 2845-2851.

Siemering, K. R., Golbik, R., Sever, R. and Haseloff, J. (1996). Mutations that suppress the thermosensitivity of green fluorescent protein. Current Biology **6**: 1653-1663.

Siuzdak, G. (1994). The emergence of mass spectrometry in biochemical research. Proceedings of the National Academy of Sciences USA **91**: 11290-11297.

Song, W. Y., Wang, G. L., Chen, L. L., Kim, H. S., Pi, L. Y., Holsten, T., Gardner, J., Wang, B., Zhai, W. X., Zhu, L. H. and et al. (1995). A receptor kinase-like protein encoded by the rice disease resistance gene, *Xa21*. Science **270**: 1804-1806.

Southgate, E. M., Davey, M. R., Power, J. B. and Marchant, R. (1995). Factors affecting the genetic engineering of plants by microprojectile bombardment. Biotechnology Advances **13**: 631-651.

Spolaore, S., Trainotti, L. and Casadoro, G. (2001). A simple protocol for transient gene expression in ripe fleshy fruit mediated by *Agrobacterium*. Journal of Experimental Botany **52**: 845-850.

Stintzi, A., Heitz, T., Prasad, V., Wiedemann-Merdinoglu, S., Kauffmann, S., Geoffroy, P., Legrand, M. and Fritig, B. (1993). Plant 'pathogenesis-related' proteins and their role in defense against pathogens. Biochimie **75**: 687-706.

Tai, T. H., Dahlbeck, D., Clark, E. T., Gajiwala, P., Pasion, R., Whalen, M. C., Stall, R. E. and Staskawicz, B. J. (1999). Expression of the *Bs2* pepper gene confers resistance to bacterial spot disease in tomato. Proceedings of the National Academy of Sciences USA **96**: 14153-14158.

Takumi, S., Murai, K., Mori, N. and Nakamura, C. (1999). *Trans*-activation of a maize *Ds* transposable element in transgenic wheat plants expressing the *Ac* transposase gene. Theoretical and Applied Genetics **98**: 947-953.

Tang, X., Frederick, R. D., Zhou, J., Halterman, D. A., Jia, Y. and Martin, G. B. (1996). Initiation of plant disease resistance by physical interaction of AvrPto and Pto kinase. Science **274**: 2060-2063.

Tarentino, A. L. and Plummer, T. H., Jr. (1994). Enzymatic deglycosylation of asparagine-linked glycans: purification, properties, and specificity of oligosaccharide-cleaving enzymes from *Flavobacterium meningosepticum*. Methods in Enzymology **230**: 44-57.

Tatu, U. and Helenius, A. (1997). Interactions between newly synthesized glycoproteins, calnexin and a network of resident chaperones in the endoplasmic reticulum. Journal of Cell Biology **136**: 555-565.

Taylor, N. J. and Fauquet, C. M. (2002). Microparticle bombardment as a tool in plant science and agricultural biotechnology. DNA and Cell Biology **21**: 963-977.

Thilmony, R. L., Chen, Z., Bressan, R. A. and Martin, G. B. (1995). Expression of the tomato *Pto* gene in tobacco enhances resistance to *Pseudomonas syringae* pv *tabaci* expressing *avrPto*. The Plant Cell **7**: 1529-1536.

Thomas, C. M., Jones, D. A., Parniske, M., Harrison, K., Balint-Kurti, P. J., Hatzixanthis, K. and Jones, J. D. G. (1997). Characterization of the tomato *Cf-4*

gene for resistance to *Cladosporium fulvum* identifies sequences that determine recognitional specificity in *Cf-4* and *Cf-9*. The Plant Cell **9**: 2209-2224.

Thomas, C. M., Tang, S., Hammond-Kosack, K. E. and Jones, J. D. G. (2000). Comparison of the hypersensitive response induced by the tomato *Cf-4* and *Cf-9* genes in *Nicotiana spp*. Molecular Plant-Microbe Interactions **13**: 465-469.

Tillmann, U., Viola, G., Kayser, B., Siemeister, G., Hesse, T., Palme, K., Lobler, M. and Klambt, D. (1989). cDNA clones of the auxin-binding protein from corn coleoptiles (Zea mays L.): isolation and characterization by immunological methods. EMBO Journal **8**: 2463-2467.

Timpte, C. (2001). Auxin binding protein: curiouser and curiouser. Trends in Plant Science **6**: 586-590.

Tornero, P., Conejero, V. and Vera, P. (1996). Primary structure and expression of a pathogen-induced protease (PR- P69) in tomato plants: similarity of functional domains to subtilisin- like endoproteases. Proceedings of the National Academy of Sciences USA **93**: 6332-6337.

Torres, E., Gonzalez-Melendi, P., Stoger, E., Shaw, P., Twyman, R. M., Nicholson, L., Vaquero, C., Fischer, R., Christou, P. and Perrin, Y. (2001). Native and artificial reticuloplasmins co-accumulate in distinct domains of the endoplasmic reticulum and in post-endoplasmic reticulum compartments. Plant Physiology **127**: 1212-1223.

Townsley, F. M., Wilson, D. W. and Pelham, H. R. (1993). Mutational analysis of the human KDEL receptor: distinct structural requirements for Golgi retention, ligand binding and retrograde transport. EMBO Journal **12**: 2821-2829.

Toyooka, K., Okamoto, T. and Minamikawa, T. (2000). Mass transport of proform of a KDEL-tailed cysteine proteinase (SH-EP) to protein storage vacuoles by endoplasmic reticulum-derived vesicle is involved in protein mobilization in germinating seeds. Journal of Cell Biology **148**: 453-463.

Tsien, R. Y. (1998). The green fluorescent protein. Annual Review of Biochemistry **67**: 509-544.

Tzfira, T. and Citovsky, V. (2002). Partners-in-infection: host proteins involved in the transformation of plant cells by *Agrobacterium*. Trends in Cell Biology **12**: 121-129.

Van den Ackerveken, G. F., Vossen, P. and de Wit, P. J. G. M. (1993). The AVR9 race-specific elicitor of *Cladosporium fulvum* is processed by endogenous and plant proteases. Plant Physiology **103**: 91-96.

Van den Ackerveken, G. F., Marois, E. and Bonas, U. (1996). Recognition of the bacterial avirulence protein AvrBs3 occurs inside the host plant cell. Cell **87**: 1307-1316.

van den Hooven, H. W., Appelman, A. W., Zey, T., de Wit, P. J. G. M. and Vervoort, J. (1999). Folding and conformational analysis of AVR9 peptide elicitors of the fungal tomato pathogen *Cladosporium fulvum*. European Journal of Biochemistry **264**: 9-18.

van den Hooven, H. W., van den Burg, H. A., Vossen, P., Boeren, S., de Wit, P. J. G. M. and Vervoort, J. (2001). Disulfide bond structure of the AVR9 elicitor of the fungal tomato pathogen *Cladosporium fulvum*: evidence for a cystine knot. Biochemistry **40**: 3458-3466.

van der Biezen, E. A. and Jones, J. D. G. (1998). Plant disease-resistance proteins and the gene-for-gene concept. Trends in Biochemical Sciences **23**: 454-456.

van der Biezen, E. A., Sun, J., Coleman, M. J., Bibb, M. J. and Jones, J. D. G. (2000). *Arabidopsis* RelA/SpoT homologs implicate (p)ppGpp in plant signaling. Proceedings of the National Academy of Sciences USA **97**: 3747-3752.

Van der Hoorn, R. A. L., Laurent, F., Roth, R. and de Wit, P. J. G. M. (2000). Agroinfiltration is a versatile tool that facilitates comparative analyses of *Avr9*/*Cf-9*-induced and *Avr4*/*Cf-4*-induced necrosis. Molecular Plant-Microbe Interactions **13**: 439-446.

Van der Hoorn, R. A. L., Roth, R. and de Wit, P. J. G. M. (2001a). Identification of distinct specificity determinants in resistance protein Cf-4 allows construction of a Cf-9 mutant that confers recognition of avirulence protein Avr4. The Plant Cell **13**: 273-285.

Van der Hoorn, R. A. L., Ven der Ploeg, A., de Wit, P. J. G. M. and Joosten, M. H. A. J. (2001b). The C-terminal dilysine motif for targeting to the endoplasmic reticulum is not required for Cf-9 function. Molecular Plant-Microbe Interactions **14**: 412-415.

Van der Hoorn, R. A. L., Rivas, S., Wulff, B. B. H., Jones, J. D. G. and Joosten, M. H. A. J. (2003). Rapid migration in gel filtration of the Cf-4 and Cf-9 resistance proteins is an intrinsic property of Cf proteins and not because of their association with high-molecular-weight proteins. The Plant Journal **35**: 305-315.

van Kan, J. A., van den Ackerveken, G. F. and de Wit, P. J. G. M. (1991). Cloning and characterization of cDNA of avirulence gene *Avr9* of the fungal pathogen *Cladosporium fulvum*, causal agent of tomato leaf mold. Molecular Plant-Microbe Interactions **4**: 52-59.

Vaquero, C., Sack, M., Chandler, J., Drossard, J., Schuster, F., Monecke, M., Schillberg, S. and Fischer, R. (1999). Transient expression of a tumor-specific single-chain fragment and a chimeric antibody in tobacco leaves. Proceedings of the National Academy of Sciences USA **96**: 11128-11133.

Vervoort, J., van den Hooven, H. W., Berg, A., Vossen, P., Vogelsang, R., Joosten, M. H. A. J. and de Wit, P. J. G. M. (1997). The race-specific elicitor AVR9 of the tomato pathogen *Cladosporium fulvum*: a cystine knot protein. Sequence-specific 1H NMR assignments, secondary structure and global fold of the protein. FEBS Letters **404**: 153-158.

Vitale, A. and Denecke, J. (1999). The endoplasmic reticulum-gateway of the secretory pathway. The Plant Cell **11**: 615-628.

von Arnim, A. G., Deng, X.-W. and Stacey, M. G. (1998). Cloning vectors for the expression of green fluorescent protein fusion proteins in transgenic plants. Gene **221**: 35-43.

Wales, R., Chaddock, J. A., Roberts, L. M. and Lord, J. M. (1992). Addition of an ER retention signal to the ricin A chain increases the cytotoxicity of the holotoxin. Experimental Cell Research **203**: 1-4.

Wang, Z., Russon, L., Li, L., Roser, D. C. and Long, S. R. (1998). Investigation of spectral reproducibility in direct analysis of bacteria proteins by matrix-assisted laser desorption/ionization time-of-flight mass spectrometry. Rapid Communications in Mass Spectrometry **12**: 456-464.

Weeks, J. T., Anderson, O. D. and Blechl, A. E. (1993). Rapid production of multiple independent lines of fertile transgenic wheat (*Triticum aestivum*). Plant Physiology **102**: 1077-1084.

Weir, B., Gu, X., Wang, M., Upadhyaya, N., Elliott, A. R. and Brettell, R. I. S. (2001). *Agrobacterium tumefaciens*-mediated transformation of wheat using suspension cells as a model system and green fluorescent protein as a visual marker. Australian Journal of Plant Physiology **28**: 807-818.

Whitham, S., McCormick, S. and Baker, B. (1996). The *N* gene of tobacco confers resistance to tobacco mosaic virus in transgenic tomato. Proceedings of the National Academy of Sciences USA **93**: 8776-8781.

Wu, H., Sparks, C., Amoah, B. and Jones, H. D. (2003). Factors influencing successful *Agrobacterium*-mediated transformation of wheat. Plant Cell Reports **21**: 659-668.

Xiao, S., Ellwood, S., Calis, O., Patrick, E., Li, T., Coleman, M. and Turner, J. G. (2001). Broad-spectrum mildew resistance in *Arabidopsis thaliana* mediated by *RPW8*. Science **291**: 118-120.

Xiao, S., Charoenwattana, P., Holcombe, L. and Turner, J. G. (2003). The *Arabidopsis* genes *RPW8.1* and *RPW8.2* confer induced resistance to powdery mildew diseases in tobacco. Molecular Plant-Microbe Interactions **16**: 289-294.

Yang, Y., Li, R. and Qi, M. (2000). *In vivo* analysis of plant promoters and transcription factors by agroinfiltration of tobacco leaves. The Plant Journal **22**: 543-551.

Yates, J. R., 3rd (1998). Mass spectrometry and the age of the proteome. Journal of Mass Spectrometry **33**: 1-19.

Zagouras, P. and Rose, J. K. (1989). Carboxy-terminal SEKDEL sequences retard but do not retain two secretory proteins in the endoplasmic reticulum. Journal of Cell Biology **109**: 2633-2640.

Zambre, M., Terryn, N., De Clercq, J., De Buck, S., Dillen, W., Van Montagu, M., Van Der Straeten, D. and Angenon, G. (2003). Light strongly promotes gene transfer from *Agrobacterium tumefaciens* to plant cells. Planta **216**: 580-586.

Zhan, J., Stayton, P. and Press, O. W. (1998). Modification of ricin A chain, by addition of endoplasmic reticulum (KDEL) or Golgi (YQRL) retention sequences, enhances its cytotoxicity and translocation. Cancer Immunology and Immunotherapy **46**: 55-60.